An investigation of functional brain networks in drug resistant and well-controlled Idiopathic Generalised Epilepsy

A thesis submitted to the University of Manchester for the degree of Doctor of Philosophy in the Faculty of Biology, Medicine and Health

2021

Emily J Pegg

School of Biological Sciences

Contents

List of tables **6**

List of figures **7**

Abbreviations **9**

Abstract **12**

Declaration **14**

Copyright statement **14**

Journal format statement **15**

Statement of contributions to journal papers **15**

Preface **16**

Acknowledgements **16**

Chapter 1. Introduction **17**

1.1 Idiopathic Generalised Epilepsy (IGE) 17

1.1.1 Background 17

1.1.2 Clinical features of IGE 18

1.1.3 Diagnosing IGE 19

1.1.4 Pharmacological management of IGE 21

1.2 Drug resistant IGE 22

1.2.1 Background 22

1.2.2 Proposed mechanisms of drug resistance in epilepsy 23

1.2.3 Determinants of response to antiepileptic drugs 28

1.3 Neuronal oscillations 29

1.3.1 The role of neuronal oscillations 29

1.3.2 Measuring neuronal oscillations 30

1.3.3 Oscillatory amplitude, frequency and spectral analysis in epilepsy studies 31

1.4 Network analysis in the study of epilepsy 33

1.4.1 Contextual overview 33

1.4.2 Scales of connectivity 34

1.4.3 Large-scale resting state network analysis 35

1.4.3.1 Overview..... 35
1.4.3.2 Connectivity subtypes..... 36
1.4.3.3 Neuroimaging modalities in global functional network analysis..... 37
1.4.3.4 Inferring global resting state functional connectivity..... 38
1.4.3.5 Evaluating connectivity in functional networks with graph theory..... 46
1.4.4 Overview of interictal functional network literature in IGE..... 50
1.5 Aims and objectives..... 52

Chapter 2. A spectral power investigation of the interictal EEG in drug resistant and well-controlled IGE..... 54

2.1 Authors..... 54
2.2 Abstract..... 54
2.3 Introduction..... 55
2.4 Materials and methods..... 57
2.5 Results..... 60
2.5.1 Baseline demographics..... 60
2.5.2 Outcome measures..... 60
2.6 Discussion..... 63
2.7 Conclusions..... 66
2.8 Acknowledgements..... 66
2.9 Funding..... 66

Chapter 3. Interictal structural and functional connectivity in IGE: A systematic review of graph theoretical studies..... 72

3.1 Authors..... 72
3.2 Abstract..... 72
3.3 Introduction..... 73
3.3.1 Background..... 73
3.3.2 Measuring connectivity in brain networks..... 75
3.3.3 Aim of the review..... 80
3.4 Methods..... 81
3.4.1 Search strategy..... 81
3.4.2 Data extraction..... 81
3.5 Results..... 82
3.5.1 Participant demographics..... 83
3.5.1.1 Functional network studies..... 83

3.5.1.2 Structural network studies..... 84
3.5.2 Data acquisition and network construction..... 85
3.5.2.1 Functional network studies..... 85
3.5.2.2 Structural network studies..... 86
3.5.3 Statistical considerations..... 87
3.6 Study results..... 87
3.6.1 Functional network studies..... 87
3.6.1.1 EEG/MEG studies..... 87
3.6.1.2 fMRI studies..... 90
3.6.2 Structural network studies..... 91
3.7 Discussion..... 93
3.7.1 Limitations of the review..... 98
3.8 Conclusions..... 98

Chapter 4. Interictal EEG functional network topology in drug resistant and well-controlled IGE..... 111

4.1 Authors..... 111
4.2 Abstract..... 111
4.3 Introduction..... 112
4.4 Methods..... 114
4.5 Results..... 121
4.6 Discussion..... 124
4.7 Acknowledgements..... 127
4.8 Funding..... 127
4.9 Appendix A- Supplementary data..... 133

Chapter 5. Functional network topology in drug resistant and well-controlled Idiopathic Generalised Epilepsy: A resting state fMRI study..... 137

5.1 Authors..... 137
5.2 Abstract..... 137
5.3 Introduction..... 138
5.4 Materials and methods..... 140
5.5 Results..... 146
5.6 Discussion..... 150
5.7 Conclusions..... 152
5.8 Funding..... 153

5.9 Appendix B- Discussion of atlas choice..... 160
5.10 Appendix C- Supplementary data..... 166
5.10.1 Supplementary data 1- Global outcome metric results..... 166
5.10.2 Supplementary data 2- Nodal analyses results..... 169

Chapter 6. General discussion..... 200
6.1 Summary of experimental results..... 200
6.2 Interpretation..... 201
6.3 General limitations..... 208
6.4 Future directions..... 210
6.5 Conclusions..... 213

References..... 215

Word count: 44,681

List of tables

1a. Demographic and clinical details of participants with WC-IGE..... 67

1b. Demographic and clinical details of participants with DR-IGE..... 69

1c. Demographic details of control participants..... 71

2. Commonly used measures in global network studies..... 99

3. Demographics of participants in functional connectivity studies..... 101

4. Demographics of participants included in structural connectivity studies..... 104

5. Data acquisition and graph construction for structural studies using DTI 106

6. Recommendations and considerations for future graph theoretical studies of cerebral networks..... 107

7. Participant demographics (EEG graph theoretical study)..... 128

8. Commonly used graph theoretical terms and measures applied to epilepsy research.... 154

9. Participant demographics (IGE group, fMRI study)..... 156

Appendix tables

A-1. Descriptive statistics for outcome metrics in the 6-9 Hz frequency band..... 133

A-2. Descriptive statistics for outcome metrics in the 10-12 Hz frequency band..... 134

A-3. Outcome metrics compared at the three-group level..... 135

A-4. Pairwise comparison tests of results that were significant at the three-group level.... 136

C-1. Three-group comparison of networks constructed using absolute values of edges..... 166

C-2. Two-group comparison of network constructed using absolute values of edges 167

C-3. Three-group comparison of networks constructed using positively correlated edges 167

C-4. Two-group comparison of networks constructed using positively correlated edges... 168

C-5. Statistical significance of difference in node strength between controls and people IGE for each region 169

C-6. Statistical significance of difference in betweenness centrality between controls and people with IGE for each region..... 180

List of figures

1. Typical inter-ictal EEG features of IGE..... 20

2. Example DTI image..... 36

3. Phase synchronisation and amplitude correlation..... 41

4. Schematic illustrating how PLV is determined..... 42

5. Phase locking index..... 43

6. Example of a connectivity matrix derived from a 62 channel EEG..... 46

7. A simple undirected graph..... 47

8. 'Rewiring' of a regular network to form small-world and random networks..... 49

9. Spectral power analysis..... 56

10. Power spectra plotted for each group..... 61

11. Power spectra for each group averaged within each frequency band..... 61

12. Scalp topographical images of differences in spectral power between epilepsy groups and controls..... 62

13. Summary of previous studies evaluating EEG /MEG spectral power in IGE..... 63

14. Schematic overview of graph construction using diffusion MRI, fMRI, structural covariance and EEG..... 76

15. Visual representation of different graph types according to edge features..... 78

16. Example representations of regular, random and small-world networks..... 80

17. Study flow chart..... 83

18. Result summary of clustering coefficient analyses in EEG/MEG studies..... 88

19. Result summary of path length analyses in EEG/MEG studies..... 89

20. Result summary of global efficiency analysis in EEG/MEG studies..... 90

21. Visual summary of outcome measures from fMRI functional studies..... 91

22. Visual summary of outcome measures from structural connectivity studies..... 93

23. Schematic overview of study methodology..... 115

24. Outcome metrics plotted for each group..... 123

25. Schematic overview of study methodology..... 141

26. Global outcome metrics..... 148

27. Nodal differences between IGE and controls..... 149

28. 2D state-plane representations of oscillations in a normal brain and a brain with epilepsy..... 206

29. A multifactorial network system model of antiepileptic drug resistance..... 207

Appendix figures

B-1 Illustration of the rendering of AICHA and the sulci used in anatomical labelling..... 161

C-1 Frequency of hub nodes in frontal regions plotted for each group..... 197

C-2 Frequency of hub nodes in temporal regions plotted for each group..... 197

C-3 Frequency of hub nodes in parietal regions plotted for each group..... 198

C-4 Frequency of hub nodes in occipital regions plotted for each group..... 198

C-5 Frequency of hub nodes in thalamic regions plotted for each group..... 199

Abbreviations

AAL	automated anatomical labelling
AED	antiepileptic drug
AICHA	atlas of Intrinsic Connectivity of Homotopic Areas
ANCOVA	analysis of covariance
ANOVA	analysis of variance
BBB	blood brain barrier
BOLD	blood-oxygen-level-dependent
C	clustering coefficient
CAE	childhood absence epilepsy
CONN	functional connectivity toolbox
DMN	default mode network
DRE	drug resistant epilepsy
DR-IGE	drug resistant Idiopathic Generalised Epilepsy
DTI	diffusion tensor imaging
EEG	electroencephalograph
EGTCSA	epilepsy with generalised tonic-clonic seizures alone
EOG	electrooculography
EPI	echo planar imaging
FE	focal epilepsy
fMRI	functional magnetic resonance imaging
FDR	false discovery rate
FOV	field of view
FWE	family wide error
GABA	gamma-aminobutyric acid

GTC	generalised tonic-clonic
HCP	Human Connectome Project
HFOs	high frequency oscillations
HRA	Health Research Authority
HRF	haemodynamic response function
ICA	independent component analysis
IEDs	interictal epileptiform discharges
IGE	Idiopathic Generalised Epilepsy
ILAE	International League Against Epilepsy
JAE	juvenile absence epilepsy
JME	juvenile myoclonic epilepsy
L	characteristic path length
MDR1	multidrug resistance mutation 1
MEG	magnetoencephalography
MNI	Montreal Neurological Institute
MRI	magnetic resonance imaging
NEAD	non-epileptic attack disorder
P-gp	P-glycoprotein
PLI	phase locking index
PLV	phase locking value
REC	Research Ethics Committee
RSN	resting-state network
SD	standard deviation
SUDEP	sudden unexplained death in epilepsy
SWI	small world index

TE	echo time
TR	repetition time
UK	United Kingdom
WCE	well-controlled epilepsy
WC-IGE	well-controlled Idiopathic Generalised Epilepsy
3T	3 Tesla

Abstract

Epilepsy is one of the most common neurological disorders, estimated to affect 70 million people worldwide (Ngugi et al., 2010). Around 20 % of people with Idiopathic Generalised Epilepsy (IGE) continue to have seizures despite treatment with antiepileptic medication (Brodie et al., 2012). The mechanisms of epilepsy drug resistance remain poorly understood. Previous studies have primarily investigated potential cellular or genetic explanations for drug resistance.

Epilepsy is regarded as a network disorder in which seizures arise via transient, abnormal, hypersynchronous activity of large-scale neuronal brain networks. An increasing body of literature demonstrates that people with epilepsy have different resting state networks than people without epilepsy. This thesis aims to investigate whether network alterations are also implicated in drug resistance.

Resting state networks in people with well-controlled IGE, drug resistant IGE, and healthy controls were compared using spectral power analysis and graph theoretical analysis of data derived from EEG and fMRI. Converging evidence from the results demonstrated large-scale network alterations in people with IGE compared to controls. In particular, in IGE, there was a suggestion of greater cortical hyperexcitability and an alteration in the topology of the network, which had a more regular configuration. One of the studies also suggested that network topology in well-controlled IGE differed from controls, but not between controls and drug resistant IGE. We posit that this is due to a drug induced network alteration in people who respond to medication which stabilises the network, rendering it less susceptible to the seizure state.

The cause of drug resistance in some people with IGE remains unknown, but may involve a complex interplay between multifarious brain networks, influenced by inherent epilepsy severity. The results of this thesis are of potential importance in furthering knowledge of how drug resistance arises and as a possible basis for an epilepsy biomarker.

Declaration

No portion of the work referred to in the thesis has been submitted in support of an application for another degree or qualification of this or any other university or other institute of learning.

Copyright statement

Journal format statement

Investigating functional networks in Idiopathic Generalised Epilepsy using the tools and methods outlined in the introduction to this thesis, leant itself to the creation of three separate publishable papers, with a further paper to systematically review current literature in this area. As agreed with my supervisors, it was felt that together with an introduction and synthesised discussion of the papers, the work forms a coherent body of work that is suitable for a thesis presented in the journal format.

Statement of contributions to journal papers

The participants included in the manuscripts forming Chapters 2 and 4 were all recruited by me, except three who were recruited by colleagues at the Walton Centre. The majority of participants in the study forming Chapter 5 were recruited by colleagues at the Walton Centre. Each of the study methodologies were designed by me and reviewed by co-authors, including my PhD supervisors, and revised where necessary. I performed all data collection and pre-processing for both EEG studies (Chapters 2 and 4). fMRI data was collected by colleagues at The Walton Centre and pre-processed by Yachin Chen and Andrea McKavanagh. The code used to construct networks in the studies in Chapters 4 and 5 was written by Petroula Laiou. All of the data analysis and statistical analysis for each study was performed by me. I also performed the literature search for the systematic review (Chapter 3) and extracted and synthesised data for the review. All of the papers were written by me, with co-authors critically reviewing its content, which was revised where required. All authors approved the final versions to be published.

Preface

The author studied medicine at the University of St Andrews and University of Manchester, graduating with an MBChB and MSc (medical science) in 2008. Following this, she began postgraduate training in the north west of England. She has a longstanding interest in research and completed an MRes (public health) in 2014 at the University of Manchester, alongside clinical training. In 2014, she entered a neurology training programme and whilst doing so, sought an opportunity to pursue a PhD in a research area related to epilepsy. She had time out of clinical training from 2017-2020 to work towards this. The author has now returned to her final year of postgraduate training in neurology and subsequently hopes to work as an epilepsy specialist whilst continuing epilepsy research.

Acknowledgements

I would firstly like to thank my PhD supervisors Rajiv Mohanraj and Jason Taylor for their guidance and support. I am also very grateful to Rajiv for the opportunity to undertake this project and for fostering my interest in epilepsy. Thank you to my PhD advisor, Monty Silverdale, whose wise words helped me immensely, and to senior colleagues at Salford Royal, who made it possible for me to have time out of clinical training to pursue a research project.

I am also very thankful to Anthony Jones and the Human Pain Research Group at the University of Manchester who kindly offered a share of their workspace and the use of their EEG equipment.

This research would also not have been possible without the many individuals who are acknowledged in the manuscripts within this thesis. Special thanks are owed to Simon Keller and the Liverpool Neuroimaging Group who welcomed me to join their lab meetings and provided a great source of support, and also to Petroula Laiou at Kings College London who provided friendly mathematical guidance from afar. Special thanks are also owed to all of the people who gave their time to participate in this study.

The final year of working towards this PhD coincided with a difficult time in my life (alongside a pandemic thrown into the mix, when I temporarily returned to clinical work). I will be forever grateful for the love and unwavering support of my husband Nikesh, and for my friends and family during this period.

Chapter 1. Introduction

This thesis investigates well-controlled and drug resistant Idiopathic Generalised Epilepsy (IGE) using electroencephalograph (EEG) methods to evaluate oscillatory power and EEG and functional magnetic resonance imaging (fMRI) methods to examine large-scale resting state networks. In the introduction, I will firstly review IGE and drug resistance in IGE. Neuronal oscillations will then be discussed and previous studies that have evaluated oscillations in IGE will be summarised. Next, resting state network analysis will be introduced, with a focus on graph theoretical analysis. This will be followed by a discussion of the literature on graph theoretical analytical studies of IGE. To conclude the introduction, the aims and objectives of the thesis will be presented.

1.1 Idiopathic Generalised Epilepsy

1.1.1 Background

Epilepsy is a common neurological disorder in which seizures arise via transient, abnormal, hypersynchronous activity of large-scale neuronal brain networks. It is conceptually defined as "a disorder of the brain characterized by an enduring predisposition to generate epileptic seizures, and by the neurobiologic, cognitive, psychological, and social consequences of this condition" (Fisher et al., 2005). Epilepsy affects around 70 million people worldwide (Ngugi et al., 2010) and the estimated prevalence in the United Kingdom (UK) is 0.61- 0.76% (Thomas et al., 2012). Around 15- 20% of people with epilepsy have IGE (Jallon and Latour, 2005).

IGEs are a group of electro-clinical syndromes characterised by generalised seizures in the absence of structural brain lesions or neurodevelopmental abnormalities. The EEG typically shows bilaterally synchronous, anteriorly dominant interictal discharges with a normal background. The International League Against Epilepsy (ILAE) currently define generalised seizures as "originating at some point within, and rapidly engaging bilaterally distributed networks" in contrast to focal seizures, which are thought to evolve from networks within one cerebral hemisphere (Berg et al., 2010). There is substantial evidence to suggest seizure genesis in IGE involves aberrations in the thalamocortical network, but evidence of the involvement of other networks, such as the default mode network (DMN) or large-scale 'global' networks, is also reported. This is discussed further in subsection 1.4.1. Although the precise mechanisms of epilepsy have not been elucidated, it is widely accepted that epilepsy is

a network disorder and that seizures emerge from neuronal networks via complex dynamical interactions (Richardson, 2012b).

It is presumed that IGE has an underlying genetic basis (Berg et al., 2010) but the exact nature of this has not been determined. A number of genes have been implicated and inheritance patterns may be complex polygenic or Mendelian (Helbig, 2015). In view of the presumed genetic basis of the pathophysiology of epilepsy, the ILAE have previously suggested 'Genetic Generalised Epilepsy' to be a more accurate description than IGE (Berg et al., 2010). However, this term has not been universally accepted, partly because the term may be inappropriately synonymised with 'inherited' (Scheffer et al., 2017).

1.1.2 Clinical features of IGE

The IGE syndromes encompass Childhood Absence Epilepsy (CAE), Juvenile Absence Epilepsy (JAE), Juvenile Myoclonic Epilepsy (JME) and Epilepsy with Generalised Tonic-Clonic Seizures Alone (EGTCSA) (Scheffer et al., 2017). Available evidence suggests common pathophysiological mechanisms and genetic relationships in IGEs (Helbig, 2015).

Seizure types occurring within IGE are myoclonic seizures, typical absence seizures and generalised tonic-clonic (GTC) seizures. These may occur individually or in different combinations depending upon the IGE sub-type. Myoclonic seizures, or jerks, are muscular contractions lasting milliseconds, which often occur singly but can also occur successively. They are usually seen in limb muscles but can also occur in facial, neck and trunk muscles. Typical absence seizures cause an abrupt onset of decreased, or lost, awareness. Impaired awareness may occur alone or may be accompanied by clonic movements of facial muscles or by oral and limb automatisms. Typical absence seizures can be spontaneous or provoked, classically by hyperventilation or photo stimulation. GTC seizures are usually symmetrical and bilateral causing increased muscle tone and rhythmic limb jerking. They may occur without any clear trigger or may be precipitated by photic stimulation, sleep deprivation, or alcohol. There is an association between timing of seizures in IGE and the sleep-wake cycle, with a tendency for seizures to occur after awakening (Andermann and Berkovic, 2001).

CAE and JAE are characterised by absence seizures. CAE typically affects children aged 2-12 years whereas JAE begins around the ages of 8-20 years (ILAE, 2020b). Between the ages of 8-12 years, seizure frequency can differentiate between JAE and CAE, with multiple daily absences occurring in CAE compared to less frequent absences in JAE (ILAE, 2018). Some

cases of CAE evolve into JME (ILAE, 2020c). In JME, myoclonic jerks and generalised convulsions occur. Absence seizures may also be present. The usual onset of JME is 12-18 years. EGTCSA is characterised by onset of GTC seizures alone between the ages of 5-40 years (peak 11-23 years) (ILAE, 2020a) . There is a relationship between subtype and seizure remission rates; CAE is associated with seizure freedom by adulthood in as many as 93% of patients (Callenbach et al., 2009) whereas JME has a reported remission rate as low as 2.5% without medication to 58% with medication (Martínez-Juárez et al., 2006). In JAE, the reported remission rate varies from 37-62% (Seneviratne et al., 2012, Trinka et al., 2004). A positive family history of IGE is occasionally present in JME and JAE whereas in CAE there is an affected first degree relative in up to 20% of cases (ILAE, 2018).

Epilepsy carries a higher risk of premature death compared to the general population with a standard mortality ratio of 1.66 in IGE (Neligan et al., 2011a). Death may occur via seizure related accidents or status epilepticus (Tomson, 2000). People with epilepsy are also at risk of sudden unexplained death in epilepsy (SUDEP) with reported rates varying from 0.35 per 1000 person-years in a population-based study to 4.5 per 1000 person-years in drug resistant epilepsy (DRE) (Ficker et al., 1998, Annegers et al., 2000). Alongside seizures, epilepsy also manifests in neuropsychological and social issues. In IGE, impairment of working memory (Swartz et al., 1994) and prospective memory (Wandschneider et al., 2010) is described. There is also converging evidence of executive dysfunction, particularly in JME (Wandschneider et al., 2012). Together, impairments in these domains is suggestive of frontal lobe dysfunction in IGE (Wandschneider et al., 2012). The potential social consequences of neuropsychological dysfunction in IGE include lower educational attainment and higher rates of unemployment (Iqbal et al., 2009). Epilepsy is also associated with a higher risk of mental health problems including depression, anxiety (Piazzini et al., 2001), and suicide (Jones et al., 2003) compared with people without epilepsy.

1.1.3 Diagnosing IGE

The diagnosis of IGE is clinical and is based upon onset age, seizure types, neurodevelopmental history and family history, supported by EEG findings (Scheffer et al 2017).

The characteristic interictal EEG abnormality in IGE is bilaterally synchronous, anteriorly dominant interictal discharges (IEDs) (including spike-wave complexes, spikes, and sharp waves) with a visually normal background rhythm (*figure 1*).

Figure 1. Typical interictal EEG features of IGE. Bilaterally synchronous spike-wave complexes are seen in all channels. The greatest amplitude is seen in the anterior channels. Such anteriorly dominant discharges occurring on a normal background EEG is the hallmark of Idiopathic Generalised Epilepsy syndromes. Reprinted with permission from EEG made easy, Mohanraj et al., 2020. https://books.apple.com/gb/book/eeg-made-easy/id1506475821. Copyright Rajiv Mohanraj 2020.

During a myoclonic seizure, generalised spike-wave complexes or poly-spike waves are seen. The EEG correlate of typical absence seizures is rhythmic 3-4Hz generalised spike-waves. During a GTC seizure, the scalp EEG is generally dominated by artefact but when not concealed, shows generalised rhythmic spike-waves followed by bursts of spikes-and-slow waves. Although the term 'generalised' relates to seizures that engage both hemispheres, asymmetrical and focal EEG changes are also well-described in IGE. This includes inter-hemispheric differences of 100-200 milliseconds at the onset of absence seizures and non-

localised focal interictal discharges (Leutmezer et al., 2002). However, these non-characteristic features are not used to support a diagnosis of IGE.

The presence of IEDs is determined by visual inspection. As a result, EEGs are liable to overinterpretation (Benbadis and Tatum, 2003). The yield of IEDs on a routine EEG following a first seizure is around 29% (Krumholz et al., 2007). By a fourth recording, when combined with sleep deprivation, this increases to approximately 80% (Smith, 2005). Inpatient video-EEG has a yield of 43.5 % for epileptic discharges and 43% for IEDs (Ghougassian et al., 2004), but its use in diagnosis is limited by cost and availability. Conversely patients without epilepsy may have IEDs; the rate in a study of 13000 healthy males was 0.5%, of which 58% occurred only during photic stimulation (Gregory et al., 1993).

Although the background EEG rhythm is said to be normal in IGE, it is important to note that this refers to interpretation via visual inspection. With quantitative EEG analysis, differences in EEG power spectrum and connectivity features have been described compared to healthy controls. This is discussed further in subsection 1.3.3. However, currently none of these measures are validated for use in the diagnosis of epilepsy. The availability of an objective EEG biomarker would potentially improve the diagnostic yield of EEG and would also reduce the risk of bias due to overinterpretation that exists with expert visual EEG analysis (Benbadis and Tatum, 2003).

1.1.4 Pharmacological management of IGE

There is strong evidence that sodium valproate is the most effective drug in treating IGE (Marson et al., 2021). However, owing to teratogenic effects, sodium valproate is avoided in females of childbearing potential (Tomson et al., 2015). Other first line options include lamotrigine and levetiracetam. A caveat with the use of lamotrigine is that in around 50% of patients, myoclonic jerks may worsen (Johannessen Landmark et al., 2019). Ethosuximide is a suitable option for absence seizures. If the first medication is inefficacious, a second medication may be trialled as monotherapy or as an add-on treatment. Suitable second line treatments include topiramate, zonisamide, lacosamide, perampanel, clobazam and clonazepam.

Antiepileptic drugs (AEDs) have various mechanisms of action but generally act by either modulating voltage-gated ion channels in the neuronal cell membrane, modulating neurotransmitter release by binding to synaptic vesicles, or by altering gamma-Aminobutyric

acid (GABA) or glutamate transmission at the synapses. This has the effect of reducing excitation or increasing inhibition of neuronal activity thereby supressing seizures. These effects are demonstrated in vitro, but how they exert their effects in the brain may be more complex (Sills, 2017). For example, there is evidence that some AEDs have effects on the neuronal network structure (Haneef et al., 2015b, van Veenendaal et al., 2017) or on the strength of connections in the network (Routley et al., 2017).

1.2 Drug resistant IGE

1.2.1 Background

Drug resistance is defined by the ILAE as "failure of adequate trials of two tolerated and appropriately chosen and used AED schedules (whether used as monotherapies or in combination) to achieve sustained seizure freedom" (Kwan et al., 2010). Within this definition, seizure freedom is achieved after a period of 12 months without a seizure or after three times the longest pre-treatment inter-seizure interval, whichever is longer. The definition of drug resistance reflects the fact that most people who become seizure free do so with the first or second AED (Mohanraj and Brodie, 2006, Chen et al., 2018). The response rate with a third AED is less than 3% and decreases further with subsequent schedules (Mohanraj and Brodie, 2006).

When patients meet the criteria for drug resistance, they should be referred to an epilepsy specialist for re-evaluation of diagnosis and assessment of suitability for advanced therapies. Confirmation of diagnosis involves exclusion of epilepsy mimics such as non-epileptic attack disorder (NEAD) and consideration of "pseudo-resistance", for example due to medication non-concordance, alcohol use, or poor sleep Vagal nerve stimulation may be considered, which results in around 50% seizure reduction in 50% of patients (Englot et al., 2011). The support of an epilepsy specialist nurse is also reported to improve outcomes (Pfafflin et al., 2016).

Although numerous large-scale epilepsy prognosis studies exist, cohesively interpreting their findings is challenging owing to methodological heterogeneity and the risk of bias inherent to epidemiological studies (Seneviratne et al., 2012). Notwithstanding this, it is reported that around 18% of people with IGE are resistant to medication (Semah et al., 1998, Brodie et al., 2012). IGE remission rates from 64% (Mohanraj and Brodie, 2007) to 82% (Kharazmi et al., 2010) have been described and it is reported that the majority of those who achieve seizure

freedom, do so within five years (Sander, 2003). However, some people develop a late response to treatment and approximately 16%-25% have a fluctuating course, characterised by periods of seizure freedom interspersed with seizures (Brodie et al., 2012, Neligan et al., 2011b).

Intractable seizures are only one manifestation of DRE. It is known that there is a higher rate of injury (Beghi et al., 2002) and premature death (Bell et al., 2016) in this patient group. The most common cause of premature death in DRE is SUDEP, the risk of which may be 40 times higher in people with uncontrolled seizures compared to those who are seizure free (Tomson, 2000). Cognitive decline may be intensified due to frequent seizures (de Boer et al., 2008), and may be exacerbated by medication side effects and drug interactions (Wandschneider et al., 2012). This is more likely to affect those with DRE since they are more likely to take polytherapy. People with persistent seizures are also more likely to be single, unemployed, and live in an area of deprivation compared to the general population (Ridsdale et al., 2017). In addition, patients with DRE are unlikely to have a driving licence, which may further exacerbate social issues.

A further consideration in DRE is the impact on the health care economy. As epilepsy is a common and usually life-long condition, it already carries high health care costs (Dalic and Cook, 2016). Furthermore, within epilepsy care, patients with DRE are the most expensive group after the initial costs of epilepsy surgery are excluded (Beghi et al., 2004).

1.2.2 Proposed mechanisms of drug resistance in epilepsy

A number of hypotheses exist to explain the mechanisms underlying drug resistance in epilepsy. However, none have been universally proven. The most widely studied are the drug transporter and drug target hypotheses (Tang et al., 2017). Others include the intrinsic severity and neural network hypotheses, which are of particular relevance to this thesis.

Drug transporter hypothesis

This hypothesis, also known as the 'pharmacokinetic hypothesis', proposes that DRE is due to over-expression of adenosine triphosphate binding cassette (ABC) proteins, which are multi-drug efflux transporters at the blood brain barrier (BBB). One of the most widely studied transporters is P-glycoprotein (P-gp) which prevents lipophilic substances crossing the BBB by restricting free diffusion (Miller, 2010).

The first study highlighting P-gp and its encoding gene, multidrug resistance gene-1 (MDR1) in DRE examined brain tissue samples of patients who had undergone epilepsy surgery compared to controls who had undergone surgery for arteriovenous malformations (Tishler et al., 1995). Increased MDR1 was expressed in the DRE group and there was a corresponding increase in P-gp in BBB endothelial cells and in astrocytes. Additionally, there was significantly decreased astrocyte phenytoin levels in MDR1 positive cells compared to MDR1 negative cells suggesting that P-gp may reduce availability of AEDs to the brain. This finding has been replicated in a number of in vitro and in vivo studies (Hughes, 2008). It has subsequently been shown that there a number of other efflux transporters at increased levels in the BBB and astrocytes of patients with DRE suggesting that they too could be involved in drug resistance (Löscher and Potschka, 2005).

P-gp and other transporters are also present in the gastrointestinal tract, liver and kidneys (Schinkel, 1997) and it has been proposed that increased AED clearance by these transporters may also play a role in drug resistance (Lazarowski et al., 1999). In support of this is evidence that patients who have well-controlled epilepsy on phenytoin have significantly higher mean free plasma phenytoin levels, independent of the phenytoin dose, than patients who have a 'partial response' (Iwamoto et al., 2006). In contrast, other studies evaluating plasma levels of AEDs in animal models have not found a significant difference in DRE (Brandt et al., 2006). Caution is warranted when assessing the role of peripheral P-gp expression in DRE because therapeutic ranges of AEDs vary depending on the individual and the pharmacokinetic properties of a particular drug, thus using plasma levels to explore this hypothesis is not straightforward (Tang et al., 2017).

A widely studied genetic polymorphism in relation to drug resistance is in the MDR1 drug-transporter encoding gene (C3435T). At least two meta-analyses are in support of the association (Chouchi et al., 2017, Li et al., 2015c), the latter only reporting an association in Caucasian populations.

A significant limitation of the drug transporter theory is that causality between increased efflux transporters and DRE has not been demonstrated. Seizure frequency correlates with greater P-gp levels (Feldmann et al., 2013, Shin et al., 2016, Liu et al., 2012), indicating that upregulation may be a consequence of poorly controlled epilepsy itself (Tang et al., 2017). Over-expression of multidrug efflux proteins could also be a consequence of AED use (Tang et al., 2017). Of further contradiction to the drug transporter hypothesis is that AEDs are generally considered to be weak substrates for efflux transporters (Zhang et al., 2012); if

increased efflux transporter expression leads to drug resistance, the logical presumption is that efflux transporters should be robust substrates of AEDs (Loscher et al., 2011). Overall, direct evidence in support of drug transporter over-expression causing DRE is limited.

Target hypothesis

The target hypothesis proposes that target molecules for drug ligands undergo modifications which render drugs ineffective at their target. Much of this evidence pertains to genes that encode drug targets, where it may be described as the pharmacogenetic hypothesis of drug resistance.

Evidence for this theory in DRE was first demonstrated in a study of the response of voltage gated sodium channels to carbamazepine in the hippocampal tissue of patients with temporal lobe epilepsy who had responded to carbamazepine, compared to carbamazepine resistant patients (Remy et al., 2003). In the carbamazepine resistant group, it was found that blockage of sodium channels was not achieved by carbamazepine, rendering its key mechanism of action ineffective.

In a genotyping study examining drug resistance across various types of epilepsy, a polymorphism in SCN2A, which encodes the alpha subunit of voltage gated sodium channel, (IVS7-32A>G) was associated with drug resistance (Loup et al., 2000). However, it is not known whether this polymorphism is associated with reduced sensitivity of a particular drug (Loup et al., 2000). There is also evidence of a significantly higher frequency of the AA genotype of SCN1A IVs5-91 G > A in patients resistant to carbamazepine compared to those responsive to carbamazepine (Abe et al., 2008). Other alleles which have been reported to be associated with drug resistance include SCN2A IVS7-32A>G (Kwan et al., 2008) and SCN2A c.56 G >A allele A (Lakhan et al., 2009). The SCN1A gene encodes voltage gated sodium channels which are a target for many AEDs including lamotrigine, carbamazepine, and phenytoin. In Dravet's syndrome, a mutation in the SCN1A gene results in a non-functioning sodium channel. Patients with Dravet's syndrome typically have refractory epilepsy and often seizures can be exacerbated by drugs acting on the sodium channel. Therefore, it has been suggested that the same genetic variant causing Dravet's syndrome may also be responsible for the lack of response to AEDs whose target is the voltage gated sodium channel (Sisodiya and Marini, 2009).

The target hypothesis is weakened by demonstrable lack of sensitivity to AEDs other than carbamazepine, including other voltage gated sodium channel blockers (Remy et al., 2003). Similarly, as most patients who have been diagnosed with DRE are generally resistant to all AEDs, and different AEDs act on different receptors, it would suggest that the mechanism of drug resistance is not specific to a particular receptor anomaly (Loscher and Potschka, 2002). In view of inconsistencies in genetic studies of drug resistance and the low frequency of alleles demonstrated to be associated with DRE, pharmacogenetic alterations alone do not currently sufficiently explain drug resistance (Tang et al., 2017).

Intrinsic severity hypothesis

In 2008, Johnson and Rogawski posited that exploring drug resistance from a molecular mechanism aspect was limited by not taking into account the fundamentals of epilepsy pathophysiology itself (Rogawski and Johnson, 2008). They proposed the intrinsic severity hypothesis, where the inherent severity of epilepsy determines response to medication and as a result, more severe epilepsy is more difficult to treat. Expanding on the framework of drug resistance as a physiological constraint, they suggested that if epilepsy severity is high, seizure prevention may not be possible with available AEDs without causing toxicity. In support of this theory is epidemiological data demonstrating that frequent seizures in the early period of epilepsy are associated with poorer prognosis (Mohanraj and Brodie, 2006, MacDonald et al., 2000). In addition, a correlation between high seizure frequency in the early stages and a higher dose of AEDs required to achieve seizure freedom has been reported (Schmidt and Haenel, 1984) .

Evidence against the intrinsic severity hypothesis is that some patients with 'severe epilepsy' respond to a new drug despite previous trials of a multitude of other drugs (Brodie et al., 2012). If the intrinsic severity of their epilepsy was the sole explanation for lack of medication response, the hypothesis does not explain why some drugs are an exception to the rule (Rogawski and Johnson, 2008). Similarly, it is known that some patients shift in and out of seizure freedom (Brodie et al., 2012, Neligan et al., 2011b) which is not readily accounted for by this hypothesis (Rogawski and Johnson, 2008). Further evidence that other factors are involved in DRE is provided by a large observational study of pharmacoresistance in 780 patients with various epilepsy types (Hitiris et al., 2007). In this study, it was found that drug resistance is not only associated with greater pre-treatment seizure frequency but also with family history of epilepsy, history of febrile convulsions, traumatic brain injury, recreational drug use, and depression.

In conclusion, while it is possible that intrinsic epilepsy severity may play a role in DRE it does not seem to account for the full mechanism.

Neural network hypothesis

The neural network hypothesis proposes that under the influence of genetic and 'microenvironmental' abnormalities, seizure induced changes in brain plasticity cause alterations in the neural network. This consequently prevents AEDs from exerting their effects, either by preventing their ability to act at the drug target or through decreased effectiveness of the brain's inherent inhibitory mechanisms (Fang et al., 2011). The precise mechanisms by which network alterations may result in these effects has not been theorised.

Seizure induced changes that have been proposed as support for the neural network hypothesis include axonal and dendritic sprouting, neuronal loss (Cavazos and Sutula, 1990, Pitkänen et al., 2002), gliosis, and inflammation (Sperk et al., 2009, Fang et al., 2011). Many of these factors are associated with increased seizure severity and display a kindling response, whereby repeated seizures are associated with increased microstructural alterations (Pitkänen and Sutula, 2002). These changes may contribute to a progressive worsening of epilepsy (Pitkänen and Sutula, 2002), with the result that the more seizures a person has, the more likely they are to develop DRE. This is concordant with the observation that high pre-treatment seizure frequency is associated with a poor response to AEDs (Shinnar and Berg, 1996).

A limitation of seizure induced microstructural changes as support for the neural network theory is that there is no direct quantitative evidence that network topology is consequently altered. Moreover, causation has not been demonstrated (Fang et al., 2011) and as such, microstructural abnormalities may be a consequence of DRE rather than a cause. The concept of kindling as inferred evidence for the theory is problematic since the notion that 'seizures beget seizures' (Gowers, 1881) is largely discounted (Berg and Shinnar, 1997). This is due to a wealth of epidemiological evidence demonstrating a low incidence of recurrence of acute symptomatic seizures (Hesdorffer et al., 2009, Bentes et al., 2017, Bladin et al., 2000, Lin et al., 2003, Ferro et al., 2003), resolution of some childhood epilepsies despite an association with frequent seizures (e.g. benign epilepsy with centro-temporal spikes and many cases of CAE), and evidence of spontaneous remission in over 20% of untreated people with epilepsy in resource-poor settings (Placencia et al., 1994, Shorvon and Luciano, 2007, Nicoletti et al., 2009). In addition, there is evidence that immediate treatment of epilepsy does not affect outcomes after the first two years of treatment (Marson et al., 2005). Beyond these

limitations, the described mechanisms of neuronal reorganisation have been studied in focal epilepsies and in animal studies of focal seizures, and not in generalised epilepsies, and thus cannot necessarily be extrapolated to IGE.

While there is no strong evidence to support the neural network hypothesis, proposed by Tang and colleagues, there is no evidence against the theory, to my knowledge. Although the neural network theory remains unproven, given that epilepsy is a network disorder, it seems plausible that network aberrations may vary according to seizure control. This would also be consistent with the intrinsic severity hypothesis of epilepsy and supports the notion of epilepsy drug resistance being multifactorial. Investigating epilepsy drug resistance from a network perspective, rather than at a cellular level, is consistent with the current approach to studying epilepsy as a network disorder. It may, therefore, generate a more satisfactory understanding of this issue. This concept forms the rationale for this thesis.

1.2.3 Determinants of response to anti-epileptic drugs

Various factors have been associated with response rate of AEDs in epilepsy. However, epidemiological studies exploring this area are prone to biases. As such, evidence is often conflicting and generally not deemed to be strong (Mohanraj and Brodie, 2007, Mohanraj and Brodie, 2013). One association for which there is strong evidence is early response to treatment (Mohanraj and Brodie, 2013). In a study of newly diagnosed patients, the chance of seizure freedom significantly declined following the failure of two AEDs in the first one to two years following treatment initiation (Brodie et al., 2012).

Other factors associated with a poor medication response in IGE, includes co-existent mental or psychological illness (Gelisse et al., 2001, Cutting et al., 2001), onset less than five years old (Nicolson et al., 2004), an "atypical" presentation (defined as atypical absences, myoclonic epilepsies, generalised tonic–clonic seizures with onset less than three years or 20 twenty years) (Nicolson et al., 2004), EEG asymmetries (focal slowing, focal epileptiform discharges, asymmetric generalised spike-wave discharges (Szaflarski et al., 2010), history of febrile seizures (Mohanraj and Brodie, 2007), and the presence of multiple seizure types in JME (Gelisse et al., 2001). In epilepsy generally, other associations with poor response include high pre-treatment seizure frequency (Shinnar and Berg, 1996), neurological disability and epileptic encephalopathy syndromes (Berg et al., 2001, Ko and Holmes, 1999), and response to first AED (Kwan and Brodie, 2000, Sillanpaa, 1993). With respect to non-seizure outcomes, a first

seizure at less than 18 years is reported to be a powerful predictor of neuropsychological impairment (Hessen et al., 2006).

There are some studies which have described differences in neuroimaging features in people with drug resistant IGE or those with frequent seizures compared to those with well-controlled epilepsy. Such differences include alterations in EEG alpha frequency oscillations (Abela et al., 2019), altered connectivity in the DMN (Kay et al., 2013) and cerebellar networks (Kay et al., 2014), and greater atrophy on structural imaging (Bernhardt et al., 2009). However, it is not known whether these factors have arisen as a consequence of seizure burden or medication, or if they were present from the outset. In order to clarify this, prospective studies are needed.

Thus, the prediction of DRE remains a major challenge. A reliable biomarker to identify drug resistant patients at an early stage would permit a more tailored treatment path.

1.3 Neuronal oscillations

1.3.1 The role of neuronal oscillations

Brain function relies on interactions between populations of synchronised neuronal oscillations in functionally connected areas of the brain (Siegel et al., 2012) and it is from these background oscillations that the hypersynchronous seizure state is believed to arise (Richardson, 2012a). Although it is not known what causes a transition from the normal state to the seizure state, there is evidence to support the influence of background oscillations in the temporal dynamics of neuronal excitation (Uhlhaas et al., 2009). Examples of this include synchronisation of neuronal action potentials to background beta and gamma frequency oscillations (Gray and Singer, 1989) and alterations in the rate of neuronal discharges relating to the oscillation cycle (Fries et al., 2001). Further indirect evidence of the role of oscillations in modulating neuronal excitation comes from studies that have demonstrated an alteration in oscillatory amplitude or frequency with drugs that alter GABAergic or glutamatergic synaptic transmission (Campbell et al., 2014, Saxena et al., 2013, Shaw et al., 2015).

The coordinated neuronal populations involved in brain function are often frequency band specific (Siegel et al., 2012). Thus, frequency band specific oscillations are postulated to be markers of underlying large-scale neuronal networks (Siegel et al., 2012).

The precise boundaries between traditionally defined frequency bands are debated, but are approximately as follows : delta < 3.5 Hz, theta 4-7.5 Hz, alpha 8-13 Hz, beta 14-30 Hz, gamma > 30 Hz (Schomer and Lopes da Silva, 2017). These bands were established following visual inspection of EEG data, with Hans Berger first describing the alpha frequency band in 1929 (Berger, 1929). A criticism of using this classification in quantitative studies is that these bands may not accurately represent the oscillations involved in specific cortical processes (Donner and Siegel, 2011). To address this potential limitation, frequency bands may be derived using spectral factor analytical methods (Andresen, 1993, Kubicki et al., 1979, Shackman et al., 2010), which determine the independent signals that best explain the variability in the data and thus represent a more data-driven alternative. Where frequency bands have been defined using this method, they are broadly similar to conventional bands but typically have a division of alpha rhythm into high and low bands. For example, Shackman and colleagues define frequency bands as follows: delta 1–5 Hz, low-alpha 6–9 Hz, high-alpha 10–11 Hz, beta 12–19Hz, and gamma >21 Hz.

Despite substantial literature implicating frequency band specific oscillations in various brain functions, their precise physiological functions have not been fully elucidated. Alpha, the dominant resting state rhythm of the brain, is thought to have a role in attentional processes, mainly through active inhibition (Jensen and Mazaheri, 2010, Klimesch, 2012). Beta, theta and gamma oscillations have been associated with a range of cognitive functions including memory (Düzel et al., 2010), perception, and motor control (Başar et al., 2000, Düzel et al., 2010, Schnitzler and Gross, 2005). Rather than each band having a specific function, it has been further suggested that the effects of various oscillations may be influenced by their associated characteristics (e.g., phase and amplitude) (Herrmann et al., 2016) and their synchronisation with oscillations of other frequencies. For example, synchronisation between gamma and beta band oscillations has been demonstrated to be of importance in attention (Uhlhaas et al., 2009). There is converging evidence to support a model of oscillatory interactions whereby gamma oscillations are involved in local interactions which govern encoding processes (such as motor planning) whereas low frequency oscillations are associated with top-down, long-range integrative processes (Donner and Siegel, 2011, von Stein and Sarnthein, 2000, Kopell et al., 2000). The putative mechanisms underlying inter-oscillatory interactions involve phase or amplitude coupling (Engel et al., 2013a). This is discussed further in subsection 1.4.3.4. There is also evidence that some brain processes occur across multiple frequency bands (Wilke et al., 2006) and that some functions arise within sub-categories of conventional bands (Wyart and Tallon-Baudry, 2008).

1.3.2 Measuring neuronal oscillations

Cortical oscillations are typically quantified using EEG /magnetoencephalography (MEG). These are suitable methods owing to their high temporal resolution (typically recorded at 250 Hz to 2000 Hz) which permits sampling of the dynamic activity of coordinated neuronal populations (Abreu et al., 2018). This is in contrast to fMRI, which has a temporal resolution of approximately 0.5-1.5 Hz and indirectly measures neuronal activity by using the haemodynamic response of blood oxygen dependent (BOLD) signal. In studies combining fMRI with electrophysiological data, gamma frequency power is reported to be strongly linked to the BOLD signal, but there is also evidence that BOLD signal is influenced by lower frequencies (Magri et al., 2012). As such, it is proposed that oscillations of various frequencies dynamically contribute to the BOLD signal. The use of each of these modalities in the context of network analytical studies is further discussed in subsection 1.4.3.3.

Oscillations are commonly characterised using spectral power analysis. This decomposes signal in the time domain into its independent frequency components, typically via a Fourier Transform. The frequency content of the signal can then be quantified (i.e., the power in each frequency band) and statistically analysed. The relationship between frequency and power is known to have a 1/f spectrum, where power has an inversely proportional relationship with frequency.

1.3.3 Oscillatory amplitude, frequency, and spectral analysis in epilepsy studies

Alterations in alpha rhythm have been reported in epilepsy since the 1940s when slower alpha rhythm was noted on EEG (Gibbs et al., 1943, Stoller, 1949). Subsequently other alpha band abnormalities in epilepsy have been described including absent normal posterior alpha rhythm (Aich, 2014) and reduced peak alpha frequency with reduced alpha frequency variability (Larsson and Kostov, 2005). Of particular note is a recent study which demonstrated a shift to lower peak alpha power in people with drug resistant IGE (DR-IGE) compared to well-controlled IGE (WC-IGE) (Abela et al., 2019). There is increasing literature implicating high frequency oscillations (HFOs) (>80 Hz) in epilepsy, particularly in focal epilepsy (FE) suitable for epilepsy surgery where it is suggested that HFOs are a potential marker for epileptogenic tissue (Höller et al., 2015).

Spectral analytical studies in IGE have reported greater spectral power in the interictal period in epilepsy in various frequency bands (Clemens et al., 2000, Elshahabi et al., 2015, Miyauchi et

al., 1991, Niso et al., 2015, Tikka et al., 2013, Willoughby et al., 2003, Routley et al., 2020), either globally or in spatially segregated scalp regions. It is proposed that increased spectral power reflects greater neuronal synchronisation (Clemens et al., 2000, Michel et al., 1992) and therefore higher spectral power in IGE may reflect hyperexcitability of the cortex and a greater seizure susceptibility. Similarly, increases in broadband spectral power immediately prior to a myoclonic seizure have been reported, followed by a large ictal drop in power (Sun et al., 2016).

In studies evaluating spectral entropy, where the spectral distribution of the EEG signal is determined via quantification of signal uncertainty (Powell and Percival, 1979), larger entropy values at 6.25 Hz-12.89 Hz have been reported in interictal EEGs containing IEDs compared with EEGs of people with epilepsy without IEDs, and compared to controls (Urigüen, 2017). The same study demonstrated an inverse relationship of spectral entropy with the time since the most recent seizure suggesting that when epilepsy is well-controlled, the EEG transforms to a similar state to that found in healthy controls. Increased alpha frequency spectral entropy values in patients with temporal lobe and frontal lobe epilepsy compared with people with headaches and NEAD has also been described (Pyrzowski et al., 2015). In the ictal state, lower spectral entropy has been reported at 8–15 Hz compared with the interictal state, and also compared with controls (Mirzaei et al., 2010).

It is reported that AEDs may affect spectral power. However, evidence for this is inconsistent (Holler et al., 2019). Furthermore, in studies reporting a possible medication effect, the directionality of the change varies; whilst some studies report increased power in delta, theta, alpha and beta frequency bands (Willoughby et al., 2003, Wu and Xiao, 1997, Cho et al., 2012), others report decreased power in the same frequency bands (Clemens et al., 2007, Clemens, 2008, Sannita et al., 1989, Wu and Xiao, 1997, Cho et al., 2012, Zhong et al., 2018). However, in many studies the effects of medication on background rhythm cannot be differentiated from effects due to epilepsy owing to the study design. In a spectral power study where it was possible to compare medicated with unmedicated participants, both groups were similar suggesting that the differences were due to epilepsy rather than medication (Miyauchi et al., 1991). However, in a similar comparison, a medication effect was reported at 2-4 Hz and 7-8 Hz in medicated participants (Willoughby et al., 2003).

It is suggested that spectral power analysis is conducted alongside network analysis in order to provide complementary information about brain networks (Niso et al., 2015, van Diessen et al., 2014a) and to help extricate information regarding functional network topology from disease

specific spectral power changes (van Diessen et al., 2014a). Similarly, because some methods of delineating functional connectivity are sensitive to spectral power (particularly amplitude-based techniques), exploring connectivity at the spectral level permits insight into whether apparent changes in functional networks are driven by spectral power alterations. Furthermore, if there is a correlation between spectral power and functional connectivity in the same frequency band, it may suggest that connectivity findings have been influenced by volume conduction effects (Cohen and Grafman, 2014). Volume conduction is discussed in subsection 1.4.3.3.

1.4 Network analysis in the study of epilepsy

1.4.1 Contextual overview

Numerous cellular and molecular mechanisms have been demonstrated to play a role in seizure generation. However, the precise mechanisms underlying epilepsy remain unknown. It is widely accepted that normal brain function is dependent on interconnected neuronal networks and that epilepsy is a network disorder. We have defined a neuronal network as "a system of functionally or anatomically connected areas of the brain in which activity in one component can influence the activity of all other components and affect the system as a whole" (Pegg et al., 2020a). The neuronal networks of the brain form a complex system. A key characteristic of a complex system is that its behaviour cannot be anticipated from its individual components; this is because behaviours emerge from a system due to *interactions* between individual components. This concept provides further rationale for examining epilepsy from a network perspective. The mechanisms involved in seizure genesis are generated from the same mechanisms that are present in the brain during normal brain functioning and as such, under certain conditions, any brain can transition to a seizure state. This suggests that epilepsy is a problem emerging from the dynamic properties of the brain (Richardson, 2012b). In view of this, it can be reasoned that elucidating the network properties of the brain in its resting state is the first step in understanding the complex dynamical network system from which seizures arise.

The earliest concept of the brain functioning via a network is attributed to Ramon Y Cajal in 1894 (Ramon Y Cajal, 1894), who formed the notion of a neuron and furthermore suggested that the organisation of neurones into circuits is a key principal in brain functioning (Lopez-Munoz et al., 2006). The term "synfire chains" was introduced as a concept for information

transmission along chains of connected neurones, whereby connected neurones fire synchronously when the chain is activated (Abeles, 1982). The significance of connections between cortical and subcortical structures in the genesis of generalised seizures has been acknowledged since at least 1941 following an EEG-based study of absence seizures, which suggested that seizures originate subcortically in the thalamic intralaminar nucleus then diffusely project to the cortex (Jasper and Kershman, 1941). This subsequently became known as the centrencephalic theory (Penfield, 1958). It was later suggested that epileptic discharges arise following an initial cortical discharge (Bancaud, 1969). At a similar time, the corticoreticular theory of seizure generation was suggested (Gloor, 1968). This proposed that the reticular system of the brainstem and thalamus are involved in seizure pathogenesis, in addition to the cortex. A later hypothesis, the thalamic clock theory, suggested that seizure generation occurs through "emergent network properties" in the thalamic and cortical network (Buzsaki, 1991). According to this theory, abnormal rhythmic oscillations in the thalamic network increasingly project to the cortex, with the result that the entire network is affected. Since the formation of these hypotheses, there has been further evidence of the involvement of the thalamic and thalamocortical networks in IGE (Bernhardt et al., 2009, Aghakhani et al., 2004, Gotman et al., 2005, Hamandi et al., 2006). Reduced connectivity in the DMN has also been implicated in IGE, in addition to abnormal 'global' resting state networks (RSNs) (Bonilha et al., 2014, Chavez et al., 2010, Chowdhury et al., 2014, Elshahabi et al., 2015, Lee and Park, 2019, Liao et al., 2013, Niso et al., 2015, Zhang et al., 2011). Abnormal RSNs have also been reported IGE related cognitive impairment (Li et al., 2015a, Li et al., 2017, Bonilha et al., 2014). Altered resting state connectivity in IGE is further discussed in subsection 1.4.4.

1.4.2 Scales of connectivity

The human brain is estimated to comprise approximately 100 billion neurones with 100 trillion synapses (Fornito et al., 2016). Characteristics of this complex system can be estimated at a range of scales. Spatially, brain networks can be broadly characterised at micro, meso and macro scales (Bohland et al., 2009). At the microscale, networks are formed by individual neurones and synapses. Mesoscale networks are also examined microscopically but focus on networks formed by populations of neurones that are functionally and spatially associated, for example groups of cytoarchitecturally similar neurones. Evaluation of the brain at both meso and microscales is invasive and has limited applicability in analysing whole-brain networks

(Fornito et al., 2016). Networks at the macroscale are less precise but can depict large-scale neuronal networks that represent whole-brain 'global' connectivity. The temporal scales of neuronal networks are organised over frequencies ranging from 0.05 to 500 Hz (Fornito et al., 2016) and may be delineated at scales spanning from milliseconds to years (Betzel and Bassett, 2017).

1.4.3 Large-scale resting state network analysis

1.4.3.1 Overview

Complex network systems are pervasive in the world around us and include social networks, ecological systems and the world economy. Remarkably, these diverse systems share similar organisational characteristics (Barabási and Albert, 1999, Newman, 2003) and can be evaluated using network analysis. Network analysis in epilepsy applies concepts from the field of connectomics in understanding how neuronal networks at multiple scales of time and space are organised and interact in the epileptic brain (Bullmore and Sporns, 2009).

Approximately ten distinct resting state networks have been delineated. These include networks that are associated with specific neuroanatomical systems, such as the 'motor network' or 'visual network', in addition to networks that represent less well-defined functions such as the 'DMN' and the 'thalamocortical network' (Biswal et al., 1995, Damoiseaux et al., 2006, Beckmann et al., 2005, Buckner and Vincent, 2007, Fox et al., 2005, Greicius et al., 2003). Commonly used approaches to identify such networks include independent component analysis and seed-based correlation analysis (Biswal et al., 1995).

In addition to examining the relationship between brain processes and specific networks, 'global' large-scale RSNs may be investigated, where activity from neuronal populations spanning the cortex is captured (Schölvinck et al., 2010). This seems a particularly suitable approach for exploratory studies of RSNs in epilepsy since it may capture alterations that could be overlooked by analysing specific networks and avoids assuming the relevance of a certain network in seizure susceptibility. This is particularly relevant in IGE as it is a generalised brain disorder and it seems likely that activity in one network would influence all other networks within the complex system.

Alterations in RSNs have been described in a wide range of central-nervous system disorders including schizophrenia (Liu et al., 2008, Micheloyannis et al., 2006, Rubinov and Bullmore, 2013, Cui et al., 2019) and Alzheimer's disease (Supekar et al., 2008, Stam et al., 2007a, He et

al., 2008, Dai et al., 2019), as well as epilepsy. Where differences have been found in RSNs in disease states, it has been proposed that they could form the basis of a biomarker for that condition. As such, the study of the interictal resting state in epilepsy is also of relevance in the search for a potential biomarker.

1.4.3.2 Connectivity subtypes

RSNs may be broadly evaluated from a structural or functional perspective. Structural networks refer to anatomically connected regions of the brain. Structural connectivity is typically delineated using Diffusion Tensor Imaging (DTI) which quantifies the diffusion properties of water molecules that are constrained by white matter tracts (Clayden, 2013) (*figure 2*).

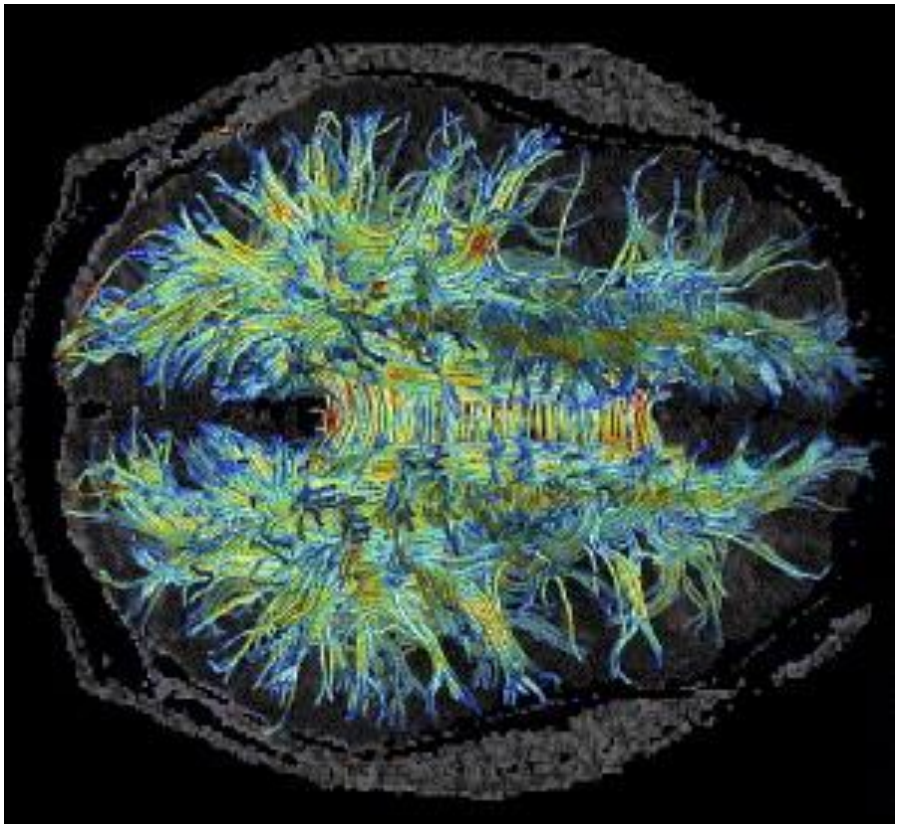

Figure 2. Example of an image obtained with DTI. Fibre bundles are coloured according to their fractional anisotropy value. Reprinted from Journal of Psychiatric research, Vol 41, Kubicki et al, a review of diffusion tensor imaging in schizophrenia., Pages 15-30. Copyright 2007, with permission from Elsevier.

Functional networks are inferred from statistically dependent correlations between spatially segregated neuronal populations or brain areas. This can be derived from fMRI, EEG or MEG. Functional connectivity may be further evaluated from an 'effective' perspective. This determines the influence of one region over another and can be used to investigate causality (Friston, 2011, Aertsen et al., 1989). This is particularly suited to the evaluation of the dynamics of epileptic discharges (Cadotte et al., 2009).

It is suggested that functional connectivity is constrained by structural connectivity (Zhang et al., 2011). However, the precise relationship between functional and structural connectivity is complex and incompletely understood (Friston, 2011). As such, the connectivity measures derived from each sub-type may not be directly comparable. However, there is evidence that functional connectivity measures that are averaged over long time frames may map onto structural connectivity (Zalesky et al., 2012b), which perhaps reflects the dynamic nature of functional networks.

1.4.3.3 Neuroimaging modalities in global functional network analysis

Data may be obtained from fMRI or EEG/MEG.

EEGs may be recorded from scalp or intracranial electrodes and measure the synchronised electrical activity of pyramidal cell dendrites. EEG has high temporal resolution, with a typical sampling frequency from 500 Hz to 2000 Hz, which is commensurate with the speed of neuronal communication in the brain (Fornito et al., 2016). A limitation of EEG is volume conduction (due to the conductive properties of the skull and scalp) and field spread, which may confound connectivity estimates. This is discussed further in subsection 1.4.4.4. A further limitation is that signal above 20-30 Hz is typically confounded by muscle artefact. Intracranial recordings attenuate these limitations. However, the use of intracranial electrodes in a study setting is limited by cost and ethical considerations regarding participant risk. In addition, intracranial recordings are spatially limited compared to the 'whole brain' recording capabilities of scalp EEG since they can only be taken from the relatively small area of exposed brain. MEG measures the magnetic fields produced by populations of underlying neurones and similarly to EEG, has a time resolution of milliseconds. An advantage of MEG compared to EEG is that the magnetic fields generated by the brain are less susceptible to volume conduction effects and also to muscle and eye movement artefacts (van den Broek et al., 1998). Disadvantages of MEG relative to EEG is that it is expensive, it necessitates the use

of a magnetically shielded room (due to being sensitive to noise from nearby electromagnetic sources), it is susceptible to head movement artefact, it is insensitive to radial sources, and it does not account for different head shapes. As a result, sensors may not be in the same location relative to the brain across subjects when the head moves relative to the sensors.

Connectivity in fMRI data is determined by measuring alterations in the BOLD response which occur in association with neuronal activity. It is, therefore, an indirect measure of neuronal activity. The chief advantage of fMRI is high spatial resolution with 3-4mm voxels typically obtained (Glover, 2011), increasing to around 1.5mm with 7T scanners (De Martino et al., 2011). However, it has poor temporal resolution relative to other modalities with a peak hemodynamic response function (HRF) of around six seconds and a typical sampling rate of 0.5 Hz (repetition time of two seconds). A further limitation of fMRI in epilepsy connectivity studies, is that the HRF may be confounded by the presence of epileptiform discharges (Bénar et al., 2002).

Comparing connectivity derived from different modalities is limited by the fact that the methods used to determine connectivity typically diverge according to the modality used. Broadly, this is a consequence of differing sensitivities to time scales (Tracy, 2015). In view of the complimentary information that may be gained from each modality, there is increasing interest in methodologies that simultaneously record EEG and fMRI data. However, the optimal methods for this complex integration remain unknown (Abreu et al., 2018). Moreover, when both modalities are used concurrently, they introduce artefact in each other.

1.4.3.4 Inferring global resting state functional connectivity

To delineate a global neural network, neuroimaging data is parcellated to represent underlying neuronal assemblies from which signal has been generated. Next, the extent of connectivity between each pair of elements is ascertained. In graph theory, discussed in subsection 1.4.3.5 these network components are known as nodes and edges, respectively. Most methods of delineating connectivity between network elements are bivariate and as such infer the nature of a connection between two network elements. Although the brain network is multivariate, models of multivariate connectivity in the brain are scarce and difficult to implement, interpret, and statistically analyse (Cohen and Grafman, 2014). As such, bivariate connectivity is used in most brain network studies and will therefore be the focus of the discussion that follows.

Data parcellation in EEG /MEG studies

In EEG and MEG studies, signal from separate network areas is detected by electrodes/sensors. Connectivity between each network element may subsequently be determined in the signal (sensor) space or the source space. In the sensor space, neuronal activity is inferred directly from each scalp electrode/sensor. A drawback of this technique is volume conduction and field spread, where signal arising from one distinct brain area is detected by two or more electrodes/sensors. This can consequently confound connectivity measures between two electrode/sensor pairs. To attenuate volume conduction effects, analysis may be performed in the source space, where signal is mapped back to the underlying source using biophysical models to take into account the effect of skull and scalp tissue conductivity. However, there is no consensus on the optimal solution for this so-called inverse problem and assumptions must be applied when performing source localisation (Darvas et al., 2004), thus analysis in the source space may also introduce some bias (Fornito et al., 2016). Moreover, it does not fully overcome potential issues of field spread because the separation of sources is never perfect (Schoffelen and Gross, 2009, Colclough et al., 2016).

Data parcellation in fMRI analysis

Parcellation of fMRI data refers to the partition and labelling of brain regions or networks. Detailed fMRI scanning creates around one million voxels; to treat each voxel as a single node would be computationally challenging, sensitive to noise (Craddock et al., 2012, Thirion et al., 2014), and statistically problematic in view of the number of tests that would be required (Zalesky et al., 2012a). In addition, the high dimensionality would render network analysis intractable (Thirion et al., 2014). To decrease dimensionality, voxels are parcellated into larger regions.

Numerous parcellation methods exist and there is no universally accepted optimal choice. One strategy is to parcellate data randomly. However, in order that parcels more accurately represent underlying brain organisation, voxels with shared structural-anatomical properties or similar connectivity features may be grouped together (Fornito et al., 2016). This may be determined at an individual level, or by applying a reference atlas. For meaningful interpretation of results in functional connectivity analysis, components represented by nodes should share similar temporal activation patterns as these reflect functionally coherent areas (Shen et al., 2013, Finn et al., 2015). Accordingly, methods of parcellation based upon connectivity information derived from the correlation of BOLD signals in the resting state are particularly suitable for functional connectivity studies (Finn et al., 2015, Eickhoff et al., 2018).

There is some evidence that functional connectivity derived parcels determined at an individual level may more accurately represent underlying functional connectivity than those defined with an atlas (Arslan et al., 2018). However, the former is limited by being time consuming for large datasets and may limit comparisons at the group-level. Therefore, applying an atlas is the more common approach for group-level analyses.

At least seven atlases are in existence that use functional connectivity features to parcellate the whole brain or cortex (Bellec et al., 2010, Craddock et al., 2012, Glasser et al., 2016, Gordon et al., 2016, Joliot et al., 2015, Schaefer et al., 2018, Shen et al., 2013). Each atlas varies in its design and there is no clear superior choice (Arslan et al., 2018). This perhaps reflects the complexity of attempting to capture brain organisation across varying scales, together with individual neurobiological variances, within the constraint of a universal atlas (Eickhoff et al., 2018). Major differences between atlases include the clustering technique used to determine similarity between voxels, the total number of parcels, the extent of brain coverage, and the characteristics of subjects used to create the atlas. Functional atlases are discussed further in Appendix 1 of Chapter 5.

Inferring connections in EEG/ MEG studies

The strength of the relationship between two network areas is ascertained according to the strength or consistency of synchronisation between two oscillating signals. The synchronisation of two signals may occur via their phase or amplitude/power (*figure 3*). Numerous measures exist to measure this relationship, each with their own advantages and disadvantages.

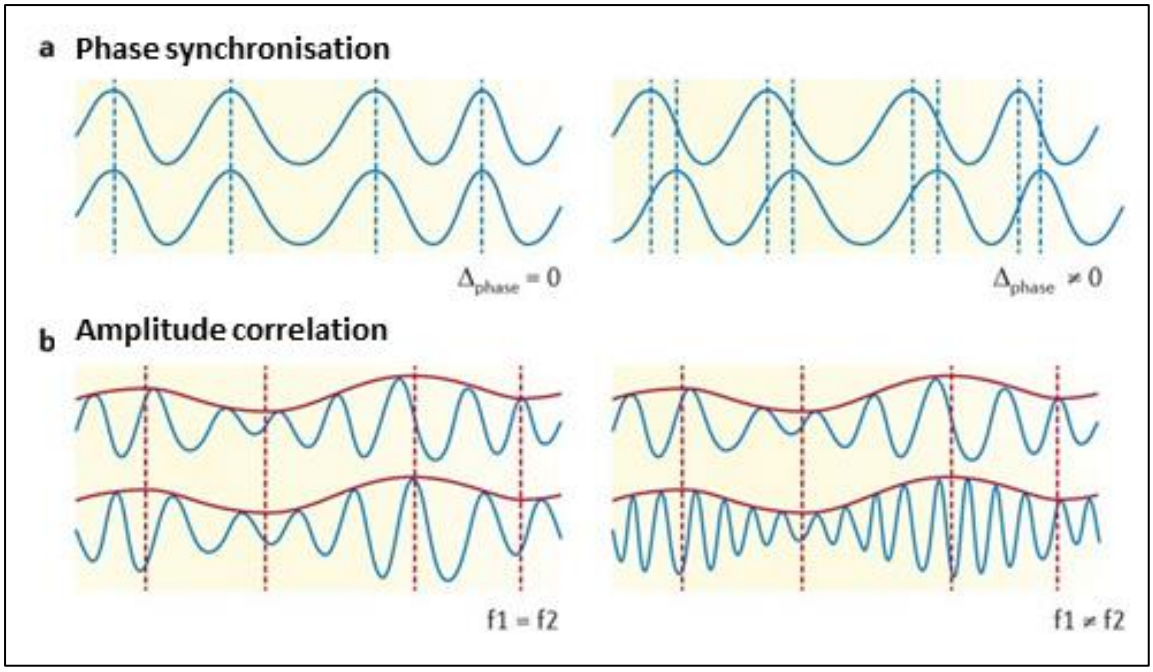

Figure 3. Phase synchronisation and amplitude correlation. a) illustrates phase synchronisation where the consistency of the phase of two signals is quantified. Signals may have zero phase lag (left panel) or may be phase shifted (right panel). b) amplitude correlation measures the correlation of the amplitude enveloped of two signals. Amplitude correlation can be determined for two signals of the same frequency (left panel) or different frequencies (right panel). Reprinted by permission from the licensor: Springer Nature, Nature Reviews Neuroscience, Spectral Fingerprints of Large-scale Neuronal Oscillations, Siegal et al. Copyright 2012.

Correlation, an amplitude-based measure, is derived from measuring the correlation of the 'amplitude envelopes' between two signals (Brazier and Barlow, 1956). Correlation produces both positive and negative edges, with positive values believed to represent integration between two network areas (Fornito et al., 2013). There is debate as to whether pre-processing techniques significantly contribute to negative correlations (Fox et al., 2009, Saad et al., 2012). Often, only absolute or positively correlated values are considered (Fornito et al., 2013). However, this may overlook potentially important information about network structure relating to negative correlations, which have been proposed to represent network segregation (Fornito et al., 2013). Phase coherence may be regarded as the frequency domain equivalent of correlation. It is derived from the cross spectral density of two signals (this is typically computed using the Fourier transform or wavelet transform and is obtained from the product of the two transforms when one is 'flipped' in its sine phase). As such, phase coherence incorporates both amplitude and phase (Adey et al., 1967). For both correlation and phase

coherence, the intrinsic non-linearity of the neural signal is not considered and the measures are sensitive to volume conduction (van Diessen et al., 2014a). Volume conduction effects can be attenuated by only using the imaginary part of coherency (Nolte et al., 2004), but this risks overlooking potentially important connections by excluding the real part of coherency (van Diessen et al., 2014a). Due to disease specific spectral alterations, power and amplitude-based methods may be influenced by the underlying spectral profile of the signal (van Diessen et al., 2014a, Donner and Siegel, 2011) and therefore methods unaffected by amplitude may be more suitable for deriving the strength of signal synchronisation. Such measures include phase locking value (PLV) and phase lag index (PLI).

The PLV (Lachaux et al., 1999) assumes that when two oscillating signals are functionally connected, the differences in the instantaneous phase of the signals will be consistent. A Hilbert transform is applied to the frequency domain signal and an average of the phase angle differences between two signals is computed over time (*figure 4*).

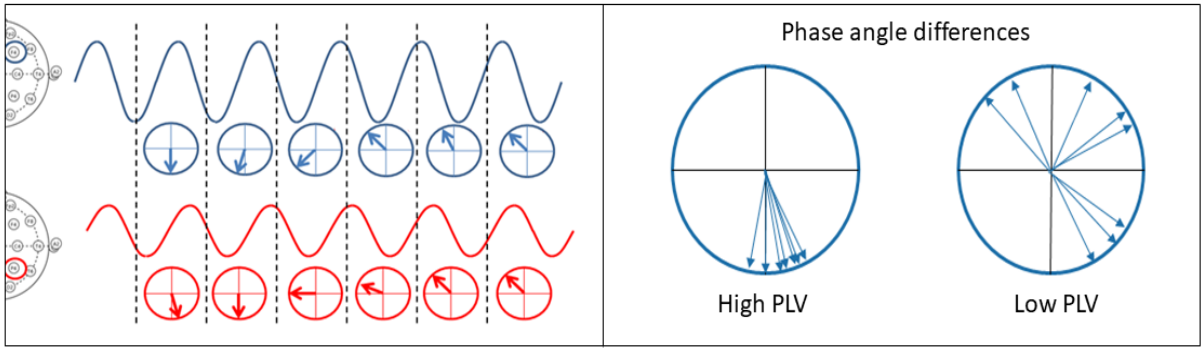

Figure 4. Schematic illustrating how PLV is determined between two simultaneously recorded signals. The phase angle of the two signals at each time point is established (left panel). The differences in phase angles at each time point between the signals are then determined. Where the phase angle differences are similar, there is a high PLV but when the differences are dissimilar, there is a low PLV (right panel).

The derived PLV lies between zero and one, where zero signifies no phase synchrony and one represents an identical phase between the signals. When two signals have zero (or Pi) lag, it is important to consider that they may have arisen as a result of volume conduction or field spread. The effect of these potential confounders on connectivity derived using PLV can be mitigated by excluding zero lagged data. Alternatively, measures which are less sensitive to these effects such as PLI may be used. The PLI (Stam et al., 2007b) is determined by the distribution of the phase angle differences between two signals. If apparent connectivity is

due to volume conduction effects, the distribution will be around zero radians whereas for non-spurious interactions, the phase angle differences will be positive or negative with respect to the real horizontal axis (*figure* 5). The PLI lies between zero and one, where zero signifies no instantaneous coupling and one indicates true lagged synchronisation.

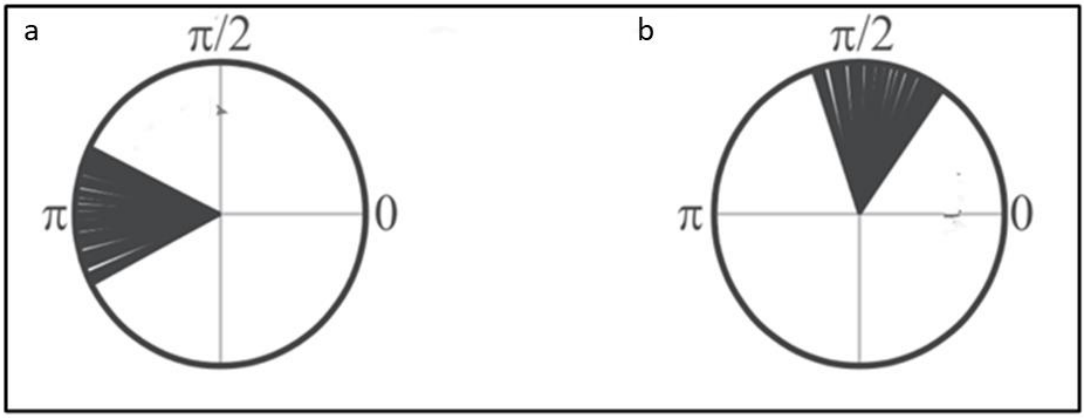

Figure 5. Phase locking index. PLI is determined by the *distribution* of the phase angle differences between two signals. a) If apparent connectivity is due to volume conduction effects, the distribution will be around zero radians. b) for non-spurious interactions, the phase angle differences will be positive or negative with respect to the real horizontal axis. Reprinted from: Journal of Neuroscience Methods, Volume 250, Cohen M, Effects of time lag and frequency matching on phase-based connectivity, Pages 137-146, Copyright 2015, with permission from Elsevier.

Using phase-based methods, the direction of information flow may also be inferred to form a directed graph by assessing whether the instantaneous phase of one signal is greater or less than the phase of another signal over time. This is potentially more informative than an undirected graph since it contains more information about the interactions between nodes.

Other methods exist that also incorporate estimates of the direction of information flow. Such measures include Granger causality (Granger, 1969), directed coherence (Wang and Takigawa, 1992), and directed transfer function (Kaminski and Blinowska, 1991). Disadvantages of these methods are that nonlinearity is not considered and the first two examples are sensitive to volume conduction (van Diessen et al., 2014a). These measures are typically used in effective connectivity studies, which seek to investigate the influence of one network region over another.

Inferring connections in fMRI studies

Edges in fMRI data are inferred from the extent of similarity of BOLD signal from time series of two different brain regions. The most common approach is to use the Pearson correlation coefficient to measure the correlations in signal amplitude fluctuations (Fornito et al., 2016). A drawback of this method is that it is sensitive to indirect connections whereby a spurious connection may be detected due to both regions being connected to an intermediary region. Using partial correlation may overcome this by regressing out the effects of other network nodes but may overcompensate thereby erroneously altering connectivity features (Smith, 2012). Furthermore, in a direct comparison of Pearson correlation and partial correlation, it was reported that there is a higher reliability when Pearson correlation is used (Liang et al., 2012). These linear methods assume that there is a temporally stable synchrony between functionally connected brain regions with zero-lag (Meszlényi et al., 2017). As with EEG/MEG derived networks, coherence-based methods may also be used.

In view of evidence that functional connectivity may comprise a more complex time lag-structure, there is increasing interest in alternative measures that account for greater complexity such as Dynamic Time Warping (Meszlényi et al., 2017) and mutual information (Fraser and Swinney, 1986).

Weighting and thresholding of connections

After connections have been detected between pairs of signals, they may be given a binary or a weighted value (corresponding to the connectivity measure) to reflect the relevance of the connection. A binary approach entails using a cut-off value to determine whether a connection is present or absent. This has the advantage of being simpler but is limited by the arbitrary nature of the selection of the cut-off point, which when too high permits inclusion of non-relevant signal and when too low may neglect functionally important connections. In weighted networks, a connection is given a value according to the strength of signal synchronisation. This attenuates the impact of statistically non-significant connections, which are postulated to be less relevant physiologically (Rubinov and Sporns, 2010).

In weighted networks, thresholding of edges is often performed with the aim of improving sensitivity to relevant connections by removing spurious connections and noise. Global thresholding, where connections less than a certain value are ignored, is a common approach in correlation analyses (Finn et al., 2015). A weakness of this method is that the threshold is arbitrary. An alternative to global thresholding is to determine the relevance of connections

statistically, at the group level. However, this may diminish the influence of important inter-individual connections and exaggerate the influence of spurious group-level confounding signal (Fornito et al., 2016). Whether weighted thresholding is performed with an arbitrary or statistical cut-off, networks with lower summed synchronisation values will become relatively less dense than networks with higher overall synchronisation values after thresholding (Fornito et al., 2013). This is a potential limitation of this method since it is known that network density may affect some network metrics (particularly clustering coefficient and characteristic path length) (van Wijk et al., 2010) and therefore, thresholding in this manner may exaggerate such effects. This issue could potentially be overcome by constructing matrices that have the same number of connections in each network. However, this may mean that networks with overall low connectivity produce fewer significant connections and potentially important connections in higher density networks may be disregarded (van Wijk et al., 2010). This issue may also be addressed with density-based thresholding where, for example, only those edges which form the highest 5% of the total number of connections between regions are included. A weakness of this method is that network density may be altered in some conditions (Cohen, 2014), including in epilepsy (Schindler et al., 2007, Kramer et al., 2010). Therefore, potentially important group differences may not be identified if this method is used.

Another commonly used approach to improve sensitivity to important connections in EEG-based studies is to construct 'surrogate' networks of the same density from the same time series (Schreiber and Schmitz, 2000, Schreiber and Schmitz, 1996). This permits the testing of a general null hypothesis for example that connections may be described by linearly correlated Gaussian noise. Connectivity values that do not exceed the statistical significance level of the distribution of the surrogate values are then discarded.

The direction of information flow may also be considered to form a 'directed network'.

The connectome

The information regarding connectivity between each region is contained within a connectivity matrix which represents the 'connectome' (Sporns et al., 2005) of the network (*figure 6*). Within this, each brain region is represented by a separate row (*i*) and column (*j*) and each element at the intersection of *i* and *j* encodes information regarding the strength of connection between regions *i* and *j*.

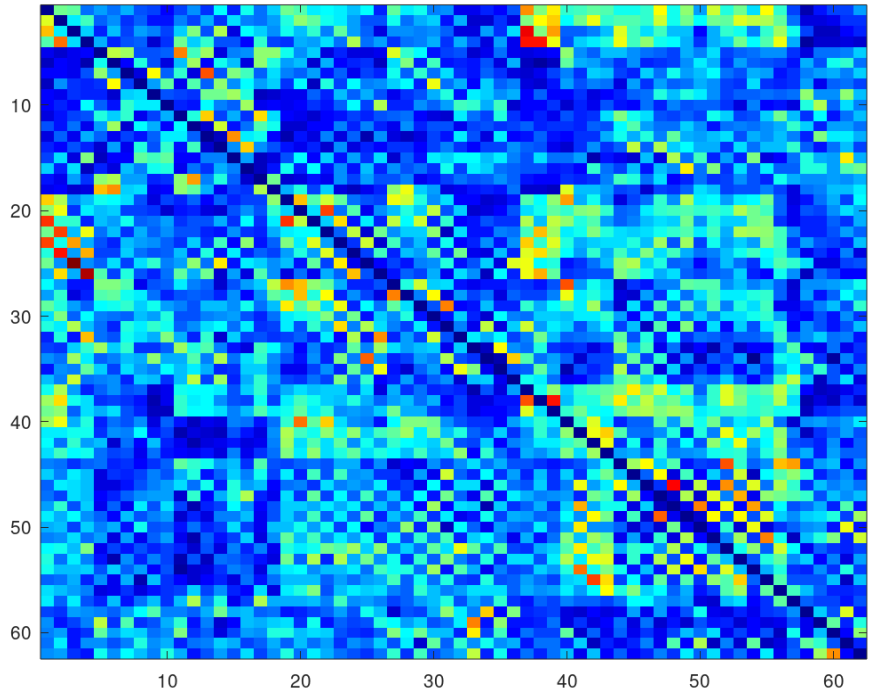

Figure 6. Example of a connectivity matrix derived from a 62 channel EEG. Each channel is represented a separate row *(i)* and column *(j)*. Each square within the matrix contains information regarding the presence and strength of connection between each electrode pair

Connectivity matrices can then be compared at the group level. One method by which to perform group level comparisons is to statistically compare the presence or strength (for unweighted or weighted networks respectively) of connections between each brain region or within specific brain networks. Alternatively, the network may be analysed according to its topology (network structure) using graph theory, as discussed in the following section.

1.4.3.5 Evaluating connectivity in functional networks with graph theory

Graph theory is an established mathematical method in which a network is represented as a graph. The graph contains 'nodes' (or 'vertices') which represent brain areas and 'edges' which represent the connections between them (*figure 7*).

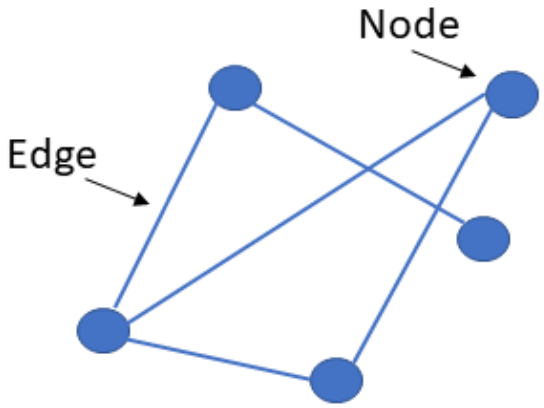

Figure 7. A simple undirected graph. Each network node is connected by an edge.

A graph is generated from a connectivity matrix whereby each row and column represent a node and each square within the matrix represents an edge. Graph theory permits modelling and analysis of various network properties, from the relationship between two structures or two communities within it, to the functioning of the entire network.

Graph theory has been widely advocated as a suitable tool for neuronal network analysis owing to its rigorously proven underlying mathematics and its generalisability to a wide range of complex systems.

Graph theory metrics

A set of definitions and statistical measures have been developed which can be used to objectively characterise various network features (Newman, 2008). Principal measures include the mean degree, degree distribution, characteristic path length, clustering coefficient and centrality measures such as betweenness centrality (*table 2, page 99)*. At the nodal level, the degree of a node represents the number of connections that it has. Nodes with a high degree are postulated to represent 'hubs' of information transfer within the network (Freeman, 1978). It has been suggested that alteration of network hubs is a final common pathway in many neurological diseases (Stam, 2014). The degree distribution provides information regarding the distribution of the number of connections of each node. Nodes within the tail of a 'long tailed distribution' contain hub nodes and thus this measure provides insight into the balance of hub nodes and low degree nodes. Betweenness centrality captures to what extent a node lies on a path between each pair of nodes in the network. The mean betweenness centrality of the network can therefore be regarded as a measure of the extent of

information flow within the network. The average clustering coefficient measures the connection between spatial neighbours of a node and reflects local connectivity or network segregation. Characteristic path length is the average distance between each pair of nodes in the network and is a measure of network integration. The small-world index is calculated as a ratio of normalised clustering coefficient to characteristic path length. Networks with a high small-world index are regarded as being efficient as they support both integration and segregation of network functions facilitating rapid transfer of information throughout the network (Bassett and Bullmore, 2006). An overall network topology can be described using the average clustering coefficient, characteristic path length and small-world index; regular networks have a high average clustering coefficient and high characteristic path length whereas random networks have a low average clustering coefficient and low characteristic path length. Small-world networks have high clustering with a low characteristic path length. This was first exemplified in seminal work by Watts and Strogatz who demonstrated that a small-world network is produced when a small number of connections in a regular graph are 'rewired' to form 'long-range' connections (Watts and Strogatz, 1998). This decreases the path length (i.e., improves integration) with little change in the average clustering coefficient (i.e., it remains strongly locally connected) (*figure 8).* It has been demonstrated that many networks, including cerebral networks, exhibit small-world properties (Stephan et al., 2000, Sporns and Zwi, 2004, Shefi et al., 2002).

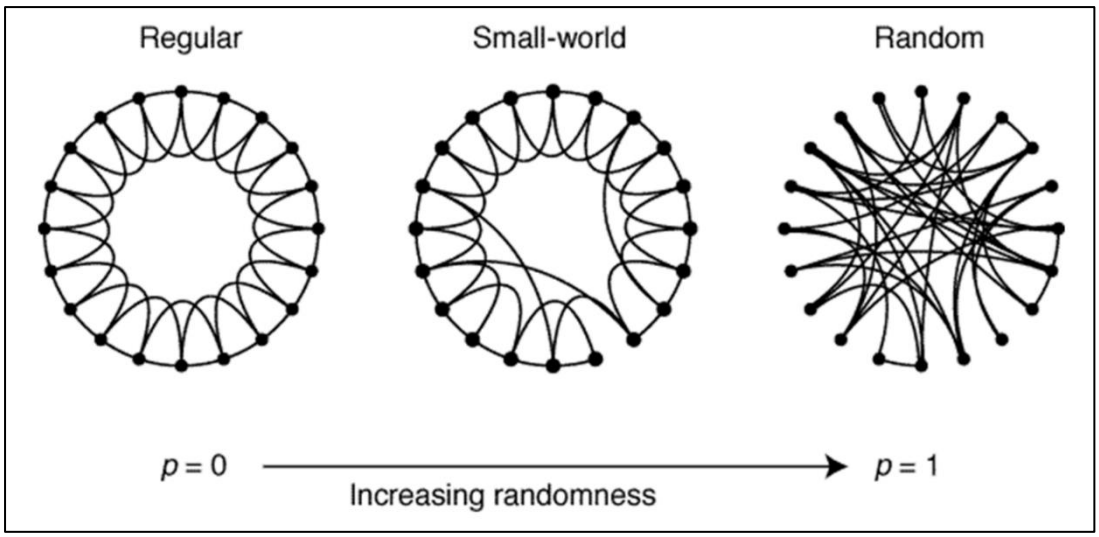

Figure 8. 'Rewiring' of a regular network to form small-world and random networks. The illustration demonstrates that a small world network occurs when a small number of connections in a regular graph are 'rewired' to form 'long-range' connections. With a probability *p*, an edge in a regular graph is reconnected to a randomly selected node. For intermediate values of *p*, the network has small-world features: high local clustering, as found in regular networks, and low characteristic path length, as found in random networks. Reprinted by permission from Springer Nature: Nature, Collective dynamics of 'small-world' networks, Watts et al., 1998. Copyright 1998.

In addition to small-world topology, there is also evidence that neuronal networks may have 'scale-free' characteristics. This concept was introduced as a generative model whereby new network nodes preferentially attach to existing nodes with a high number of connections following power-law scaling, which creates hub nodes (Barabási and Albert, 1999). As with small-worldness this topology has been recognised in a range of complex systems including in the brain (Eguíluz et al., 2005), and it has been suggested that disruption of such hub nodes may improve outcomes in epilepsy surgery (Lopes et al., 2017). However, the pervasiveness of this concept is disputed (Lima-Mendez and van Helden, 2009, Khanin and Wit, 2006). For example, in an investigation of scale-free networks, it was reported that few studies in support of the validity of such networks compared the networks to alternative distributions (Broido and Clauset, 2019). In this study, when 1000 different networks were examined, for most networks, log-normal distributions fitted the data as well as, or better than, scale-free distributions.

A third established concept in network structure is hierarchical 'modules' where subnetworks within networks exist. As with small-worldness and scale-free characteristics, modular

patterns have been reported across a range of networks. In epilepsy, higher modularity has been reported compared to controls (Chavez et al., 2010, Vaessen et al., 2014).

Since the important framework established by Watts and Strogatz (Watts and Strogatz, 1998), studies have increasingly focused on the interplay between network topology and disease (Stam and Reijneveld, 2007). Of key interest in epileptology is the contribution of resting state network topology to the collective synchronised action of the network.

1.4.4 Overview of interictal functional network literature in IGE

There is substantial literature demonstrating that people with epilepsy have different interictal networks to those without, however there are inconsistencies in findings. These differences may reflect the wide range of methodologies used, particularly differences in how the connectivity matrix was created (Pegg et al., 2020a).

We have recently published a systematic review of graph theoretical global network studies of IGE (Pegg et al., 2020a), which can be found in Chapter 3. In summary, the studies included in the review (Clemens et al., 2013, Chowdhury et al., 2014, Lee and Park, 2019, Elshahabi et al., 2015, Niso et al., 2015, Zhang et al., 2012, Liao et al., 2013, Xue et al., 2014a, Caeyenberghs et al., 2015, Qiu et al., 2017, Zhang et al., 2011) had mixed conclusions. When EEG/MEG derived functional networks were compared separately to fMRI studies, there was greater consistency with a suggestion that, compared to controls, people with IGE have a network that is more locally clustered (i.e., more regular) with increased global efficiency (i.e., more integrated). The significant findings were in various frequency bands but with overlap within the alpha frequency band. The two fMRI studies included in the review had diverging findings: one reported increased small-worldness in IGE whereas the other reported decreased small-worldness. In addition, structural network studies were evaluated, where a tendency to a decreased small-world network structure in IGE was found. Inconsistent findings in both network types may have been influenced by methodological variations in individual studies including participant demographics, post-acquisition data handling and network construction. The review paper concludes with a suggested standardised methodological framework for future studies.

Other non-graph theoretic functional connectivity studies of IGE have focused on specific networks. In a recent review of 24 fMRI studies with heterogenous study designs examining the DMN, overall there was reduced connectivity in the DMN and attention networks in IGE

compared to controls (Parsons et al., 2020). A MEG-based study reported decreased sensorimotor connectivity in JME (in the 13-30 Hz band) and increased connectivity in posterior regions (4-8 Hz and 8-13 Hz) (Routley et al., 2020). In contrast, an fMRI study reported increased sensorimotor connectivity as well as decreased connectivity in brain regions related to cognition (Zhong et al., 2018). Decreased connectivity in fMRI-derived thalamocortical networks has also been described in IGE (Wang et al., 2012, Kim et al., 2014).

Potentially relevant insights may be found in the FE network analysis literature and therefore merit discussion. In a meta-analysis of 12 studies comparing global interictal graph theoretic measures in people with various causes of FE compared to healthy controls, a more regular network in people with FE was reported (van Diessen et al., 2014c). In the EEG/MEG studies, only theta frequency band metrics were extracted as the authors deemed this to be the most relevant frequency band in focal epilepsy. The boundaries of theta frequency band were not detailed. The conclusions of this analysis should be interpreted with caution since it was based on combined data from EEG and fMRI studies, which as discussed in Section 6.2, is a complex reconciliation. Since this meta-analysis, further studies examining network properties in patients with FE have been published and have yielded mixed findings (Chiang et al., 2014, Vytvarova et al., 2017, Jiang et al., 2017, Adebimpe et al., 2016).

It is suggested that a more regular interictal network topology in epilepsy may reflect that the network is more liable to synchronisation (van Diessen et al., 2014b). This is supported by evidence that during a seizure, the network structure becomes more regular in its organisation relative to the interictal state (Ponten et al., 2007, Ponten et al., 2009, Kramer et al., 2010).

It is possible that where studies have not found differences in network topology in epilepsy, that failure to consider seizure control may be a factor. For example, between group differences may be 'cancelled out' by each other. There is evidence that connectivity in the DMN in DR-IGE compared with WC-IGE is reduced (Kay et al., 2013). Similarly, decreased resting state cerebellar connectivity in those with uncontrolled seizures in IGE compared with WC-IGE has been reported (Kay et al., 2014). To my knowledge, there is only one previous study that has compared global network differences in well-controlled epilepsy (WCE) and DRE (Kim et al., 2020). In this study, graph theoretic metrics from adults and children with controlled JME were compared with drug resistant JME and controls. Differences in global efficiency (the inverse of characteristic path length) and local efficiency between drug resistant participants and controls were found, with no differences in other group comparisons, and no differences in the other metrics used. However, this study is significantly

limited by the fact that there were only four patients with DRE. Furthermore, drug responsiveness was categorised after only one year of treatment and no information was provided regarding doses of medications reached. This is a relatively short time period in which to assess the response of two tolerated AEDs and therefore raises the possibility of incorrect classification of drug resistance.

Despite the increasing study of epileptogenesis from a network perspective, open questions include how seizures emerge from the complex network system of the brain, why the brains of people with epilepsy are particularly vulnerable to seizures, why certain conditions (such as sleep deprivation) lower the seizure threshold and why some people do not respond to antiepileptic medication. The unifying explanation is likely to relate to complex dynamical interactions (Richardson, 2012b).

1.5 Aims and objectives

Despite increasing literature regarding network anomalies in IGE and an incomplete understanding of why some people with epilepsy do not respond to AEDs, drug resistance in IGE has been seldom evaluated from a network perspective. Since seizures are an emergent phenomena arising from the same mechanisms that support normal brain functioning (Richardson, 2012b), investigating network features of the brain in its resting state may provide greater understanding of the complex dynamical network system that determines seizure susceptibility.

The analysis of EEG and fMRI-derived neuronal signal using spectral power analysis and graph theory are suitable techniques by which to understand potential alterations of neuronal oscillations and functional network topology in relation to IGE and AED resistance. Using these methods, the experimental chapters in this thesis (Chapters 2, 4, and 5) aim to evaluate network features in DR-IGE, WC-IGE and healthy controls with the intention of gaining further insight into epilepsy drug resistance.

In Chapter 2, an EEG spectral power analysis of WC-IGE, DR-IGE, and controls is presented. In Chapter 3, our published systematic review of graph theoretical studies of resting state global functional networks in IGE is presented. In Chapter 4, resting state functional network topology in WC-IGE, DR-IGE, and controls is evaluated using EEG and graph theory. Chapters 2 and 4 are based on a single EEG data set. Chapter 5 comprises a functional resting state network topological study of WC-IGE, DR-IGE and controls using fMRI and graph

theory, in a different participant cohort. Chapter 6 concludes this thesis with a synthesised discussion of the results of the analyses, including potential interpretations, limitations, and implications for further work.

Chapter 2. A spectral power investigation of the interictal EEG in drug resistant and well-controlled IGE

This manuscript is published in Epilepsy & Behavior (November 2020). Footnotes in this chapter contain additional information regarding methodological considerations, which were not included in the published paper.

2.1 Authors

Emily J. Pegg[1,2], Jason R. Taylor[2,3], Rajiv Mohanraj[1,2]

[1] Department of Neurology, Manchester Centre for Clinical Neurosciences.

[2] Division of Neuroscience and Experimental Psychology, School of Biological Sciences, Faculty of Biology, Medicine and Health, University of Manchester.

[3] Manchester Academic Health Sciences Centre.

2.2 Abstract

Introduction

Idiopathic generalised epilepsies (IGE) are characterised by generalised interictal epileptiform discharges (IEDs) on a normal background EEG. However, the yield of IEDs can be low. Approximately 20% of patients with IGE do not gain seizure control with antiepileptic drug (AED) treatment. Currently, there are no reliable prognostic markers for early identification of drug resistant epilepsy. We examined spectral power of the interictal EEG background in patients with IGE and normal controls, to identify potential diagnostic and prognostic biomarkers of IGE.

Methods

A 64 channel EEG was recorded under standardised conditions in patients with well-controlled IGE (WC-IGE, n=19), drug resistant IGE (DR-IGE, n=18) and age-matched controls (n=20). After pre-processing, fast Fourier transform was performed to obtain 1D frequency spectra for each EEG channel. 1D spectra (averaged over channels) and 2D topographic maps

(averaged over canonical frequency bands) were computed for each participant. Power spectra in the three cohorts were compared using one way analysis of variance (ANOVA), and power spectra images were compared using t contrast tests. A post-hoc analysis compared peak alpha frequency between the groups.

Results

Compared to controls, participants with IGE had higher interictal EEG spectral power in the delta band in the midline central region, in the theta band in the midline, in the beta band over the left hemisphere, and in the gamma band over the right hemisphere and left central regions. There were no differences in spectral power between the WC-IGE and DR-IGE cohorts. Peak alpha frequency was lower in WC-IGE and DR-IGE than controls.

Conclusions

EEG spectral power analysis could form part of a clinically useful diagnostic biomarker for IGE; however, it did not correlate with response to AED in this study.

2.3 Introduction

Epileptic seizures are generated by hyper-synchronised activity of neuronal networks, which can be detected by electroencephalography (EEG) in the ictal and interictal states. Idiopathic generalised epilepsies (IGE) comprise a group of electro-clinical syndromes including Childhood Absence Epilepsy (CAE), Juvenile Absence Epilepsy (JAE), Juvenile Myoclonic Epilepsy (JME) and Epilepsy with Generalised Tonic-Clonic Seizures Alone (EGTCSA), which are characterised by the occurrence of absence, myoclonic, and tonic–clonic seizures (Scheffer et al., 2017). The hallmarks of IGE syndromes on conventional visual analysis of EEG are a normal background, and bilaterally synchronous interictal epileptiform discharges (IEDs) (Wolf and Beniczky, 2014). Detection of IEDs on EEG can serve as a biomarker for epilepsy, and thus aid diagnosis and classification. However, the yield of IEDs on routine EEG can be as low as 50% in adult patients with epilepsy (van Donselaar et al., 1992). Ascertainment of IEDs by visual analysis of EEG is also limited by lack of objective definition of IEDs, resulting in high inter-observer variability, which can contribute to misdiagnosis of epilepsy (Benbadis and Tatum, 2003). Therefore, identifying an objective EEG biomarker for IGE could improve the utility of EEG in the diagnosis of IGE.

While many IGE syndromes have a good prognosis with remission of seizures achieved in 64–82% with antiepileptic drug (AED) treatment, a significant number of patients do not become seizure free (Mohanraj and Brodie, 2007, Szaflarski et al., 2010). Approximately 18% of patients with IGE do not achieve seizure control for one year with AED treatment (Brodie et al., 2012), and can be considered to have drug resistant epilepsy (DRE). DRE leads to significant physical, psychological and socioeconomic consequences for patients, and represents a significant public health problem (Kwan et al., 2011). Identifying patients at risk of developing DRE at an early stage may help to better target specialist services and non-pharmacological treatments, and potentially reduce the incidence and consequences of DRE.

Spectral power analysis is a method of decomposing EEG signal in the time domain, into its independent oscillatory components in the frequency domain (*figure 9*). This permits quantification and comparison of the EEG signal across groups of subjects in terms of power in relevant frequency bands.

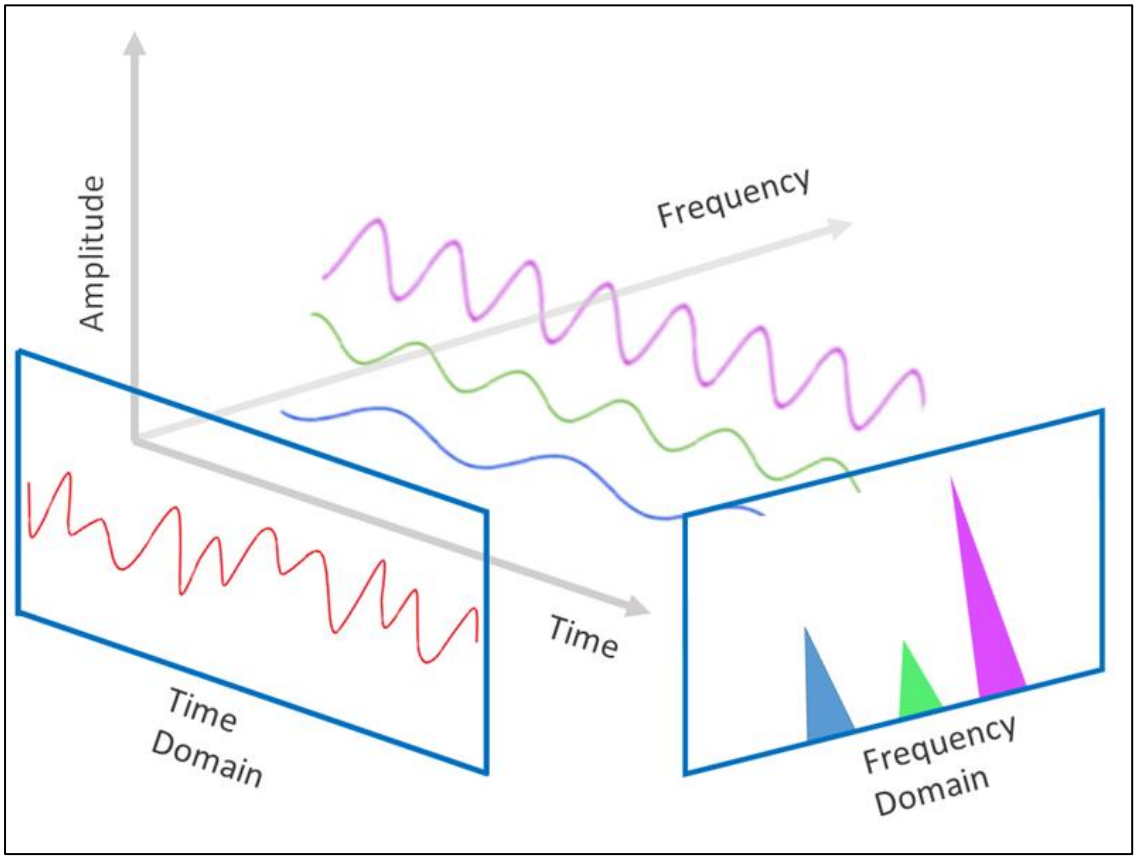

Figure 9. Spectral power analysis. EEG signal in the time domain is decomposed into its oscillatory components and expressed in the frequency domain.

Previous studies of spectral power analysis of interictal EEG have found higher spectral power across the frequency bands, across several brain regions, in people with IGE compared to controls (Miyauchi et al., 1991, Tikka et al., 2013, Clemens et al., 2000, Elshahabi et al., 2015, Willoughby et al., 2003, Niso et al., 2015, Santiago-Rodríguez et al., 2008). Findings from these studies, however, have been variable in terms of the frequency bands and scalp regions where differences were identified. Some studies have examined the prognostic utility of EEG spectral power in IGE. These have suggested that various features such as shift in alpha power from high to low alpha frequency band, (Abela et al., 2019) increase in interictal spectral entropy values (Urigüen, 2017) and increase in gamma power (Willoughby et al., 2003) as potential markers for DRE. Another study has reported 'normalisation' of EEG spectral power with AEDs, which could indicate the likelihood of seizure control with a particular AED (Clemens et al., 2007). These results suggest that EEG spectral power analysis could reveal potentially useful prognostic biomarkers.

We compared interictal EEG spectral power in people with drug resistant IGE (DR-IGE), well-controlled IGE (WC-IGE) and controls, to identify differences between patients with epilepsy compared to controls, and between DR-IGE and WC-IGE.

2.4 Materials and Methods

Participants

Participants with epilepsy were recruited from epilepsy clinics at the Manchester Centre for Clinical Neurosciences, The Walton Centre, and general neurology clinics in the Greater Manchester area. Controls were recruited via advertisements in Salford Royal Hospital, the University of Manchester and the Citizen Scientist website.

All participants were over the age of 16 years. Inclusion criteria for participants with IGE syndrome were a diagnosis of IGE and taking at least one AED. IGE syndromes were classified by the authors based on age of onset, seizure types, neurodevelopmental history, EEG findings and family history of epilepsy, based on criteria set out by the ILAE Commission on Classification and Terminology (Scheffer et al., 2017). The diagnosis was subsequently reviewed by a senior epileptologist not involved in the study, and patients who did not satisfy the diagnostic criteria were excluded from the analysis.

Exclusion criteria for all groups included a history of other neurological or developmental disorders and current or recent use of central nervous system acting drugs (other than AEDs). People with a vagal nerve stimulator were excluded. The WC-IGE group had no seizures, including myoclonic jerks and absences, for a minimum period of one year. To meet the study criteria for drug resistance, participants had continuing seizures despite having taken at least two appropriate AEDs for at least six months, one of which had to be sodium valproate, at a minimum dose of 1000 mg per day.

In total, 60 participants were recruited comprising 20 with WC-IGE, 20 with DR-IGE and 20 controls. One participant in the group with WC-IGE was reclassified as probable focal epilepsy at diagnosis review and was, therefore, excluded from the analysis. We excluded two participants with DR-IGE due to an abnormally slow background rhythm on the study EEG. Therefore, the total number of participants included in the analysis was 57 (WC-IGE n = 19, DR-IGE n = 18, controls n = 20).

Data collection

Each participant had a 12-minute 64 channel EEG recording in the 10-10 configuration using the Brain Vision system [1]. A 3-minute eyes closed sample was used for the analysis [2]. Sampling rate was 1000 Hz. The recording was carried out in a quiet, naturally lit room. All participants were seated in a cushioned chair and wore passive ear defenders. The impedance of the reference and ground electrode was always less than 10 kΩ. An impedance of less than 20 kΩ was aimed for with remaining electrodes.

---

1 Inter-subject variability in resting state EEG data may arise through differences in both the subjective experience of the recording (Diaz et al., 2013) and the immediate pre-recording cognitive state (Lopez Zunini et al., 2013). To create a similar pre-recording experience, all participants were given the same instruction "to sit and relax" and initially had their eyes open for three minutes, before the eye-closed recording began.

2 Eyes closed data is more commonly used in spectral power analysis and is less likely to contain oculomotor artefact. Although such artefacts can be removed, it is preferable to have as clean data as possible from the outset to reduce the chance of rejecting neural activity which is mixed with artefact.

EEG pre-processing

Using EEGLAB (Delorme and Makeig, 2004), data were down-sampled to 250 Hz and referenced to the common average. A 45-55 Hz notch filter was applied to attenuate contamination from mains electricity. Independent Component Analysis (ICA) of 64 components was carried out to detect artifact from oculomotor movements and muscle activity.

This was carried out using SASICA software (Chaumon et al., 2015) and included ADJUST measurements (Mognon et al., 2011), which enable the identification of oculomotor movements in the absence of an electrooculography (EOG) channel. In total, 7.95% of components were rejected, with no significant difference between groups. Following removal of rejected components, data were referenced again to the common average and converted for analysis in SPM 12 (Penny et al., 2006). Epochs containing epileptiform discharges were removed by setting a rejection threshold of 80 μV in channels Fp1, Fp2 and Fpz. Using these automated artifact rejection methods, in some instances epochs without any obvious artifact were rejected. However, the proportion of removed epochs was low (1.91% in total), which was felt to be acceptable.

Data analysis

Frequency spectra were calculated using fast Fourier transform with a Hanning window for each channel and epoch, resulting in power estimates at whole number frequencies between 1 and 70Hz. Power values were log-transformed and then averaged over epochs. 1D spectra were computed by averaging over all EEG channels, and topographic images were created to summarise the spatial distributions of log-transformed power in each standard frequency band (delta 1-3 Hz, theta 4-7 Hz, alpha 8-12 Hz, beta 13-30 Hz and gamma 31-70 Hz).

A one-way ANOVA test was carried out in SPM to compare differences between the 1D power spectraof the three groups. T contrast tests were used to compare the power at each frequency for 1) all participants with epilepsy with controls and 2) DRE-IGE with WC-IGE. Testing was corrected for multiple comparisons using a family-wise error (FWE) value of 0.05 determined using random field theory (Kilner et al., 2005), which is less conservative than traditional correction (e.g. Bonferonni) as it takes into account the smoothness of the data (dependencies between neighbouring data points). Masking was applied at 45-55 Hz where the data had been notch-filtered. 2D scalp images of power in each frequency band were

analysed using the same approach in order to evaluate the regions in which there is a significant difference in spectral power.

Ethical approval

This study has approval from the Health Research Authority (HRA), Research Ethics Committee (REC) and the hospital's Research & Development department.

2.5 Results

2.5.1 Baseline demographics

Demographic and clinical data of the three cohorts are presented in *tables 1a-c,* which can be found at the end of this chapter (pages 67-71). Where the diagnosis of an IGE syndrome had not been supported by a previous clinical EEG recording, the classification was based on other relevant clinical factors such as the presence of generalised seizure types (myoclonic and absence) appropriate age of onset, normal neurodevelopmental history and family history in first degree relatives. The median age of all participants was 26 years (range: 17-57). There were no differences between the groups in age (DR-IGE = 26.5 years, range: 18-57; WC-IGE = 24 years, range: 17- 54; controls = 25 years, range: 19-57, Kruskal-Wallis H = 1.016, p = 0.602), or gender (52.6 % in total were female. Chi-square = 0.7401 p=0.690). The DR-IGE group had a mean epilepsy duration of 16.6 years (standard deviation 9.92) compared to 11.26 years (standard deviation 9.1) in the WC-IGE group, but this difference was not statistically significant using a t test (t = -1.59, df =30 p= 0.12). The DR-IGE group took more AEDs (mode = 2, range 1-4) compared to the WC-IGE group (mode = 1, range 1-3). The majority of participants in both groups with epilepsy had JME. This was evolved from CAE in one participant in each group. Exceptions were two participants with WC-IGE and one participant with DR-IGE who had EGTCSA and two participants with WC-IGE with JAE. No participant had a seizure in the 24 hours before the EEG recording.

2.5.2 Outcome measures

There was significantly higher (FWE <0.05) EEG spectral power in the IGE cohorts (DRE-IGE and WC-IGE combined) compared to controls at 4-8 Hz, 15-20 Hz, 25-31 Hz and 39-42 Hz (*figures 10 and 11*).

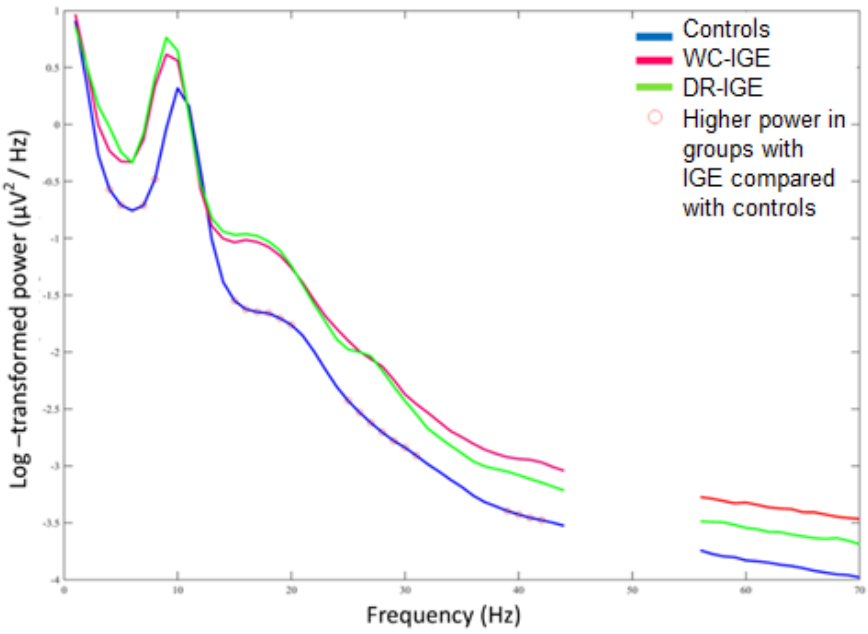

Figure 10. Power spectra plotted for each group. Log rescaled power spectra are plotted for each group, showing significant differences between the control group compared to the epilepsy group. Circles indicate frequencies at which there was a significantly lower power ($p < 0.05$, corrected for all frequencies tested FWE < 0.05) in the controls compared to the epilepsy group as a whole. Absent data at 45-55 Hz reflects notch filtering.

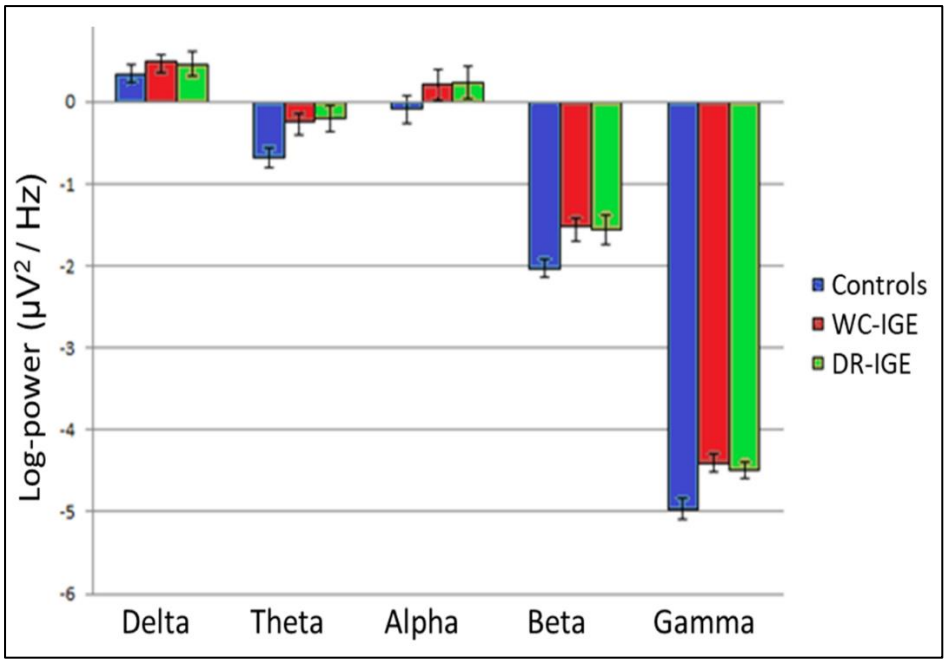

Figure 11. Power spectra for each group averaged within each frequency band. Bars denote standard errors.

There was no difference in spectral power between WC-IGE and DR-IGE. Analysis of scalp images found higher power in the delta band in a small central cluster in the epilepsy groups compared to normal controls. In the theta band, increase in power was widespread, and predominantly along the midline and over the left hemisphere. In the beta band, widespread, predominantly right sided higher power was seen in the epilepsy cohorts compared to controls, while in the gamma band, the difference was most marked over the right hemisphere and left central regions (*figure 12*). No differences were found between scalp images in WC-IGE and DR-IGE. No differences in spectral power were found between the IGE groups and controls in the alpha band. However, a post hoc analysis of individual alpha frequency revealed higher peak alpha frequency in the control group (10.15 Hz, SD 0.67) compared to WC-IGE (9.58 Hz, SD 0.96, p=0.004) and DR-IGE (9.33 Hz, SD 0.97, p = 0.037).

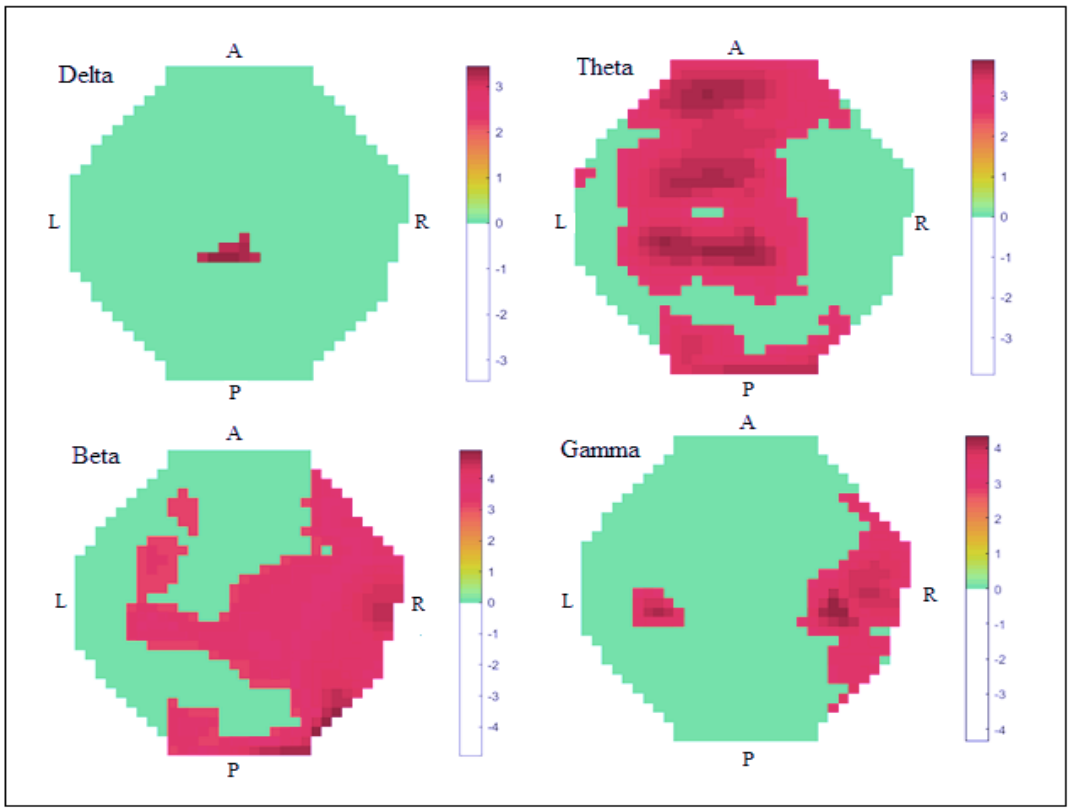

Figure 12. Scalp topographical images of differences in spectral power between epilepsy groups and controls. Images indicate the location of significantly different spectral power in the epilepsy group compared to controls for delta, theta, beta and gamma frequency bands ($p < 0.05$, FWE corrected). Red = higher spectral power in epilepsy compared to controls. Green = no difference. Colour bar represents t-statistic at each pixel. There were no significant differences in the alpha frequency band (not

2.6 Discussion

Differences in EEG background have been described in patients with epilepsy since early EEG studies, when it was noted that patients with epilepsy have slower alpha activity than controls (Gibbs et al., 1943, Stoller, 1949). We found significantly higher interictal EEG spectral power in the theta band (4-7 Hz) along the midline and left hemisphere, in the beta band (15-20 Hz and 25-31 Hz) over the right hemisphere, and gamma band (39-42 Hz) over the right hemisphere/left central regions in patients with IGE compared to controls. We did not find significant differences between IGE cohorts and controls in the alpha frequency band, but a post hoc analysis revealed significantly higher peak alpha frequency in the control subjects compared to the epilepsy cohorts. There were no significant differences in spectral power between DR-IGE and WC-IGE.

The finding of higher EEG interictal spectral power in IGE in this study is consistent with similar previous studies, albeit with some differences in the frequency bands and scalp regions with higher power (Clemens et al., 2000, Elshahabi et al., 2015, Miyauchi et al., 1991, Tikka et al., 2013, Willoughby et al., 2003, Niso et al., 2015, Santiago-Rodríguez et al., 2008) (*figure 13*). There are methodological differences in previous studies; in the modalities used (EEG or MEG), number of electrodes, number of participants, and IGE subtypes, which could account for some variation in the findings.

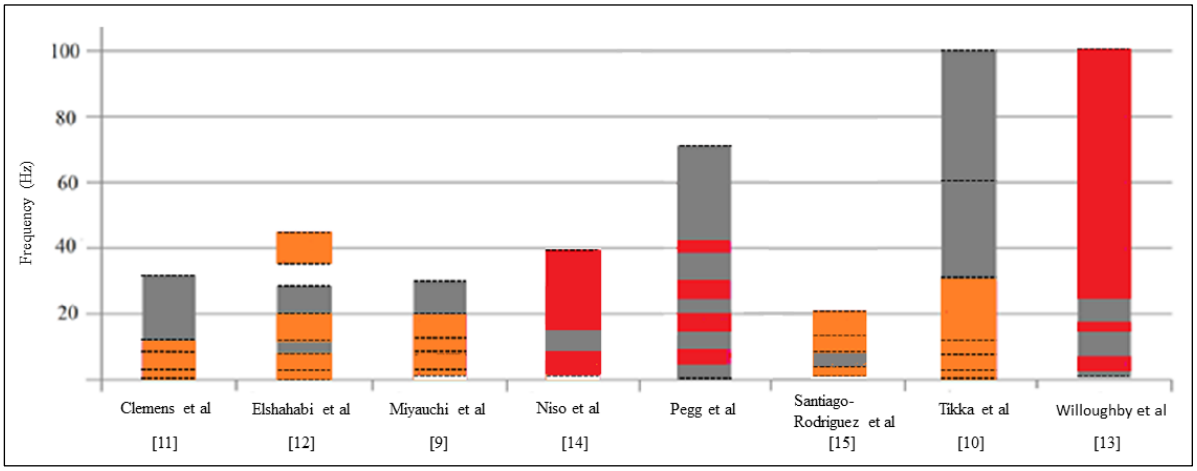

Figure 13. Summary of previous studies evaluating EEG/MEG spectral power in IGE. Orange = higher power in IGE compared with controls, averaged over frequency band subdivisions. Frequency band boundaries are indicated by dashed lines. Red = higher power in IGE compared to controls, tested in 1 or 2 Hz frequency increments. The dashed lines represent upper and lower frequencies tested. Grey= no difference in spectral power between IGE and controls.

It has been proposed that increased spectral power observed in IGE reflects greater neuronal synchronisation (Clemens et al., 2000, Michel et al., 1992), occurring as a result of an altered neuronal extracellular ionic environment (Willoughby et al., 2003) leading to hyper-excitability of the cortex. Increase in power across all frequency bands has been observed immediately before myoclonic seizures, which supports the notion of higher spectral power indicating seizure susceptibility (Sun et al., 2016).

The finding of spectral power differences in the interictal EEG in patients with IGE compared to controls may be of potential value in improving the diagnostic capability of EEG. The clinical utility of such objective measures of EEG analysis is yet to be fully established. In one study comparing three candidate interictal EEG biomarkers for the diagnosis of IGE (Schmidt et al., 2016), the sensitivity for two biomarkers (peak occipital alpha power and the mean degree- a functional network measure) was found to be very low. In the same study, a computational local coupling measure based on a dynamic network model performed better, with 56.7% sensitivity for IGE. Further work is therefore needed to develop clinically useful diagnostic EEG biomarkers in IGE.

All participants with IGE in our study were taking an AED, and therefore it is possible that the effect of AEDs has confounded our results. AEDs are reported to affect spectral power in some studies, but not in others (Holler et al., 2019). In other similar studies of IGE, some participants were not taking an AED, thus enabling comparison between medicated and unmedicated patients with IGE. In one such study, findings in the untreated group were similar to the treated group suggesting that differences were due to IGE itself rather than medication effects (Miyauchi et al., 1991). Another study only found a medication effect at 2-4Hz and at 7-8 Hz, with increased power in medicated compared to unmedicated participants with IGE (Willoughby et al., 2003). Lamotrigine, sodium valproate and levetiracetam were the most commonly taken AEDs in our study cohorts. Both lamotrigine and sodium valproate have been shown to reduce spectral power in the delta, theta, alpha and beta frequency bands (Clemens et al., 2007, Clemens, 2008, Sannita et al., 1989, Wu and Xiao, 1997). Valproate has also been reported to increase upper alpha power in the occipital areas, with a decrease in beta power in another study (Wu and Xiao, 1997). A study evaluating the effect of levetiracetam in patients before and after medication initiation reported a decrease in delta and theta and an increase in alpha and beta power (Cho et al., 2012). Overall, evidence from the majority of studies of these three AEDs suggests that they result in a reduced spectral power in epilepsy in at least one frequency band, suggesting that the differences observed in our study are unlikely to be due to AED effects.

There were no differences in spectral power between the DR-IGE group and the WC-IGE group in this study. Previous studies have identified a shift in alpha power from high to low alpha frequency band in patients with IGE, which was suggested to be a marker for DRE (Abela et al., 2019). We obtained similar results in a post hoc analysis of individual alpha frequency, with significantly lower peak alpha frequency in people with IGE compared to controls, but there were no significant differences between DR-IGE and WC-IGE. Another study reported greater interictal spectral entropy values in patients with IGE compared to controls, which had an inversely proportional relationship to the time since last seizure (Urigüen, 2017). It has also been suggested that an increase in background EEG gamma power may have an inverse relationship with seizure control (Willoughby et al., 2003). Potential differences in background rhythm between patients with DR-IGE compared to those with WC-IGE have only been previously explored within the alpha frequency band (Abela et al., 2019), to the best of our knowledge. In a study of focal and generalised epilepsy in children, relative power of delta and gamma (in addition to other quantitative EEG background parameters) were evaluated and alterations between WCE and DRE were described (Lin et al., 2014). If, as discussed above, increase in spectral power represents greater cortical excitability, the lack of difference between DR-IGE and WC-IGE cohorts in our study would suggest that the cortex remains hyperexcitable irrespective of seizure control in IGE. However, it is possible that our study was underpowered to detect a difference between the two IGE groups. The DR-IGE group were taking more AEDs, therefore it is possible that this analysis was confounded by medication effects. In addition, classification of seizure control can be challenging due to the natural history of epilepsy, as a proportion of patients may have a fluctuating course, with relapse of seizures following periods of seizure freedom (Brodie et al., 2012). Lack of concordance with prescription and co-existing non-epileptic attacks may also lead to inaccurate classification of DR-IGE.

A further limitation of this study is its cross-sectional design, which does not permit solid conclusions regarding potential prognostic biomarkers to be drawn. It is also important to note that our findings only apply to IGE. Spectral power alterations have also been reported in focal epilepsies (Yaakub et al., 2020, Kim et al., 2002, Bettus et al., 2008, Díaz et al., 1998, Miyauchi et al., 1991); however, the directionality of alterations in these studies is inconsistent. A prospective study design, which also includes other types of epilepsy, would be informative and help overcome these limitations.

2.7 Conclusions

People with IGE have higher EEG interictal spectral power than healthy controls across multiple scalp regions, with a lower peak alpha frequency. These findings could be refined to develop an interictal biomarker for IGE, which could improve the speed and accuracy of diagnosis. Future work should focus on evaluating the frequency bands and scalp regions which best capture interictal changes, independent of drug effects, which could then be prospectively tested in a prediction model. The inclusion of a subgroup of patients with other types of epilepsy in such a study would broaden the generalisability of significant findings. We did not find significant differences in EEG spectral power between DR-IGE and WC-IGE. Mechanisms of action of AED at the cellular level, although well characterised, cannot predict clinical effect of AEDs in patients. As seizures involve large-scale neuronal networks, the effects of AEDs should also be examined at the level of neuronal networks. Further work, using EEG or MEG based techniques to study functional network effects of AEDs may be more successful in identifying potential prognostic biomarkers in IGE (Yaakub et al., 2020).

2.8 Acknowledgements

We are grateful to Dr Paul Cooper MA, DM, FRCP, FAES for reviewing diagnosis and classification of patients with IGE recruited into the study.

2.9 Funding

This research did not receive any specific grant from funding agencies in the public, commercial, or not-for-profit sectors. The project was sponsored by the department of research and development at Salford Royal NHS Foundation Trust.

Table 1a. Demographic and clinical details of participants with WC-IGE

Participant	Age	Sex	Seizure types	Age at onset	Neuro-developmental history	EEG	Epilepsy in first degree relatives	IGE subtype	Current medication (total daily dose)
W01	22	M	GTC, Abs	13	Normal	Typical	No	JAE	Valproate 2100mg, Levetiracetam 500mg
W02	21	F	GTC, MJ	14	Normal	Normal	No	JME	Levetiracetam 1000mg
W03	21	F	GTC, MJ, Abs	12	Normal	Normal	Mother	JME	Levetiracetam 1000mg
W04	24	F	Abs, GTC	18	Normal	Typical	No	JAE	Valproate 1000mg, Lamotrigine 200mg, Levetiracetam 4000mg
W05	37	F	GTC, MJ	23	Normal	NA	No	JME	Lamotrigine 250mg, Levetiracetam 2500mg
W06	21	F	GTC, MJ	14	Normal	Typical	Yes	JME	Lamotrigine 300mg
W07	17	M	GTC, MJ	15	Normal	Typical	Father	JME	Levetiracetam 1000mg
W08	34	F	GTC, MJ	14	Yes	NA	No	JME	Valproate 400mg, Levetiracetam 3000mg
W09	37	M	GTC	13	Normal	NA	Brother	EGTCSA	Valproate 300mg, Lamotrigine 300mg
W10	37	M	GTC, MJ	16	Normal	NA	Father	JME	Lamotrigine 400mg
W11	28	F	GTC, MJ	20	Normal	Typical	Brother	JME	Levetiracetam 1000mg
W12	20	M	GTC, MJ, Abs	5-10	Normal	Typical	No	CAE>JME	Valproate 1700mg Ethosuximide 500mg
W13	28	F	GTC, MJ	18	Normal	NA	No	JME	Levetiracetam 1250mg
W14	54	M	GTC, MJ	16	Normal	NA	no	JME	Valproate 2200mg, Clonazepam 2mg, Lamotrigine 100mg

W15	23	M	GTC	20	Normal	Typical	No	EGTSCA	Valproate 800mg
W16	34	F	GTC, MJ	15	Normal	Normal	Mother	JME	Levetiracetam 1500mg
W17	20	F	GTC, MJ	16	Normal	Typical	No	JME	Levetiracetam 2000mg
W19	50	M	GTC, MJ	13	Normal	Typical	No	JME	Valproate 1000mg, Levetiracetam 2000mg
W20	21	M	GTC, MJ	12	Normal	Typical	No	JME	Valproate 1000mg

W18 was excluded from the analysis following independent diagnosis review. F – female, M-male, GTC- generalised tonic-clonic, MJ- myoclonic jerk, Abs- absence, JAE- juvenile absence epilepsy, CAE- childhood absence epilepsy, JME- juvenile myoclonic epilepsy, EGTSCA- IGE with generalised tonic-clonic seizures alone, NA - not available, typical - previous EEG recording showing bilaterally synchronous spike/polyspike wave discharges on normal background.

Table 1 b. Demographic and clinical details of participants with DR-IGE

Participant	Age	Sex	Seizure types	Age at onset	Neuro-developmental history	EEG	Epilepsy in first degree relatives	IGE subtype	Current medication (total daily dose)
R01	45	F	GTC, MJ, Abs	18	Normal	Typical	No	JME	Perampanel 2mg, Brivaracetam 100mg
R02	23	M	GTC, MJ	16	Normal	Typical	No	JME	Valproate 3000mg, Zonisamide 300mg, Levetiracetam 1000mg
R04	57	F	GTC, MJ	17	Normal	Typical	Un-known	JME	Valproate 1000mg, Zonisamide 400mg, Clonazepam 1.5mg
R05	32	F	GTC, MJ, Abs	11	Normal	Typical	No	JME	Levetiracetam 3000mg, Perampanel 6mg
R06	22	M	GTC, MJ	13	Normal	Normal	No	JME	Valproate 2000mg, Lamotrigine 150mg
R07	20	F	GTC, MJ	15	Normal	Typical	Mother	JME	Valproate 1500mg, Levetiracetam 2500mg
R08	36	M	GTC, MJ	<20	Normal	N/A	Un-known	JME	Valproate 1800mg, Topiramate 100mg, clobazam 10mg PRN
R09	43	M	GTC, MJ	19	Normal	N/A	Sister	JME	Valproate 2000 mg
R10	23	M	GTC, MJ, Abs	19	Normal	Typical	No	JME	Brivaracetam 100mg, Zonisamide 200mg
R11	23	F	GTC, MJ	10	Normal	Typical	No	JME	Valproate 600mg, Levetiracetam 500mg, Lamotrigine 300mg
R12	30	M	GTC	11	Memory and executive deficits on neuropsychological tests	Typical	Brother	EGTCSA	Lamotrigine 250mg, Valproate 1400mg, Clonazepam 0.5mg
R13	24	F	GTC, Abs	4	Normal	Typical	No	CAE>JME	Lamotrigine 450mg, Clobazam 10mg, Brivaracetam 100mg, Lacosamide 300mg

R14	26	M	GTC, MJ	17	Normal	Typical	No	JME	Levetiracetam 3000mg, Lamotrigine 450mg
R15	27	F	GTC, MJ	11	Normal	Typical	No	JME	Zonisamide 400mg, Clonazepam 1mg, Brivaracetam 150mg
R16	34	F	GTC, MJ	24	Normal	N/A	No	JME	Levetiracetam 3000mg, Clobazam 15mg, Gabapentin 300mg
R17	37	F	GTC, MJ, Abs	17	Normal	N/A	No	JME	Valproate 1500mg, Levetiracetam 1500mg
R18	26	F	GTC, MJ, Abs	10	Normal	Typical	No	JME	Valproate 1000mg, Clobazam 10mg
R20	18	M	Abs	10	Normal	Typical	No	JAE	Valproate 2000mg, Ethosuximide 500mg

*R03 and R19 excluded from analysis to slow background rhythm of EEG. F – female, M-male, GTC- generalised tonic-clonic, MJ- myoclonic jerk, Abs- absence, JAE- juvenile absence epilepsy, CAE- childhood absence epilepsy, JME- juvenile myoclonic epilepsy, EGTSCA- IGE with generalised tonic-clonic seizures alone, NA- not available, typical - previous EEG recording showing bilaterally synchronous spike/polyspike wave discharges on normal background.

Table 1 c. Demographic details of control participants

Participant	**Age**	**Sex**
C01	25	F
C02	57	M
C03	36	M
C04	40	M
C05	27	M
C06	22	F
C07	32	F
C08	29	F
C09	27	M
C10	22	M
C11	26	M
C12	19	M
C13	22	F
C14	22	F
C16	30	M
C17	24	M
C18	21	F
C19	25	F
C20	22	M
C21	23	F

M- male, F-female

Chapter 3. Interictal structural and functional connectivity in IGE: A systematic review of graph theoretical studies

This manuscript is published in Epilepsy & Behavior (March 2020).

3.1 Authors

Emily J. Pegg[1,2], Jason R. Taylor[2,3], Simon S. Keller[4,5], Rajiv Mohanraj[1,2]

[1] Department of Neurology, Manchester Centre for Clinical Neurosciences, Salford Royal NHS Foundation Trust.

[2] Division of Neuroscience and Experimental Psychology, School of Biological Sciences, Faculty of Biology, Medicine and Health, University of Manchester.

[3] Manchester Academic Health Sciences Centre.

[4] Department of Molecular and Clinical Pharmacology, Institute of Translational Medicine, University of Liverpool.

[5] The Walton Centre NHS Foundation Trust, Liverpool.

3.2 Abstract

The evaluation of the role of anomalous neuronal networks in epilepsy using a graph theoretical approach is of growing research interest. There is currently no consensus on optimal methods for performing network analysis and it is possible that variations in study methodology account for diverging findings. This review focuses on global functional and structural interictal network characteristics in people with Idiopathic Generalised Epilepsy (IGE) with the aim of appraising the methodological approaches used and assessing for meaningful consensus.

Thirteen studies were included in the review. Data were heterogenous and not suitable for meta-analysis. Overall, there is a suggestion that the cerebral neuronal networks of people with IGE have different global structural and functional characteristics to people without

epilepsy. However, the nature of the aberrations is inconsistent with some studies demonstrating a more regular network configuration in IGE, and some, a more random topology. There is greater consistency when different data modalities and connectivity subtypes are compared separately, with a tendency towards increased small-worldness of networks in functional EEG/MEG studies and decreased small-worldness of networks in structural studies.

Prominent variation in study design at all stages is likely to have contributed to differences in study outcomes. Despite increasing literature surrounding neuronal network analysis, systematic methodological studies are lacking. Absence of consensus in this area significantly limits comparison of results from different studies, and the ability to draw firm conclusions about network characteristics in IGE.

3.3 Introduction

3.3.1 Background

Epilepsy is estimated to affect around 70 million people worldwide (Ngugi et al., 2010), 15- 20% of whom have Idiopathic Generalised Epilepsy (IGE) (Jallon and Latour, 2005). IGE comprises a group of electro-clinical syndromes including Childhood Absence Epilepsy (CAE), Juvenile Absence Epilepsy (JAE), Juvenile Myoclonic Epilepsy (JME) and Epilepsy with Generalised Tonic-Clonic Seizures Alone (EGTCSA) (Scheffer et al., 2017). The hallmark of IGE is the occurrence of bilateral symmetric and synchronous epileptiform discharges on electroencephalography (EEG) in the ictal and interictal states, which represents hyper-synchronised activity of large-scale brain networks (Wolf and Beniczky, 2014). It is likely that seizures occur as emergent phenomena from dynamics of brain networks (Richardson, 2012b). Elucidating the properties of interictal brain networks is therefore vital in understanding the complex dynamical system from which seizures arise.

Brain networks have been described as "maps of structural or functional interactions (termed links) between brain regions (termed nodes)" (Rubinov and Bullmore, 2013). Another, commonly quoted, definition of a neuronal network is a "functionally and anatomically connected, bilaterally represented, set of cortical and subcortical brain structures and regions in which activity in one part affects activity in all the others" (Spencer, 2002). However, a cerebral neuronal network may not necessarily be bilaterally derived and can be delineated at the anatomical *or* functional level. We suggest that a neuronal network be defined as 'a

system of functionally or structurally connected areas of the brain in which activity in one component can influence the activity of all other components, and can affect the system as a whole'. This definition also emphasises the concept of the brain functioning via a system comprising numerous, interacting networks.

Since the corticoreticular theory of seizure generation was proposed (Gloor, 1968), evidence of the involvement of the thalamic and thalamocortical networks in IGE has accumulated (Bernhardt et al., 2009, Aghakhani et al., 2004, Gotman et al., 2005, Hamandi et al., 2006). A recent review of 24 studies reported reduced connectivity in the Default Mode Network (DMN) across the IGE subtypes (Parsons et al., 2020). Abnormal resting state networks are also associated with cognitive impairment in IGE (Li et al., 2015a, Li et al., 2017). Unanswered questions include how the multifarious networks of the brain interact, how seizures emerge from these networks, and how certain influences (e.g., sleep deprivation) render networks vulnerable to seizures. The answer to this is likely to involve complex dynamical interactions (Richardson, 2012b).

Graph theory is a mathematical technique which generates representation of any complex system as a collection of nodes (vertices) and links (edges) between pairs of nodes. Graph theory-based methods are well established in analysing structural and functional brain networks (Sporns, 2018). Using this framework, it may be ultimately possible to predict ictal onset or develop anti-epileptogenic (as opposed to anti-seizure) medication. Graph theoretical analyses of neuroimaging data have the potential to identify objective biomarkers of epilepsy. This could improve diagnostic utility of these modalities, compared to conventional visual analysis alone, and help reduce the rate of misdiagnosis of epilepsy (Smith et al., 1999, Benbadis and Allen Hauser, 2000). Graph theory approaches may also aid syndromic classification of epilepsy, and serve as a prognostic biomarker of cognitive impairment and response to treatment (Tavakol et al., 2019). In focal epilepsy, there is growing interest in the use of graph theory in the identification of surgical targets and in the prediction of post-surgical outcomes (Tavakol et al., 2019).

Numerous studies suggest that people with epilepsy have different global interictal network characteristics to those without epilepsy (Chowdhury et al., 2014, Elshahabi et al., 2015, Chavez et al., 2010, Lee and Park, 2019, Liao et al., 2013, Zhang et al., 2011, Xue et al., 2014a, Qiu et al., 2017, Bonilha et al., 2014). In focal epilepsy, a meta-analysis of studies of global connectivity measures showed more segregated and more regular networks in patients compared to controls (van Diessen et al., 2014b). However, similar studies in IGE show inconsistent results.

Studies have adopted a variety of approaches to network analysis, which may account for differences in observed results. To our knowledge, there is no published review summarising global connectivity studies in IGE.

3.3.2 Measuring connectivity in brain networks

Types of connectivity

Network studies may examine the global network, or specific networks (e.g., the thalamocortical network). Structural connectivity refers to anatomical connections between spatially separate brain areas. Functional networks are inferred connections between distinct brain areas, based on statistically correlated measures of neuronal activity (Friston, 2011). Effective connectivity measures the influence of activity in one area over another and is thus a dynamic measurement which may be used to examine causality (Friston, 2011, Aertsen et al., 1989). Most studies of IGE have examined structural or functional connectivity of brain networks. The relationship between structural and functional connectivity is unclear, and therefore the results from the two types of studies should not be interpreted in a combined fashion. Functional networks derived from different techniques (EEG/ magnetoencephalography (MEG) versus functional magnetic resonance imaging (fMRI)) may also have different properties, due to differences in data acquisition, and therefore are not directly comparable.

Data collection modalities

Structural connectivity data can be acquired from structural magnetic resonance imaging (MRI) or from diffusion tensor imaging (DTI). Using structural MRI, connections are derived from covariance patterns- i.e., morphologic correlations of structural anatomical features. DTI relies on measuring diffusivity of water molecules, which is constrained by white matter tracts. From the unevenness of water diffusivity (the anisotropy), white matter tracts can be delineated (Clayden, 2013).

Functional connectivity data may be obtained from fMRI using Blood Oxygen Level-Dependent (BOLD) techniques, EEG, or MEG. Compared to EEG and MEG, fMRI provides improved spatial resolution, although this may still be insufficient to detect all relevant connections (Engel et al., 2013b). fMRI has poor temporal resolution relative to other modalities with a typical sampling rate of 0.5 Hz (repetition time of 2 seconds) and a peak haemodynamic response function of around 6 seconds. EEG and MEG have superior temporal

resolution compared to fMRI with a typical sampling rate of 500-1000 Hz. Both techniques, therefore, provide time resolution in the order of milliseconds, which reflects neuronal communication in real time (Fornito et al., 2016). Both scalp EEG and MEG may be limited by 'field spread', where numerous electrodes detect signal from a single source (Sarvas, 1987) and volume conduction – a "data blurring" effect caused by conduction properties of the skull and scalp (van den Broek et al., 1998). This particularly affects EEG and both factors can complicate connectivity analysis.

Network construction and analysis

(Figure 14) Graph theory offers a mathematical/computational framework for analysing networks. Within this construct, networks are represented as a graph, with brain areas represented by 'nodes' (or 'vertices') and the connections between them by 'edges'. A large number of different approaches have been employed in network construction in both structural and functional connectivity studies, the choice of which affects interpretation of network characteristics (Stanley et al., 2013, Butts, 2009).

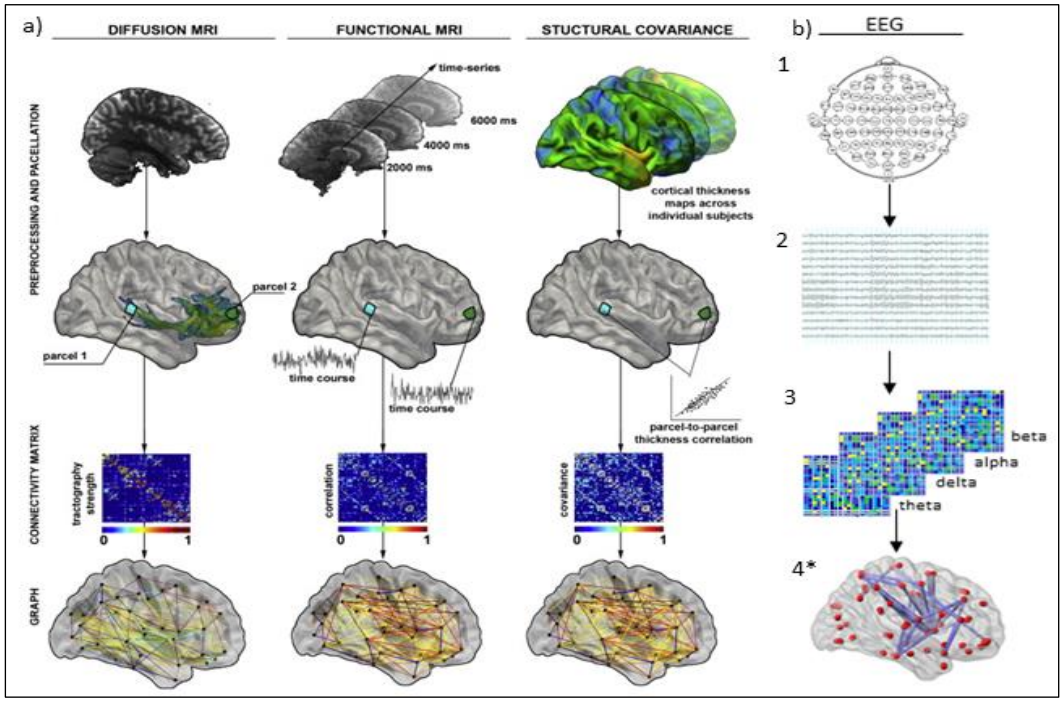

Figure 14. Schematic overview of graph construction using diffusion MRI, fMRI, structural covariance and EEG. a) Reproduced with permission from the publisher. Network analysis for a network disorder: The emerging role of graph theory in the study of epilepsy. Bernhardt et al. Epilepsy and Behavior, 2015. b) Figs. 1, 2, and 4 reproduced from Wikimedia Commons. http://www.plosone.org/article/info%3Adoi%2F10.1371%2Fjournal.pone.00578314* A separate graph for each frequency band is produced.

In network studies derived from MRI, a common approach to represent nodes is to parcellate co-registered anatomical MRI using a validated scheme. This includes schemes based on macroscopic landmarks, for example Automated Anatomical Labelling (Tzourio-Mazoyer et al., 2002) or FreeSurfer parcellation atlases (Fischl, 2012), or on cytoarchitecture, for example Brodmann areas. These have the advantage of being standardised methods (Stanley et al., 2013) but limitations are that nodes may not reflect meaningful separations of the brain at a functional level and bias may be introduced due to varying size of parcellation areas (Fornito et al., 2016). The issue of unequal node sizes may be addressed by parcellating data into random, evenly sized parcels or by grouping together measurement points (i.e., voxels) based on shared connectivity features, which have been determined *a priori* (Fornito and Bullmore, 2010, Zalesky et al., 2010, Hagmann et al., 2007). Alternatively, each voxel can be treated as a node. This has the advantage of being data-driven rather than being constrained by interpretation based on anatomical boundaries (Stanley et al., 2013). Disadvantages of this approach are that data may be noisy (Stanley et al., 2013, Fornito et al., 2016), connections between neighbouring nodes may be spurious (Stanley et al., 2013) and it is computationally demanding. In EEG and MEG studies, nodes are represented by electrodes, sensors, or sources.

Edges in structural networks can be inferred from anatomical MRI alone, or more typically by combining MRI with DTI. Using structural MRI alone, connections are derived from covariance patterns (i.e. morphologic correlations) of features such as cortical thickness or volume (Mechelli et al., 2005). Such correlations suggest a functional-trophic connection, but do not correspond to a direct anatomical connection (Bernhardt et al., 2013). Using DTI, estimates of structural connections can be derived using deterministic tractography, which relies on following the direction of water diffusion from a voxel seed location until a new measurement is reached, with the process continuing until all the DTI streamline has been outlined (Conturo et al., 1999, Mori et al., 1999). However, the direction and distribution of diffusion at each measurement point is uncertain since each voxel contains many connections on a very small scale (Fornito et al., 2016). Probabilistic tractography takes into account these uncertainties by producing estimates for each, and incorporating them into a model based on the likelihood of each estimate (Behrens et al., 2003). This approach is reported to produce better sensitivity for determining connections (Behrens et al., 2007).

In functional connectivity studies, edges are typically determined using correlation coefficients (or similar measures) in the time domain or coherence measures in the frequency domain (Fornito et al., 2016). A binary approach means that a connection is determined as

either being absent or present using a selected threshold value. An alternative is to weight edges according to the strength of the signal. This reduces the influence of statistically non-significant connections, which are postulated to be physiologically less important (Rubinov and Sporns, 2010). The directionality of a connection may also be incorporated to form a directed graph *(Figure 15)*.

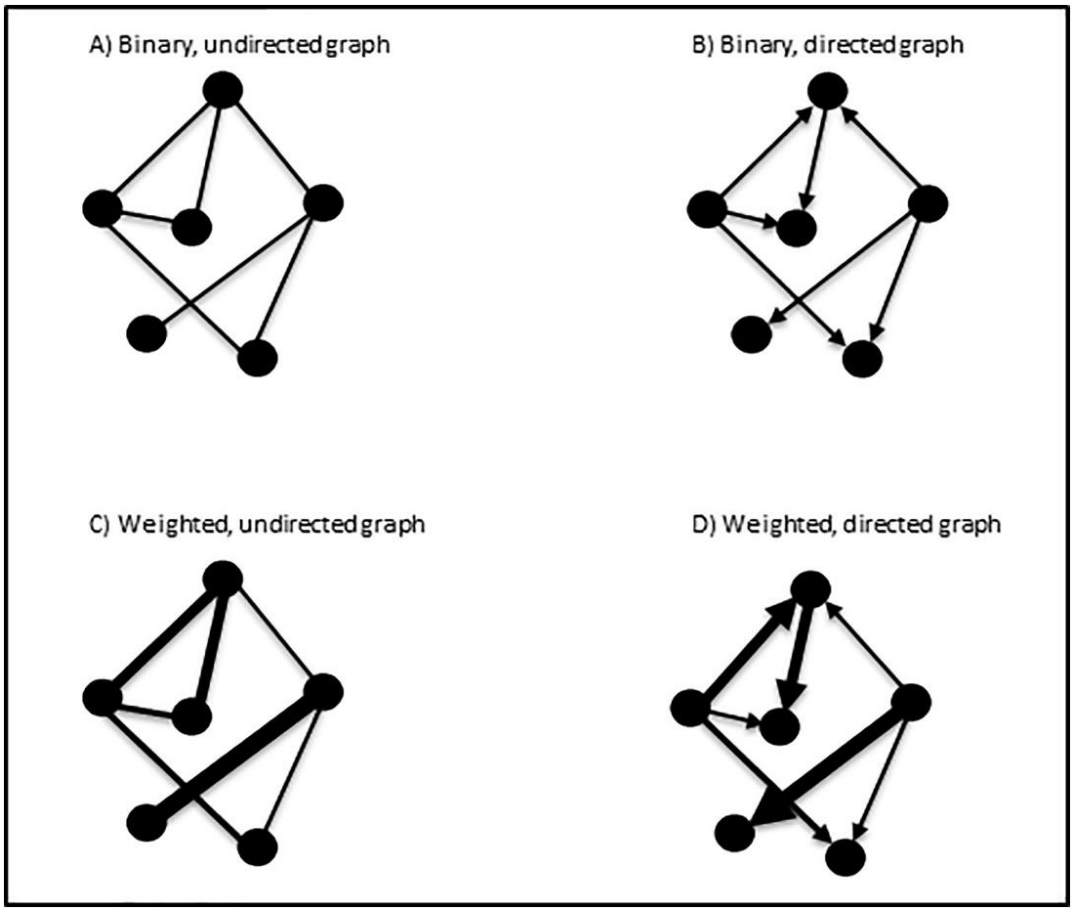

Figure 15. Visual representation of different graph types according to edge features. Images A–D depict graph types according to whether edges are binary or weighted and directed or undirected. The thickness of an edge represents the connection strength.

Measures of network connectivity

There are many graph theoretic metrics, each providing different characterisations of network organisation (for review see (Rubinov and Sporns, 2010)). Principal measures in epilepsy network studies include clustering coefficient, path length, global efficiency, and centrality measures *(table 2, page 99)*. Clustering coefficient is a measure of connectivity between neighbours of a node and represents local network connectivity or segregation. Mean path length is the average distance between each pair of nodes in the network and is a measure of network integration. Regular networks are those which have a high clustering coefficient and high path length. Conversely, random networks have a low clustering coefficient and low path length. Global efficiency is the inverse of the mean path length, and is a measure of efficiency of information transfer. Centrality measures evaluate the importance of particular nodes in networks. Nodes with high centrality are believed to represent network hubs, which play an important role in the transfer of information through the network (Freeman, 1978). It has been proposed that altered network topology, as a result of a change in network hubs, is the final common pathway in many neurological diseases (Stam, 2014).

When a small number of connections in a regular graph are 'rewired' to form 'long-range' connections, there is a drop in path length with very little change in the clustering coefficient: this is a key feature of networks with small-world properties *(figure 16)*.

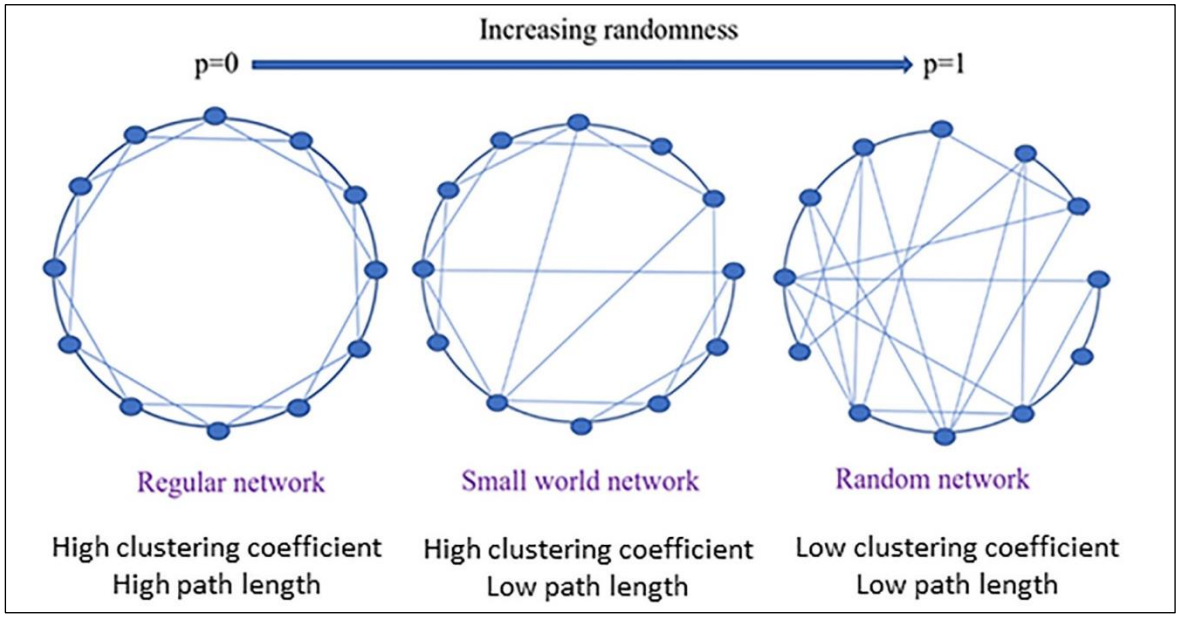

Figure 16. Example representations of regular, random and small-world networks. Connections in a regular graph are 'rewired' to form 'long-range' connections resulting in a drop in path length with minimal change in clustering coefficient. This is a key feature of networks with small-world properties (Watts and Strogatz, 1998).

In their seminal study, Watts and Strogatz (Watts and Strogatz, 1998) demonstrated small-worldness to be a feature of the electrical grid of the USA, a network of film actors, and the whole neuronal network of the *Caenorhabditis elegans* worm. Since then, small-worldness has been demonstrated to exist in various human cerebral cortical network studies at a macroscopic level (e.g., (Achard et al., 2006, He et al., 2007, Iturria-Medina et al., 2008)). A small-world network is regarded to be efficient as it facilitates rapid transmission and integration of information throughout the network (Bassett and Bullmore, 2006).

It is important to note that the number of nodes of a graph and the number of connections from each node (degree) affects connectivity measures (the node-degree dependency) (van Wijk et al., 2010). This highlights the importance of the choice of node and edge representation but also makes comparison of networks of different sizes and densities challenging.

3.3.3 Aim of the review

The aim of this systematic review is to summarise the outcome measures of graph theoretical studies of global functional and structural interictal networks in IGE, to examine for meaningful consensus and to discuss potential methodological limitations in this research area.

3.4 Methods

3.4.1 Search strategy

PRISMA guidelines were used to conduct the review (Moher et al., 2009). Studies were identified following a PubMed search using the following search strategy:

(Epilepsy[Text Word]) AND ((((((((((network analysis[Text Word]) OR network[Text Word]) OR graph theory[Text Word]) OR graph theoretical analysis[Text Word]) OR small world[Text Word]) OR path length[Text Word]) OR clustering coefficient[Text Word]) OR connectivity[Text Word] OR global efficiency[Text Word] OR hub nodes [Text word] or centrality [Text word]) Filters: Humans; English

Study titles and abstracts were screened by me. Studies were included that compared the networks of people with IGE to controls using measures of clustering coefficient, path length,

small-worldness, global efficiency or centrality measures. These measures were selected as they are frequently used in network studies and provide broad representation of key network characteristics. Included IGE syndromes, or terms, were: Idiopathic Generalised Epilepsy (IGE), Idiopathic Generalised Epilepsy with generalised tonic-clonic seizures alone (EGTCSA), Idiopathic Generalised Epilepsy with generalised tonic-clonic seizures (IGE-GTCS), Juvenile Myoclonic Epilepsy (JME), Juvenile Absence Epilepsy (JAE), Childhood Absence Epilepsy (CAE), Jeavons syndrome, genetic generalised epilepsy, primary generalised epilepsy. Reviews, focal epilepsy studies, animal studies, non-English language studies, studies which did not have a control group, and studies where results were obtained via visual inspection rather than statistical analysis were excluded. There were some studies which included both focal epilepsy and IGE (Garcia-Ramos et al., 2017). Where it was not possible to separate the results of the IGE group, or where it was not possible to separate IGE data from other generalised epilepsies (e.g., metabolic aetiologies (van Diessen et al., 2016)), data were not included. The date of the last search was the 18th of July 2019.

3.4.2 Data extraction

The following aspects of each study were recorded: Data acquisition modality and parameters (e.g., number of EEG channels, field strength of MRI scanner, parcellation scheme), participant numbers, medication use, network construction, network metrics used and outcomes for each metric. For the majority of studies, quantitative result data was not provided; rather comparative results were expressed e.g., an outcome measure was said to be higher to or lower than controls. If relevant information was not explicit, the corresponding study author was contacted with the aim of obtaining it.

3.5 Results

(Figure 17) The search strategy identified 2728 papers. After exclusion based on titles and abstracts, 30 potentially eligible full studies were reviewed and 13 met the eligibility criteria. These comprised seven structural connectivity analyses (Xue et al., 2014a, Bonilha et al., 2014, Qiu et al., 2017, Zhang et al., 2011, Caeyenberghs et al., 2015, Lee and Park, 2019, Liao et al., 2013) and nine functional connectivity analyses (Clemens et al., 2013, Chowdhury et al., 2014,

Chavez et al., 2010, Elshahabi et al., 2015, Niso et al., 2015, Lee and Park, 2019, Wang et al., 2017, Liao et al., 2013, Zhang et al., 2011). Three studies evaluated both functional and structural connectivity (Zhang et al., 2011, Lee and Park, 2019, Liao et al., 2013).

Data has been presented separately for structural and functional studies because the precise relationship between structural and functional connectivity is not known, as discussed above. Furthermore, it has been demonstrated that there is uncoupling between functional and structural networks in epilepsy (Zhang et al., 2011). Therefore, assimilating the results may not be appropriate. Within the functional studies, EEG/MEG and fMRI outcome data has also been presented separately because reconciling outcomes using these two distinct methods is complex (Chowdhury et al., 2014) and therefore combined results may obscure any differences.

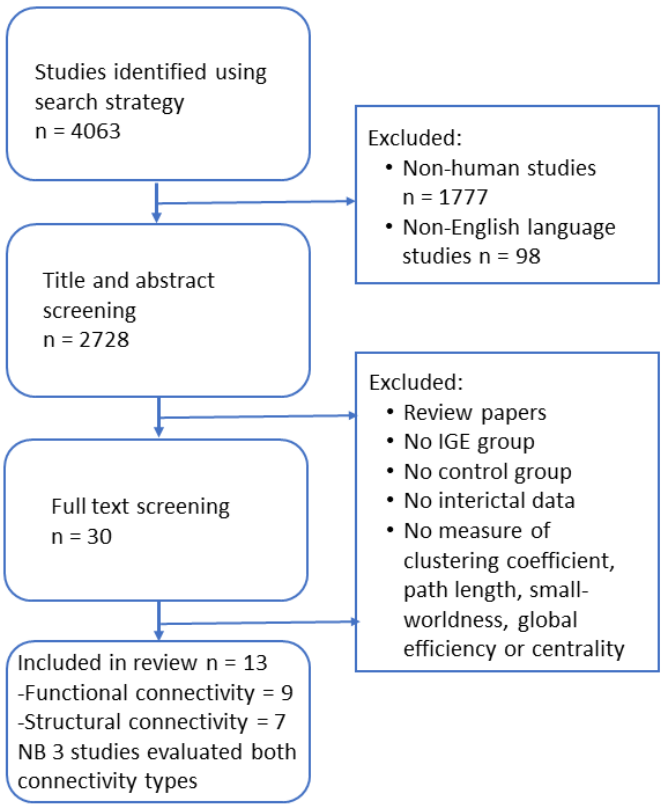

Figure 17. Review flow diagram

3.5.1 Participant demographics

3.5.1.1 Functional network studies *(table 3, page 101)*

MEG/EEG studies

A total of 123 people with IGE were included (range n=5 to n=36) in the six studies of functional connectivity using EEG/MEG (Clemens et al., 2013, Chowdhury et al., 2014, Elshahabi et al., 2015, Niso et al., 2015, Chavez et al., 2010, Lee and Park, 2019, Liao et al., 2013). This group comprised the following IGE subtypes: EGTCSA (n=17), JME (n=64), CAE (n=10), JAE (n=6), Jeavons syndrome (n=1), unclassified / unspecified (n=20), and absences (without further clarification) (n=5). Average age of participants in each study ranged from 18.2 years to 38.6 years. One study did not report the age and sex of all five subjects included in that investigation (Elshahabi et al., 2015). In the remaining studies, 61.9% (n=73) of participants were female. Epilepsy duration was not reported in two studies (Niso et al., 2015, Chavez et al., 2010). In one study the mean epilepsy duration was four months (range up to five years) (Clemens et al., 2013) and in the remaining, median duration ranged from 2.25 years to 21.5 years. Medication information was not provided for all five patients in one study (Elshahabi et al., 2015). In two studies, no participants were taking medication on account of being newly diagnosed (Clemens et al., 2013, Lee and Park, 2019). In the other studies, 12.3% (n=11) were not taking an AED, despite some having uncontrolled epilepsy.

All studies had a similar number of participants in the control group. In one study there was no demographic information regarding the controls (n=5) (Elshahabi et al., 2015). In the remaining five studies, there was no significant difference in age or sex of controls compared to IGE groups.

fMRI studies

These three studies (Zhang et al., 2011, Wang et al., 2017, Liao et al., 2013) comprised a total of 110 participants with IGE, of whom 85 (77.3 %) had EGTCSA (Zhang et al., 2011, Liao et al., 2013) and 25 (22.3%) had CAE (Wang et al., 2017). The same 26 participants took part in both the study by Zhang et al and by Liao et al. Mean age was 24.12 years in the EGTCSA studies and 10.5 +/- 3.3 years in the CAE study. In total, 44.5% (n=49) were female. Mean epilepsy duration was 6.92 years in one EGTCSA study (Zhang et al., 2011), 7.83 years in another (Liao et al., 2013), and 3.7 years in the CAE study (Wang et al., 2017). 39% (n=43) of participants with epilepsy were not taking an AED. There were an equal number of controls and they did not significantly differ from the IGE group in age or sex in any study.

3.5.1.2 Structural network studies *(table 4, page 104)*

A total of 211 participants with IGE were included from seven studies (Zhang et al., 2011, Xue et al., 2014a, Bonilha et al., 2014, Qiu et al., 2017, Caeyenberghs et al., 2015, Lee and Park, 2019, Liao et al., 2013). Thirty-eight (18%) were diagnosed with CAE, 70 (33%) with JME, 85 (40%) with IGE-GTCS and in 18 (8.5%) (Bonilha et al., 2014) the subtype was not specified. Mean age ranged from 8.05 years to 26 years. It was not possible to combine age data due to lack of individual participant information in one study (Bonilha et al., 2014). 49.2% (n=104) of patients were female. Median duration of epilepsy in each study ranged from less than one year (Bonilha et al., 2014, Qiu et al., 2017) to 16.1 years (Caeyenberghs et al., 2015). In one study, it was not clear how many participants were taking an AED (Bonilha et al., 2014). In one study no participant was taking an AED (Caeyenberghs et al., 2015) and in the others 26.1% (n= 41) of patients were not taking an AED.

One study used first cousins as controls (Bonilha et al., 2014). There was no difference in age or sex between epilepsy groups and controls in any study.

3.5.2 Data acquisition and network construction

3.5.2.1 Functional network studies

Data collection modalities comprised fMRI in three studies (Zhang et al., 2011, Liao et al., 2013, Wang et al., 2017), EEG in three (Clemens et al., 2013, Chowdhury et al., 2014, Lee and Park, 2019) and MEG in three (Chavez et al., 2010, Elshahabi et al., 2015, Niso et al., 2015).

EEG/MEG studies

The number of electrodes in two EEG studies was 19 (Clemens et al., 2013, Chowdhury et al., 2014) and in the other 18 (Lee and Park, 2019). All used a 10-20 montage. One MEG study used 151 axial gradiometer sensors (Chavez et al., 2010), one used 275 axial gradiometer sensors (Elshahabi et al., 2015) and the third used 306 channels (102 magnetometers and 204 planar gradiometers) (Niso et al., 2015). All EEG/MEG studies used eyes-closed resting state data, except possibly in one where this information was not provided (Lee and Park, 2019). Length of data used ranged from a total of 5 seconds to 300 seconds. One EEG study re-referenced to the common average (Chowdhury et al., 2014), one used Fpz as an online reference then re-referenced offline to linked earlobes (Clemens et al., 2013), and in the other the method of re-

referencing is unclear (Lee and Park, 2019). There were no studies where automated artefact removal was used, and in all instances artefact free epochs were chosen using 'expert selection'. Each EEG/MEG study used slightly different frequency bands (see figures 18-20) and in one study the frequency bands were not stated (Lee and Park, 2019). Data were downsampled to between 200 Hz and 1250 Hz. Bandpass filtering was inconsistent between studies with the narrowest range 0.7-70 Hz and the widest 0.1-330 Hz. Synchronisation between nodes in the EEG/MEG studies was identified using phase-based methods in three studies (Elshahabi et al., 2015, Niso et al., 2015, Chowdhury et al., 2014). One study used spectral coherence (Chavez et al., 2010), one used a power-based method (Lee and Park, 2019) and the remaining used spatial-temporal correlation coefficient of current source density (Clemens et al., 2013). All created weighted networks.

fMRI studies

The fMRI study data were acquired using a 3 Tesla (3T) scanner whilst participants rested with eyes closed. In two of the three studies, there were 250 whole-brain echo-planar image volumes (Zhang et al., 2011, Liao et al., 2013), and in the other 210 (Wang et al., 2017). Data were parcellated into 210 regions in one study using a voxel-wise approach (Wang et al., 2017) and the other two used Automated anatomical labelling (AAL) (Tzourio-Mazoyer et al., 2002) with 90 and 1024 parcellations (Zhang et al., 2011, Liao et al., 2013). In all, Pearson correlation coefficients between time courses were used to produce edges and a threshold applied to outcomes to produce weighted graphs.

3.5.2.2 Structural network studies

Four studies used DTI to acquire data (Xue et al., 2014a, Qiu et al., 2017, Zhang et al., 2011, Caeyenberghs et al., 2015) and three derived networks via structural covariance analysis using 1.5 or 3T structural MRI (Bonilha et al., 2014, Lee and Park, 2019, Liao et al., 2013).

DTI based studies (table 5, page 106)

All four DTI-based studies used 3T MRI. The number of diffusion directions was 30 in three studies (Qiu et al., 2017, Zhang et al., 2011, Caeyenberghs et al., 2015) and 50 in the other (Xue et al., 2014a). Only one study stated the use of cardiac gating (Caeyenberghs et al., 2015).

Number of slices ranged from 45 to 60. All four studies used AAL (Tzourio-Mazoyer et al., 2002) to parcellate data. Three studies used DTI deterministic tractography to define the network edges and one used probabilistic tractography (Qiu et al., 2017). The scale of parcellation i.e., the number of nodes, was 116 in one study (Caeyenberghs et al., 2015). The other three studies all used 90 nodes (Xue et al., 2014b, Qiu et al., 2017) and one of these studies also constructed a 'high density' network comprising 1024 nodes (Zhang et al., 2011). The graph was weighted in three studies (Xue et al., 2014a, Qiu et al., 2017, Zhang et al., 2011) and unweighted in the other (Caeyenberghs et al., 2015).

Structural covariance-based studies

Of the three structural covariance studies, one used the AAL atlas to parcellate data into 90 and 1024 nodes (Liao et al., 2013), another used the Destrieux atlas (Destrieux et al., 2010) with 171 nodes (Bonilha et al., 2014) and the third parcellated data into 80 regions (Lee and Park, 2019) using FreeSurfer (Fischl, 2012). All created weighted graphs.

3.5.3 Statistical considerations

All EEG/MEG studies with significant results except one (Elshahabi et al., 2015) corrected for multiple comparisons for the frequency bands tested. One functional study adjusted for age and sex of participants (Xue et al., 2014a). The remaining studies did not control for these factors.

3.6 Study Results

Network measurements were not suitable for statistical meta-analysis because in most studies quantitative results were not provided. Instead, results were generally expressed in terms of the IGE group relative to the control group. Furthermore, there was heterogeneity in outcome measures used and how the measures were calculated i.e., whether mean or normalised values were used.

For brevity, where the terms 'increased' and 'decreased' or 'greater' have been used in this section, it refers to the result of participants with IGE compared to controls. In this section, clustering coefficient is abbreviated to C, and path length to L.

3.6.1 Functional network studies

3.6.1.1 EEG/MEG studies

a. Clustering coefficient (C) *(figure 18)*

Four of six studies reported this outcome (Chowdhury et al., 2014, Lee and Park, 2019, Chavez et al., 2010, Elshahabi et al., 2015). Two studies found an increase in C. In one study this was found in the 6-9 Hz band (EEG study; no difference found at 1-5 Hz, 10-11 Hz, 12-19 Hz or 21-70 Hz) (Chowdhury et al., 2014). In the other study with increased C, this was found in the 5-14 Hz band (MEG study; no difference found at <5 Hz, 15-24 Hz or 24 -35 Hz) (Chavez et al., 2010). The other two studies did not find a difference.

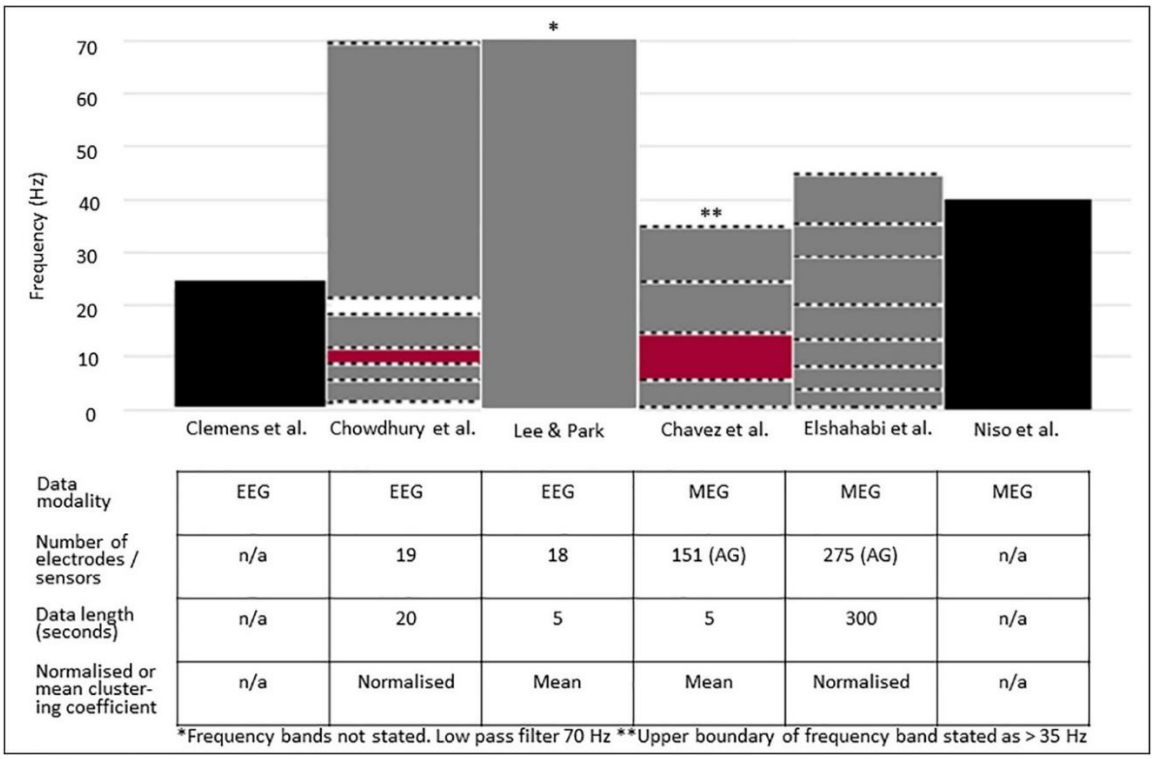

Data modality	EEG	EEG	EEG	MEG	MEG	MEG
Number of electrodes / sensors	n/a	19	18	151 (AG)	275 (AG)	n/a
Data length (seconds)	n/a	20	5	5	300	n/a
Normalised or mean clustering coefficient	n/a	Normalised	Mean	Mean	Normalised	n/a

*Frequency bands not stated. Low pass filter 70 Hz **Upper boundary of frequency band stated as > 35 Hz

Figure 18. Result summary of clustering coefficient analyses in EEG/MEG studies. Dotted line shows boundary lines for the frequency bands tested. ■ = Clustering coefficient not tested. ■ = No difference found between groups. ■ = Statistically significant greater value in IGE compared with controls. AG = axial gradiometer. n/a = not applicable.

b. Characteristic path length (L) *(figure 19)*

This was evaluated in three EEG/MEG studies (Chowdhury et al., 2014, Lee and Park, 2019, Elshahabi et al., 2015). One study, using MEG, reported a decreased value in the 12-20 Hz

band (no difference found at 0-4 Hz, 4-8 Hz, 8-12 Hz, 21-29 Hz or 35- 45 Hz) (Elshahabi et al., 2015). The other two studies (both EEG) did not find a difference between the groups.

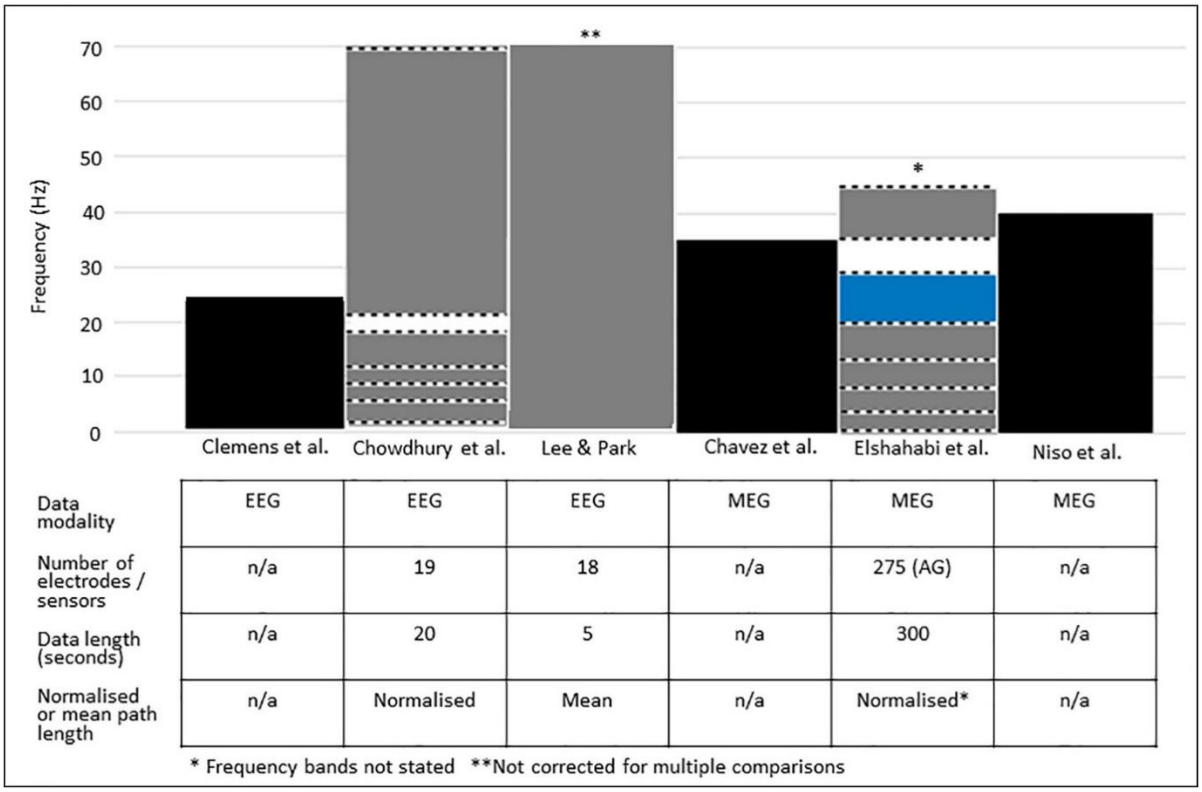

Data modality	EEG	EEG	EEG	MEG	MEG	MEG
Number of electrodes / sensors	n/a	19	18	n/a	275 (AG)	n/a
Data length (seconds)	n/a	20	5	n/a	300	n/a
Normalised or mean path length	n/a	Normalised	Mean	n/a	Normalised*	n/a

* Frequency bands not stated **Not corrected for multiple comparisons

Figure 19. Result summary of path length analyses in EEG/MEG studies. – Dotted line shows boundary lines for the frequency bands tested. ■ = Path length not tested. ■ = No difference found between groups. ■ = Statistically significant lower value in IGE compared with controls.

c. Small-worldness

Only one EEG study (Lee and Park, 2019) reported this outcome and no difference was found.

d. Global efficiency *(figure 20)*

Four studies measured global efficiency. Two reported greater efficiency (both MEG). In one the difference was found only in the 5-14 Hz frequency band (Chavez et al., 2010). (No difference found at <5 Hz, 15-24 Hz or 24 -35Hz). In the other study the difference was found at 12-20 Hz and 28-40 Hz (Niso et al., 2015). (No difference found at 0.1-4 Hz, 4-8 Hz, 8-12 Hz or 20-28 Hz). In the remaining two studies (both EEG), there was no difference found.

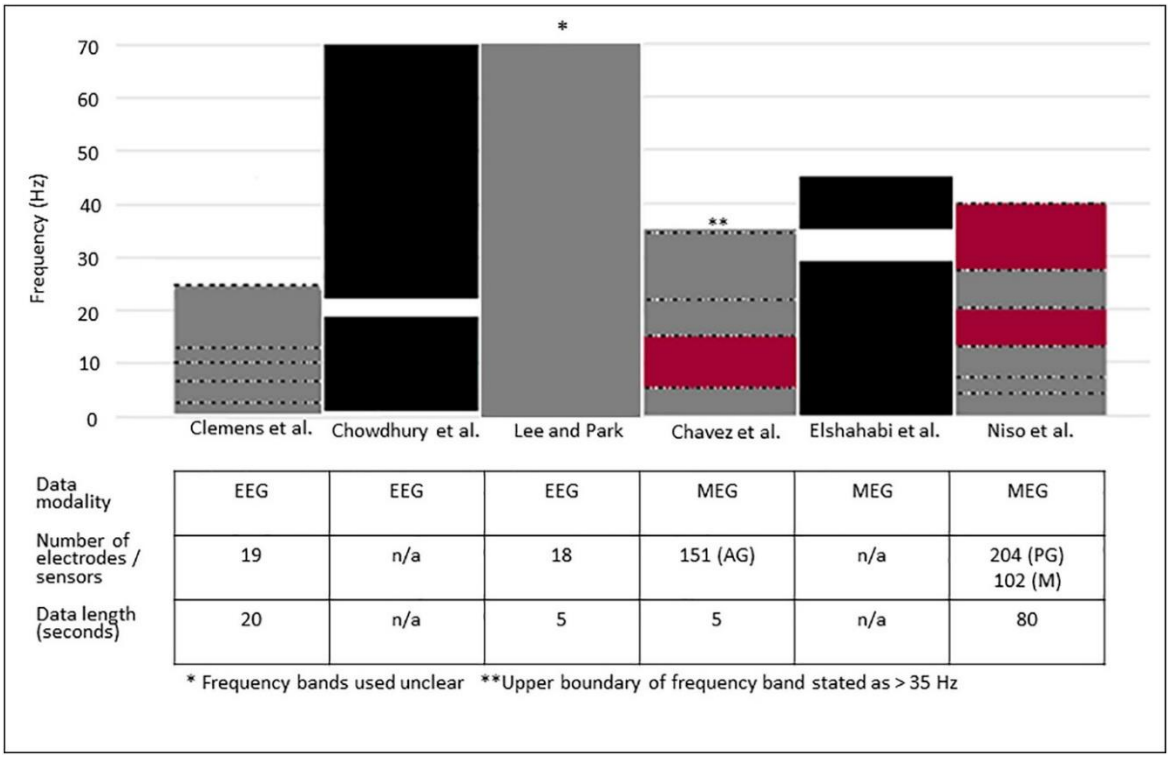

Figure 20. Result summary of global efficiency analysis in EEG/MEG studies. Dotted line shows boundary lines for the frequency bands tested. ■ = Global efficiency not tested. ■ = No difference found between groups. ■ = Statistically significant greater value in IGE compared with controls. AG = axial gradiometer. PG = planar gradiometer. M = magnetometer.

e. Centrality measures

This was evaluated in one EEG study and increased betweenness centrality at the F8 and C4 electrodes was found (Lee and Park, 2019).

3.6.1.2 fMRI studies

a. C, L, small-worldness and global efficiency (*figure 21*)

Two fMRI functional connectivity studies measured C, L and small-worldness. C was decreased in one study (90 nodes) (Zhang et al., 2011) with no difference in the other (Liao et al., 2013). Small-worldness was decreased in one study (90 nodes) (Zhang et al., 2011) and increased in the other (1024 nodes) (Liao et al., 2013). There was no difference in L in either

case. Global efficiency was unchanged in one study (Liao et al., 2013) and not tested in the others.

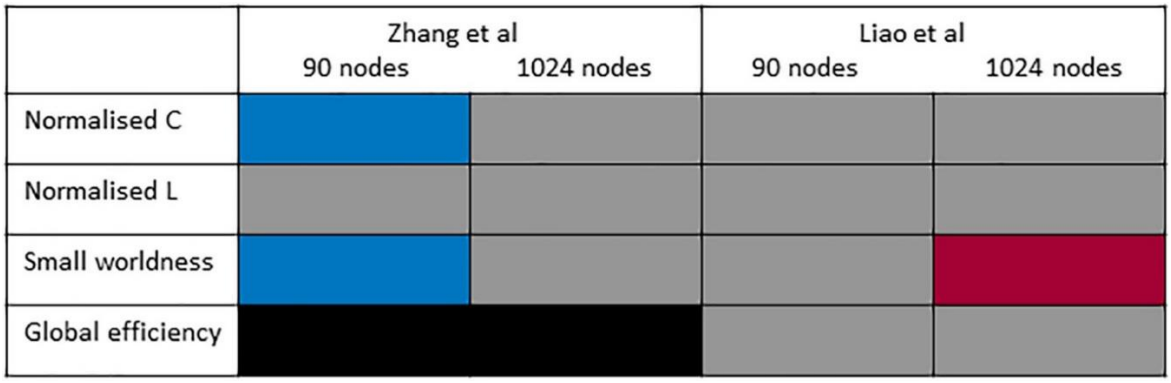

Figure 21. Visual summary of outcome measures from fMRI functional studies. This figure summarizes the results of the fMRI functional connectivity study for the following measures: Correlation coefficient (C) (mean and/or normalized value), path length (L) (mean and/or normalized value), small-worldness, and global efficiency. ■ = No significant difference between groups. ■ = Statistically significant lower value in the group with IGE relative to controls. ■ = Statistically significant higher value in group with IGE relative to controls. ■ = Not tested.

b. Centrality measures

Two studies reported this outcome measure. One reported decreased degree centrality in the following regions: Bilateral medial prefrontal cortex, left posterior cingulate gyrus, bilateral precuneus cortex, bilateral middle temporal cortex. Degree centrality was increased in the thalami bilaterally (Wang et al., 2017). Another fMRI study found increased betweenness centrality in the left calcarine fissure and a decreased value in the left lingual gyrus and left Heschl's gyrus (Zhang et al., 2011).

3.6.2 Structural network studies (*figure 22*)

a. Clustering coefficient (C)

This was calculated in all seven studies. Three studies reported decreased C (Zhang et al., 2011, Xue et al., 2014a, Qiu et al., 2017). In one of the studies reporting a decreased mean C, there

was no difference when normalised C was used (Xue et al., 2014a). In another of the studies reporting decreased C, this difference was only found in the lower density network (Zhang et al., 2011). One study did not find a difference between the groups (Lee and Park, 2019) and two studies reported an increased C (Bonilha et al., 2014, Liao et al., 2013). In the latter, this was in the lower density network only.

b. Path length (L)

This was evaluated in six studies. Three studies reported no difference between groups (Zhang et al., 2011, Caeyenberghs et al., 2015, Liao et al., 2013) and three reported an increased L (Xue et al., 2014a, Qiu et al., 2017, Lee and Park, 2019). Of the three reporting increased L, one study reported an increased mean L (Lee and Park, 2019), one reported no difference in normalised L but an increased mean L (Xue et al., 2014a), and the other study reported an increased mean and normalised L (Qiu et al., 2017).

c. Small-worldness

This was evaluated directly in six studies. Three reported no difference between the groups (Xue et al., 2014a, Caeyenberghs et al., 2015, Liao et al., 2013) and the other three found decreased small-worldness (Zhang et al., 2011, Qiu et al., 2017, Lee and Park, 2019). In one study this was in the low-resolution network only (Zhang et al., 2011).

d. Global efficiency

This was measured in five studies. Four reported it to be decreased (Xue et al., 2014a, Qiu et al., 2017, Bonilha et al., 2014, Lee and Park, 2019). In the remaining study, no difference between groups was found (Liao et al., 2013).

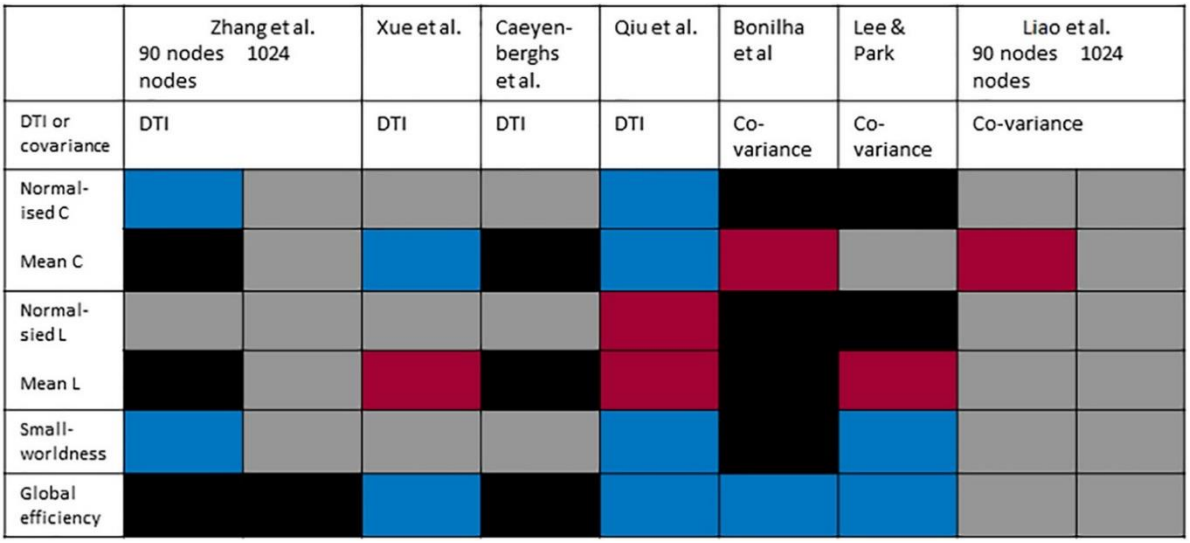

Figure 22. Visual summary of outcome measures from structural connectivity studies. This figure summarizes the results of the structural connectivity studies for the following measures: Correlation coefficient (C) (mean and/or normalized value), path length (L) (mean and/or normalized value), small-worldness, and global efficiency. ■ = No significant difference between groups. ■ = Statistically significant lower value in group with IGE relative to controls. ■ = Statistically significant higher value in group with IGE relative to controls. ■ = Not tested.

e. Centrality measures

Two structural studies measured this. One reported increased betweenness centrality in the following cortical areas: left caudal anterior cingulate, left precentral, left superior parietal, right precentral, right superior frontal. There was a decreased value in the left hippocampus (Lee and Park, 2019). In the other study there was increased betweenness centrality in the left superior parietal gyrus, right orbital part of superior frontal gyrus, and the right middle temporal gyrus. There was decreased centrality in the left cuneus, left superior occipital gyrus and right insula (Zhang et al., 2011).

3.7 Discussion

Most structural and functional connectivity studies in this review report altered connectivity in IGE. However, the results are inconsistent, with a large proportion of outcomes showing no difference and one study in each subset reporting a conflicting finding to the others (Zhang et al., 2011, Bonilha et al., 2014, Liao et al., 2013). Studies are notably heterogeneous in terms of sample size, participant demographics, data collection modalities, frequency bands used (for

EEG/MEG data), length of data used, scan acquisition parameters, post-acquisition data handling, graph construction, outcome metrics and statistical methods. These factors limit comparability between studies and may explain the variation in findings. Methodological studies to inform the various choices are currently lacking but would be of much benefit. In the meantime, a standardised method of performing and reporting graph theoretical analysis in neuroscience studies would greatly improve study comparability. In view of this, we have proposed a suggested framework for analysis and reporting of methods (t*able 6, page 107*).

In the functional EEG/MEG studies in which a difference was detected between groups, there was a higher clustering coefficient and higher global efficiency in the IGE group with some overlap in the frequencies at which this was detected (6-9 Hz for clustering coefficient and 12 Hz for global efficiency). This suggests that people with IGE have a functional network which is more locally clustered and more integrated i.e., more small-world. One fMRI study also reported greater small-worldness in the IGE group. However, the other fMRI study reported a lower clustering coefficient and lower small-world value. In the structural connectivity studies, there was generally lower local connectivity, lower global efficiency and a less small-world network in IGE. There were two exceptions to this, where a higher clustering coefficient was reported. However, these two studies used a different parcellation scheme than the others. There was some overlap in increased centrality measures in the following brain regions in two out of three structural studies: right superior frontal region, left superior parietal region and the precentral gyrus (left in one study and right in the other). Similarly, in the functional EEG study measuring betweenness centrality, there were increased values at the F8 and C_4 electrodes approximating to the right fronto-central area. This suggests that these nodes function as hub nodes in IGE. Differences in the study that did not find similar hub nodes are that the epilepsy group all had CAE (the other two were JME and IGE-GTCS) and a different centrality measure than the other two was used (degree centrality rather than betweenness centrality).

Considered as a whole, studies to date suggest that basic IGE network topology differs depending on whether structural or functional networks are evaluated, with a tendency towards increased small-worldness of networks in functional EEG/MEG studies and decreased small-worldness of networks in structural studies. However, the outcomes of the two fMRI functional studies were inconsistent with each other, thus adding to the complexity of synthesising results. There was more consistency between functional and structural studies for centrality measures. However, the low number of studies evaluating this caution against drawing firm conclusions.

fMRI and MEG/EEG connectivity data are not readily comparable, in part due to differing sensitivity of each modality to different time scales (Tracy, 2015, Singh, 2012). EEG and MEG are typically recorded at sampling rates of 200-1000+ Hz, enabling the detection of neuronal oscillations from sub-1Hz to 100Hz or higher. By contrast, fMRI is typically sampled at a rate of 0.5 Hz, corresponding to a repetition time (TR) of 2 seconds, and it is only indirectly sensitive to neuronal activity after convolution with the haemodynamic response function (HRF), which effectively low-pass filters the signal below about 0.1 Hz (Josephs and Henson, 1999). Both MEG and EEG have certain 'blind spots' – MEG has low sensitivity for deep sources and the sensitivity of both modalities is low for spherically arranged (therefore 'self-cancelling') sources such as the thalamus. fMRI data may be confounded by the presence of epileptiform activity, which is associated with increased long-range connections and reduced small-worldness (Lee et al., 2017). It is therefore possible that inherent properties of the modalities used are responsible for the variation in findings.

The relationship between functional and structural connectivity is not fully elucidated. The literature suggests that structural connectivity constrains functional connectivity, and that structural connectivity is more stable (Zhang et al., 2011). In IGE studies which have examined both types of connectivity, decoupling between functional and structural connectivity was found in one fMRI and DTI study (Zhang et al., 2011), whereas increased correlation was reported in another (Liao et al., 2013). However, these 2 studies used different methods to examine structural connectivity (DTI based and covariance methods respectively). It is possible that the contrasting outcomes between structural and functional studies, particularly when different data collection modalities are used, reflects failure to capture the complexity of the relationship.

There is evidence that small-world topology is affected by epilepsy duration (Dyhrfjeld-Johnsen et al., 2007, Haneef et al., 2015a). However, no studies controlled for this. Given the considerable range of epilepsy duration in the studies (from less than 1 year to 21.5 years), it is possible that this has confounded overall outcomes. Age and sex of participants were similar in patients and controls in all studies where this information was provided. Controlling for age and sex is an important consideration in network studies as both have been demonstrated to affect connectivity (Sala-Llonch et al., 2015, Donishi et al., 2018).

Antiepileptic medication is a potential confounder and is an issue inherent to studies of this nature. In two studies (Clemens et al., 2013, Lee and Park, 2019) participants were not taking any medication and in both, there were no significant differences in the functional network

for most measures when the epilepsy group was compared to controls. However, both studies reported greater connectivity in nodal measures in the epilepsy group and one study found differences in structural connectivity suggesting that network changes were not medication related. In the remaining studies (where relevant information was provided) overall, 28.8% of patients were not taking an AED yet a separate analysis of these patients was not reported in any of the relevant studies. The authors of one of the studies set in China (Xue et al., 2014a), noted that patients may have been taking traditional Chinese medication for epilepsy, which could also confound results. Of note in the study by Chowdhury et al (Chowdhury et al., 2014), is that network differences were also found between controls and relatives of people with epilepsy, which also goes against the results being due to medication.

The number of participants in each study was typically low- one study had only 5 participants in each group. Furthermore, none of the studies performed a power calculation. This raises the possibility of a type 2 error in some studies. Under-powering may also explain inter-study inconsistencies in the frequency bands where significant results were found. There is no consensus for normal network characteristics, thus deciding upon a parameter to include in a power calculation is challenging.

The patients in the IGE groups had a range of IGE subtypes. In some studies, the IGE group had only one subtype whereas in another study the IGE group comprised five different subtypes. None of the studies carried out sub-group comparative analyses, perhaps due to the number of participants being too low. It is possible that IGE syndromes have differing pathophysiologies and some believe that they should be treated as separate conditions (Panayiotopoulos and Koutroumanidi, 2017). Thus, analysing different subtypes together may complicate result interpretation. However, it is generally accepted that seizure onset in the corticothalamic networks is common to all forms of generalised epilepsies (Gloor, 1968, Wolf and Beniczky, 2014), which provides justification for analysing IGE subtypes as one. None of the studies controlled for seizure frequency, which varied from seizure freedom in some patients to multiple attacks in others. This could introduce methodological error because seizure frequency may modify network properties (Douw et al., 2010, van Dellen et al., 2012).

Artefact handling and data pre-processing (for example sampling rate and re-referencing of EEG/MEG) is a key methodological consideration in all connectivity studies and techniques varied between studies. Pre-processing and artefact removal is not a standardised process and choices made at this stage may have a significant influence on the results (van Diessen et al.,

2014a). In most studies reviewed, justification for the steps used is not provided which further limits comparability and assessment of reliability.

Differences in post-acquisition processing and network construction were particularly marked, including within studies using the same data modality. In the case of fMRI/DTI studies, differences in how data was parcellated is likely to be a consequence of the lack of consensus on how this should be performed to best reflect network nodes (Zalesky et al., 2010). Furthermore, within all study modalities, a wide range of scales were used. The number of nodes used is a vital consideration when comparing study outcomes since it has been demonstrated that there is disproportionately higher clustering and small-worldness in larger networks (Zalesky et al., 2010).

The method of graph construction also varied between studies. All graphs in the studies bar one were weighted; i.e., the strength of the communication between nodes was factored in. Weighting may result in a more realistic representation of a neuronal network than an unweighted graph and also removes the arbitrariness of threshold selection which occurs in unweighted network construction (van Diessen et al., 2014a). Seven studies subsequently normalised the graphs, i.e., bootstrapped data from random graphs were used to normalise graph measures. This approach is typically used to reduce the effect of node-degree dependency- an intrinsic characteristic of networks whereby estimates of topology are dependent upon the quantity of nodes and number of connections of each node (van Wijk et al., 2010). Although normalised graphs may reduce sensitivity to degree distribution and number of nodes, it has been demonstrated that this dependence increases with more regular networks, particularly small networks (van Wijk et al., 2010). This introduces the potential for further bias depending on overall network topology. Of note is that one study evaluated both mean and normalised values with different results for each approach, highlighting the importance of interpreting results in the context of the calculation method used.

Finally, it should be noted that the physiological implications of altered measures of connectivity, and the directionality of these measures within the construct of a dynamical system, is not fully elucidated. Interpretation of results may be limited by the reduction of a complex dynamical system to the few outcome measures used (Tracy, 2015). As such, it is possible that conflicting study outcomes reflect dynamic alterations that are not yet understood.

3.7.1 Limitations of the review

This review is limited by the fact that just one database was searched by one reviewer which increases the possibility of a relevant study not being identified. Furthermore, it is possible that pertinent studies were excluded due to not being published in English.

3.8 Conclusions

Most studies included in this review suggest that interictal networks of people with IGE have different global structural and functional network characteristics to people without epilepsy. However, the nature of individual network parameter aberrations is inconsistent with some studies demonstrating a more regular topology and some a more random topology in IGE. There is more consistency between results when different data modalities and connectivity sub-types are compared separately. EEG/MEG functional studies suggest that people with epilepsy have a network which is more locally clustered and more integrated i.e., more small-world. The fMRI study outcomes were inconsistent with each other. In contrast to the functional studies, structural connectivity studies suggest lower local connectivity, lower global efficiency and a less small-world network in IGE. This highlights the difficulty in reconciling results of studies using different analytical approaches. In view of the reasons discussed above, we suggest that future meta-analyses also consider the results of structural and functional network studies separately. Marked variations in data collection, post-acquisition data handling, network construction, outcome measures and statistical analysis are also likely to have contributed to differences in study outcomes. Studies to guide methodological choices are greatly needed. Until then, a standardised methodological approach to network analysis, such as the framework suggested in this paper *(table 5)*, would improve study comparability and enable better understanding of network aberrations in epilepsy.

Disclosure of Conflicts of Interest

None of the authors has any conflict of interest to disclose.

Table 2. Commonly used measures in global network studies

Clustering coefficient *(C)*	The probability that the neighbouring nodes of 2 given nodes are themselves connected.
Mean clustering coefficient *(Ci)*	*C* is averaged to calculate the clustering coefficient of the whole graph. (A measure of network segregation).
Normalised clustering coefficient ($\hat{C}$)	$\hat{C} = C / C^{Surr}$ where C^{Surr} is the mean *C* of *X* randomly generated networks This controls for differences in the number of nodes and number of nodal connections in the network.
Path length *(d)*	Minimum number of edges (or shortest path) connecting 2 nodes.
Mean path length *(L)*	Mean of the shortest path length between all pairs of network nodes (a measure of network integration).
Normalised path length ($\hat{L}$)	$\hat{L} = L / L^{Surr}$ where L^{Surr} is the mean *L* of *X* randomly generated networks This controls for differences in the number of nodes and number of nodal connections in the network.
Global efficiency	Inverse of characteristic path length. Used to analyse weighted graphs since the shortest path is not necessarily the path with the fewest edges,
Small- worldness	Ratio of mean clustering coefficient of the graph to the mean clustering coefficient of a similar size random graph as a proportion of the ratio of the characteristic path length of the graph compared to the path length of a random graph. $\frac{[C / C\ random]}{[P / P\ random]}$ Small-world networks have higher than expected clustering coefficient with a characteristic path length of equal or lower value than a a random graph.
Centrality measures e.g.:	Evaluate the importance of an individual node in information transfer in a network.
Degree centrality	Equivalent to the node degree- the assumption being that nodes with more connections are more important.

Betweenness centrality	The number of shortest paths between all network pairs that pass-through a given node.

Table 3. Demographics of participants in functional connectivity studies

Study and modality	Number of participants with epilepsy	Number of controls	IGE subtypes	Mean or median age of epilepsy group (years)	Sex of epilepsy group	Difference in age or sex between controls and epilepsy group	Number of epilepsy group not taking AED	Median/ mean epilepsy duration
Clemens et al. (Clemens et al., 2013) -EEG	19	19	19 x JME	18.2	14 F (74%) 5 M (26%)	No	19 (100%)	4 months
Chowdhury et al. (Chowdhury et al., 2014) -EEG	35	40	12 x EGTCSA 6 x CAE 4 x JAE 8 x JME 4 x UC 1 x Jeavons	34.4	21 F (60%) 14 M (40%)	No	10 (28.5%)	21.5 years
Lee and Park. (Lee and Park, 2019)	36	39	36 x JME	22 +/-6.8	20 F (56%) 16 M (44%)	No	100%	2.25 years

-EEG								
Chavez et al. (Chavez et al., 2010) -MEG	5	5	Absences *	Not stated	Not stated	Not stated	Not stated	Not stated
Elshahabi et al. (Elshahabi et al., 2015) -MEG	13	19	5 x EGTCSA 4 x CAE 2 x JAE 1x JME 1 x UC	38.6	9 F (69%) 4 M (30%)	No	1 (7.7%)	17 years
Niso et al. (Niso et al., 2015) -MEG	15	15	15 x "JME or presumed Genetic"	24 +/- 6	9 F (60%) 6 M (40%)	No	0	Not stated
Zhang et al. (Zhang et al., 2011) -fMRI	26 **	26	26 x EGTCSA	24.12 +/- 6.85	9 F (35%) 17 M (65%)	No	11 (42%)	6.92 +/- 5.8 years
Liao (Liao et al., 2013)	59**	59	59 x EGTCSA	24.9 +/- 7.07	21 F (25.6%) 38 M (64.4%)	No	13 (22%)	7.83 +/- 7.51 years

-fMRI								
Wang (Wang et al., 2017) -fMRI	25	25	25 x CAE	10.5 +/-3.3	11 F (44%) 14 M (56%)	No	19 (76%)	3.6 years

* Further information regarding epilepsy subtype not provided. ** 26 had participated in the Zhang et al study. JME- Juvenile Myoclonic Epilepsy, EGTCSA- Idiopathic Generalised Epilepsy with generalised tonic-clonic seizures alone, CAE – Childhood Absence Epilepsy, JME- Juvenile Myoclonic Epilepsy, UC- unclassified, F- female, M - male.

Table 4. Demographics of participants included in structural connectivity studies

Study and modality	Number of participants with epilepsy	Number of controls	IGE subtype	Mean / median age of epilepsy group (years)	Sex of epilepsy group	Difference in age/ sex between epilepsy group and controls	Number of participants with epilepsy not taking medication	Median epilepsy duration (years)
Xue et al. (Xue et al., 2014a) -DTI	17	18	17 x CAE	8.9 +/- 1.8	8 F (44 %)** 10M (56%)**	No	13 (76%)	3
Bonilha et al. (Bonilha et al., 2014) - MRI (1.5T)	18	28	Subtype not stated	15 +/- 3.3	11 F (61%) 7 M (39%)	No	Not clear	Less than 1
Qiu et al.(Qiu et al., 2017) -DTI	21	24	21 x CAE	Mean 8.05 +/- 1.99	11 F (52%) 10 M (48%)	No	4 (19%)	0.58
Zhang et al. (Zhang et al., 2011) -DTI	26	26	26 x EGTCSA	24.12 +/- 6.85	9 F (35%) 17 M (65%)	No	11 (42%)	4.5
Liao et al. (Liao et al., 2013) -MRI (3T)	59	59	59 x EGTCSA	24.9 +/- 7.07	21 F (25.6%) 38 M (64.4%)	No	13 (22%)	7.83 +/- 7.51 years

Caeyenberghs et al. (Caeyenberghs et al., 2015) -DTI	34	34	34 x JME*	26 +/- 7.8	25 F (71%)** 10 M (29%)	No	0	16.1
Lee and Park (Lee and Park, 2019) -MRI (3T)	36	30	26 x JME	22 +/- 6.8	20 F (56%) 16 M (44%)	Age- No difference Sex- yes (M 87%)	0	2.25

*6 did not have myoclonic jerks. **Data from 1 participant excluded from analysis- demographics of the removed subject are unclear. JME- Juvenile Myoclonic Epilepsy, EGTCSA- Idiopathic Generalised Epilepsy with generalised tonic-clonic seizures alone, CAE – Childhood Absence Epilepsy, JME- Juvenile Myoclonic Epilepsy, UC- unclassified, F- female, M -male.

Table 5. Data acquisition and graph construction for structural studies using DTI

Study	Number of diffusion directions	Number of slices	Slice thickness (mm)	Parcellation scheme	Tractography method	Weighted or unweighted graph	Scale (number of nodes)
Xue et al. (Xue et al., 2014a)	50	50	3	AAL	Deterministic	Weighted	90
Qiu et al. (Qiu et al., 2017)	30	45	3	AAL	Probabilistic	Weighted	90
Zhang et al. (Zhang et al., 2011)	30	45	Not stated	AAL	Deterministic	Weighted	90 1024
Caeyenberghs et al. (Caeyenberghs et al., 2015)	30	60	2.4	AAL	Deterministic	Unweighted	116

AAL- automated anatomical labelling.

Table 6. Recommendations and considerations for future graph theoretical studies of cerebral networks

1. Reporting and pre-processing recommendations (general points for all modalities)	
• For neuroimaging studies across all modalities, it is important that data collection methods and pre-processing steps are explicit to enable interstudy comparability. • The minimum sample number to achieve an adequately powered graph theoretical study has not been elucidated. Reporting of mean / median results for each outcome metric (rather than only one group relative to another) along with effect sizes, would facilitate estimation of adequate power and permit meta-analyses. • A consensus on whether eyes-closed or eyes-open data should be used has not been established. Differences in connectivity measures have been reported between the two states (Horstmann et al., 2010) and may depend on the network of interest (Agcaoglu et al., 2019). For fMRI, eyes-open fixated data is commonly used whereas EEG/MEG data is often eyes-closed. Performing analysis using data from both states would add further information to this area of uncertainty.	
1.1 EEG/ MEG	• For EEG and MEG, general standards for recording and reporting have been previously recommended (Picton et al., 2000, Gross et al., 2013). • The common average is the most frequently used method of re-referencing and has been presented as the gold standard (Kayser and Tenke, 2010) *. • For study comparability, it is recommended that data is filtered into conventional frequency bands e.g., Delta 1-3 Hz, Theta 4-7 Hz, Alpha 8-12 Hz, Beta 13-30 Hz, Gamma 31-70 Hz. Further research should evaluate the use of bands identified by spectral factor analysis, which have been demonstrated to be robust to a range of measures (Shackman et al., 2010).

	• A minimum duration of 12 seconds of data should be used. Functional connectivity measures have been shown to stabilise at this duration (Fraschini et al., 2016). • The first artefact-free epochs should be used. The use of the earliest possible epochs decreases the risk of inclusion of data with reduced vigilance (which are more likely to occur later in the recording (Maltez et al., 2004)), and reduces risk of selection bias (van Diessen et al., 2014a). Epochs should be selected in a manner whereby the investigator is blinded to subject group.
1.2 fMRI	• The following information relating to data acquisition should be stated: o Manufacturer, model and field strength of scanner o Pulse sequence information o Duration of acquisition o Repetition time (TR), echo time (TE), flip angle data o Sequence / volume length o Slice thickness o Field of view o Data acquisition orientation • Optimum duration of acquisition is widely debated. The Human Connectome Project (HCP) acquires a total of 1 hour of data (4 x 15 minutes) (Smith et al., 2013). A long duration increases statistical sensitivity and permits analysis of a greater range of fluctuating resting states (Smith et al., 2013). Whilst implementing the HCP protocol may not always be practicable, it is suggested that factors deviating from it are made explicit. • The following information relating to pre-processing should be stated as a minimum: o Order of pre-processing operations o Methods for slice time correction, motion correction and echo-planar imaging (EPI) distortion correction o Describe transformation model (linear/affine, nonlinear) or type of any

	non-linear transformations (polynomial, discrete cosine basis) ○ Anatomical atlas information including total number of parcellations ○ Smoothing kernel size and type ○ Version number and date of last application for each piece of software used • The use of a particular atlas for node generation should be justified. Using a functional-based atlas may be preferential to a structural-based atlas for the analysis of the functional connectome (and vice versa) given the discordance between structural and functional connectomes (Yao et al., 2015) Furthermore, there is evidence for the superiority of fMRI-driven parcellations (Sala-Llonch et al., 2019). • In view of issues in comparing networks of different densities (van Wijk et al., 2010), it is suggested that the analysis is repeated over different densities to support that any findings are stable.
2. Graph Construction (general points for all modalities)	
• Weighting of connections should be carried out. This may reduce the influence of weak and physiologically insignificant connections (Rubinov and Sporns, 2010). • The construction of both normalised (via random graphs) and non-normalised graphs should be considered. Normalisation may lessen the effect of node-degree dependency for some measures (but not others), which may reduce issues in comparing of networks of different sizes (van Wijk et al., 2010). Further research is needed to optimise methods of reducing node-degree dependency. Reporting both measures would allow further evaluation of this. • The method of synchronisation identification should be specified. For EEG /MEG, measures based on phase (e.g. phase locking) rather than power are less likely to be confounded by disease specific spectral differences (van Diessen et al., 2014a).	

- As a minimum, the following metrics should be reported to facilitate study comparability: Mean clustering coefficient, mean path length (or global efficiency), small-world index, mean degree.

* There is some literature (Zheng et al., 2018, Chella et al., 2016) to suggest superiority of Reference Electrode Standardisation Technique (REST) (Yao, 2001) in network analysis. Further research is suggested to add further information to this area.

AEDs - antiepileptic drugs, CNS - central nervous system

Chapter 4. Interictal EEG functional network topology in drug resistant and well-controlled IGE

This manuscript forming this chapter is published in Epilepsia (Pegg et al., 2021). Since the publication of this paper, an error in the results has been discovered. The error has been rectified in this chapter and an erratum for the paper has been requested. The footnotes contain additional information providing justification for the some of the methodological choices which were not described in the paper due to the word count limit.

4.1 Authors

Emily J. Pegg[1,2], Jason R. Taylor[2,3], Petroula Laiou[4], Mark Richardson[5], Rajiv Mohanraj[1,2]

[1] Department of Neurology, Manchester Centre for Clinical Neurosciences.

[2] Division of Neuroscience and Experimental Psychology, School of Biological Sciences, Faculty of Biology, Medicine and Health, University of Manchester.

[3] Manchester Academic Health Sciences Centre.

[4] Department of Biostatistics and Health Informatics, Institute of Psychiatry, Psychology and Neuroscience, King's College London, London, UK

[5]Department of Basic and Clinical Neuroscience, Institute of Psychiatry, Psychology and Neuroscience, King's College London, London, UK

4.2 Abstract

Objective

The study aim was to compare interictal encephalograph (EEG) functional network topology between people with well-controlled Idiopathic Generalised Epilepsy (WC-IGE) and drug resistant IGE (DR-IGE).

Methods

The data used in this chapter was the same as the data in chapter 2. 19 participants with WC-IGE, 18 with DR-IGE and 20 controls underwent a resting state, 64 channel EEG. An artefact

free epoch was bandpass filtered into the frequency range of high and low extended alpha. Weighted functional connectivity matrices were calculated. Mean degree, degree distribution variance, characteristic path length (L), clustering coefficient, small-world index (SWI), and betweenness centrality were measured. A Kruskal-Wallis H test assessed effects across groups. Where significant differences were found, Bonferroni corrected Mann-Whitney pairwise comparisons were calculated.

Results

There were no significant differences at the three-group level in the 6-9 Hz frequency band. Mean degree (p=0.031), degree distribution variance (p = 0.032), SWI (p = 0.023) differed across the three groups in the high alpha band (10-12 Hz). Mean degree and degree distribution variance was lower in WC-IGE than controls (p = 0.029 for both) and SWI was higher in WC-IGE compared with controls (p = 0.038), with no differences in other pairwise comparisons.

Significance

. WC-IGE network topology is different from controls in the high alpha band. This may reflect drug induced network changes that have stabilised the WC-IGE network by rendering it less likely to synchronise. These results are of potential importance in advancing the understanding of mechanisms of epilepsy drug resistance and as a possible basis for a biomarker of DR-IGE.

4.3 Introduction

Idiopathic (or genetic) Generalised Epilepsies (IGEs) are a group of electro-clinical syndromes characterised by generalised seizures in the absence of structural brain lesions or neurodevelopmental abnormalities. The electroencephalogram (EEG) in IGE syndromes characteristically shows a normal background, with bilaterally synchronous interictal and ictal discharges, which arise as a result of abnormal oscillatory activity in the thalamocortical system (Wolf and Beniczky, 2014). Approximately 18% of people with IGE develop drug resistant epilepsy (DRE) (Brodie et al., 2012), defined by the ILAE as “failure of adequate trials of two tolerated and appropriately chosen and used Anti-Epileptic Drugs (AEDs) to achieve sustained seizure freedom” (Kwan et al., 2010). Seizure freedom is defined as a period of 12 months without a seizure, or after three times the longest pre-treatment inter-seizure interval, whichever is longer. DRE is associated with significant risk of psychosocial morbidity (Piazzini

et al., 2001) and increased mortality (Tomson, 2000). The reason for such variable response to AED treatment in this relatively homogenous group of electro-clinical syndromes is not clear. A number of potential cellular and genetic mechanisms for DRE have been investigated, but the neurobiology of DRE remains largely unexplained (Tang et al., 2017).

Epilepsy is now understood as a disorder of rhythmic activity of brain networks, with epileptic seizures generated by hypersynchronous activity in large-scale neuronal networks (Richardson, 2012a). It is therefore appropriate to examine response to AED treatment from a global cerebral network perspective. A number of studies have found alterations of global functional network structure and function in IGE (Xue et al., 2014b, Chowdhury et al., 2014, Zhang et al., 2011, Chavez et al., 2010, Elshahabi et al., 2015, Liao et al., 2013), some of which may also be important in determining response to treatment (Pegg et al., 2020a). Other studies have identified reduced functional connectivity in specific networks (cerebellar and default mode networks) in patients with drug resistant IGE (DR-IGE) compared to well-controlled IGE (WC-IGE) (Kay et al., 2013, Kay et al., 2014). However, to our knowledge, no functional connectivity studies have investigated global network topology in DR-IGE.

Structural and functional brain networks may be represented as a graph, in which brain areas are represented by 'nodes', which interact with each other via connections known as 'edges'. In functional network studies using EEG, each electrode is considered a node in the graph, and connectivity between nodes is inferred from the quantification of synchronous oscillatory activity at each electrode, within a frequency band. The strength of functional connectivity may be incorporated into the graph by 'weighting' each connection according to the magnitude of the measure of synchronisation used. Properties (metrics) of the graph may then be compared between cohorts under study. Graph theoretical metrics used in brain network studies include mean degree (average number of connections of nodes), degree distribution variance (a measure of the variance of number of connections per node in the graph), centrality measures (a measure of 'hub nodes'- those which transfer a high proportion of signal within the network), clustering coefficient (a measure of connectivity between neighbours of a node, an indicator of network segregation), characteristic path length (average distance between each pair of nodes in the network, an indicator of network integration) small-world index (a measure of network efficiency) (Newman, 2008, Rubinov and Sporns, 2010). Networks which have a high clustering coefficient and high characteristic path length have a regular topology, whereas those with a low clustering coefficient and low path length have a 'random' topology. Networks which are 'small-world' have a high clustering coefficient

and low characteristic path length, which represents high local connectivity in addition to strong integration of distant network regions (Watts and Strogatz, 1998).

There is a suggestion that the extended alpha frequency band (6-12 Hz) is particularly important in IGE. It is proposed that alpha rhythm arises through cortico-thalamic interactions and has roles in attention (Halgren et al., 2019) and functional inhibition (Jensen and Mazaheri, 2010). Changes in alpha rhythm have been reported since early EEG studies when it was noted that people with epilepsy have slower alpha activity than controls (Gibbs et al., 1943). Similarly, reduced peak alpha frequency (Larsson and Kostov, 2005, Pegg et al., 2020b), lower alpha frequency variability (Larsson and Kostov, 2005), and increased alpha spectral power in IGE (Clemens et al., 2000, Miyauchi et al., 1991, Tikka et al., 2013) have been described. Of further relevance are findings of a shift from 10-11 Hz to 6-9 Hz power in poorly controlled IGE (Abela et al., 2019), alterations in graph theoretical metrics within the alpha band in IGE (Chavez et al., 2010, Niso et al., 2015, Chowdhury et al., 2014) and coupling changes in the 6-9 Hz band in a dynamic modelling study of IGE (Schmidt et al., 2014).

Considering the literature described above, the present study investigates network topology in the extended alpha frequency band in IGE, according to seizure control.

Aims

The aim of this study was to compare interictal functional network properties in the alpha frequency band, derived from graph theoretical analysis of EEG in people with DR-IGE, WC-IGE and controls.

4.4 Methods

(figure 23)

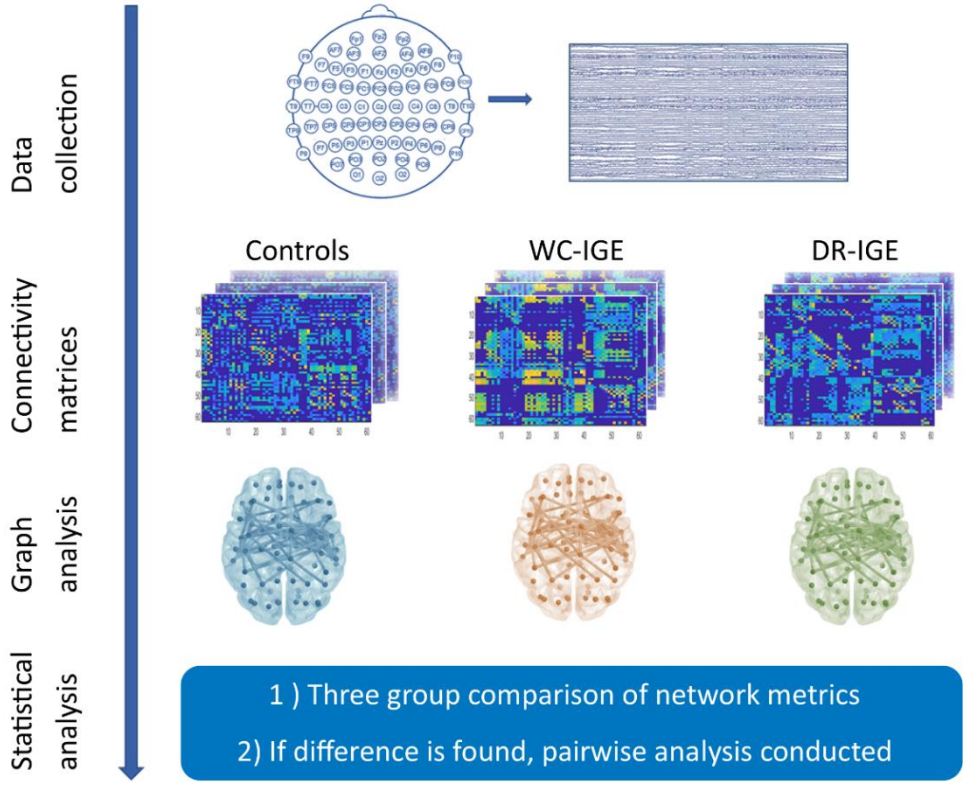

Figure 23. Schematic overview of study methodology

Recruitment

People with DR-IGE and WC-IGE were identified from an audit database of patients attending a tertiary epilepsy clinic at Salford Royal NHS Foundation Trust, general neurology clinics within Greater Manchester, and tertiary epilepsy clinics at The Walton Centre NHS Foundation Trust, Merseyside. Controls were recruited via advertisements in the hospitals, the Citizen Scientist website and on a University of Manchester study volunteering webpage.

The aim was to recruit 15-20 participants into each group. Because normal values and effect sizes for differences between normal and epileptic networks have not been established, a meaningful *a priori* power calculation was not possible. However, this sample number is

similar to, or greater than, previous studies which have reported significant results (Chowdhury et al., 2014, Chavez et al., 2010, Niso et al., 2015, Elshahabi et al., 2015).

Inclusion and exclusion criteria

All participants in the epilepsy groups were over 16 years old and had a diagnosis of IGE. IGE syndrome was determined by an epilepsy specialist based on onset age, seizure types, neurodevelopmental history, family history, and EEG findings in accordance with ILAE criteria (Scheffer et al., 2017). A diagnostic review was subsequently undertaken by a second epileptologist who was not part of the study team. Any participants not meeting the diagnostic criteria for IGE were not included in the analysis. All participants with IGE were taking at least one appropriate AED. Participants in the WC-IGE group were seizure free, including from myoclonic jerks, for a minimum period of one year. Participants in the DR-IGE group must have experienced myoclonus or generalised tonic-clonic seizures at least once per three months in the preceding 12-month period.

Exclusion criteria in the groups with IGE included those who continue to have seizures whilst on AED treatment, but have not been treated with adequate doses of sodium valproate, either through patient - physician preference, or due to adverse reactions or intolerable side effects occurring at doses <1000mg per day. Patients with ongoing seizures taking an AED known to worsen myoclonic epilepsies (phenytoin, carbamazepine, oxcarbazepine, eslicarbazepine, tiagabine, vigabatrin) were also excluded. For patients taking lamotrigine, an investigator ascertained whether seizure aggravation had occurred from the history on a case-by-case basis. Participants with a vagal nerve stimulator were excluded.

Controls were all over 16 years old and were sex and age matched (+/-5 years) with participants with IGE, as these variables have been reported to affect connectivity (Sala-Llonch et al., 2015, Donishi et al., 2018).

All participants with a history of a neurological disorder (other than epilepsy), or with recent use of brain active drugs (antipsychotics, antidepressants, sedative / hypnotic and recreational drugs), were excluded.

Data acquisition

A 64 channel EEG cap in the 10-10 configuration using the BrainVision system was used. Sampling rate was 1000 Hz. A twelve-minute resting state recording was undertaken. Six minutes of the recording was with eyes opened and six with eyes closed[1]. To reduce the chance of drowsiness, this was done as four three-minute recordings. The recording was

carried out in a quiet, naturally lit room. Participants were seated in a cushioned chair and wore passive ear defenders. Participants were instructed to sit still with their eyes closed. Impedance was less than 10 kΩ in the reference and ground electrode. An impedance of less than 20 kΩ was aimed for with remaining electrodes and was always under 30 kΩ.

A 20 second[2] eyes-closed[3] epoch, free from artefact, signs of drowsiness or epileptiform discharges was selected by a trained member of the study team who was blinded to the study groups. The first epoch of adequate quality was selected (van Diessen et al., 2014a) in order to reduce the risk of selection bias. In 21 participants, one channel was faulty and was, therefore, removed from those datasets. There was no difference between groups in the number of datasets this affected (controls n = 6, WC-IGE n = 7, DR-IGE n=10. Chi squared = 2.72, p = 0.26).

---

1. Inter-subject variability in resting state EEG data may arise through differences in the subjective experience of the recording (Diaz et al., 2013) and the immediate pre-recording cognitive state (Lopez Zunini et al., 2013). These variables may affect connectivity measures. All participants were given the same instructions and data collection began with the eyes opened for three minutes followed by the eyes being closed. This was so that a similar experience was created in participants prior to the recording of the eyes closed data that was subsequently used in the analysis.

2. A more regular network topology has been reported with the eyes closed in EEG and MEG studies (Horstmann et al., 2010, Tan et al., 2013, Jin et al., 2013). Eyes closed data is more commonly used in EEG / MEG connectivity analysis and has the advantage of containing less oculomotor artefact and facilitates the selection of epochs without signs of drowsiness (since alpha rhythm is more pronounced).

3. Epoch lengths in existing studies range from seconds to several hours (Chu et al., 2012). At 12 seconds, the phase locking index becomes stabilised across epochs (Fraschini et al., 2016). It can therefore be reasoned that 12 seconds should be the minimum epoch duration for phase-based connectivity. The use of a short epoch also reduces variance of vigilance, which is reported to increase with the length of the recording (Maltez et al., 2004). In our study, in order to also provide consistency with similar studies, a 20 second epoch was used (Chowdhury et al., 2014, Schmidt et al., 2016).

Network construction

A custom MATLAB (R2019a) script was applied each 20 second epoch. Data were re-referenced to the average[4] and downsampled to 256 Hz. Next, data were analysed into an extended high and low alpha band (10-12 Hz and 6-9 Hz respectively). These frequency bands are based on a classification derived using Spectral Factor Analysis, and probably better reflect underlying neural generators than conventional frequency bands (Shackman et al., 2010). Subsequent steps were performed for both frequency bands. A fourth-order Butterworth filter with forward and backward filtering was applied to minimize phase distortions. Weighted phase synchronization was calculated for each pair of electrodes using the phase locking value (PLV)[5].

---

4. Referencing can introduce spurious zero lagged connections and may create time varying activity at each electrode, both of which may potentially affect connectivity measures (Chella et al., 2016). In a study comparing the effect of four different references, a distortion of connectivity was found to be greatest for the Cz reference and became progressively less for the mean mastoids, average reference, and REST respectively (Chella et al., 2016). This study also demonstrated that node degree and local efficiency are sensitive to the reference choice in relation to different parts of the scalp (higher values were seen occipitally using REST and average reference). Mastoid references have been shown to have larger distortions in derived connectivity values than both the average reference and REST (Qin et al., 2017). It has also been reported that small-world effects are more clearly seen using REST reference, compared to an average reference in 64 channel recordings (Zheng et al., 2018). Reference-free techniques such as the surface Laplacian (Hjorth, 1975) may also be used, which have the advantage of not spuriously inflating connectivity. However, it is limited by being insensitive to deep sources and distributed sources (Qin et al., 2017). In view of its common usage and relatively strong performance in studies comparing different references, the average reference was used in this study. Furthermore, it has been demonstrated that when the average reference is used in combination with phase- based connectivity measures (as used in our study), the risk of introducing erroneous connections is reduced (Stam et al., 2007b).

5. There is no clear best measure of connectivity method (Cohen, 2014). In our study, PLV with zero lagged data excluded was selected. Advantages of this measure is that it mitigates the possible effects of disease specific spectral alterations, non-linearity of the neural signal is taken into account (David et al., 2004), and volume conduction effects are attenuated. PLI has similar advantages however PLV has been used in similar studies (Chowdhury et al., 2014, Niso et al., 2015), thereby readily facilitating comparison.

In particular, electrodes were considered as nodes in the functional network and the phase locking values as connectivity weights (Lachaux et al., 1999). For every pair of (i, j) nodes we computed the PLV,

$$1. \qquad PLV_{i,j} = \frac{1}{N}\left|\sum_{k=1}^{N} e^{i\Delta\phi_{i,j}(t_k)}\right|$$

where N is the number of samples and $\Delta\phi_{i,j}(t_k)$ is the instantaneous phase difference between the i, j signals at time t_k. The phase differences were calculated using the Hilbert transform on the filtered signals.

The time-lag, $\tau_{i,j}$, was also computed between the i, j nodes in order to infer the direction of the functional network, where arg is the angle of the complex number that is inside the parenthesis (i.e., the mean of the phase difference).

$$2. \qquad \tau\, i, j = \arg\left(\frac{1}{N}\sum_{k=1}^{N} e^{i\Delta\phi_{i,j}(t_k)}\right)$$

Connections at zero time-lag were discarded to account for possible effects from volume conduction (Bastos and Schoffelen, 2016). In addition, for every (i, j) pair of nodes, 99 pairs of surrogate signals using the iterative amplitude-adjusted Fourier transform (IAAFT) with 10 iterations were computed (Schreiber and Schmitz, 1996). Connections between the (i, j) pair of nodes were discarded if their PLV values did not exceed the 95% significance level of the PLV values distribution of the surrogates (Schmidt et al., 2014)[6]. This reduces the probability of including connections that are due to chance.

---

6 Each methodological option for network thresholding carries potential limitations. The risk of concealing significant results with density thresholding, due to possible inter-group differences in network density, is an important consideration for this analysis and was therefore discounted as an option.

Graph theoretical analysis

Directed, weighted graphs were constructed with electrodes representing nodes, and the edges weighted according to the connectivity matrix data. Following this, global measures of mean degree, degree distribution variance, clustering coefficient (C), characteristic path length (L), small-world index (SWI) and betweenness centrality were calculated for the graph for each individual participant in each frequency band (Newman, 2008, Rubinov and Sporns, 2010). These are commonly used metrics in graph theoretical analysis and were selected to provide representation of the global topological features of the network. Both C and L are sensitive to the number of network nodes. Therefore, normalised metrics for C and L (^C and ^L respectively) were obtained by dividing C and L by the mean of the C and L distributions of 500 surrogate networks respectively, which were produced by random shuffling of the edge weights (Stam et al., 2008, Stam et al., 2007a).

Statistical analysis

Statistical analysis was carried out in SPSS version 25 (IBM-Corp, 2017). After assessment of normality (evaluated using skewness, kurtosis, histograms and Q-Q plots), potential differences in baseline characteristics were tested using either a Kruskal-Wallis H test, Chi-squared test or Mann-Whitney U test, as appropriate. A Kruskal-Wallis H test was used to examine for potential differences in each metric across the three groups for each frequency band (2-sided, significance level $p < 0.05$).

For statistically significant results, effect sizes were calculated using Epsilon squared (ε^2). If results were significantly different at the three-group level, further analysis was performed to compare pairs of groups using the Mann-Whitney test. This was Bonferroni corrected for between-group comparisons with a significance level of $p < 0.05$.

Ethical considerations

The study was conducted in accordance with Research Governance Framework (v.2, 2005). The study was approved by the Health Research Authority (HRA), Research Ethics Committee (REC) and local Research & Development department.

4.5 Results

Participant demographics (table 7, page 128)

In total, 60 participants were enrolled in the study (N= 20 in each group). Data were excluded from two participants with DR-IGE due to a slow background EEG rhythm (a presumed medication or post-ictal cause). Data from one participant in the WC-IGE group were excluded due to reclassification of epilepsy type. In the remaining 57 participants (WC-IGE =19, DR-IGE =18, Controls = 20), median age was 26 years and there was no difference between groups (DR-IGE = 26.5 years; WC-IGE = 24 years; Controls = 25 years. Kruskal-Wallis H = 1.016, p = 0.602). 50.8% of participants were female, with no differences between groups (DR-IGE n = 10; WC-IGE n = 10; Controls n = 9, Chi-square = 0.7401, p = 0.690). Mean epilepsy duration was higher in DR-IGE than WC-IGE but was not statistically different (DR-IGE = 15.8 years, standard deviation (SD): 8.96; WC-IGE = 13 years, SD:10.2. t = -0.89, df = 34.8, p = 0.38). Most participants in the epilepsy groups had Juvenile Myoclonic Epilepsy (JME). In one in each group this had evolved from Childhood Absence Epilepsy (CAE). Exceptions were three participants with IGE with Generalised Tonic-Clonic Seizures Alone (EGTCSA) (two in the WC-IGE group and one in the DR-IGE group), and two with well-controlled Juvenile Absence Epilepsy (JAE). In the 24 hours prior to the EEG recording, no seizures were reported by participants. The DR-IGE group took more AEDs (mode = 2, range 1-4) compared with the WC-IGE group (mode = 1, range 1-3, Mann-Whitney U = 276, p = 0.01).

Outcome metrics

(figure 24, page 123)

There were no significant differences at the three-group level in the 6-9 Hz frequency band *(tables A-1, A-3, A-4, section 4.9).*

In the 10-12 Hz band, there was a significant difference between the three groups in mean degree (Kruskal-Wallis H = 6.956, p=0.031, ε^2 = 0.124), degree distribution variance (Kruskal-Wallis H = 6.855, p=0.032, ε^2= 0.122) and small-world index (Kruskal-Wallis H = 7.071, p=0.023, ε^2 = 0.126). Subsequent pairwise analyses found that mean degree and degree distribution was lower in WC-IGE than controls (p = 0.029 for both measures, Bonferroni corrected), with no difference in other pairwise comparisons. Small-world index was higher in WC-IGE compared with controls (p = 0.038, Bonferroni corrected). There was no difference in betweenness centrality, characteristic path length, or clustering coefficient between groups in this band *(tables A-2 to A-4, section 4.9).*

A post-hoc analysis found that there was no correlation between epilepsy duration, or number of medications taken, and outcome metrics (using Pearson's correlation, significant at $p < 0.05$, uncorrected for multiple comparisons).

Post-hoc analyses also compared outcome metrics between i) WC-IGE and DR-IGE and ii) Both IGE groups combined and controls. Compared to DR-IGE, small-world index was higher in WC-IGE in the 10-12 Hz frequency band (Mann Whitney $U = 106$, $p = 0.049$) and characteristic path length was lower in the 10-12 Hz frequency band (Mann-Whitney $U= 236$, $p = 0.046$). Compared with controls, mean degree and degree distribution variance were lower in the 10-12 Hz frequency band (Respectively: Mann-Whitney $U = 490$, $p = 0.045$; Mann-Whitney $U = 491$, $p = 0.043$). There were no other statistically significant results in the post-hoc analyses.

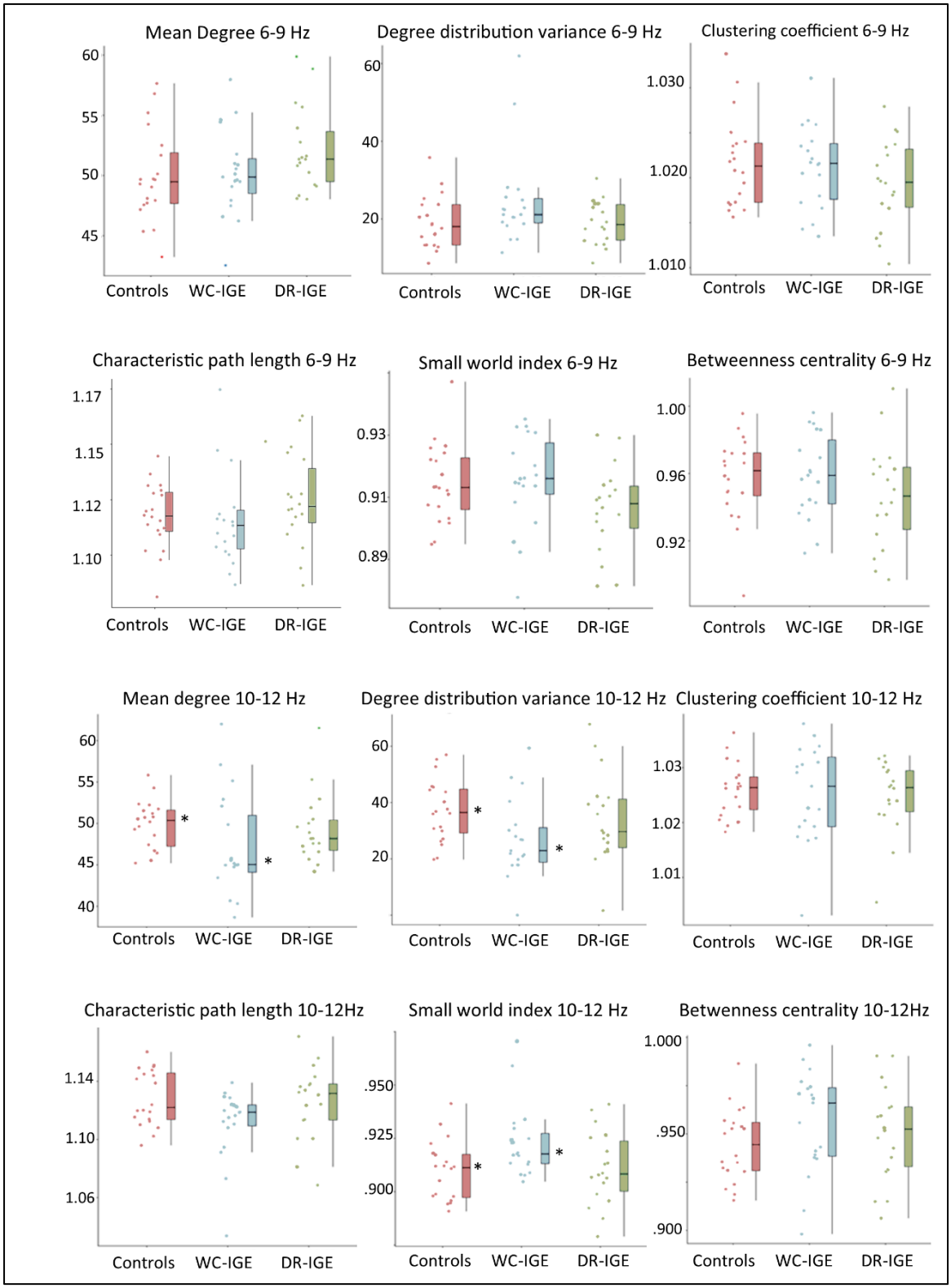

Figure 24. Outcome metrics plotted for each group (controls, well-controlled idiopathic generalized epilepsy [WC-IGE], drug-resistant idiopathic generalized epilepsy [DR-IGE]). Statistically significant results ($p < .05$) are indicated by *: mean degree 10–12 Hz controls–WC-IGE $p = .029$; degree distribution variance 10–12 Hz controls–WC-IGE $p = .029$; small world index controls–WC-IGE $p = .38$

4.6 Discussion

In contrast to the overall findings of our recent review of graph theoretical EEG-based graph theoretical studies in IGE (Pegg et al., 2020a), we did not find an alteration in network topology in the IGE group as a whole compared to controls. However, it should be noted that findings in the literature at the level of specific metrics, rather than overall topological descriptions, are inconsistent. This may reflect varying methodologies including different network sizes, different measures of connectivity and failure to consider seizure control (Pegg et al., 2020a).

Interestingly, network topology in the high-alpha frequency band, differed between WC-IGE and controls, but not in other group comparisons. Compared to controls, WC-IGE networks have a reduced number of connections (weighted mean degree), lower variation in the number of nodal connections (i.e., fewer network hubs, evidenced by a lower degree distribution) and a greater network efficiency (a higher small-world index (SWI)). Considering evidence that people with poorly controlled IGE may have more visually identifiable EEG anomalies than those with better controlled epilepsy (Seneviratne et al., 2017), it may have been anticipated that the group with DR-IGE would have the most pronounced network abnormalities. Instead, our results suggest that differences observed between WC-IGE and controls in this frequency band reflect specific drug induced topological changes in the WC-IGE group, that do not occur in the DR-IGE group. It may be postulated that at the start of epilepsy, network topology is more regular compared to controls, but in those who respond to medication, the network becomes more small-world (i.e., less regular), and therefore less vulnerable to transitioning to a seizure state. The fact that there was no significant difference in SWI between DR-IGE and controls may be consistent with this, in that healthy controls may have a network at the more random end of the spectrum and DR-IGE at the more regular end of the spectrum, both of which may result in a low SWI (since SWI is a ratio of randomised clustering coefficient to characteristic path length, two networks may have a very different overall topology with a similar SWI). It is also possible that there were differences between WC-IGE and DR-IGE but that this study was underpowered to detect them. In support of this is that there was a significant difference in SWI between these two groups in the 10-12 Hz frequency band, but it did not survive correction for multiple comparisons. Similarly, in the post-hoc comparison of DR-IGE and WC-IGE, there was a significant difference in SWI in both frequency bands, and in characteristic path length at 10-12 Hz.

Mechanisms of action of AEDs are well characterised at a cellular level, but how those relate to anti-seizure effects is incompletely understood. Our results support the notion of a common pathway of AED effects, arising through a large-scale network effect (Woldman et al., 2019). Studies in other epilepsy cohorts have reported changes in global efficiency (the inverse of path length) with topiramate but not with lamotrigine, levetiracetam or valproate (van Veenendaal et al., 2017). Another study found altered betweenness centrality with carbamazepine (Haneef et al., 2015a).

To our knowledge, this is the first study comparing global network connectivity in DR-IGE to WC-IGE using graph theory. Considering the results of the current study, it is possible that significant findings in the existing literature that compare IGE with controls, are driven by network features of WCE. Similarly, where differences have not been found, this may be due to the network effects of drug responders 'cancelling out' the differences in DRE networks. This potential confounder is highlighted by the post hoc comparison of both IGE cohorts with controls where there was no difference in SWI, yet a difference was revealed between WC-IGE and controls. This is a pertinent point for consideration in the design of future epilepsy network studies.

A potential limitation of our study relates to challenges in classifying drug response. Patients may not be concordant with AEDs and may, therefore, be inaccurately categorised as drug resistant. This is an inherent difficulty in studies of drug resistance and there is no optimal solution. It is possible that people with DRE are less likely to be taking their prescribed AEDs than those with WCE, although there is no literature to suggest this to our knowledge. If this were the case, it is possible that the results reflect drug effects irrespective of seizure control. However, existing studies on network effects of AEDs, outlined above, do not provide evidence that AEDs commonly taken by participants in this study (levetiracetam, valproate, lamotrigine) directly explain the result. A further limitation of our study is that the groups with IGE differed in terms of number of medications and epilepsy duration, although the latter did not reach statistical significance. Both have been associated with changes in network metrics (Haneef et al., 2015a, van Veenendaal et al., 2017), but the fact that these variables were lower in the WC-IGE group (where the significant differences were found compared to controls), goes against the results being due to either of these factors. Additionally, the sample size was relatively small, which may introduce type one errors. However, the effect sizes of the significant results were medium or strong, which is in support of the findings not being due to statistical chance.

It should be noted that the physiological implications and directionality of network metrics within a complex dynamical system, are not fully understood (Tracy, 2015) and thus our interpretation of the results is necessarily speculative. Longitudinal studies with large sample sizes are required to validate this finding in order to better understand dynamical network features in IGE and their relationship with seizure control.

In conclusion, our results suggest that WC-IGE is associated with altered network features compared to controls. It is possible that large-scale network alterations arise as a downstream effect of AEDs, rendering the network less prone to synchronisation and therefore less susceptible to transitioning to the seizure state. The results potentially demonstrate new insight into DRE and represent a possible avenue for the development of a biomarker of drug resistance. This study also highlights that drug responsiveness should be taken into account in the design of future epilepsy network analytical studies.

Key points

1. WC-IGE is associated with altered network topology in the 10-12 Hz frequency band, compared to controls.
2. The alterations in WC-IGE networks may arise as a downstream effect of AEDs, rendering the network more stable.

4.7 Acknowledgements

We are grateful to Professor Tony Marson and Dr Simon Keller and colleagues (University of Liverpool) for recruiting participants, to Dr Paul Cooper for reviewing diagnosis and classification of patients with IGE recruited into the study, to Tim Rainey and Dr Sarah Martin for assistance with EEG recordings, and to Calvin Heal for statistical advice (University of Manchester).

4.8 Funding

PL is supported by the following: National Institute for Health Research (NIHR) Biomedical Research Centre at South London; Maudsley NHS Foundation Trust; King's College London; Innovative Medicines Initiative 2 Joint Undertaking, Grant/Award Number: 115902; European

Union's Horizon 2020 research and innovation programme; EFPIA. EP is supported by Salford Royal NHS Foundation Trust.

Table 7. Participant demographics

Participant	Group	Age	Sex	Seizure types	Age at onset	Neuro-developmental history	EEG	Epilepsy in first degree relatives	IGE subtype	Current medication (total daily dose)
W01	WC-IGE	22	M	GTC, Abs	13	Normal	Typical	No	JAE	Valproate 2100mg, Levetiracetam 500mg
W02	WC-IGE	21	F	GTC, MJ	14	Normal	Normal	No	JME	Levetiracetam 1000mg
W03	WC-IGE	21	F	GTC, MJ, Abs	12	Normal	Normal	Mother	JME	Levetiracetam 1000mg
W04	WC-IGE	24	F	Abs, GTC	18	Normal	Typical	No	JAE	Valproate 1000mg, Lamotrigine 200mg, Levetiracetam 4000mg
W05	WC-IGE	37	F	GTC, MJ	23	Normal	NA	No	JME	Lamotrigine 250mg, Levetiracetam 2500mg
W06	WC-IGE	21	F	GTC, MJ	14	Normal	Typical	Yes	JME	Lamotrigine 300mg,
W07	WC-IGE	17	M	GTC, MJ	15	Normal	Typical	Father	JME	Levetiracetam 1000mg
W08	WC-IGE	34	F	GTC, MJ	14	Yes	NA	No	JME	Valproate 400mg, Levetiracetam 3000mg
W09	WC-IGE	37	M	GTC	13	Normal	NA	Brother	EGTCSA	Valproate 300mg, Lamotrigine 300mg

W10	WC-IGE	37	M	GTC, MJ	16	Normal	NA	Father	JME	Lamotrigine 400mg
W11	WC-IGE	28	F	GTC, MJ	20	Normal	Typical	Brother	JME	Levetiracetam 1000mg
W12	WC-IGE	20	M	GTC, MJ, Abs	5-10	Normal	Typical	No	CAE>JME	Valproate 1700mg, Ethosuximide 500mg
W13	WC-IGE	28	F	GTC, MJ	18	Normal	NA	No	JME	Levetiracetam 1250mg
W14	WC-IGE	54	M	GTC, MJ	16	Normal	NA	no	JME	Valproate 2200mg, Clonazepam 2mg, Lamotrigine 100mg
W15	WC-IGE	23	M	GTC	20	Normal	Typical	No	IGE-GTSCA	Valproate 800mg
W16	WC-IGE	34	F	GTC, MJ	15	Normal	Normal	Mother	JME	Levetiracetam 1500mg
W17	WC-IGE	20	F	GTC, MJ	16	Normal	Typical	No	JME	Levetiracetam 2000mg
W19	WC-IGE	50	M	GTC, MJ	13	Normal	Typical	No	JME	Valproate 1000mg, Levetiracetam 2000mg
W20	WC-IGE	21	M	GTC, MJ	12	Normal	Typical	No	JME	Valproate 1000mg
R01	DR-IGE	45	F	GTC, MJ, Abs	18	Normal	Typical	No	JME	Perampanel 2mg, Brivaracetam 100mg
R02	DR-IGE	23	M	GTC, MJ	16	Normal	Typical	No	JME	Valproate 3000 mg, Zonisamide 300mg, Levetiracetam 1000mg

R04	DR-IGE	57	F	GTC, MJ	17	Normal	Typical	unknown	JME	Valproate 1000mg, Zonisamide 400mg, Clonazepam 1.5mg
R05	DR-IGE	32	F	GTC, MJ, Abs	11	Normal	Typical	No	JME	Levetiracetam 3000 mg, Perampanel 6mg
R06	DR-IGE	22	M	GTC, MJ	13	Normal	Normal	No	JME	Valproate 2000 mg, Lamotrigine 150mg
R07	DR-IGE	20	F	GTC, MJ	15	Normal	Typical	Mother	JME	Valproate 1500mg, Levetiracetam 2500mg
R08	DR-IGE	36	M	GTC, MJ	<20	Normal	N/A	unknown	JME	Valproate 1800mg, Topiramate 100mg, clobazam 10mg PRN
R09	DR-IGE	43	M	GTC, MJ	19	Normal	N/A	Sister	JME	Valproate 2000 mg
R10	DR-IGE	23	M	GTC, MJ, Abs	19	Normal	Typical	No	JME	Brivaracetam 100mg, Zonisamide 200mg
R11	DR-IGE	23	F	GTC, MJ	10	Normal	Typical	No	JME	Valproate 600mg, Levetiracetam 500mg, Lamotrigine 300mg
R12	DR-IGE	30	M	GTC	11	Memory, language and executive deficits on neuropsychological tests	Typical	Brother	EGTCSA	Lamotrigine 250mg, Valproate 1400mg, Clonazepam 0.5mg
R13	DR-IGE	24	F	GTC, Abs	4	Normal	Typical	No	CAE>JME	Lamotrigine 450mg, Clobazam 10mg, Brivaracetam 100mg, Lacosamide 300mg

R14	DR-IGE	26	M	GTC, MJ	17	Normal	Typical	No	JME	Levetiracetam 3000mg, Lamotrigine 450mg
R15	DR-IGE	27	F	GTC, MJ	11	Normal	Typical	No	JME	Zonisamide 400mg, Clonazepam 1mg, Brivaracetam 150mg
R16	DR-IGE	34	F	GTC, MJ	24	Normal	N/A	No	JME	Levetiracetam 3000mg, Clobazam 15mg, Gabapentin 300mg
R17	DR-IGE	37	F	GTC, MJ, Abs	17	Normal	N/A	No	JME	Valproate 1500mg, Levetiracetam 1500mg
R18	DR-IGE	26	F	GTC, MJ, Abs	10	Normal	Typical	No	JME	Valproate 1000mg, Clobazam 10mg
R20	DR-IGE	18	M	Abs	10	Normal	Typical	No	JAE	Valproate 2000mg, Ethosuximide 500mg
C01	Con	25	F	-	-	-	-	-	-	-
C02	Con	57	M	-	-	-	-	-	-	-
C03	Con	36	M	-	-	-	-	-	-	-
C04	Con	40	M	-	-	-	-	-	-	-
C05	Con	27	M	-	-	-	-	-	-	-
C06	Con	22	F	-	-	-	-	-	-	-
C07	Con	32	F	-	-	-	-	-	-	-
C08	Con	29	F	-	-	-	-	-	-	-

C09	Con	27	M	-	-	-	-	-	-	-
C10	Con	22	M	-	-	-	-	-	-	-
C11	Con	26	M	-	-	-	-	-	-	-
C12	Con	19	M	-	-	-	-	-	-	-
C13	Con	22	F	-	-	-	-	-	-	-
C14	Con	22	F	-	-	-	-	-	-	-
C15	Con	30	M	-	-	-	-	-	-	-
C16	Con	24	M	-	-	-	-	-	-	-
C17	Con	21	F	-	-	-	-	-	--	-
C18	Con	25	F	-	-	-	-	-	-	-
C19	Con	22	M	-	-	-	-	-	-	-
C20	Con	23	F	-	-	-	-	-	-	-

W18 was excluded from the analysis following independent diagnosis review. R03 and R19 were excluded from analysis to slow background rhythm of EEG.

Abbreviations. WC-IGE = well-controlled Idiopathic Generalised Epilepsy, DR-IGE = drug resistant Idiopathic Generalised epilepsy, Con= control, F= female, M= male, GTC = Generalised tonic-clonic seizure, MJ = myoclonic jerk, Abs = absence seizure, IGE = Idiopathic Generalised Epilepsy, Con= Control, CAE = Childhood Absence Epilepsy, EGTCSA= IGE with generalised tonic-clonic seizures alone, JAE = Juvenile Absence Epilepsy, JME = Juvenile Myoclonic Epilepsy, N/A = not available. EEG findings were classified as typical if bilaterally synchronous spike/polyspike wave discharges on normal background were recorded previously.

4.9 Appendix A- Supplementary data

Table A-1. Descriptive statistics for outcome metrics in the 6-9 Hz frequency band

Group	Descriptive statistic		Mean Degree 6-9 Hz	Degree variance 6-9 Hz	Clustering coefficient 6-9 Hz	Path length 6-9 Hz	Small world index 6-9 Hz	Betweennes s centrality 6-9 Hz
Control	Mean		49.90619	19.063225	1.02174	1.1175	0.914435	0.9573
	95% CI for Mean	Lower Bound	48.124219	15.905231	1.01941	1.1106	0.908482	0.945741
		Upper Bound	51.688161	22.221219	1.02407	1.1245	0.920388	0.968859
	SE of mean		0.8513857	1.508819	0.0011133	0.0032	0.0028441	0.0055225
	Median		49.47055	18.03635	1.0213	1.1177	0.91315	0.9617
	Std. Deviation		3.8075126	6.7476437	0.0049789	0.1486	0.0127191	0.0246972
WC-IGE	Mean		50.262921	24.516716	1.021158	1.116100	0.915200	0.958589
	95% CI for Mean	Lower Bound	48.541125	18.737697	1.018932	1.105883	0.907872	0.946673
		Upper Bound	51.984717	30.2957340	1.0233840	1.1263170	0.9225280	0.9705060
	SE of mean		0.819543	2.7507058	0.0010596	0.0048631	.0034881	0.0056719
	Median		49.873	21.1219	1.0216	1.1135	0.9160	0.9589
	Std. Deviation		3.572305	11.990049	0.004619	0.021198	0.015204	0.024723
DR-IGE	Mean		52.1049330	19.0126890	1.0193500	1.1250390	0.9062940	0.9466560
	95% CI for Mean	Lower Bound	50.3570500	16.2116930	1.0169310	1.1146000	0.8993050	0.9313610
		Upper Bound	53.8528	21.8137	1.0218	1.1355	0.9133	0.9620
	SE of mean		0.8285	1.3276	0.0011	0.0049	0.0033	0.0072
	Median		51.354800	18.555000	1.019500	1.122000	0.907950	0.946600
	Std. Deviation		3.5148287	5.6325394	0.0048645	0.0209911	0.0140545	0.0307564

Table A-2. Descriptive statistics for outcome metrics in the 10-12 Hz frequency band

Group	Descriptive statistic		Mean Degree 10-12 Hz	Degree variance 10-12 Hz	Clustering coefficient 10-12 Hz	Path length 10-12 Hz	Small world index 10-12 Hz	Between-ness centrality 10-12 Hz
Control	Mean		49.847495	37.09385	1.02596	1.128485	0.909375	0.944265
	95% CI for Mean	Lower Bound	48.498919	31.945553	1.023677	1.119512	0.902807	0.935454
		Upper Bound	51.196071	42.242147	1.028243	1.137458	0.915943	0.953076
	SE of mean		0.6443192	2.459741	0.001091	0.0042871	0.003138	0.0042095
	Median		50.3651	36.48975	1.02635	1.122	0.91125	0.94445
	Std. Deviation		2.8814832	11.0002964	0.004879	0.0191723	0.0140335	0.0188256
WC-IGE	Mean		47.061768	27.030211	1.025242	1.111174	0.922995	0.955711
	95% CI for Mean	Lower Bound	44.061828	20.352618	1.021031	1.099428	0.914807	0.942866
		Upper Bound	50.0617080	33.7078030	1.0294530	1.1229190	0.9311830	0.9685550
	SE of mean		1.4279159	3.1784103	0.0020045	0.0055907	0.0038973	0.0061135
	Median		45.0476	22.9085	1.0266	1.1187	0.9177	0.9660
	Std. Deviation		6.224141	13.854369	0.008737	0.024369	0.016988	0.026648
DR-IGE	Mean		49.3082280	33.9993610	1.0247000	1.1253610	0.9109280	0.9506440
	95% CI for Mean	Lower Bound	47.2443040	26.1313650	1.0213850	1.1125560	0.9023510	0.9382550
		Upper Bound	51.3722	41.8674	1.0280	1.1382	0.9195	0.9630
	SE of mean		0.9782	3.7292	0.0016	0.0061	0.0041	0.0059
	Median		48.176100	29.647300	1.026350	1.131600	0.908300	0.952500
	Std. Deviation		4.1503566	15.8217997	0.0066653	0.0257497	0.0172474	0.0249144

Table A-3. Outcome metrics compared at the three-group level.

Outcome metric	H	Sig.
Mean degree 6-9 Hz	4.446	.108
Degree distribution 6-9 Hz	3.409	.182
Clustering coefficient 6-9 Hz	1.647	.439
Characteristic path length 6-9 Hz	3.241	.198
Small world index 6-9 Hz	5.043	.080
Betweenness centrality 6-9 Hz	2.180	.336
Degree distribution 10-12 Hz	6.855	.032*
Clustering coefficient 10-12 Hz	0.04	.980
Characteristic path length 10-12 Hz	5.097	.078
Small world index 10-12 Hz	7.071	0.029*
Betweenness centrality 10-12 Hz	3.193	.203

Sig = significance level. H = H statistic of Kruskal-Wallis test.

* statistically significant at $p < 0.05$ level (2 sided).

Table A-4. Pairwise comparison tests of results that were significant at the three-group level.

Outcome metric	Pairwise group comparisons		Test statistic	Standard error	Significance	Adjusted significance (2-sided)
Mean degree 10-12 Hz	WC-IGE	DR-IGE	-9.345	5.459	.087	.261
	WC-IGE	Controls	13.789	5.317	.01	.029*
	DR-IGE	Controls	4.444	5.393	.410	1
Degree distribution 10-12 Hz	WC-IGE	DR-IGE	-9.073	5.459	.07	.290
	WC-IGE	Controls	13.734	5.317	.01	.029*
	DR-IGE	Controls	4.661	5.393	.387	1
Small world index 10-12 Hz	WC-IGE	DR-IGE	11.212	5.459	.04	.120
	WC-IGE	Controls	-12.234	5.317	.013	.038*
	DR-IGE	Controls	-2.022	5.392	.708	1
Characteristic path length 6-9 Hz	WC-IGE	DR-IGE	-6.058	5.459	.267	.801
	WC-IGE	Controls	-25.553	-4.805	<0.0001*	<0.0001*
	DR-IGE	Controls	-31.611	5.393	<0.0001*	<0.0001*

*Statistically significant at $p < 0.05$, Bonferroni corrected

Chapter 5. Functional network topology in drug resistant and well-controlled IGE: A resting state fMRI study

This manuscript is submitted for publication to Brain Communications. The footnotes within this chapter contain additional information regarding methodological choices, which were not discussed in the submitted paper. Appendix B of this chapter (*section 5.9*) was not included in the paper and has been added to this thesis chapter to provide richer discussion of the choice of atlas.

5.1 Authors

Emily J Pegg[1,2], Andrea McKavanagh[3], R Martyn Bracewell[4], Yachin Chen[3], Kumar Das[4], Christine Denby[4], Petroula Laiou[5], Tony Marson[3], Rajiv Mohanraj[1,2], Jason R Taylor[2,6], Simon S Keller[3].

[1] Department of Neurology, Manchester Centre for Clinical Neurosciences, Salford Royal NHS Foundation Trust.

[2] Division of Neuroscience and Experimental Psychology, School of Biological Sciences, Faculty of Biology, Medicine and Health, University of Manchester.

[3] Department of Pharmacology and Therapeutics, Institute of Systems, Molecular and Integrative Biology, University of Liverpool.

[4] The Walton Centre NHS Foundation Trust, Liverpool.

[5] Department of Biostatistics and Health Informatics, Institute of Psychiatry, Psychology and Neuroscience, King's College London, London.

6 Manchester Academic Health Sciences Centre, University of Manchester.

5.2 Abstract

Despite an increasing number of drug treatment options for people with Idiopathic Generalised Epilepsy (IGE), drug resistance remains a significant issue and the mechanisms

underlying it remain poorly understood. Previous studies have largely focused on potential cellular or genetic explanations for drug resistance. However, epilepsy is understood to be a network disorder and there is a growing body of literature suggesting altered topology of large-scale resting networks in people with epilepsy compared to controls. We hypothesise that network alterations may also play a role in seizure control.

The study aim was to compare resting state functional network structure between well-controlled IGE (WC-IGE), drug resistant IGE (DR-IGE), and healthy controls.

Thirty-five participants with IGE (12 with WC-IGE and 23 with DR-IGE) and 34 controls were recruited. Resting state functional MRI networks were reconstructed using the Functional Connectivity Toolbox (CONN). Global graph theoretic network measures of average node strength (an equivalent measure to mean degree in a network that is fully connected), node strength distribution variance, characteristic path length, average clustering coefficient, small-world index, and average betweenness centrality were computed. Graphs were constructed separately for positively weighted connections and for absolute values. Individual nodal values of strength and betweenness centrality were also measured and 'hub nodes' were compared between groups. Outcome measures were assessed across the three groups and between both groups with IGE and controls.

The IGE group as a whole had a higher average node strength, characteristic path length, and average betweenness centrality, irrespective of seizure control. Outcome metrics were sensitive to whether negatively correlated connections were included in network construction. There were no clear differences in the location of 'hub nodes' between groups.

The results suggest that irrespective of seizure control, the IGE interictal network topology is more regular and has a higher global connectivity compared to controls, with no alteration in the location of hub nodes. These alterations may produce a resting state network that is more vulnerable to transitioning to the seizure state. It is also demonstrated that network topological features are influenced by the sign of connectivity weights and therefore future methodological work is warranted to account for anticorrelations in graph theoretic studies.

5.3 Introduction

Epilepsy affects around 70 million people worldwide (Ngugi et al., 2010), of whom 15-20% are estimated to have Idiopathic Generalised Epilepsy (IGE) (Jallon and Latour, 2005). IGEs comprise a group of syndromes characterised by the occurrence of generalised seizures in the

absence of neurodevelopmental abnormalities or structural brain lesions (Scheffer et al., 2017). Approximately 18% of people with IGE do not become seizure free despite an adequate trial of at least two appropriate and tolerated antiepileptic drugs (AEDs) (Semah et al., 1998, Brodie et al., 2012). Subsequent changes to drug regimens have a low chance of resulting in seizure freedom (Mohanraj and Brodie, 2006) and, therefore, such patients are considered to have drug resistant epilepsy (Kwan et al., 2010). In addition to a high seizure burden, people with drug resistant epilepsy have a higher rate of injury (Beghi et al., 2002), sudden unexplained death in epilepsy (SUDEP) (Tomson, 2000), and social difficulties (Ridsdale et al., 2017), compared to those with controlled seizures.

Traditionally, drug resistance in epilepsy has been examined from a cellular or genetic perspective. However, such approaches have failed to fully explain the underlying mechanisms of drug resistance (Tang et al., 2017). Since epilepsy is now understood to be a network disorder, in which seizures emerge from the dynamic resting state of the brain (Richardson, 2012b), investigating epilepsy drug resistance from a resting state network perspective may facilitate greater understanding of this important issue.

Resting state brain networks may be examined using functional magnetic resonance imaging (fMRI), whereby blood oxygen level dependent (BOLD) signal is statistically analysed to establish the extent of connectivity between regions. Graph theory provides a robust mathematical method to subsequently delineate and analyse network topology (structure). Within this framework, each brain area is termed a 'node' and the connections between nodes are termed 'edges'. Edges may be weighted according to the strength of correlation of BOLD signal between nodes. Information regarding the presence and strength of pairs of connections within a network is contained within a connectivity matrix and from this, a range of network metrics and features can be determined (*table 8, page 154*) (Rubinov and Sporns, 2010, Newman, 2008). Overall evidence from graph theoretical studies derived from electroencephalography (EEG), magnetoencephalography (MEG) and MRI suggests that networks of people with focal epilepsy and IGE have a more regular topology compared to controls (van Diessen et al., 2014c, Pegg et al., 2020a). It has been proposed that this regularity may render the network more likely to synchronise than a network that has a more random structure (van Diessen et al., 2014a). However, there are inconsistencies within the literature, with some studies consistent with a more random network structure in epilepsy and others not identifying any differences in network regularity (Zhang et al., 2011, Lee and Park, 2019, Elshahabi et al., 2015).

To our knowledge, analysing fMRI-derived functional connectivity from a global network perspective in IGE according to seizure control has not previously been considered. However, reduced connectivity in specific networks (cerebellar and default mode networks) in drug resistant IGE (DR-IGE) compared with well-controlled IGE (WC-IGE) has been described (Kay et al., 2013, Kay et al., 2014). In an EEG topology study by our group, in a different patient cohort, differences were found between controls and WC-IGE in the 10-12 Hz frequency band (compared with controls, mean degree and degree distribution variance was lower in WC-IGE and SWI was higher) (Pegg et al., 2021). This perhaps suggests that in people who respond to medication, drug induced alterations to the network render the network less susceptible to seizures.

Considering that network topology may play a role in seizure control in IGE, and that diverging findings in the literature of IGE network topology may be influenced by a lack of evaluation according to seizure control (Pegg et al., 2020a), the aim of this study was to compare resting state global network topology in people with DR-IGE, WC-IGE, and controls, using fMRI. Consistent with the intrinsic severity hypothesis of drug resistant epilepsy, where the inherent severity of epilepsy determines medication response (Rogawski and Johnson, 2008), we hypothesise that network aberrations in epilepsy lie on a spectrum according to seizure control, with alterations in WC-IGE lying between those of DR-IGE and controls. We also tested the hypothesis that specific nodes which play a prominent role in network integration (so called 'hub nodes'), differ between people with IGE and controls (Frei et al., 2010, Zhang et al., 2011). The potential importance of hub nodes in seizure susceptibility in focal epilepsy is well described (Lopes et al., 2017, Lee et al., 2018), but hub nodes have been seldom explored in IGE.

5.4 Materials and methods

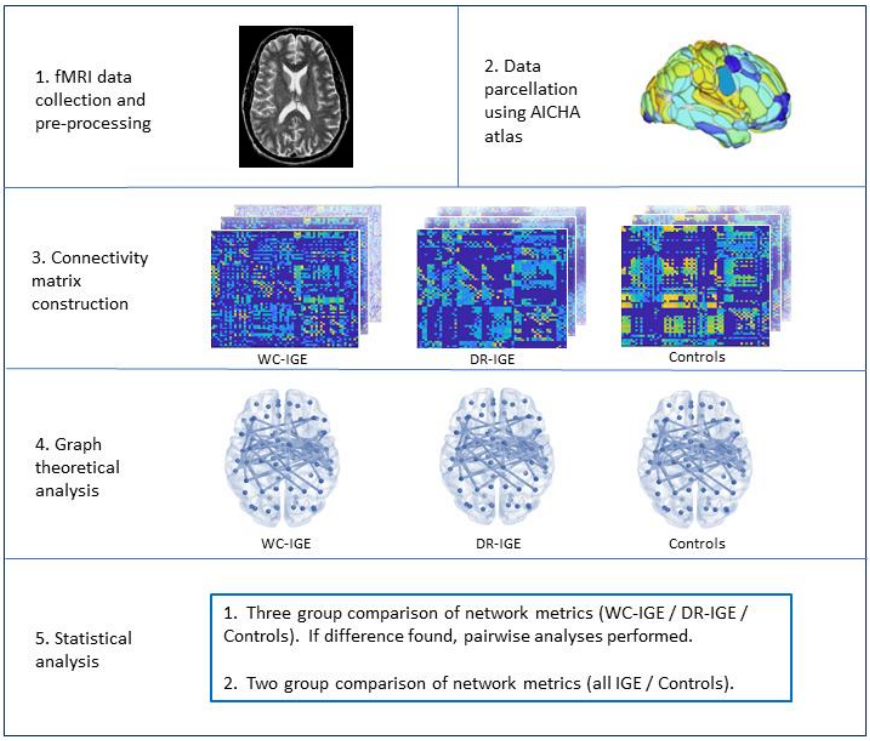

Figure 25. Schematic overview of study methodology. After data were collected and pre-processed, parcellation into network nodes was performed. Connectivity matrices were constructed for each participant. Graphs were created for each participant in each group, followed by group-level statistical analysis.

Recruitment

Thirty-five participants with IGE were recruited from the Walton Centre NHS Foundation Trust and from Salford Royal NHS Foundation Trust. All participants with IGE had been diagnosed by an experienced epileptologist according to current ILAE criteria (Scheffer et al., 2017) based on patient history, seizure semiology and EEG. Two participants were subsequently excluded. This was due to re-classification of epilepsy type in one case and in the other, there was an MRI finding of focal cortical dysplasia (this was an incidental finding, the syndromic classification of IGE remains following review of diagnosis). Twenty-three participants had DR-IGE (persistent seizures despite AED treatment) and 10 were seizure free for at least one year and therefore were classified as having WC-IGE. Thirty-four healthy controls were recruited. Informed, written consent was obtained for all participants (UK Research Ethical Committee reference 14/NW/0332).

Data collection and pre-processing[1]

3D T1 weighted and resting state fMRI images were obtained for each participant using a 3T GE Discovery MR 750 MR system. Scanning was performed supine in the head-first orientation. Participants were instructed to close their eyes[2] and to remain awake. T1-weighted data was acquired using the following parameters: Pulse sequence = BRAVO; echo time (TE) = 3.22 ms; repetition time (TR) = 8.2 ms; field of view (FOV) = 24, TI = 450 ms; slice thickness = 1 mm; voxel size = 1 mm × 1 mm x 1 mm; 140 slices; flip angle = 12. RS-fMRI was obtained with a 6-minute[3] T2*-weighted sequence with the following parameters: Pulse sequence = echo planar imaging (EPI) ; TE = 25 ms; TR = 2,000 ms; FOV= 24 cm; slice thickness = 2.4 mm; voxel size = 3mm x 3mm x 3mm; 180 volumes; 38 slices; flip angle = 75 degrees.

---

1 A number of artefacts may affect connectivity measures including those from head movement and cardio-respiratory sources (Finn et al., 2015). A variety of toolboxes exist to remove such artefacts as part of a pre-processing pipeline but there is no consensus on the optimal way in which to perform pre-processing. Although many pre-processing pipelines contain broadly similar steps, it has been demonstrated that both the included steps, and the order in which they are performed may affect graph theoretical measures (Gargouri et al., 2018, Aurich et al., 2015). In our study, pre-processing was performed using the standard pipeline in SPM12 and the CONN toolbox (Whitfield-Gabrieli and Nieto-Castanon, 2012). Steps which are regarded as being standard, include slice timing correction, head movement correction, EPI distortion correction, spatial normalisation, smoothing, removal of noise from cardio-respiratory sources, and band pass filtering. Additional steps such as scrubbing or global signal regression were not implemented with the aim of preserving as much neuronal signal as possible.

2 Whether the eyes are closed or open (typically fixated) is reported to affect functional connectivity derived from fMRI, and there is no consensus on which should be used. Several studies suggest that specific networks may be affected by this including the default node network, somatosensory network and visual networks (Jao et al., 2013, Liang et al., 2014, Yang et al., 2007, Marx et al., 2004). However, there are inconsistencies as to whether the networks are more or less connected in each state. To my knowledge, there are no studies that have assessed whether the eyes being open or closed affects global connectivity analysed using graph theory. One study suggested that there was greater variance in characteristic path length with the eyes closed in a range of specific networks, but with no difference in clustering coefficient or efficiency measures (Weng et al., 2020). From this, the authors postulated that eyes open state networks may be more stable. Consistent with similar studies (Zhang et al., 2011, Liao et al., 2013), the eyes closed state was used in our study.

3 The optimal duration of data acquisition is debated. Considerations include stability of networks over time, participant tolerability and a possible increased risk of drowsiness with longer recordings. A typical acquisition duration of many resting state fMRI connectivity studies is five to seven minutes (Birn et al., 2013), a range that has been demonstrated to provide stable estimates of networks (van Wijk et al., 2010, Fox et al., 2005).

Spatial pre-processing was implemented in SPM12 using the standard SPM pipeline. Slice timing correction of the fMRI time series was performed using the first slice as the reference. Head motion and EPI distortion were corrected to the first functional volume. The estimated movement parameters (3 translation; 3 rotation) were saved and later included as covariates for each subject in the first level analysis to produce the connectivity matrix. Data were normalised into MNI (Montreal Neurological Institute) space using the ICBM 152 template of European brains (Mazziotta et al., 2001); the mean functional image was registered to the template image via a direct affine and interpolated into 2 x 2 x 2 mm voxel space using 4th degree B-Spline method. The resulting warp parameter was then applied to all volumes. Gaussian kernel smoothing with an 8mm full width half-maximum Gaussian kernel was employed at each data point and neighbourhood voxel. Tissue segmentation was performed using the SPM add-on CAT12 toolbox (http://www.neuro.uni-jena.de/cat/). This spatially normalises the T1 weighted image into the MNI space then segments it into skull-stripped brain. Following this, adaptive maximum a posteriori segmentation (AMAP) (Rajapakse et al., 1997) was performed to quantify estimates of grey matter, white matter and cerebrospinal fluid present at each element. An exclusion threshold for motion > 3mm translation and >1^{0} rotation was set (Fallon et al., 2016).

Spatially pre-processed data were next temporally pre-processed using the Functional Connectivity Toolbox (CONN) (Whitfield-Gabrieli and Nieto-Castanon, 2012). Component-based noise correction using the CompCor method (Behzadi et al., 2007) was performed to reduce voxel specific noise. Potential confounds from white matter and cerebrospinal fluid (based on Principal Component Analysis (PCA) of the multivariate BOLD signal within masks produced from T1 weighted tissue segmentation for each subject) were added as co-variates in CONN. Head motion effects that were detected in spatial pre-processing (6 estimated movement parameters per volume) were used as co-variates to further reduce noise. These steps are reported to increase sensitivity of results of both correlated and anticorrelated networks (Whitfield-Gabrieli and Nieto-Castanon, 2012). Bandpass filtering was also implemented to further remove physiological noise and to limit BOLD to between 0.01 and 0.08 Hz. Networks within this frequency range are widely reported to represent the resting state of the brain (Biswal et al., 1995, Buckner et al., 2008, Fox and Raichle, 2007, Whitfield-Gabrieli and Nieto-Castanon, 2012).

Network construction

Weighted functional connectivity matrices were constructed using the CONN functional connectivity toolbox. Data were parcellated using AICHA (Atlas of Intrinsic Connectivity of Homotopic Areas) (Joliot et al., 2015). This functional resting state connectivity atlas segregates data into 384 regions comprising 244 gyral regions, 100 sulcal regions and 40 grey matter nuclei. Network edges were defined using a weighted least squares linear model, where Pearson's correlation of average BOLD signal was determined between each pair of regions, with the strength of correlation forming the weight[4]. This was Fisher transformed to provide normally distributed scores, producing Z, representing the weighted matrix of Fisher transformed correlation coefficients.

Weighted, undirected, graphs were subsequently constructed using a custom script implemented in Matlab (R2019a). Thresholding was performed in order to improve sensitivity to physiologically relevant connections versus noise (Rubinov and Sporns, 2010), with connections with weights between -0.25 and + 0.25 excluded. There is no universally agreed threshold value, with variations from r = 0.1 to r = 0.8 seen in the literature (Garrison et al., 2015). A threshold of r = 0.25 was selected as it is a commonly used threshold (Eickhoff et al., 2015). There is no optimal solution to handle negative values in graph theoretical analysis (Fornito et al., 2016); typically either positively correlated values or absolute values are used (Fornito et al., 2013). The rationale for discarding negatively correlated edges comes from studies demonstrating that anticorrelated networks reflect artefact generated in pre-processing (Murphy et al., 2009, Saad et al., 2012). However, there is also evidence to suggest that anticorrelated networks have an important role in brain functioning (De Pisapia et al., 2012, Kelly et al., 2008) and as such, relevant connectivity information may be overlooked if negative correlations are ignored (Fornito et al., 2016). In view of this debate, and the fact that graph theoretic measures cannot account for signed weights, two separate analyses were performed for global metrics; one based on networks created from only positive correlations, and the other using absolute correlations.

4 As there is no clear optimal approach to delineating network edges, correlation was selected as it is the most conventional technique in fMRI studies (Fornito et al., 2013, Sala-Llonch et al., 2019) and therefore facilitates comparison of results from similar studies.

Graph analysis

Global measures of average node strength, node strength distribution variance, average clustering coefficient, characteristic path length, small-world index, and average betweenness centrality were calculated. These metrics were chosen to provide a broad overview of network topology. Because clustering coefficient and characteristic path length are sensitive to degree, normalised metrics were calculated for each by dividing average clustering coefficient and characteristic path length by the mean of the clustering coefficient and characteristic path length distributions of 500 surrogate random networks respectively (Stam et al., 2008, Stam et al., 2006).

As a post hoc analysis, strength and betweenness centrality were also calculated for each node individually. Subsequently, 'hub nodes' were identified for each participant. Nodes were considered as hubs if both strength and betweenness centrality were greater than one standard deviation above the corresponding mean network value (He et al., 2009, Bernhardt et al., 2011, Tian et al., 2011). The nodal metric analysis was carried out using absolute values only, and compared IGE with controls, in view of the results of the global network analysis.

Statistical analysis

Demographic and outcome metric results were firstly assessed for normality (by reviewing kurtosis, skewness, histograms and Q-Q plots). Next, potential differences in demographics and outcome metrics between the three groups were evaluated using Kruskal-Wallis tests or one-way analysis of covariance (ANCOVA), as appropriate. Age and epilepsy duration were included as co-variates. Where differences were found, pairwise comparisons were evaluated using a Mann-Whitney U or Tukey test. This was Bonferroni corrected for multiple comparisons. In addition, both groups with epilepsy were combined into one cohort and global outcome metrics were compared with controls using an independent t-test, controlled for participant age.

Potential differences in connectivity between individual nodes in IGE compared to controls were evaluated by comparing the strength and betweenness centrality of each node, using a Mann-Whitney U test. Correction for multiple comparisons was implemented using the False Discovery Rate (FDR) (Benjamini and Hochberg, 1995) with a q-value of 0.1. Following the identification of hub nodes, the total number of times a node was considered a hub in each

group was calculated and displayed visually. The number of hub nodes in each group was compared using a Kruskal-Wallis test.

5.5 Results

Participant demographics

(Table 9, page 156)

Median age significantly differed between groups (DR-IGE = 31 years; WC-IGE = 22.5 years; Controls = 32 years. Kruskal-Wallis H = 8.02, p = 0.018). Pairwise comparisons found a difference in age between WC-IGE and controls (p = 0.014), with no significant differences between WC-IGE and DR-IGE (p = 0.094), DR-IGE and controls (p = 1.00), or between both IGE groups (combined) and controls (p=0.066). Females comprised 59.7% of participants, with no significant difference across groups (Pearson Chi-square = 0.84, p = 0.656). Median duration of epilepsy was 14.5 years in DR-IGE and 6.5 years in WC-IGE. This difference was not statistically significant (Kruskal-Wallis H = 2.715, p = 0.099). The mean number of AEDs taken in the group with WC-IGE was 1.14 (range 1-2) and in the DR-IGE group was 1.9 (range 1-4). This difference was not statistically significant (Mann-Whitney U = 1.937, p = 0.524).

Global outcome metrics

(*Figure 26, page1 48, and tables C-1 to C4, section 5.10.1).* In the graphs constructed using absolute values, there was a difference between the three groups in average betweenness centrality (one-way ANOVA F = 4.657, p = 0.013). Pairwise comparisons identified a significantly higher average betweenness centrality in WC-IGE compared with controls (p = 0.048) and a possible trend towards a significantly higher average betweenness centrality in DR-IGE compared with controls (p = 0.057), with no difference between WC-IGE and DR-IGE (p = 1). There were no other differences in global metrics at the three-group level. When both IGE groups (WC-IGE and DR-IGE combined) were compared with controls, a higher average node strength *(figure 26 a)* and average betweenness centrality *(figure 26 f)* were found in the group with IGE (respectively; t = 5.956, p =0.017; t = 8.963, p= 0.004). A trend toward a significantly higher characteristic path length (*figure 2d*) and lower small-world index (*figure 26 e*) was seen in IGE (respectively; t = 3.864, p = 0.054; t= 3.787, p = 0.056). There were no differences in node strength distribution variance (*figure 2b*) or clustering coefficient (*figure 26 c*) between the two groups.

In the graphs constructed using positively correlated edges only, there were no significant results at the three-group level. A higher average node strength (*figure 26 g*) and greater characteristic path length (*figure 26 j*) was identified in IGE (WC-IGE and DR-IGE combined) compared to controls (respectively; $t = 6.200$, $p = 0.015$; $t = 4.717$ $p = 0.034$). The remaining outcome metrics did not significantly differ between the two groups (*figure 26 h, j, k, l*).

There was no correlation between age or epilepsy duration with any outcome metric (Pearson's correlation $p > 0.05$ in all comparisons).

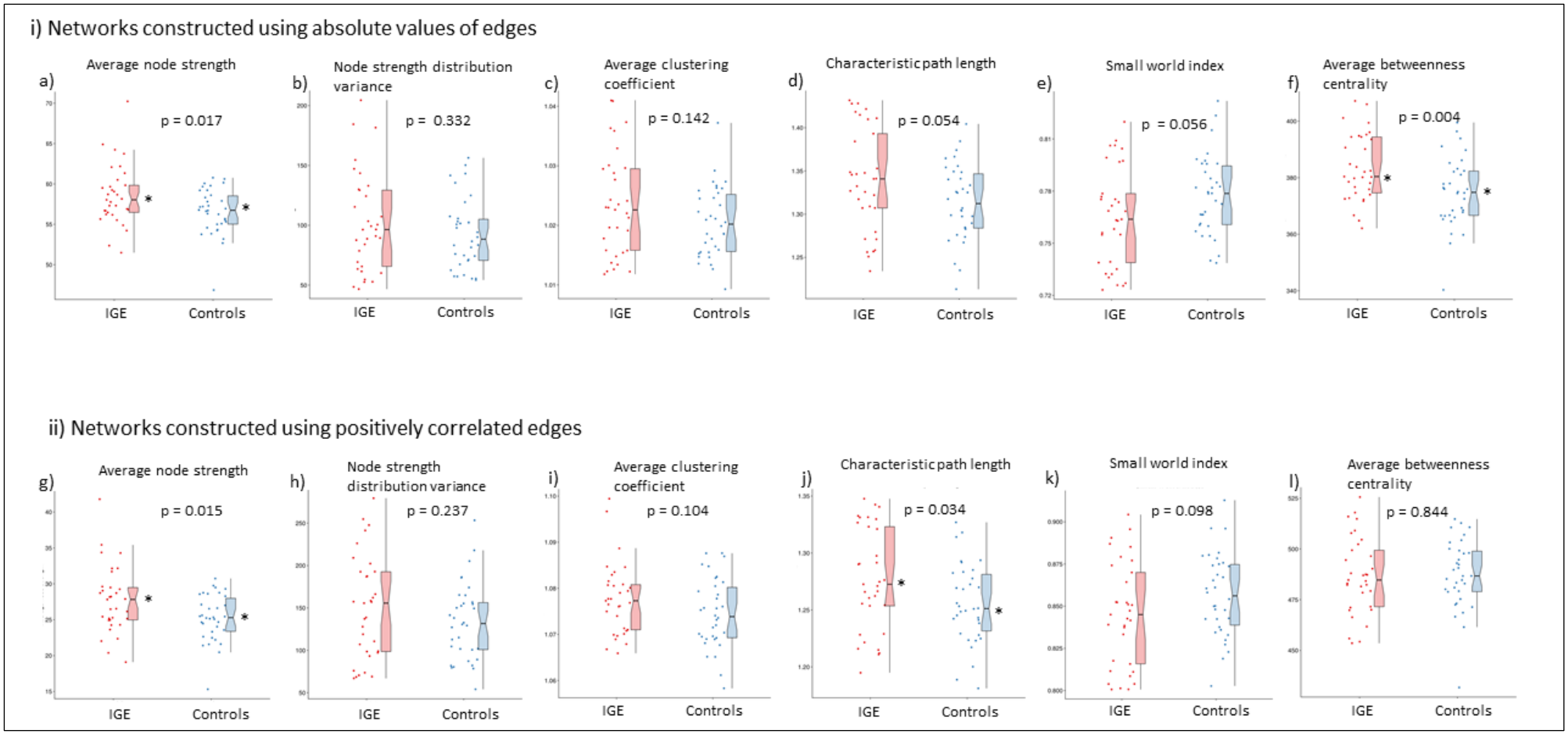

Figure 26. Global outcome metrics. Data is plotted for IGE (both groups combined) and controls. * = statistically significant difference between groups at $p < 0.05$.

Nodal outcome metrics

Neither betweenness centrality nor node strength survived correction for multiple comparisons. This was an exploratory study with 384 comparisons and therefore, results of uncorrected significant results, which may suggest a trend towards significance, are presented together with effect sizes (Althouse, 2016). Uncorrected significant differences in betweenness centrality and node strength at the level of individual nodes between the IGE group and controls were found in 37 and 35 nodes respectively *(tables C-5 and C-6 section 5.10.2).* Node strength was higher in IGE in each of the 35 nodes (*figure 27 a*), whereas there was a greater betweenness centrality at some of the 37 nodes in IGE and a lower value in others *(figure 27 b).*

The median number of hub nodes in each group was 38 and there was no significant difference in the total number of hub nodes between each group, in either the three group or two group comparison (respectively; Kruskal Wallis U = 0.593, p = 0.743; Mann-Whitney U = 617, p = 0.671). On inspection of plots of the frequency of hub nodes at each location, there were no clear group differences between the location of hub nodes *(table c-7, section 5.10.2 and figures C-1 to C-5, section 5.10.2).*

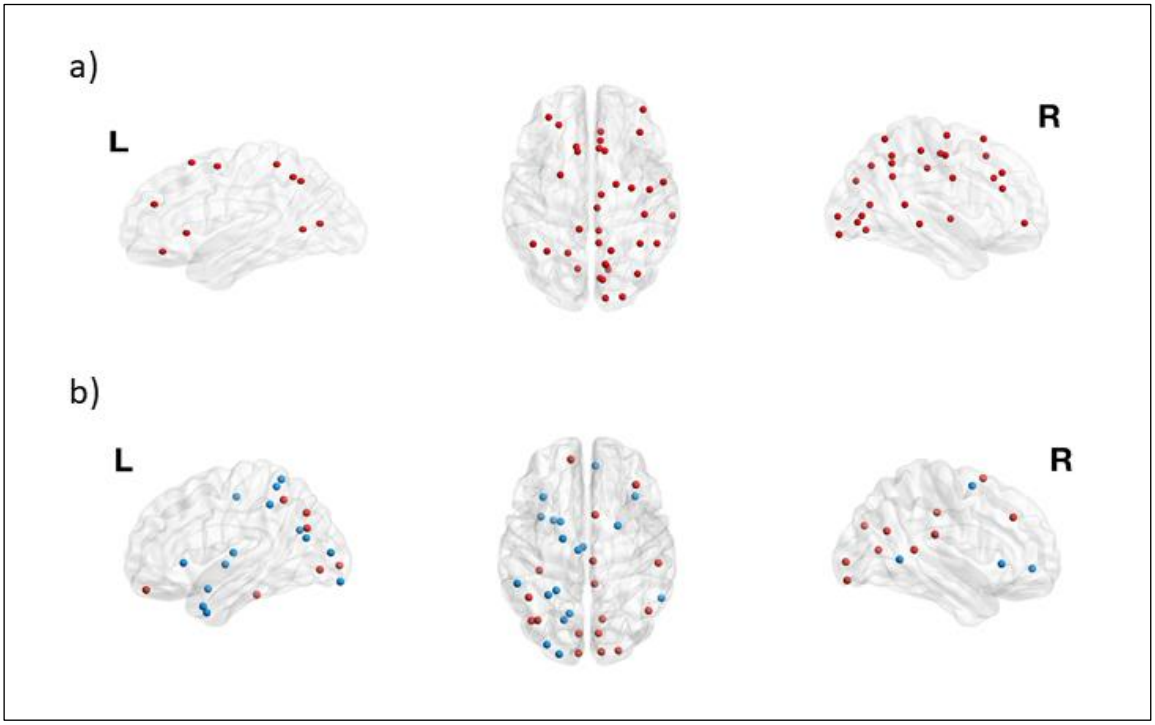

Figure 27. Nodal differences between IGE and controls. This illustrates the location of nodes that have significantly different *uncorrected* outcome metrics. a) node strength b) betweenness centrality. Red dots indicate a higher value in IGE, blue dots represent a lower value in IGE. L= left side of brain, R = right side of brain. This figure was created using BrainNet Viewer (Xia et al., 2013).

5.6 Discussion

This study investigated global resting state fMRI network features in people with drug resistant IGE, well-controlled IGE and healthy controls. The results suggest that compared to controls, network topology in IGE is less integrated (as evidenced by a higher path length) and has a generally greater connectivity across the network nodes (demonstrated by a higher average node strength and average betweenness centrality), without a clear difference in the location of hub nodes. Network topology did not vary according to seizure control.

A higher characteristic path length results in a more regular network topology (Watts and Strogatz, 1998). It has been suggested that a regular configuration may render a network more vulnerable to synchronisation (van Diessen et al., 2014b). The finding of a higher characteristic path length in IGE, is consistent with the findings from a meta-analysis of functional connectivity studies in focal epilepsy using fMRI and EEG (van Diessen et al., 2014c), and in structural studies in IGE (Xue et al., 2014a, Qiu et al., 2017, Lee and Park, 2019). However, in the two fMRI-derived functional connectivity studies (Zhang et al., 2011, Liao et al., 2013) identified in our systematic review (Pegg et al., 2020a), there was no difference in characteristic path length between people with IGE and controls. However, in both previous studies, networks were constructed using absolute correlations whereas the finding of altered characteristic path length in the present study was in positively correlated networks. In these same studies, also in contrast to the present study, one reported a lower clustering coefficient and small-world index in IGE (Zhang et al., 2011), and the other reported a higher small-world index in IGE (Liao et al., 2013). Average betweenness centrality and average node strength were not considered in these two studies. An important difference of our study compared to both of these studies is the method by which data were parcellated into nodes; in our study, a functional connectivity atlas was used, whereas the others used an anatomical atlas. It is known that the technique of data parcellation may affect connectivity measures (Arslan et al., 2018) and as such this is an important methodological decision. In functionally derived data parcellation schemes, nodes comprise components with similar temporal activation patterns. As such, it is suggested that such atlases are particularly suitable for functional connectivity analysis as the nodes reflect functionally coherent areas (Finn et al., 2015, Eickhoff et al., 2018, Shen et al., 2013).

The average node strength of a network reflects the strength of connections of each node across the network. Therefore, networks which have a higher average node strength perhaps reflect networks with generally greater connectivity. Similarly, networks with higher average

betweenness centrality (a measure of the extent of 'information flow' within a network), may also reflect a greater resting state hyperexcitability of the epileptic brain (Grobelny et al., 2018). There are limited studies within the IGE literature that have considered these metrics. Increased average betweenness centrality, average node strength, or mean degree have been reported in at least two EEG/MEG studies (Chavez et al., 2010, Chowdhury et al., 2014). However, other studies have reported no difference between groups (Caeyenberghs et al., 2015), or a decreased value (Xue et al., 2014b). It should be noted that the comparison between fMRI and EEG/MEG is challenging owing to their differing sensitivities to temporal and spatial resolution, which may account for diverging findings (Pegg et al., 2020a).

Previous fMRI connectivity studies have reported widespread locations of specific nodes that display altered connectivity in IGE, with a similar location of hub nodes in IGE and controls (Zhang et al., 2011, Liao et al., 2013). Both studies corrected for multiple comparisons using the FDR, but the threshold used is unclear. In the Liao at al study, significance levels did not survive this correction. Notwithstanding the fact that the individual nodal comparisons did not survive correction for multiple comparisons in our study, there is no suggestion from our study or from these previous studies, that there are specific regions of altered resting state connectivity in IGE. Whilst corticothalamic regions have been implicated in seizure genesis, it is possible that in generalised seizure disorders, the precise area of network aberration from where a seizure is initiated may vary between, or within, individuals (Anderson and Hamandi, 2011).

The additional findings depending on whether negatively correlated edges were discarded highlights that network topology is sensitive to the sign of the edge. As discussed above, the significance of anticorrelated networks and the extent to which they are influenced by pre-processing techniques is not fully elucidated. We suggest that by using absolute values, correlation values may be regarded as a reflection of the strength of neural connectivity, irrespective of the nature of the relationship. The similarity of results of both analyses suggests that the results are not confounded by taking into account negative correlations and in fact, their inclusion may improve sensitivity to the detection of network differences. How negative correlations may be mathematically accounted for in graph theoretic analysis is an important consideration for future graph theoretical studies.

It is possible that differences in network features in the group with IGE compared to controls represent medication effects. Previous studies have described alterations in global efficiency (inverse of characteristic path length) with topiramate, but not with valproate, lamotrigine or

levetiracetam (van Veenendaal et al., 2017). Another study reported altered betweenness centrality (but not other network metrics) with carbamazepine, but not with other commonly used AEDs (Haneef et al., 2015b). Therefore, overall, there is no strong evidence that medication effects directly explain the results. The inclusion of a group with epilepsy not taking an AED would help clarify this, but this would be practically difficult since AEDs are typically started at diagnosis.

This study did not find any differences in network topology dependent upon seizure control. One limitation of this interpretation is the small sample size of the WC-IGE group, which may have been underpowered to detect a possible difference. The low number of participants recruited with WC-IGE reflects the fact that they are less likely to remain under long-term follow up. Larger collaborations between institutions could help increase sample numbers (Whelan et al., 2018, Hatton et al., 2020). The study groups also differed in terms of age and epilepsy duration (although the latter was not statistically significant). The inclusion of these factors as covariates in the statistical analysis guards against confounding, however it remains possible that the results were influenced by these differences (Haneef et al., 2015a, Varangis et al., 2019). A further potential limitation relates to the difficulties in classifying response to AEDs; Patients may not be concordant with their antiepileptic medication and therefore may be inaccurately categorised as drug resistant. Alternatively, they may have unrecognised co-existent non-epileptic attacks, which could result in a seemingly higher seizure frequency. In addition, it is known that a proportion of patients follow a fluctuating course, shifting in and out of seizure control (Brodie et al., 2012). A larger study may enable the inclusion of this subgroup as a third category.

A further limitation of this study is that interictal epileptiform discharges (IEDs) in the group with IGE may have confounded the results. IEDs are associated with co-localised BOLD activation, in addition to BOLD activation in distant areas (Aghakhani et al., 2015). A combined EEG-fMRI study could overcome this limitation.

5.7 Conclusions

In summary, this study demonstrates that the network structure in IGE is more regular and has higher global connectivity, with no evidence of systematic alteration in the location of nodes with high connectivity. This was found to be the case irrespective of seizure control.

We suggest that examining drug resistance from a network perspective warrants further exploration in a larger, longitudinal, multimodal study.

5.8 Funding

SSK was supported by the Medical Research Council (grant numbers MR/S00355X/1 and MR/K023152/). EP is supported by Salford Royal NHS Foundation Trust.

Table 8. Commonly used graph theoretical terms and measures applied to epilepsy research

Node (vertex) *(n)*	The unit which forms a graph and represents an underlying brain region
Edge Directed edge Undirected edge Weighted edge	Connection between two nodes Information flows in one direction only Information flows in either direction A value given to an edge according to the strength of the connection
Degree distribution variance / node strength distribution variance	The variance of the node degree /node strength distribution
Degree (*k)* Node strength Average node strength	Number of connections of a node The summed strength of connections of a node Nodes with a high number of connections or a high connectivity strength may be regarded as 'hub nodes' The mean value of the node strengths of all network nodes (this is an equivalent measure to mean degree in a network that is not fully connected)
Clustering coefficient *(C)* Mean clustering coefficient *(Ci)*	The probability that the neighbouring nodes of a given node are themselves connected C is averaged to calculate the clustering coefficient of the whole graph. (A measure of network segregation)
Path length *(d)* Characteristic path length *(L)*	Minimum (or shortest) number of edges connecting 2 nodes Mean of the shortest path length between all pairs of network nodes (a measure of network integration)
Small- worldness	Ratio of average clustering coefficient of the graph to the mean clustering coefficient of a similar size random graph as a proportion of the ratio of the characteristic path length of the graph compared to the path length of a random graph [C / C *random*]

	[P / P *random*] Small-world networks have higher than expected clustering coefficient with a characteristic path length of equal or lower value than a random graph
Betweenness centrality	A measure of to what extent a node lies on all shortest paths between each pair of network nodes. A measure of the importance of a node within the network. Nodes with high betweenness centrality may be regarding as 'hub nodes'
Average betweenness centrality	The mean value of the betweenness centrality values of all network nodes

Table 9. Participant demographics (IGE group)

ID	Group	Age (years)	Gender	Onset age (years)	Seizure types	Antiepileptic medication	EEG findings
4	WC-IGE	25	M	19	MJ	Levetiracetam 1500mg, valproate 1600mg	Typical
18	WC-IGE	24	F	16	Abs, GTCS	Not known	n/a
23	WC-IGE	23	M	16	Abs, GTCS	Not known	n/a
24	WC-IGE	19	F	13	GTCS	Levetiracetam 3000mg	n/a
26	WC-IGE	18	F	15	Abs, eyelid myoclonus	Levetiracetam 2000mg	Typical
27	WC-IGE	22	M	2	Abs, MJ	Valproate 1400mg	n/a
29	WC-IGE	56	F	3	Abs	Valproate 1500mg	n/a
31	WC-IGE	33	M	7	Abs	Valproate 1800mg	Typical
32	WC-IGE	19	F	14	Abs, MJ	Levetiracetam 1000mg	n/a
34	WC-IGE	20	M	16	Abs	Levetiracetam 2000mg	n/a

1	DR-IGE	23	F	14	Abs, MJ	Levetiracetam 3000mg, topiramate 300mg, clobazam 10mg	Typical
2	DR-IGE	19	M	16	IGE	Valproate 1000mg	Typical
3	DR-IGE	19	F	8	GTCS, Abs	Lamotrigine 200mg	Normal
5	DR-IGE	60	F	13	GTCS, Abs	Valproate 2500mg	Typical
6	DR-IGE	24	M	15	GTC, MJ, abs	Levetiracetam 3000mg, valproate 2500mg, carbamazepine 1000mg	Typical
7	DR-IGE	21	F	15	GTC, MJ, abs	Levetiracetam 4000mg, valproate 2000mg	Typical
8	DR-IGE	32	F	23	GTC, MJ	Levetiracetam 3500mg, clobazam 15mg	Normal
9	DR-IGE	38	M	18	GTC, MJ	Valproate 600mg, lamotrigine 50mg	Typical
10	DR-IGE	67	M	29	GTC, Abs	Valproate 2000mg, lamotrigine 200mg, clobazam 10mg, phenobarbital 150mg	n/a
11	DR-IGE	46	F	7	Abs	Valproate 1200mg, lamotrigine 200mg, levetiracetam 2500mg	Normal

13	DR-IGE	20	M	8	GTC, Abs	Valproate 2000mg	Typical
14	DR-IGE	24	F	13	GTC, MJ	Topiramate 100mg	n/a
15	DR-IGE	35	M	6	GTC	Levetiracetam 2000mg, valproate 2000mg	Typical
16	DR-IGE	18	M	14	GTC, Abs	Valproate 1500mg, zonisamide 350mg	Typical
17	DR-IGE	39	M	17	GTC	Lamotrigine 75mg	Typical
19	DR-IGE	21	M	16	GTC, abs, MJ	Valproate 2400mg	n/a
20	DR-IGE	36	F	17	GTC	Levetiracetam 1250mg, lamotrigine 75mg	Typical
21	DR-IGE	31	F	15	GTC	Levetiracetam 2000mg, lamotrigine 400mg	Normal
22	DR-IGE	31	F	16	GTC, MJ, Abs	Valproate 1500mg, levetiracetam 3500mg	Typical
25	DR-IGE	58	F	15	GTC, Abs	Unknown	n/a
28	DR-IGE	24	M	13	MJ, abs	Valproate 1700mg	Typical

30	DR-IGE	57	F	7	GTC, abs	Valproate 1200mg, carbamazepine 600mg	Typical
33	DR-IGE	57	F	7	GTC, abs	Valproate 2000mg, lamotrigine 75mg	Typical

Table 9 displays participant information for the group with IGE. WC-IGE = well-controlled IGE, DR-IGE = drug resistant IGE. F = female, M = male, GTC = generalised tonic-clonic, MJ = myoclonic jerk, Abs = absence, typical= EEG findings in support of IGE, n/a = EEG not available.

5.9 Appendix B- Discussion of atlas choice

Methods of fMRI data parcellation based upon connectivity derived from the correlation of BOLD signals in the resting state are particularly suitable for functional connectivity studies (Finn et al., 2015, Eickhoff et al., 2018). This is because parcels share similar temporal activation patterns that are reflective of functionally coherent areas (Shen et al., 2013, Finn et al., 2015). Such connectivity may be derived at an individual level; however, this is time consuming for large datasets and can limit group-level comparisons (Arslan et al., 2018). Therefore, typically, an atlas is applied to the dataset. This integrates the dataset by aligning data from individual subjects to the atlas. At least seven such atlases exist, (Bellec et al., 2010, Craddock et al., 2012, Glasser et al., 2016, Gordon et al., 2016, Joliot et al., 2015, Schaefer et al., 2018, Shen et al., 2013) with no clear optimum choice. Differences in the available atlases include the number of parcels, the characteristics of subjects used in the development of the atlas, the amount of brain covered, and how similarity between voxels is determined in order to segregate data into parcels.

Data in our study were parcellated using AICHA (Joliot et al., 2015). AICHA defines 384 regions, delineated in the volumetric MNI space, comprising 244 gyral regions, 100 sulcal regions and 40 grey matter nuclei (*figure B-1*). This functional resting state connectivity atlas accounts for brain homotopy - an aspect of brain organisation relating to the fact that each region in a cerebral hemisphere has a corresponding region in the other hemisphere, which has comparable anatomical and functional features (Fuster, 1998, Mesulam, 1990). The rationale for selecting this atlas will be discussed herein.

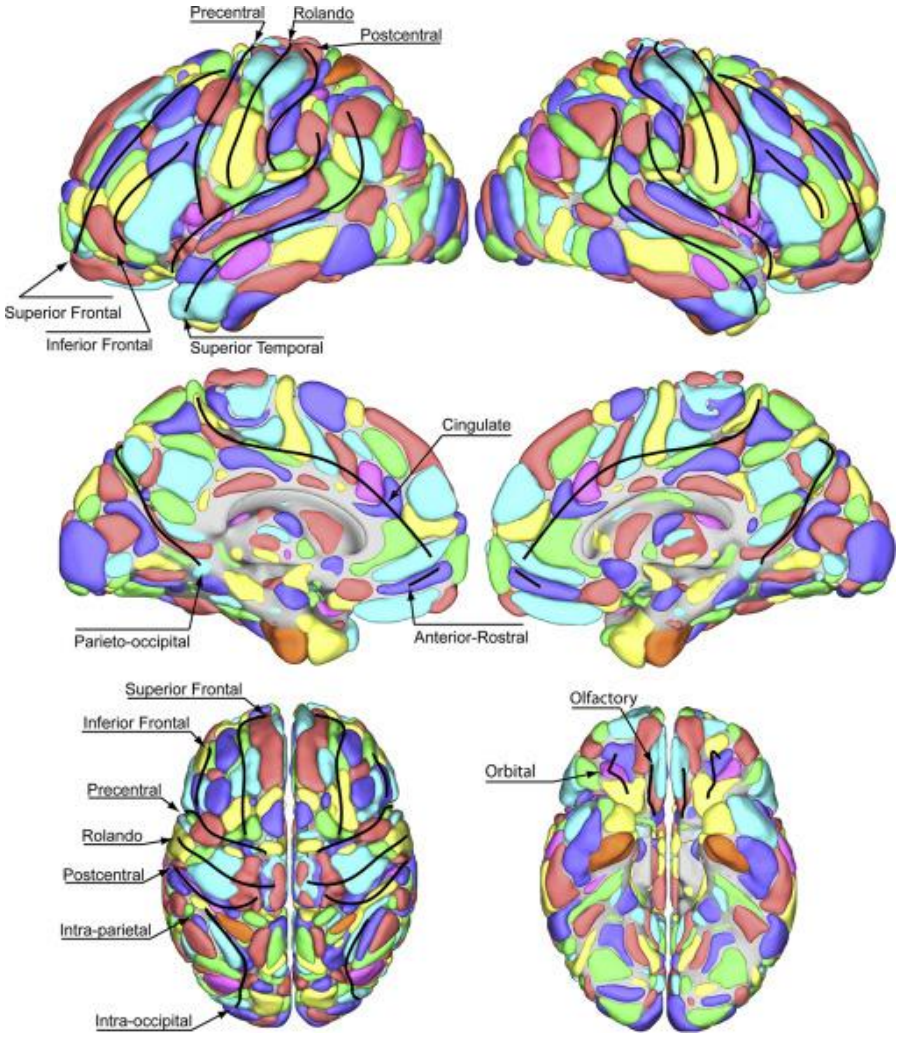

Figure B-1. Illustration of the rendering of AICHA and the sulci used in anatomical labelling. Reprinted from Journal of Neuroscience Methods, Vol 254, Joliot et al, AICHA: An atlas of intrinsic connectivity of homotopic areas., Pages 46-59., Copyright 2015, with permission from Elsevier.

Several clustering methods and algorithms exist to group data, each with their own advantages and biases (Eickhoff et al., 2015). However, theoretical studies to evaluate the comparative merits of each are lacking (Eickhoff et al., 2018). The construction of AICHA was based on k-means clustering, which is probably the most widely used approach in neuroimaging studies (Eickhoff et al., 2015). A potential limitation of this and other clustering methods is that assumptions must be applied to initialise clustering and to select the final number of clusters. Such assumptions can be avoided by using 'data-driven' or 'factorisation' techniques, where components are parcellated to best represent variations in data (for

example, using principal component analysis or independent component analysis). However, identified components are not always functionally relevant and may, for example, represent artifact (Finn et al., 2015). Although artifact can be removed via manual evaluation of components, this could also introduce bias.

An optimal number of parcellations has not been defined (Finn et al., 2015) and the scale of parcellations in available atlases ranges from seven (Yeo et al., 2011) to one-thousand (Craddock et al., 2012, Schaefer et al., 2018). It has been suggested that there is no "correct" number because the brain has multi-level organisation and, therefore, representation at different scales of parcellation may best reflect this feature (Eickhoff et al., 2018, Bellec et al., 2010, Yeo et al., 2011). It has been demonstrated that parcellations of 200 areas provides reproducibility across subjects (Shen et al., 2013). However, at more than 400 parcels reproducibility decreases (Shen et al., 2013). Befittingly, AICHA contains 384 parcels.

Atlases also vary according to whether they are constructed in the surface space (covering the cortex) or the volume space (providing coverage of the whole brain or parts of the whole brain). Four out of seven of the aforementioned atlases are in the volume space, one of which is AICHA, which parcellates the cortex and grey matter nuclei. A drawback of population-averaged volumetric templates compared to surface templates is reduced alignment of cortical folding (Mangin et al., 2010). This is of particular relevance for studies where greater cortical spatial localisation is of interest (Glasser et al., 2016). A benefit of a volume space atlas, such as AICHA, in a study of connectivity in epilepsy is that it includes the thalami, which are widely regarded to be an important part of the seizure network.

Whilst the optimal strategy to determine parcellation is debated, selecting an atlas that is generalisable to the study population seems more straightforward. It has been suggested that this should include consideration of subject ages, sex, cognition, medical history and ethnicity (Dickie et al., 2017). The first three of these factors, together with neurological and psychiatric conditions, have been reported to affect connectivity (Sala-Llonch et al., 2015, Donishi et al., 2018). However, to my knowledge, connectivity effects relating to ethnicity are not described and this detail has only been provided, to an extent, for one atlas where 63% of participants were described as white (Schaefer et al., 2018). There is no agreement on how subjects should be selected for the purpose of atlas construction. It has been proposed that the optimal solution is to create an atlas via random sampling of the general population (Joliot et al., 2015). However, a drawback of this approach is that it would result in the inclusion of people with

neurological or structural brain disorders (Joliot et al., 2015) and therefore would not be generalisable to healthy subjects.

AICHA was constructed from a relatively large dataset derived from 281 healthy volunteers who were aged 18-57 years. 48.75% of subjects were female and 10% were left-handed. There is wide variety in the number of individuals from whom atlases have been constructed, ranging from just one (Tzourio-Mazoyer et al., 2002, Destrieux et al., 2010, Power et al., 2011), to 1489 subjects (Schaefer et al., 2018). Within the subcategory of functional connectivity atlases which parcellate cortical *and* subcortical regions, AICHA was derived from the largest dataset (others range from 41- 79 subjects). The creators of AICHA state that the ages of the subjects had a "consistent range in variability". However, there is no explicit information on the age distribution of participants. Younger subjects are typically more likely to be recruited into studies (Joliot et al., 2015), which may result in an atlas that is less generalisable to older subjects. However, the age range of subjects used to construct AICHA (18 to 57), was comparable to the age range of participants in our study (18 to 67). As such, AICHA was a suitable choice with respect to age. 10% of subjects included in AICHA were left-handed. Since left-handedness is associated with organisational structures that differ from right-handedness, inclusion of subjects with left handedness at the prevalent general population level may also be regarded as a strength of AICHA. Around 10% of subjects in the Schaefer atlas were also left-handed (Schaefer et al., 2018). However, this atlas only covers the cortex, which makes it a less preferable option for this study. The handedness of subjects is reported in two other atlases (Shen et al., 2013, Gordon et al., 2016) but in these instances all are right-handed. Most atlases are balanced in terms of gender, including AICHA. This is reflective of our study participants, where there are similar numbers of male and female participants.

A unique feature of AICHA is that it takes into account homotopy between cerebral hemispheres. The existence of functional homotopy has been described in several studies (Van Den Heuvel and Pol, 2010, Jo et al., 2012, Beckmann et al., 2005, Yeo et al., 2011) and the connectivity between corresponding inter-hemispheric regions is demonstrated to be greater than between other inter or intra-hemispheric regions (Stark et al., 2008). This highlights the importance of homotopy in functional organisation of the brain and provides further support for the use of AICHA.

Each available atlas has been validated against alternatives (Arslan et al., 2018). However, assessing the quality of different approaches is limited by the fact that there is no empirical evidence for parcellation definition, and consequently there is a lack of reference parcellation

scheme with which to make comparisons. A widely accepted technique used to assess parcellation is to measure the homogeneity of parcels based upon the rationale that the more functionally similar parcellated brain regions are, the less homogenous intra-parcel connectivity will be. This is of particular relevance for fMRI network analysis since nodes are averages of the BOLD signals within each parcel (Arslan et al., 2018). Appraisal of homogeneity is commonly carried out using cluster validity analysis techniques, which assess the similarity of BOLD signal in voxels that have been parcelled together. Based upon the premise that parcellations reflecting biological processes should be stable, the quality of an atlas may also be assessed via its reproducibility, where alignment between parcel boundaries is measured. This can be performed across different acquisitions from the same subject, or by comparison with a different dataset.

In the validation of AICHA, parcel homogeneity was compared to another functional atlas (Craddock et al., 2012), as well as two macroscopic anatomically-derived atlases (Tzourio-Mazoyer et al., 2002, Desikan et al., 2006), and the Julich cytoarchitectonic atlas (Caspers et al., 2006). Both AICHA and Craddock atlases significantly outperformed the others, with greater homogeneity in the Craddock atlas than AICHA (0.18 and 0.2 respectively). It is possible that the greater homogeneity of the Craddock atlas relates to the smaller size of parcellations, which were determined via normalised-cut spectral clustering (whereas in AICHA, k-means clustering was used) (Joliot et al., 2015) ; It has been demonstrated that homogeneity correlates with parcel size, with some random and subject-level parcellation schemes exceeding the performance of functionally derived atlases (Urchs et al., 2017). Although the compactness of parcels produced by the Craddock atlas may favour higher homogeneity than AICHA, a drawback of the parcellation technique used in the Craddock atlas is the assumption that functionally independent areas are constrained by the same geometric shape (Joliot et al., 2015). In a review comparing 5 resting state fMRI derived atlases (Power et al., 2011, Yeo et al., 2011, Glasser et al., 2016, Shen et al., 2013, Gordon et al., 2016), alongside some structural atlases and subject-level parcellation methods, no clear method was consistently superior (Arslan et al., 2018); Homogeneity was highest for subject-level k-means clustering and low for anatomical atlases, whereas anatomical parcellations correlated best with cytoarchitecture, and subject level parcellations tended towards poorer reproducibility. Importantly, this study also demonstrated that connectivity-derived atlases had superior agreement with graph theoretic measures of connectivity than other atlas categories.

A key question for graph theoretical studies is how different parcellations may affect topological properties of the network. Converging evidence suggests that overall network

structure, for example small-worldness and regularity, is relatively consistent across parcellation schemes (Hayasaka and Laurienti, 2010, Fornito et al., 2010, Zalesky et al., 2010, Wang et al., 2009). However, quantitative measures pertaining to overall topology may vary (Fornito et al., 2016); increased normalised clustering, path length and degree with increased parcellation resolution have been reported (Arslan et al., 2018). This cautions against comparing the magnitude of alterations in network topology between studies when different atlases and different resolutions are used but suggests that choice of atlas does not affect overall conclusions regarding network topology.

In summary, AICHA is a suitable atlas choice for parcellating the fMRI data used in our study as it is derived from functional connectivity, its coverage extends to the thalami, it has good homogeneity, and the number of nodes is within a range that has demonstrated reproducibility. Although these features also apply to some other validated atlases (Bellec, Craddock, Shen), AICHA is generalisable to the characteristics of the study population and was constructed from the largest population.

5.10 Appendix C- Supplementary data

Supplementary data 1 - Global outcome metric results

	3 group comparison			Pairwise comparisons for statistically significant results		
	F stat-istic	P value	Partial Eta Squared	Groups Compared	P value	Std Error
Average node strength	2.97	0.059	0.086			
Node strength distribution variance	.988	0.378	0.030			
Average clustering coefficient	1.11	0.337	0.034			
Characteristic path length	2.11	0.130	0.063			
Small-world index	2.13	0.127	0.063			
Average betweenness centrality	4.66	0.013	0.129	WC-IGE – Con	0.048	4.455
				DR-IGE – Con	0.057	3.288
				WC-IGE – DR-IGE	1.000	4.742

Table C-2. Two-group comparison of networks constructed using absolute values of edges (Both IGE groups combined / Controls)

	F statistic	P value	Partial Eta Squared
Average node strength	5.956	0.017	0.085
Node strength distribution variance	.995	0.332	0.015
Average clustering coefficient	2.216	0.142	0.033
Characteristic path length	3.864	0.054	0.057
Small-world index	3.787	0.056	0.056
Average betweenness centrality	8.963	0.004	0.123

Table C-3. Three-group comparison of networks constructed using positively correlated edges only (WC-IGE / DR- IGE / Controls)

	F statistic	P value	Partial Eta Squared
Average node strength	3.072	0.053	0.89
Node strength distribution variance	0.949	.392	0.029
Average clustering coefficient	1.815	.171	0.054
Characteristic path length	2.689	.076	0.079
Small-world index	1.587	.213	0.048
Average betweenness centrality	0.405	.669	0.013

Table C-4. Two-group comparison of networks constructed using positively correlated edges only (Both IGE groups combined / Controls)

	F statistic	P value	Partial Eta Squared
Average node strength	6.200	0.015	0.088
Node strength distribution variance	1.425	0.237	0.022
Average clustering coefficient	2.725	0.104	0.041
Characteristic path length	4.717	0.034	0.069
Small-world index	2.827	0.098	0.042
Average betweenness centrality	0.039	.844	0.001

5.10.2 Supplementary data 2 - results of nodal analysis

Table C-5. Statistical significance of difference in node strength between IGE group (WC-IGE and DR-IGE combined) and controls for each region

AICHA region	AICHA region name	P value (un-corrected)	Mann-Whitney U	IGE mean rank	Control mean rank	Effect size
1	G_Frontal_Sup-1-L	NS				
2	G_Frontal_Sup-1-R	NS				
3	G_Frontal_Sup-2-L	NS				
4	G_Frontal_Sup-2-R	NS				
5	G_Frontal_Sup-3-L	NS				
6	G_Frontal_Sup-3-R	NS				
7	S_Sup_Frontal-1-L	NS				
8	S_Sup_Frontal-1-R	NS				
9	S_Sup_Frontal-2-L	0.009	352	40.33	27.85	-0.13
10	S_Sup_Frontal-2-R	NS				
11	S_Sup_Frontal-3-L	0.004	331	40.97	27.24	-0.15
12	S_Sup_Frontal-3-R	NS				
13	S_Sup_Frontal-4-L	NS				
14	S_Sup_Frontal-4-R	NS				
15	S_Sup_Frontal-5-L	NS				
16	S_Sup_Frontal-5-R	NS				
17	S_Sup_Frontal-6-L	NS				
18	S_Sup_Frontal-6-R	NS				
19	G_Frontal_Mid-1-L	NS				
20	G_Frontal_Mid-1-R	NS				
21	G_Frontal_Mid-2-L	NS				
22	G_Frontal_Mid-2-R	NS				
23	G_Frontal_Mid-3-L	0.014	365	39.94	28.24	-0.13
24	G_Frontal_Mid-3-R	NS				
25	G_Frontal_Mid-4-L	NS				

26	G_Frontal_Mid-4-R	NS				
27	G_Frontal_Mid-5-L	NS				
28	G_Frontal_Mid-5-R	NS				
29	S_Inf_Frontal-1-L	NS				
30	S_Inf_Frontal-1-R	NS				
31	S_Inf_Frontal-2-L	NS				
32	S_Inf_Frontal-2-R	NS				
33	G_Frontal_Inf_Tri-1-L	NS				
34	G_Frontal_Inf_Tri-1-R	NS				
35	G_Frontal_Sup_Orb-1-L	NS				
36	G_Frontal_Sup_Orb-1-R	NS				
37	G_Frontal_Mid_Orb-1-L	NS				
38	G_Frontal_Mid_Orb-1-R	NS				
39	G_Frontal_Mid_Orb-2-L	NS				
40	G_Frontal_Mid_Orb-2-R	NS				
41	G_Frontal_Inf_Orb-1-L	NS				
42	G_Frontal_Inf_Orb-1-R 4	NS				
43	G_Frontal_Inf_Orb-2-L	NS				
44	G_Frontal_Inf_Orb-2-R	NS				
45	S_Orbital-1-L	NS				
46	S_Orbital-1-R	NS				
47	S_Orbital-2-L	NS				
48	S_Orbital-2-R	NS				
49	S_Olfactory-1-L	NS				
50	S_Olfactory-1-R	NS				
51	S_Precentral-1-L	NS				
52	S_Precentral-1-R	NS				
53	S_Precentral-2-L	NS				
54	S_Precentral-2-R	0.032	390	39.18	28.97	-0.11
55	S_Precentral-3-L	NS				

56	S_Precentral-3-R	0.034	392	39.12	29.03	-0.11
57	S_Precentral-4-L	NS				
58	S_Precentral-4-R	NS				
59	S_Precentral-5-L	NS				
60	S_Precentral-5-R	NS				
61	S_Precentral-6-L	NS				
62	S_Precentral-6-R	NS				
63	S_Rolando-1-L	NS				
64	S_Rolando-1-R	NS				
65	S_Rolando-2-L	NS				
66	S_Rolando-2-R	NS				
67	S_Rolando-3-L	NS				
68	S_Rolando-3-R	NS				
69	S_Rolando-4-L	NS				
70	S_Rolando-4-R	NS				
71	S_Postcentral-1-L	NS				
72	S_Postcentral-1-R	NS				
73	S_Postcentral-2-L	NS				
74	S_Postcentral-2-R	NS				
75	S_Postcentral-3-L	NS				
76	S_Postcentral-3-R	NS				
77	G_Parietal_Sup-1-L	NS				
78	G_Parietal_Sup-1-R	NS				
79	G_Parietal_Sup-2-L	NS				
80	G_Parietal_Sup-2-R	NS				
81	G_Parietal_Sup-3-L	NS				
82	G_Parietal_Sup-3-R	NS				
83	G_Parietal_Sup-4-L	NS				
84	G_Parietal_Sup-4-R	NS				
85	G_Parietal_Sup-5-L	NS				
86	G_Parietal_Sup-5-R	NS				
87	G_Supramarginal-1-L	NS				
88	G_Supramarginal-1-R	NS				
89	G_SupraMarginal-2-L	NS				
90	G_SupraMarginal-2-R	NS				

91	G_Supramarginal-3-L	NS				
92	G_Supramarginal-3-R	NS				
93	G_Supramarginal-4-L	NS				
94	G_Supramarginal-4-R	NS				
95	G_SupraMarginal-5-L	NS				
96	G_SupraMarginal-5-R	NS				
97	G_SupraMarginal-6-L	NS				
98	G_SupraMarginal-6-R	NS				
99	G_SupraMarginal-7-L	NS				
100	G_SupraMarginal-7-R	NS				
101	G_Angular-1-L	NS				
102	G_Angular-1-R	NS				
103	G_Angular-2-L	NS				
104	G_Angular-2-R	NS				
105	G_Angular-3-L	NS				
106	G_Angular-3-R	NS				
107	G_Parietal_Inf-1-L	NS				
108	G_Parietal_Inf-1-R	NS				
109	S_Intraparietal-1-L	NS				
110	S_Intraparietal-1-R	NS				
111	S_Intraparietal-2-L	NS				
112	S_Intraparietal-2-R	0.024	381	39.45	28.71	-0.12
113	S_Intraparietal-3-L	NS				
114	S_Intraparietal-3-R	NS				
115	S_Intraoccipital-1-L	NS				
116	S_Intraoccipital-1-R	NS				
117	G_Occipital_Pole-1-L	NS				
118	G_Occipital_Pole-1-R	NS				
119	G_Occipital_Lat-1-L	NS				
120	G_Occipital_Lat-1-R	0.026	384	39.36	28.79	-0.11
121	G_Occipital_Lat-2-L	NS				
122	G_Occipital_Lat-2-R	NS				
123	G_Occipital_Lat-3-L	NS				
124	G_Occipital_Lat-3-R	NS				
125	G_Occipital_Lat-4-L	NS				
126	G_Occipital_Lat-4-R	NS				
127	G_Occipital_Lat-5-L	NS				
128	G_Occipital_Lat-5-R	NS				
129	G_Occipital_Sup-1-L	NS				
130	G_Occipital_Sup-1-R	NS				
131	G_Occipital_Sup-2-L	NS				
132	G_Occipital_Sup-2-R	NS				
133	G_Occipital_Mid-1-L	NS				
134	G_Occipital_Mid-1-R	NS				
135	G_Occipital_Mid-2-L	NS				
136	G_Occipital_Mid-2-R	NS				

137	G_Occipital_Mid-3-L	NS				
138	G_Occipital_Mid-3-R	NS				
139	G_Occipital_Mid-4-L	NS				
140	G_Occipital_Mid-4-R	NS				
141	G_Occipital_Inf-1-L	NS				
142	G_Occipital_Inf-1-R	NS				
143	G_Occipital_Inf-2-L	NS				
144	G_Occipital_Inf-2-R	NS				
145	G_Insula-anterior-1-L	0.036	394	39.06	29.09	-0.11
146	G_Insula-anterior-1-R	NS				
147	G_Insula-anterior-2-L	NS				
148	G_Insula-anterior-2-R	NS				
149	G_Insula-anterior-3-L	NS				
150	G_Insula-anterior-3-R	0.024	381	39.45	28.71	-0.12
151	G_Insula-anterior-4-L	NS				
152	G_Insula-anterior-4-R	NS				
153	G_Insula-anterior-5-L	NS				
154	G_Insula-anterior-5-R	NS				
155	G_Insula-posterior-1-L	NS				
156	G_Insula-posterior-1-R	NS				
157	G_Rolandic_Oper-1-L	NS				
158	G_Rolandic_Oper-1-R	NS				
159	G_Rolandic_Oper-2-L	NS				
160	G_Rolandic_Oper-2-R	NS				
161	G_Temporal_Sup-1-L	NS				
162	G_Temporal_Sup-1-R	NS				
163	G_Temporal_Sup-2-L	NS				
164	G_Temporal_Sup-2-R	NS				
165	G_Temporal_Sup-3-L	NS				
166	G_Temporal_Sup-3-R	NS				
167	G_Temporal_Sup-4-L	NS				
168	G_Temporal_Sup-4-R	NS				
169	S_Sup_Temporal-1-L	NS				
170	S_Sup_Temporal-1-R	NS				
171	S_Sup_Temporal-2-L	NS				
172	S_Sup_Temporal-2-R	NS				
173	S_Sup_Temporal-3-L	NS				
174	S_Sup_Temporal-3-R	0.021	377.5	39.56	28.6	-0.12
175	S_Sup_Temporal-4-L	NS				
176	S_Sup_Temporal-4-R	NS				
177	S_Sup_Temporal-5-L	NS				
178	S_Sup_Temporal-5-R	NS				
179	G_Temporal_Mid-1-L	NS				
180	G_Temporal_Mid-1-R	NS				
181	G_Temporal_Mid-2-L	NS				
182	G_Temporal_Mid-2-R	NS				

183	G_Temporal_Mid-3-L	NS				
184	G_Temporal_Mid-3-R	NS				
185	G_Temporal_Mid-4-L	NS				
186	G_Temporal_Mid-4-R	NS				
187	G_Temporal_Inf-1-L	NS				
188	G_Temporal_Inf-1-R	NS				
189	G_Temporal_Inf-2-L	NS				
190	G_Temporal_Inf-2-R	NS				
191	G_Temporal_Inf-3-L	NS				
192	G_Temporal_Inf-3-R	NS				
193	G_Temporal_Inf-4-L	NS				
194	G_Temporal_Inf-4-R	NS				
195	G_Temporal_Inf-5-L	NS				
196	G_Temporal_Inf-5-R	NS				
197	G_Temporal_Pole_Sup-1-L	NS				
198	G_Temporal_Pole_Sup-1-R	NS				
199	G_Temporal_Pole_Sup-2-L	NS				
200	G_Temporal_Pole_Sup-2-R	NS				
201	G_Temporal_Pole_Mid-1-L	NS				
202	G_Temporal_Pole_Mid-1-R	NS				
203	G_Temporal_Pole_Mid-2-L	NS				
204	G_Temporal_Pole_Mid-2-R	0.022	378	39.55	28.62	-0.12
205	G_Temporal_Pole_Mid-3-L	NS				
206	G_Temporal_Pole_Mid-3-R	NS				
207	G_Frontal_Sup_Medial-1-L	NS				
208	G_Frontal_Sup_Medial-1-R	NS				
209	G_Frontal_Sup_Medial-2-L	NS				
210	G_Frontal_Sup_Medial-2-R	NS				
211	G_Frontal_Sup_Medial-3-L	NS				
212	G_Frontal_Sup_Medial-3-R	NS	393	39.09	29.06	-0.11
213	S_Anterior_Rostral-1-L	NS				
214	S_Anterior_Rostral-1-R	NS				
215	G_Frontal_Med_Orb-1-L	NS				
216	G_Frontal_Med_Orb-1-R	NS				
217	G_Frontal_Med_Orb-2-L	NS				

218	G_Frontal_Med_Orb-2-R	NS				
219	G_subcallosal-1-L	NS				
220	G_subcallosal-1-R	NS				
221	G_Supp_Motor_Area-1-L	NS				
222	G_Supp_Motor_Area-1-R	NS				
223	G_Supp_Motor_Area-2-L	0.031	389	39.21	28.94	-0.11
224	G_Supp_Motor_Area-2-R	0.028	386	39.3	28.85	-0.11
225	G_Supp_Motor_Area-3-L	0.001	302	41.85	26.38	-0.17
226	G_Supp_Motor_Area-3-R	NS				
227	S_Cingulate-1-L	NS				
228	S_Cingulate-1-R	NS				
229	S_Cingulate-2-L	0.039	396	39	29.15	-0.12
230	S_Cingulate-2-R	NS				
231	S_Cingulate-3-L	NS				
232	S_Cingulate-3-R	NS				
233	S_Cingulate-4-L	NS				
234	S_Cingulate-4-R	NS				
235	S_Cingulate-5-L	0.045	401	38.85	29.29	-0.10
236	S_Cingulate-5-R	NS				
237	S_Cingulate-6-L	NS				
238	S_Cingulate-6-R	NS				
239	S_Cingulate-7-L	NS				
240	S_Cingulate-7-R	NS				
241	G_Cingulum_Ant-1-L	NS				
242	G_Cingulum_Ant-1-R	NS				
243	G_Cingulum_Ant-2-L	0.029	387	39.27	28.88	-0.11
244	G_Cingulum_Ant-2-R	NS				
245	G_Cingulum_Mid-1-L	NS				
246	G_Cingulum_Mid-1-R	NS				
247	G_Cingulum_Mid-2-L	NS				
248	G_Cingulum_Mid-2-R	0.022	378	39.55	28.62	-0.12
249	G_Cingulum_Mid-3-L	NS				
250	G_Cingulum_Mid-3-R	NS				
251	G_Cingulum_Post-1-L	NS	445	37.52	30.59	-0.14
252	G_Cingulum_Post-1-R	NS				
253	G_Cingulum_Post-2-L	NS				
254	G_Cingulum_Post-2-R	NS				
255	G_Cingulum_Post-3-L	NS				
256	G_Cingulum_Post-3-R	0.008	350	40.39	27.79	-0.13
257	G_Paracentral_Lobule-1-L	NS				
258	G_Paracentral_Lobule-1-R	NS				
259	G_Paracentral_Lobule-2-L	NS				
260	G_Paracentral_Lobule-2-R	NS				
261	G_Paracentral_Lobule-3-L	NS				
262	G_Paracentral_Lobule-3-R	NS				
263	G_Paracentral_Lobule-4-L	NS				

264	G_Paracentral_Lobule-4-R	NS				
265	G_Precuneus-1-L	NS				
266	G_Precuneus-1-R	NS				
267	G_Precuneus-2-L	NS				
268	G_Precuneus-2-R	NS				
269	G_Precuneus-3-L	NS				
270	G_Precuneus-3-R	NS				
271	G_Precuneus-4-L	NS				
272	G_Precuneus-4-R	NS				
273	G_Precuneus-5-L	NS				
274	G_Precuneus-5-R	NS				
275	G_Precuneus-6-L	NS				
276	G_Precuneus-6-R	NS				
277	G_Precuneus-7-L	NS				
278	G_Precuneus-7-R	NS				
279	G_Precuneus-8-L	NS				
280	G_Precuneus-8-R	NS				
281	G_Precuneus-9-L	NS				
282	G_Precuneus-9-R	NS				
283	S_Parietooccipital-1-L	NS				
284	S_Parietooccipital-1-R	0.012	360	40.09	28.09	-0.14
285	S_Parietooccipital-2-L	NS				
286	S_Parietooccipital-2-R	NS				
287	S_Parietooccipital-3-L	NS				
288	S_Parietooccipital-3-R	NS				
289	S_Parietooccipital-4-L	NS				
290	S_Parietooccipital-4-R	NS				
291	S_Parietooccipital-5-L	NS				
292	S_Parietooccipital-5-R	NS				
293	S_Parietooccipital-6-L	NS				
294	S_Parietooccipital-6-R	NS				
295	G_Cuneus-1-L	NS				
296	G_Cuneus-1-R	NS				
297	G_Cuneus-2-L	NS				
298	G_Cuneus-2-R	NS				
299	G_Calcarine-1-L	NS				
300	G_Calcarine-1-R	NS				
301	G_Calcarine-2-L	NS				
302	G_Calcarine-2-R	NS				
303	G_Calcarine-3-L	0.028	386	39.3	28.85	-0.11
304	G_Calcarine-3-R	0.029	387	39.27	28.88	-0.11
305	G_Lingual-1-L	NS				
306	G_Lingual-1-R	0.017	371	39.76	28.41	-0.12
307	G_Lingual-2-L	NS				
308	G_Lingual-2-R	NS				
309	G_Lingual-3-L	NS				

310	G_Lingual-3-R	NS				
311	G_Lingual-4-L	NS				
312	G_Lingual-4-R	NS				
313	G_Lingual-5-L	NS				
314	G_Lingual-5-R	0.027	385	39.33	28.82	-0.11
315	G_Lingual-6-L	NS				
316	G_Lingual-6-R	NS				
317	G_Hippocampus-1-L	0.005	337	40.79	27.41	-0.14
318	G_Hippocampus-1-R	NS				
319	G_Hippocampus-2-L	NS				
320	G_Hippocampus-2-R	0.001	293	42.12	26.12	-0.17
321	G_ParaHippocampal-1-L	0.024	381	39.45	28.71	-0.12
322	G_ParaHippocampal-1-R	NS				
323	G_ParaHippocampal-2-L	NS				
324	G_ParaHippocampal-2-R	NS				
325	G_ParaHippocampal-3-L	NS				
326	G_ParaHippocampal-3-R	NS				
327	G_ParaHippocampal-4-L	0.022	378	39.55	28.62	-0.12
328	G_ParaHippocampal-4-R	NS				
329	G_ParaHippocampal-5-L	NS				
330	G_ParaHippocampal-5-R	NS				
331	G_Fusiform-1-L	NS				
332	G_Fusiform-1-R	0.01	356	40.21	27.97	-0.13
333	G_Fusiform-2-L	NS				
334	G_Fusiform-2-R	NS				
335	G_Fusiform-3-L	NS				
336	G_Fusiform-3-R	NS				
337	G_Fusiform-4-L	NS				
338	G_Fusiform-4-R	NS				
339	G_Fusiform-5-L	NS				
340	G_Fusiform-5-R	0.034	392	39.12	29.03	-0.11
341	G_Fusiform-6-L	NS				
342	G_Fusiform-6-R	0.022	378	39.55	28.62	-0.12
343	G_Fusiform-7-L	NS				
344	G_Fusiform-7-R	0.007	346	40.52	27.68	-0.14
345	N_Amygdala-1-L	NS				
346	N_Amygdala-1-R	NS				
347	N_Caudate-1-L	NS				
348	N_Caudate-1-R	0.006	341	40.67	27.53	-0.14
349	N_Caudate-2-L	NS				
350	N_Caudate-2-R	0.015	367	39.88	28.29	-0.12
351	N_Caudate-3-L	NS				
352	N_Caudate-3-R	NS				
353	N_Caudate-4-L	NS				
354	N_Caudate-4-R	NS				
355	N_Caudate-5-L	NS				

356	N_Caudate-5-R	NS				
357	N_Caudate-6-L	NS				
358	N_Caudate-6-R	NS				
359	N_Caudate-7-L	NS				
360	N_Caudate-7-R	NS				
361	N_Pallidum-1-L	NS				
362	N_Pallidum-1-R	NS				
363	N_Putamen-2-L	NS				
364	N_Putamen-2-R	NS				
365	N_Putamen-3-L	NS				
366	N_Putamen-3-R	NS				
367	N_Thalamus-1-L	NS				
368	N_Thalamus-1-R	NS				
369	N_Thalamus-2-L	NS				
370	N_Thalamus-2-R	NS				
371	N_Thalamus-3-L	NS				
372	N_Thalamus-3-R	NS				
373	N_Thalamus-4-L	0.016	368	39.85	28.32	-0.12
374	N_Thalamus-4-R	NS				
375	N_Thalamus-5-L	NS				
376	N_Thalamus-5-R	NS				
377	N_Thalamus-6-L	NS				
378	N_Thalamus-6-R	NS				
379	N_Thalamus-7-L	NS				
380	N_Thalamus-7-R	NS				
381	N_Thalamus-8-L	NS				
382	N_Thalamus-8-R	NS				
383	N_Thalamus-9- L	NS				
384	N_Thalamus-9-R	NS				

NS = not significant at $p < 0.05$. Effect size calculated as $r=Z/\sqrt{N}$. All results displayed to two decimal points.

Table C-6. Statistical significance of difference in betweenness centrality between controls and people with IGE for each region

AICHA region	AICHA region name	p value (uncorrected)	Mann-Whitney U	IGE mean rank	Control mean rank	Effect size
1	G_Frontal_Sup-1-L	NS				
2	G_Frontal_Sup-1-R	NS				
3	G_Frontal_Sup-2-L	NS				
4	G_Frontal_Sup-2-R	NS				
5	G_Frontal_Sup-3-L	NS				
6	G_Frontal_Sup-3-R	NS				
7	S_Sup_Frontal-1-L	NS				
8	S_Sup_Frontal-1-R	NS				
9	S_Sup_Frontal-2-L	NS				
10	S_Sup_Frontal-2-R	NS				
11	S_Sup_Frontal-3-L	NS				
12	S_Sup_Frontal-3-R	NS				
13	S_Sup_Frontal-4-L	NS				
14	S_Sup_Frontal-4-R	NS				
15	S_Sup_Frontal-5-L	NS				
16	S_Sup_Frontal-5-R	NS				
17	S_Sup_Frontal-6-L	NS				
18	S_Sup_Frontal-6-R	0.005	339	40.73	28.32	-0.14
19	G_Frontal_Mid-1-L	NS				
20	G_Frontal_Mid-1-R	NS				
21	G_Frontal_Mid-2-L	NS				
22	G_Frontal_Mid-2-R	NS				
23	G_Frontal_Mid-3-L	NS				
24	G_Frontal_Mid-3-R	NS				
25	G_Frontal_Mid-4-L	NS				
26	G_Frontal_Mid-4-R	NS				
27	G_Frontal_Mid-5-L	NS				
28	G_Frontal_Mid-5-R	NS				
29	S_Inf_Frontal-1-L	NS				
30	S_Inf_Frontal-1-R	NS				
31	S_Inf_Frontal-2-L	NS				
32	S_Inf_Frontal-2-R	NS				
33	G_Frontal_Inf_Tri-1-L	NS				
34	G_Frontal_Inf_Tri-1-R	NS				
35	G_Frontal_Sup_Orb-1-L	NS				
36	G_Frontal_Sup_Orb-1-R	NS				
37	G_Frontal_Mid_Orb-1-L	NS				
38	G_Frontal_Mid_Orb-1-R	NS				
39	G_Frontal_Mid_Orb-2-L	0.017	751	28.24	40.6	0.15
40	G_Frontal_Mid_Orb-2-R	NS				
41	G_Frontal_Inf_Orb-1-L	NS				

42	G_Frontal_Inf_Orb-1-R 4	NS				
43	G_Frontal_Inf_Orb-2-L	NS				
44	G_Frontal_Inf_Orb-2-R	NS				
45	S_Orbital-1-L	NS				
46	S_Orbital-1-R	NS				
47	S_Orbital-2-L	NS				
48	S_Orbital-2-R	NS				
49	S_Olfactory-1-L	0.031	733	28.97	39.56	0.11
50	S_Olfactory-1-R	NS				
51	S_Precentral-1-L	NS				
52	S_Precentral-1-R	0.042	399	38.91	29.41	-0.10
53	S_Precentral-2-L	0.027	284.5	39.35	29.75	-0.11
54	S_Precentral-2-R	0.026	383	39.39	29	-0.11
55	S_Precentral-3-L	NS				
56	S_Precentral-3-R	NS				
57	S_Precentral-4-L	NS				
58	S_Precentral-4-R	NS				
59	S_Precentral-5-L	0.046	720	29.18	36.68	0.10
60	S_Precentral-5-R	NS				
61	S_Precentral-6-L	NS				
62	S_Precentral-6-R	NS				
63	S_Rolando-1-L	0.008	771.5	27.62	40.25	0.13
64	S_Rolando-1-R	NS				
65	S_Rolando-2-L	NS				
66	S_Rolando-2-R	NS				
67	S_Rolando-3-L	NS				
68	S_Rolando-3-R	NS				
69	S_Rolando-4-L	NS				
70	S_Rolando-4-R	NS				
71	S_Postcentral-1-L	NS				
72	S_Postcentral-1-R	NS				
73	S_Postcentral-2-L	0.007	776.5	27.47	41.25	0.14
74	S_Postcentral-2-R	NS				
75	S_Postcentral-3-L	0.007	777	27.45	41.35	0.14
76	S_Postcentral-3-R	NS				
77	G_Parietal_Sup-1-L	NS				
78	G_Parietal_Sup-1-R	NS				
79	G_Parietal_Sup-2-L	NS				
80	G_Parietal_Sup-2-R	NS				
81	G_Parietal_Sup-3-L	NS				
82	G_Parietal_Sup-3-R	NS				
83	G_Parietal_Sup-4-L	NS				
84	G_Parietal_Sup-4-R	NS				
85	G_Parietal_Sup-5-L	NS				
86	G_Parietal_Sup-5-R	NS				
87	G_Supramarginal-1-L	NS				

88	G_Supramarginal-1-R	NS				
89	G_SupraMarginal-2-L	NS				
90	G_SupraMarginal-2-R	NS				
91	G_Supramarginal-3-L	NS				
92	G_Supramarginal-3-R	NS				
93	G_Supramarginal-4-L	NS				
94	G_Supramarginal-4-R	NS				
95	G_SupraMarginal-5-L	NS				
96	G_SupraMarginal-5-R	NS				
97	G_SupraMarginal-6-L	NS				
98	G_SupraMarginal-6-R	NS				
99	G_SupraMarginal-7-L	NS				
100	G_SupraMarginal-7-R	NS				
101	G_Angular-1-L	NS				
102	G_Angular-1-R	0.014	756.5	28.08	39.75	0.13
103	G_Angular-2-L	0.04	724.5	29.05	39.72	0.10
104	G_Angular-2-R	NS				
105	G_Angular-3-L	NS				
106	G_Angular-3-R	NS				
107	G_Parietal_Inf-1-L	NS				
108	G_Parietal_Inf-1-R	NS				
109	S_Intraparietal-1-L	NS				
110	S_Intraparietal-1-R	NS				
111	S_Intraparietal-2-L	NS				
112	S_Intraparietal-2-R	NS				
113	S_Intraparietal-3-L	NS				
114	S_Intraparietal-3-R	NS				
115	S_Intraoccipital-1-L	NS				
116	S_Intraoccipital-1-R	NS				
117	G_Occipital_Pole-1-L	NS				
118	G_Occipital_Pole-1-R	NS				
119	G_Occipital_Lat-1-L	NS				
120	G_Occipital_Lat-1-R	NS				
121	G_Occipital_Lat-2-L	NS				
122	G_Occipital_Lat-2-R	NS				
123	G_Occipital_Lat-3-L	NS				
124	G_Occipital_Lat-3-R	NS				
125	G_Occipital_Lat-4-L	NS				
126	G_Occipital_Lat-4-R	NS				
127	G_Occipital_Lat-5-L	NS				
128	G_Occipital_Lat-5-R	NS				
129	G_Occipital_Sup-1-L	0.004	789	27.09	41.35	0.15
130	G_Occipital_Sup-1-R	NS				
131	G_Occipital_Sup-2-L	NS				
132	G_Occipital_Sup-2-R	NS				
133	G_Occipital_Mid-1-L	NS				

134	G_Occipital_Mid-1-R	NS				
135	G_Occipital_Mid-2-L	NS				
136	G_Occipital_Mid-2-R	NS				
137	G_Occipital_Mid-3-L	NS				
138	G_Occipital_Mid-3-R	NS				
139	G_Occipital_Mid-4-L	NS				
140	G_Occipital_Mid-4-R	NS				
141	G_Occipital_Inf-1-L	NS				
142	G_Occipital_Inf-1-R	NS				
143	G_Occipital_Inf-2-L	0.023	742.5	28.5	39.34	0.12
144	G_Occipital_Inf-2-R	NS				
145	G_Insula-anterior-1-L	NS				
146	G_Insula-anterior-1-R	0.017	750.5	28.26	39.57	0.12
147	G_Insula-anterior-2-L	NS				
148	G_Insula-anterior-2-R	NS				
149	G_Insula-anterior-3-L	NS				
150	G_Insula-anterior-3-R	NS				
151	G_Insula-anterior-4-L	NS				
152	G_Insula-anterior-4-R	0.043	399.5	38.89	29.25	-0.10
153	G_Insula-anterior-5-L	NS				
154	G_Insula-anterior-5-R	NS				
155	G_Insula-posterior-1-L	NS				
156	G_Insula-posterior-1-R	NS				
157	G_Rolandic_Oper-1-L	NS				
158	G_Rolandic_Oper-1-R	0.034	391.5	39.14	29.16	-0.11
159	G_Rolandic_Oper-2-L	NS				
160	G_Rolandic_Oper-2-R	NS				
161	G_Temporal_Sup-1-L	NS				
162	G_Temporal_Sup-1-R	NS				
163	G_Temporal_Sup-2-L	NS				
164	G_Temporal_Sup-2-R	NS				
165	G_Temporal_Sup-3-L	NS				
166	G_Temporal_Sup-3-R	NS				
167	G_Temporal_Sup-4-L	NS				
168	G_Temporal_Sup-4-R	0.048	403.5	38.77	29.72	-0.10
169	S_Sup_Temporal-1-L	NS				
170	S_Sup_Temporal-1-R	NS				
171	S_Sup_Temporal-2-L	NS				
172	S_Sup_Temporal-2-R	NS				
173	S_Sup_Temporal-3-L	NS				
174	S_Sup_Temporal-3-R	NS				
175	S_Sup_Temporal-4-L	NS				
176	S_Sup_Temporal-4-R	NS				
177	S_Sup_Temporal-5-L	NS				
178	S_Sup_Temporal-5-R	NS				
179	G_Temporal_Mid-1-L	NS				

180	G_Temporal_Mid-1-R	NS				
181	G_Temporal_Mid-2-L	0.012	761.5	27.92	40.09	0.13
182	G_Temporal_Mid-2-R	NS				
183	G_Temporal_Mid-3-L	NS				
184	G_Temporal_Mid-3-R	NS				
185	G_Temporal_Mid-4-L	NS				
186	G_Temporal_Mid-4-R	NS				
187	G_Temporal_Inf-1-L	0.042	723	29.09	39.65	0.10
188	G_Temporal_Inf-1-R	NS				
189	G_Temporal_Inf-2-L	NS				
190	G_Temporal_Inf-2-R	NS				
191	G_Temporal_Inf-3-L	NS				
192	G_Temporal_Inf-3-R	NS				
193	G_Temporal_Inf-4-L	NS				
194	G_Temporal_Inf-4-R	NS				
195	G_Temporal_Inf-5-L	NS				
196	G_Temporal_Inf-5-R	NS				
197	G_Temporal_Pole_Sup-1-L	NS				
198	G_Temporal_Pole_Sup-1-R	NS				
199	G_Temporal_Pole_Sup-2-L	NS				
200	G_Temporal_Pole_Sup-2-R	NS				
201	G_Temporal_Pole_Mid-1-L	0.035	729	28.91	39.76	0.11
202	G_Temporal_Pole_Mid-1-R	NS				
203	G_Temporal_Pole_Mid-2-L	NS				
204	G_Temporal_Pole_Mid-2-R	0.005	337.5	40.77	27.69	-0.14
205	G_Temporal_Pole_Mid-3-L	NS				
206	G_Temporal_Pole_Mid-3-R	NS				
207	G_Frontal_Sup_Medial-1-L	NS				
208	G_Frontal_Sup_Medial-1-R	NS				
209	G_Frontal_Sup_Medial-2-L	NS				
210	G_Frontal_Sup_Medial-2-R	NS				
211	G_Frontal_Sup_Medial-3-L	NS				
212	G_Frontal_Sup_Medial-3-R	NS				

213	S_Anterior_Rostral-1-L	NS				
214	S_Anterior_Rostral-1-R	NS				
215	G_Frontal_Med_Orb-1-L	NS				
216	G_Frontal_Med_Orb-1-R	NS				
217	G_Frontal_Med_Orb-2-L	NS				
218	G_Frontal_Med_Orb-2-R	NS				
219	G_subcallosal-1-L	NS				
220	G_subcallosal-1-R	NS				
221	G_Supp_Motor_Area-1-L	NS				
222	G_Supp_Motor_Area-1-R	NS				
223	G_Supp_Motor_Area-2-L	NS				
224	G_Supp_Motor_Area-2-R	NS				
225	G_Supp_Motor_Area-3-L	NS				
226	G_Supp_Motor_Area-3-R	NS				
227	S_Cingulate-1-L	NS				
228	S_Cingulate-1-R	NS				
229	S_Cingulate-2-L	NS				
230	S_Cingulate-2-R	NS				
231	S_Cingulate-3-L	NS				
232	S_Cingulate-3-R	NS				
233	S_Cingulate-4-L	NS				
234	S_Cingulate-4-R	NS				
235	S_Cingulate-5-L	NS				
236	S_Cingulate-5-R	0.034	392	39.12	29.56	-0.11
237	S_Cingulate-6-L	NS				
238	S_Cingulate-6-R	NS				
239	S_Cingulate-7-L	NS				
240	S_Cingulate-7-R	NS				
241	G_Cingulum_Ant-1-L	NS				
242	G_Cingulum_Ant-1-R	NS				
243	G_Cingulum_Ant-2-L	NS				
244	G_Cingulum_Ant-2-R	NS				
245	G_Cingulum_Mid-1-L	0.047	403	38.79	29.47	0.10
246	G_Cingulum_Mid-1-R	NS				
247	G_Cingulum_Mid-2-L	NS				
248	G_Cingulum_Mid-2-R	NS				
249	G_Cingulum_Mid-3-L	NS				
250	G_Cingulum_Mid-3-R	NS				
251	G_Cingulum_Post-1-L	0.009	354	40.27	28.29	-0.13
252	G_Cingulum_Post-1-R	NS				
253	G_Cingulum_Post-2-L	NS				
254	G_Cingulum_Post-2-R	NS				
255	G_Cingulum_Post-3-L	NS				
256	G_Cingulum_Post-3-R	NS				

257	G_Paracentral_Lobule-1-L	NS				
258	G_Paracentral_Lobule-1-R	NS				
259	G_Paracentral_Lobule-2-L	NS				
260	G_Paracentral_Lobule-2-R	NS				
261	G_Paracentral_Lobule-3-L	NS				
262	G_Paracentral_Lobule-3-R	NS				
263	G_Paracentral_Lobule-4-L	NS				
264	G_Paracentral_Lobule-4-R	NS				
265	G_Precuneus-1-L	NS				
266	G_Precuneus-1-R	NS				
267	G_Precuneus-2-L	0.03	734	28.76	39.35	0.11
268	G_Precuneus-2-R	NS				
269	G_Precuneus-3-L	NS				
270	G_Precuneus-3-R	NS				
271	G_Precuneus-4-L	NS				
272	G_Precuneus-4-R	NS				
273	G_Precuneus-5-L	NS				
274	G_Precuneus-5-R	NS				
275	G_Precuneus-6-L	NS				
276	G_Precuneus-6-R	NS				
277	G_Precuneus-7-L	NS				
278	G_Precuneus-7-R	NS				
279	G_Precuneus-8-L	NS				
280	G_Precuneus-8-R	NS				
281	G_Precuneus-9-L	NS				
282	G_Precuneus-9-R	NS				
283	S_Parietooccipital-1-L	NS				
284	S_Parietooccipital-1-R	NS				
285	S_Parietooccipital-2-L	0.036	632	31.85	36.09	-0.11
286	S_Parietooccipital-2-R	NS				
287	S_Parietooccipital-3-L	NS				
288	S_Parietooccipital-3-R	NS				
289	S_Parietooccipital-4-L	NS				
290	S_Parietooccipital-4-R	NS				
291	S_Parietooccipital-5-L	NS				
292	S_Parietooccipital-5-R	NS				
293	S_Parietooccipital-6-L	NS				
294	S_Parietooccipital-6-R	NS				
295	G_Cuneus-1-L	NS				
296	G_Cuneus-1-R	NS				

297	G_Cuneus-2-L	NS				
298	G_Cuneus-2-R	NS				
299	G_Calcarine-1-L	0.037	727.5	28.95	38.9	0.11
300	G_Calcarine-1-R	NS				
301	G_Calcarine-2-L	NS				
302	G_Calcarine-2-R	NS				
303	G_Calcarine-3-L	NS				
304	G_Calcarine-3-R	NS				
305	G_Lingual-1-L	0.036	394	39.06	39.06	-0.11
306	G_Lingual-1-R	NS				
307	G_Lingual-2-L	NS				
308	G_Lingual-2-R	NS				
309	G_Lingual-3-L	NS				
310	G_Lingual-3-R	NS				
311	G_Lingual-4-L	NS				
312	G_Lingual-4-R	NS				
313	G_Lingual-5-L	NS				
314	G_Lingual-5-R	NS				
315	G_Lingual-6-L	NS				
316	G_Lingual-6-R	NS				
317	G_Hippocampus-1-L	0.024	381.5	39.44	29.51	-0.11
318	G_Hippocampus-1-R	NS				
319	G_Hippocampus-2-L	NS				
320	G_Hippocampus-2-R	0.032	390	39.18	29.03	-0.11
321	G_ParaHippocampal-1-L	NS				
322	G_ParaHippocampal-1-R	NS				
323	G_ParaHippocampal-2-L	NS				
324	G_ParaHippocampal-2-R	NS				
325	G_ParaHippocampal-3-L	NS				
326	G_ParaHippocampal-3-R	NS				
327	G_ParaHippocampal-4-L	NS				
328	G_ParaHippocampal-4-R	NS				
329	G_ParaHippocampal-5-L	NS				
330	G_ParaHippocampal-5-R	NS				
331	G_Fusiform-1-L	NS				
332	G_Fusiform-1-R	NS				
333	G_Fusiform-2-L	NS				
334	G_Fusiform-2-R	NS				
335	G_Fusiform-3-L	NS				
336	G_Fusiform-3-R	NS				
337	G_Fusiform-4-L	NS				
338	G_Fusiform-4-R	NS				
339	G_Fusiform-5-L	NS				
340	G_Fusiform-5-R	0.034	392	39.12	29.21	-0.11
341	G_Fusiform-6-L	NS				
342	G_Fusiform-6-R	0.04	397	38.97	29.79	-0.10

343	G_Fusiform-7-L	NS				
344	G_Fusiform-7-R	0.008	348	40.75	28.53	-0.14
345	N_Amygdala-1-L	NS				
346	N_Amygdala-1-R	NS				
347	N_Caudate-1-L	NS				
348	N_Caudate-1-R	NS				
349	N_Caudate-2-L	NS				
350	N_Caudate-2-R	NS				
351	N_Caudate-3-L	NS				
352	N_Caudate-3-R	NS				
353	N_Caudate-4-L	NS				
354	N_Caudate-4-R	NS				
355	N_Caudate-5-L	NS				
356	N_Caudate-5-R	NS				
357	N_Caudate-6-L	NS				
358	N_Caudate-6-R	NS				
359	N_Caudate-7-L	NS				
360	N_Caudate-7-R	NS				
361	N_Pallidum-1-L	NS				
362	N_Pallidum-1-R	NS				
363	N_Putamen-2-L	NS				
364	N_Putamen-2-R	NS				
365	N_Putamen-3-L	NS				
366	N_Putamen-3-R	NS				
367	N_Thalamus-1-L	NS				
368	N_Thalamus-1-R	NS				
369	N_Thalamus-2-L	NS				
370	N_Thalamus-2-R	NS				
371	N_Thalamus-3-L	NS				
372	N_Thalamus-3-R	NS				
373	N_Thalamus-4-L	NS				
374	N_Thalamus-4-R	NS				
375	N_Thalamus-5-L	NS				
376	N_Thalamus-5-R	NS				
377	N_Thalamus-6-L	NS				
378	N_Thalamus-6-R	NS				
379	N_Thalamus-7-L	NS				
380	N_Thalamus-7-R	NS				
381	N_Thalamus-8-L	NS				
382	N_Thalamus-8-R	NS				
383	N_Thalamus-9- L	NS				
384	N_Thalamus-9-R	NS				

NS = not significant at $p < 0.05$. Effect size calculated as $r = Z/\sqrt{N}$. All results displayed to two decimal points.

Table C-7. Frequency of hub nodes in each region

AICHA region	AICHA region name	Controls	IGE (both groups)	WC-IGE	DR-IGE
1	G_Frontal_Sup-1-L	3	1	0	1
2	G_Frontal_Sup-1-R	1	0	0	0
3	G_Frontal_Sup-2-L	12	11	5	6
4	G_Frontal_Sup-2-R	14	20	3	17
5	G_Frontal_Sup-3-L	1	3	1	2
6	G_Frontal_Sup-3-R	0	1	0	1
7	S_Sup_Frontal-1-L	0	0	0	0
8	S_Sup_Frontal-1-R	1	4	1	3
9	S_Sup_Frontal-2-L	0	2	1	1
10	S_Sup_Frontal-2-R	3	2	1	1
11	S_Sup_Frontal-3-L	3	1	0	1
12	S_Sup_Frontal-3-R	2	5	1	4
13	S_Sup_Frontal-4-L	8	11	6	5
14	S_Sup_Frontal-4-R	9	8	3	5
15	S_Sup_Frontal-5-L	5	3	0	3
16	S_Sup_Frontal-5-R	4	5	1	4
17	S_Sup_Frontal-6-L	7	3	0	3
18	S_Sup_Frontal-6-R	4	12	4	8
19	G_Frontal_Mid-1-L	4	4	1	3
20	G_Frontal_Mid-1-R	5	6	1	5
21	G_Frontal_Mid-2-L	2	3	0	3
22	G_Frontal_Mid-2-R	8	8	3	5
23	G_Frontal_Mid-3-L	0	2	2	0
24	G_Frontal_Mid-3-R	4	6	0	6
25	G_Frontal_Mid-4-L	4	8	2	6
26	G_Frontal_Mid-4-R	1	4	1	3
27	G_Frontal_Mid-5-L	2	4	2	2
28	G_Frontal_Mid-5-R	4	4	0	4
29	S_Inf_Frontal-1-L	3	4	1	3
30	S_Inf_Frontal-1-R	2	2	1	1
31	S_Inf_Frontal-2-L	5	2	0	2
32	S_Inf_Frontal-2-R	4	4	0	4
33	G_Frontal_Inf_Tri-1-L	3	3	0	3
34	G_Frontal_Inf_Tri-1-R	2	3	2	1
35	G_Frontal_Sup_Orb-1-L	1	1	1	0
36	G_Frontal_Sup_Orb-1-R	0	0	0	0
37	G_Frontal_Mid_Orb-1-L	0	1	0	1
38	G_Frontal_Mid_Orb-1-R	0	1	0	1
39	G_Frontal_Mid_Orb-2-L	4	3	0	3
40	G_Frontal_Mid_Orb-2-R	2	4	2	2
41	G_Frontal_Inf_Orb-1-L	0	0	0	0
42	G_Frontal_Inf_Orb-1-R 4	4	1	0	1

43	G_Frontal_Inf_Orb-2-L	0	0	0	0
44	G_Frontal_Inf_Orb-2-R	1	0	0	0
45	S_Orbital-1-L	1	0	0	1
46	S_Orbital-1-R	1	1	0	0
47	S_Orbital-2-L	0	0	0	0
48	S_Orbital-2-R	1	0	0	4
49	S_Olfactory-1-L	13	4	0	0
50	S_Olfactory-1-R	0	0	1	2
51	S_Precentral-1-L	3	3	3	6
52	S_Precentral-1-R	4	9	0	0
53	S_Precentral-2-L	0	0	0	2
54	S_Precentral-2-R	0	2	1	0
55	S_Precentral-3-L	0	1	1	0
56	S_Precentral-3-R	2	1	0	2
57	S_Precentral-4-L	2	2	1	5
58	S_Precentral-4-R	7	6	0	1
59	S_Precentral-5-L	2	1	1	3
60	S_Precentral-5-R	1	4	0	1
61	S_Precentral-6-L	0	1	1	1
62	S_Precentral-6-R	0	2	0	0
63	S_Rolando-1-L	1	0	1	3
64	S_Rolando-1-R	4	4	1	2
65	S_Rolando-2-L	2	3	0	2
66	S_Rolando-2-R	2	2	1	2
67	S_Rolando-3-L	3	3	1	4
68	S_Rolando-3-R	4	5	1	7
69	S_Rolando-4-L	7	8	1	3
70	S_Rolando-4-R	7	4	1	1
71	S_Postcentral-1-L	2	2	0	2
72	S_Postcentral-1-R	2	2	0	6
73	S_Postcentral-2-L	13	6	2	6
74	S_Postcentral-2-R	5	8	0	4
75	S_Postcentral-3-L	2	4	0	3
76	S_Postcentral-3-R	6	3	1	0
77	G_Parietal_Sup-1-L	2	1	1	1
78	G_Parietal_Sup-1-R	1	2	1	3
79	G_Parietal_Sup-2-L	7	4	4	3
80	G_Parietal_Sup-2-R	7	7	1	5
81	G_Parietal_Sup-3-L	8	6	0	5
82	G_Parietal_Sup-3-R	6	5	1	3
83	G_Parietal_Sup-4-L	7	4	1	3
84	G_Parietal_Sup-4-R	4	4	1	6
85	G_Parietal_Sup-5-L	9	7	1	4
86	G_Parietal_Sup-5-R	10	5	3	4
87	G_Supramarginal-1-L	11	7	2	6
88	G_Supramarginal-1-R	7	8	1	6

89	G_SupraMarginal-2-L	6	7	1	8
90	G_SupraMarginal-2-R	10	9	4	5
91	G_Supramarginal-3-L	8	9	2	5
92	G_Supramarginal-3-R	8	7	1	5
93	G_Supramarginal-4-L	9	6	2	8
94	G_Supramarginal-4-R	9	10	0	1
95	G_SupraMarginal-5-L	1	1	1	3
96	G_SupraMarginal-5-R	3	4	1	4
97	G_SupraMarginal-6-L	1	5	1	3
98	G_SupraMarginal-6-R	10	4	1	4
99	G_SupraMarginal-7-L	4	5	0	1
100	G_SupraMarginal-7-R	6	1	3	9
101	G_Angular-1-L	18	12	3	6
102	G_Angular-1-R	14	9	6	13
103	G_Angular-2-L	23	19	6	13
104	G_Angular-2-R	17	19	5	7
105	G_Angular-3-L	14	12	3	7
106	G_Angular-3-R	9	10	1	4
107	G_Parietal_Inf-1-L	8	5	1	7
108	G_Parietal_Inf-1-R	9	8	1	8
109	S_Intraparietal-1-L	12	9	3	10
110	S_Intraparietal-1-R	14	13	4	7
111	S_Intraparietal-2-L	10	11	1	9
112	S_Intraparietal-2-R	6	10	3	10
113	S_Intraparietal-3-L	8	13	3	4
114	S_Intraparietal-3-R	8	7	2	1
115	S_Intraoccipital-1-L	0	3	1	0
116	S_Intraoccipital-1-R	3	1	3	1
117	G_Occipital_Pole-1-L	1	4	1	2
118	G_Occipital_Pole-1-R	2	3	2	0
119	G_Occipital_Lat-1-L	1	2	0	1
120	G_Occipital_Lat-1-R	0	1	1	2
121	G_Occipital_Lat-2-L	3	3	2	4
122	G_Occipital_Lat-2-R	1	6	0	0
123	G_Occipital_Lat-3-L	1	0	0	1
124	G_Occipital_Lat-3-R	2	1	4	1
125	G_Occipital_Lat-4-L	6	5	1	1
126	G_Occipital_Lat-4-R	3	2	6	8
127	G_Occipital_Lat-5-L	13	14	5	8
128	G_Occipital_Lat-5-R	8	13	1	2
129	G_Occipital_Sup-1-L	9	3	1	0
130	G_Occipital_Sup-1-R	3	1	1	4
131	G_Occipital_Sup-2-L	10	5	2	6
132	G_Occipital_Sup-2-R	6	8	3	5
133	G_Occipital_Mid-1-L	11	8	3	7
134	G_Occipital_Mid-1-R	7	10	1	1

135	G_Occipital_Mid-2-L	5	2	1	2
136	G_Occipital_Mid-2-R	3	3	1	4
137	G_Occipital_Mid-3-L	3	5	4	4
138	G_Occipital_Mid-3-R	2	8	3	5
139	G_Occipital_Mid-4-L	6	8	3	5
140	G_Occipital_Mid-4-R	4	8	0	1
141	G_Occipital_Inf-1-L	1	1	2	2
142	G_Occipital_Inf-1-R	2	4	0	3
143	G_Occipital_Inf-2-L	6	3	2	4
144	G_Occipital_Inf-2-R	3	6	0	2
145	G_Insula-anterior-1-L	0	2	0	0
146	G_Insula-anterior-1-R	1	0	0	0
147	G_Insula-anterior-2-L	1	0	0	2
148	G_Insula-anterior-2-R	1	2	1	0
149	G_Insula-anterior-3-L	1	1	2	4
150	G_Insula-anterior-3-R	4	6	3	3
151	G_Insula-anterior-4-L	5	6	4	11
152	G_Insula-anterior-4-R	9	15	1	0
153	G_Insula-anterior-5-L	6	1	2	4
154	G_Insula-anterior-5-R	10	6	1	2
155	G_Insula-posterior-1-L	1	3	0	0
156	G_Insula-posterior-1-R	2	0	6	4
157	G_Rolandic_Oper-1-L	7	10	3	7
158	G_Rolandic_Oper-1-R	4	10	3	3
159	G_Rolandic_Oper-2-L	3	6	1	2
160	G_Rolandic_Oper-2-R	2	3	1	2
161	G_Temporal_Sup-1-L	6	3	1	5
162	G_Temporal_Sup-1-R	2	6	0	1
163	G_Temporal_Sup-2-L	0	1	1	0
164	G_Temporal_Sup-2-R	1	1	1	3
165	G_Temporal_Sup-3-L	8	4	4	4
166	G_Temporal_Sup-3-R	7	8	0	3
167	G_Temporal_Sup-4-L	4	3	1	0
168	G_Temporal_Sup-4-R	2	1	0	0
169	S_Sup_Temporal-1-L	3	0	0	1
170	S_Sup_Temporal-1-R	1	1	0	1
171	S_Sup_Temporal-2-L	1	1	2	6
172	S_Sup_Temporal-2-R	5	8	1	2
173	S_Sup_Temporal-3-L	0	3	2	1
174	S_Sup_Temporal-3-R	1	3	1	1
175	S_Sup_Temporal-4-L	1	2	1	2
176	S_Sup_Temporal-4-R	3	3	6	11
177	S_Sup_Temporal-5-L	17	17	4	11
178	S_Sup_Temporal-5-R	14	15	3	3
179	G_Temporal_Mid-1-L	5	6	1	6
180	G_Temporal_Mid-1-R	3	7	2	2

181	G_Temporal_Mid-2-L	11	4	4	6
182	G_Temporal_Mid-2-R	5	10	2	2
183	G_Temporal_Mid-3-L	3	4	2	1
184	G_Temporal_Mid-3-R	0	3	3	1
185	G_Temporal_Mid-4-L	4	4	0	2
186	G_Temporal_Mid-4-R	6	2	0	0
187	G_Temporal_Inf-1-L	1	0	0	1
188	G_Temporal_Inf-1-R	0	1	0	0
189	G_Temporal_Inf-2-L	1	0	0	1
190	G_Temporal_Inf-2-R	4	1	1	2
191	G_Temporal_Inf-3-L	5	3	0	2
192	G_Temporal_Inf-3-R	1	2	2	3
193	G_Temporal_Inf-4-L	7	5	0	4
194	G_Temporal_Inf-4-R	6	4	0	0
195	G_Temporal_Inf-5-L	0	0	3	1
196	G_Temporal_Inf-5-R	4	4	1	1
197	G_Temporal_Pole_Sup-1-L	0	2	1	0
198	G_Temporal_Pole_Sup-1-R	1	1	1	0
199	G_Temporal_Pole_Sup-2-L	0	1	1	0
200	G_Temporal_Pole_Sup-2-R	0	1	1	3
201	G_Temporal_Pole_Mid-1-L	7	4	2	6
202	G_Temporal_Pole_Mid-1-R	2	8	0	0
203	G_Temporal_Pole_Mid-2-L	0	0	0	0
204	G_Temporal_Pole_Mid-2-R	1	0	0	1
205	G_Temporal_Pole_Mid-3-L	0	1	0	0
206	G_Temporal_Pole_Mid-3-R	0	0	1	7
207	G_Frontal_Sup_Medial-1-L	6	8	2	4
208	G_Frontal_Sup_Medial-1-R	6	6	3	9
209	G_Frontal_Sup_Medial-2-L	6	12	3	3
210	G_Frontal_Sup_Medial-2-R	9	6	1	1
211	G_Frontal_Sup_Medial-3-L	0	2	1	1
212	G_Frontal_Sup_Medial-3-R	0	2	2	8
213	S_Anterior_Rostral-1-L	12	10	1	3

214	S_Anterior_Rostral-1-R	7	4	1	4
215	G_Frontal_Med_Orb-1-L	4	5	0	1
216	G_Frontal_Med_Orb-1-R	4	1	1	11
217	G_Frontal_Med_Orb-2-L	13	12	2	4
218	G_Frontal_Med_Orb-2-R	3	6	1	0
219	G_subcallosal-1-L	0	1	0	0
220	G_subcallosal-1-R	0	0	0	0
221	G_Supp_Motor_Area-1-L	0	0	0	1
222	G_Supp_Motor_Area-1-R	2	1	0	2
223	G_Supp_Motor_Area-2-L	2	2	0	1
224	G_Supp_Motor_Area-2-R	0	1	1	1
225	G_Supp_Motor_Area-3-L	0	2	0	3
226	G_Supp_Motor_Area-3-R	2	3	0	1
227	S_Cingulate-1-L	0	1	0	1
228	S_Cingulate-1-R	2	1	0	1
229	S_Cingulate-2-L	2	1	1	9
230	S_Cingulate-2-R	5	10	0	2
231	S_Cingulate-3-L	6	2	4	11
232	S_Cingulate-3-R	10	15	1	4
233	S_Cingulate-4-L	4	5	3	7
234	S_Cingulate-4-R	9	10	0	1
235	S_Cingulate-5-L	1	1	0	2
236	S_Cingulate-5-R	0	2	1	2
237	S_Cingulate-6-L	2	3	2	3
238	S_Cingulate-6-R	6	5	1	1
239	S_Cingulate-7-L	2	2	2	3
240	S_Cingulate-7-R	3	5	0	2
241	G_Cingulum_Ant-1-L	2	2	1	6
242	G_Cingulum_Ant-1-R	6	7	0	0
243	G_Cingulum_Ant-2-L	0	0	3	0
244	G_Cingulum_Ant-2-R	1	3	0	0
245	G_Cingulum_Mid-1-L	1	0	0	0
246	G_Cingulum_Mid-1-R	1	0	0	0
247	G_Cingulum_Mid-2-L	0	0	0	0
248	G_Cingulum_Mid-2-R	0	0	1	1
249	G_Cingulum_Mid-3-L	2	2	1	2
250	G_Cingulum_Mid-3-R	2	3	1	0
251	G_Cingulum_Post-1-L	0	1	1	1
252	G_Cingulum_Post-1-R	0	2	1	4
253	G_Cingulum_Post-2-L	1	5	4	5
254	G_Cingulum_Post-2-R	4	9	1	3
255	G_Cingulum_Post-3-L	0	4	0	4
256	G_Cingulum_Post-3-R	1	4	0	1
257	G_Paracentral_Lobule-1-	0	1	0	3

	L				
258	G_Paracentral_Lobule-1-R	1	3	0	1
259	G_Paracentral_Lobule-2-L	0	1	0	2
260	G_Paracentral_Lobule-2-R	2	2	1	1
261	G_Paracentral_Lobule-3-L	0	2	1	2
262	G_Paracentral_Lobule-3-R	1	3	1	0
263	G_Paracentral_Lobule-4-L	0	1	0	1
264	G_Paracentral_Lobule-4-R	0	1	2	12
265	G_Precuneus-1-L	9	14	4	5
266	G_Precuneus-1-R	6	9	3	8
267	G_Precuneus-2-L	14	11	4	7
268	G_Precuneus-2-R	12	12	5	14
269	G_Precuneus-3-L	17	19	6	10
270	G_Precuneus-3-R	24	16	1	2
271	G_Precuneus-4-L	2	3	1	7
272	G_Precuneus-4-R	6	8	0	1
273	G_Precuneus-5-L	4	1	1	2
274	G_Precuneus-5-R	6	3	1	6
275	G_Precuneus-6-L	6	7	1	6
276	G_Precuneus-6-R	9	7	1	6
277	G_Precuneus-7-L	9	7	2	6
278	G_Precuneus-7-R	12	8	0	3
279	G_Precuneus-8-L	4	3	3	9
280	G_Precuneus-8-R	10	12	1	4
281	G_Precuneus-9-L	5	5	4	3
282	G_Precuneus-9-R	7	7	2	7
283	S_Parietooccipital-1-L	5	9	4	7
284	S_Parietooccipital-1-R	5	12	1	1
285	S_Parietooccipital-2-L	1	2	1	2
286	S_Parietooccipital-2-R	3	3	0	3
287	S_Parietooccipital-3-L	7	3	1	5
288	S_Parietooccipital-3-R	6	6	1	2
289	S_Parietooccipital-4-L	3	3	1	1
290	S_Parietooccipital-4-R	3	2	0	1
291	S_Parietooccipital-5-L	1	1	0	2
292	S_Parietooccipital-5-R	0	2	0	4
293	S_Parietooccipital-6-L	4	4	0	1
294	S_Parietooccipital-6-R	2	1	0	3
295	G_Cuneus-1-L	6	3	1	1
296	G_Cuneus-1-R	1	2	1	2

297	G_Cuneus-2-L	0	3	1	1
298	G_Cuneus-2-R	1	2	1	3
299	G_Calcarine-1-L	3	4	1	3
300	G_Calcarine-1-R	1	4	0	5
301	G_Calcarine-2-L	6	5	2	4
302	G_Calcarine-2-R	5	6	0	4
303	G_Calcarine-3-L	1	4	2	3
304	G_Calcarine-3-R	2	5	0	1
305	G_Lingual-1-L	0	1	0	1
306	G_Lingual-1-R	1	1	1	1
307	G_Lingual-2-L	3	2	0	1
308	G_Lingual-2-R	1	1	2	1
309	G_Lingual-3-L	1	3	1	1
310	G_Lingual-3-R	3	2	0	1
311	G_Lingual-4-L	2	1	0	0
312	G_Lingual-4-R	1	0	0	0
313	G_Lingual-5-L	1	0	0	1
314	G_Lingual-5-R	1	1	0	1
315	G_Lingual-6-L	0	1	0	2
316	G_Lingual-6-R	0	2	0	0
317	G_Hippocampus-1-L	0	0	0	2
318	G_Hippocampus-1-R	0	2	0	0
319	G_Hippocampus-2-L	1	0	0	0
320	G_Hippocampus-2-R	1	0	0	1
321	G_ParaHippocampal-1-L	1	1	0	0
322	G_ParaHippocampal-1-R	0	0	0	1
323	G_ParaHippocampal-2-L	1	1	0	1
324	G_ParaHippocampal-2-R	1	1	0	1
325	G_ParaHippocampal-3-L	0	1	0	1
326	G_ParaHippocampal-3-R	0	1	0	1
327	G_ParaHippocampal-4-L	0	1	1	0
328	G_ParaHippocampal-4-R	4	1	0	0
329	G_ParaHippocampal-5-L	3	0	0	2
330	G_ParaHippocampal-5-R	1	2	1	1
331	G_Fusiform-1-L	0	2	0	1
332	G_Fusiform-1-R	0	1	0	1
333	G_Fusiform-2-L	0	1	0	0
334	G_Fusiform-2-R	0	0	0	0
335	G_Fusiform-3-L	0	0	1	0
336	G_Fusiform-3-R	0	2	0	0
337	G_Fusiform-4-L	2	0	1	2
338	G_Fusiform-4-R	0	3	0	0
339	G_Fusiform-5-L	0	0	1	1
340	G_Fusiform-5-R	0	2	1	1
341	G_Fusiform-6-L	2	2	1	1
342	G_Fusiform-6-R	1	2	0	0

343	G_Fusiform-7-L	1	0	2	1
344	G_Fusiform-7-R	0	3	0	1
345	N_Amygdala-1-L	0	1	0	0
346	N_Amygdala-1-R	0	0	0	1
347	N_Caudate-1-L	0	1	0	1
348	N_Caudate-1-R	0	1	0	2
349	N_Caudate-2-L	1	2	0	1
350	N_Caudate-2-R	0	1	1	2
351	N_Caudate-3-L	0	3	0	1
352	N_Caudate-3-R	1	1	0	2
353	N_Caudate-4-L	0	2	0	2
354	N_Caudate-4-R	0	2	0	2
355	N_Caudate-5-L	0	2	0	1
356	N_Caudate-5-R	0	1	0	1
357	N_Caudate-6-L	0	1	0	1
358	N_Caudate-6-R	0	1	0	0
359	N_Caudate-7-L	0	0	0	0
360	N_Caudate-7-R	0	0	0	0
361	N_Pallidum-1-L	0	0	0	0
362	N_Pallidum-1-R	0	0	0	0
363	N_Putamen-2-L	0	0	0	0
364	N_Putamen-2-R	0	0	0	1
365	N_Putamen-3-L	0	1	0	0
366	N_Putamen-3-R	0	0	0	0
367	N_Thalamus-1-L	0	0	0	0
368	N_Thalamus-1-R	0	0	0	1
369	N_Thalamus-2-L	1	1	0	0
370	N_Thalamus-2-R	0	0	0	1
371	N_Thalamus-3-L	0	1	0	0
372	N_Thalamus-3-R	0	0	0	2
373	N_Thalamus-4-L	0	2	0	2
374	N_Thalamus-4-R	1	2	0	0
375	N_Thalamus-5-L	0	0	0	0
376	N_Thalamus-5-R	0	0	0	0
377	N_Thalamus-6-L	0	0	0	0
378	N_Thalamus-6-R	0	0	0	0
379	N_Thalamus-7-L	0	0	0	0
380	N_Thalamus-7-R	0	0	0	0
381	N_Thalamus-8-L	0	0	0	0
382	N_Thalamus-8-R	1	0	0	0
383	N_Thalamus-9- L	0	0	0	0
384	N_Thalamus-9-R	0	0	0	0

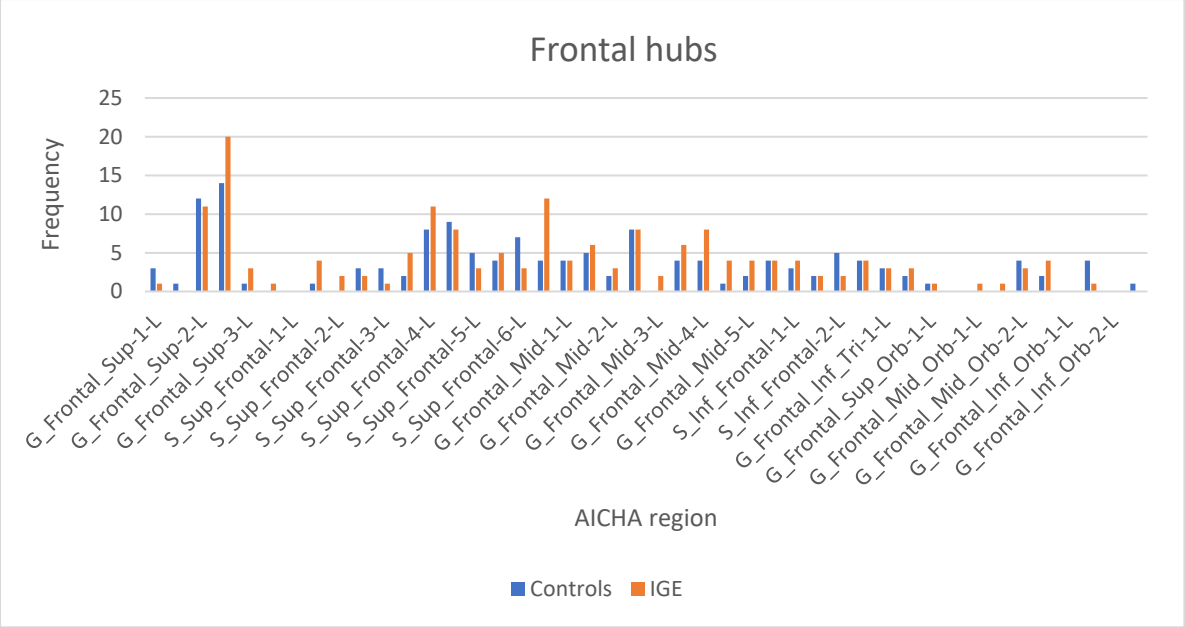

Figure C-1. Frequency of hub nodes in the frontal regions plotted for controls and IGE group (WC-IGE and DR-IGE combined). Nodes are defined as network hubs if both the strength and betweenness centrality are greater than one standard deviation above corresponding mean network metric.

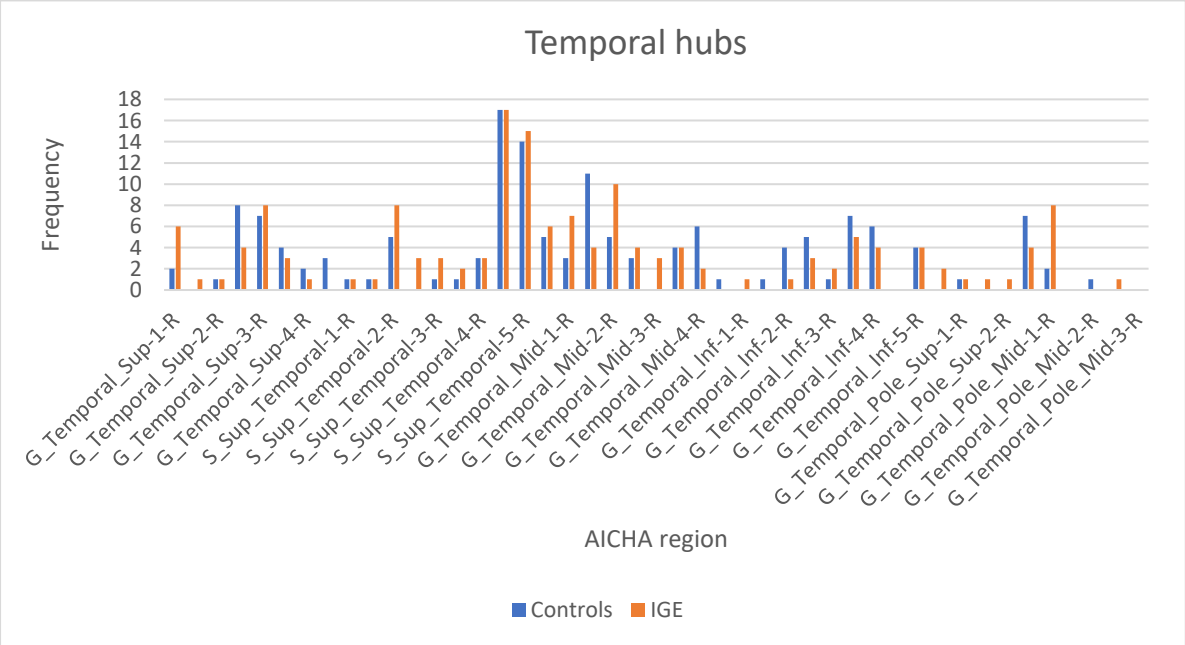

Figure C-2. Frequency of hub nodes in the temporal regions plotted for controls and IGE group (WC-IGE and DR-IGE combined). Nodes are defined as network hubs if both the strength and betweenness centrality are greater than one standard deviation above corresponding mean network metric.

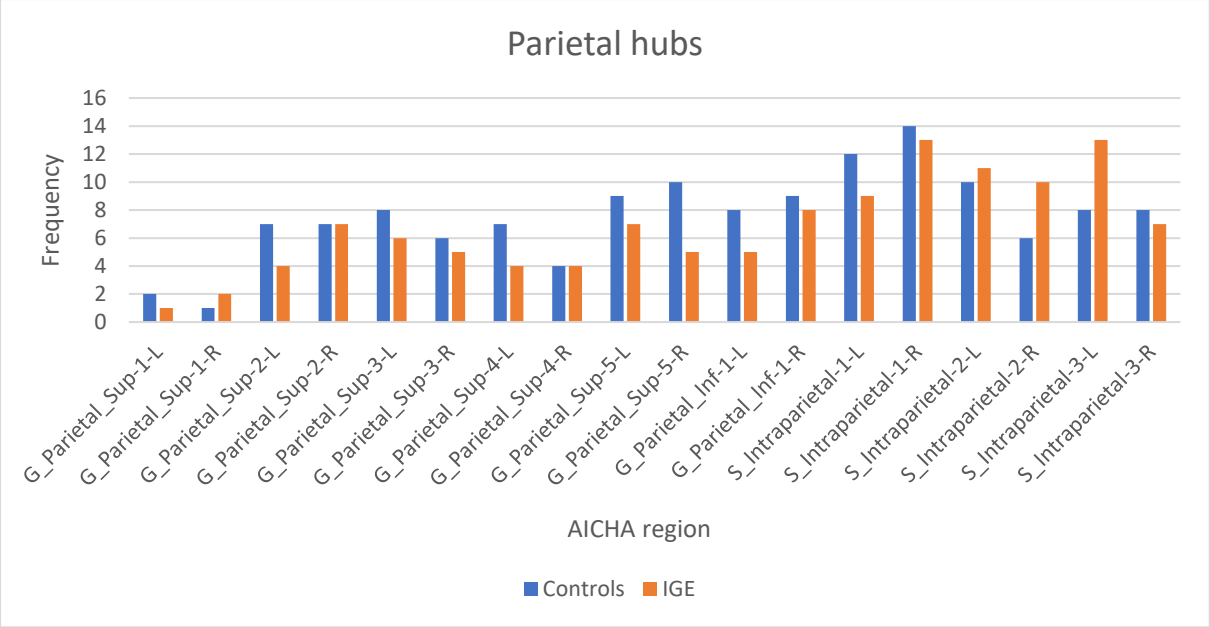

Figure C-3. Frequency of hub nodes in the parietal regions plotted for controls and IGE group (WC-IGE and DR-IGE combined). Nodes are defined as network hubs if both the strength and betweenness centrality are greater than one standard deviation above corresponding mean network metric.

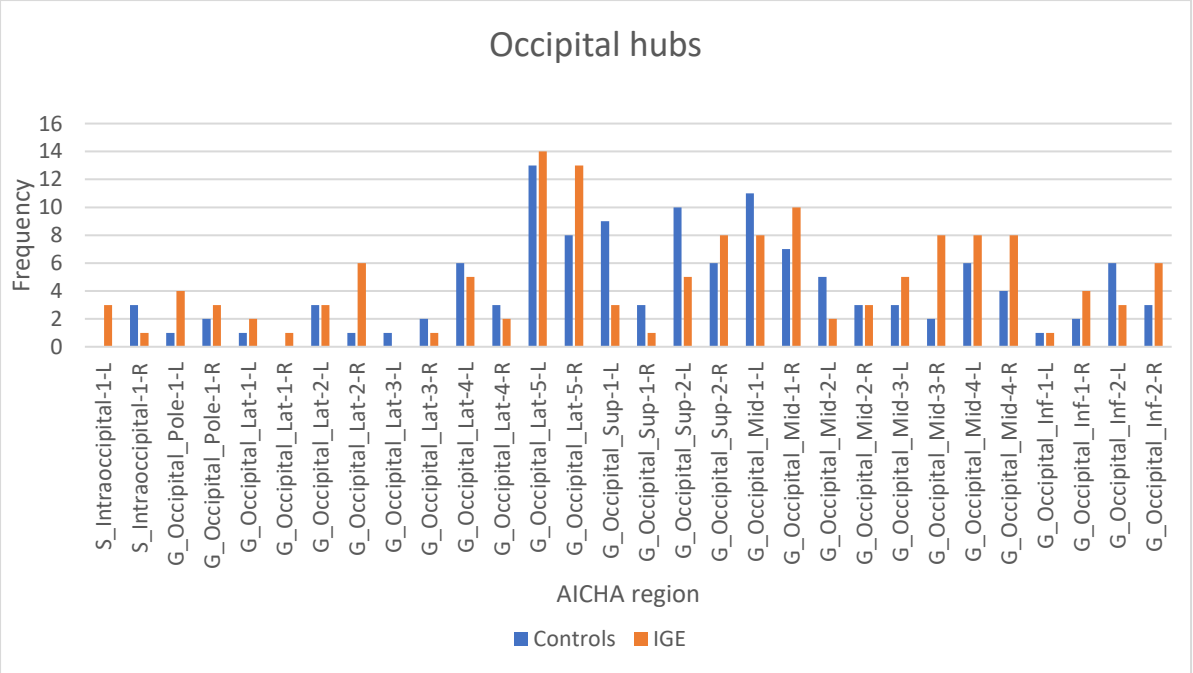

Figure C-4. Frequency of hub nodes in the occipital regions plotted for controls and IGE group (WC-IGE and DR-IGE combined). Nodes are defined as network hubs if both the strength and betweenness centrality are greater than one standard deviation above corresponding mean network metric.

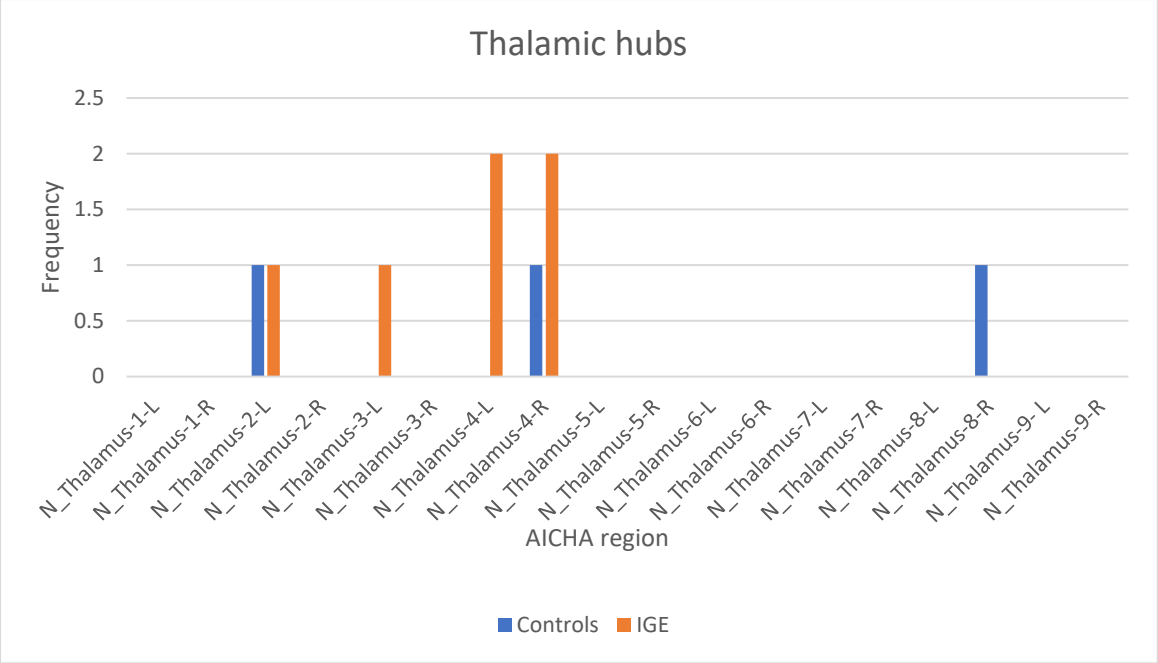

Figure C-5. Frequency of hub nodes in the thalamic regions plotted for controls and IGE group (WC-IGE and DR-IGE combined). Nodes are defined as network hubs if both the

Chapter 6. General Discussion

The aim of this thesis was to investigate the effect of seizure control on global interictal network features in IGE, with a focus on functional connectivity. In conjunction, global network features in people with IGE compared to healthy controls were also examined. Since seizures are believed to emerge from the same mechanisms that underlie normal brain function (Richardson, 2012b), it was postulated that the same network alterations underlying epilepsy are also implicated in drug resistance. This envisages a spectrum of network abnormality, with healthy controls and DR-IGE at opposite ends of the spectrum, and WC-IGE positioned between them. As such, it was hypothesised that any aberrations in network features would reflect this spectrum.

6.1 Summary of experimental results

I performed an EEG spectral power analysis to compare global network oscillatory activity between WC-IGE, DR-IGE and controls (Pegg et al., 2020b), presented in *Chapter 2*. Irrespective of seizure control, a higher spectral power in participants with IGE compared with controls at 4-8 Hz, 15–20 Hz, 25-31 Hz, and 39-42 Hz was found in widespread scalp regions, with a lower peak alpha frequency. Topological features of networks derived from EEG in WC-IGE, DR-IGE and controls were investigated using graph theory in *Chapter 4* (Pegg et al., 2021). ~~Irrespective of seizure control, a more regular network topology (higher characteristic path length) in IGE was found in the 6-9 Hz frequency band in IGE, compared with controls.~~ An altered network topology in WC-IGE compared with controls was found at 10-12 Hz; the group with WC-IGE had a more efficient network (greater small-world index) and a difference in hub node connectivity (lower mean degree and lower degree distribution variance). A post hoc comparison also suggested a difference between WC-IGE and DR-IGE in the same frequency band with a higher small-world index and lower characteristic path length in WC-IGE (consistent with a more efficient and less regular network). I also investigated topological features of the global network derived from fMRI in WC-IGE, DR-IGE and controls with a different participant cohort. This is presented in *Chapter 5*. Compared with controls, the network structure in IGE was more regular (higher path length), with altered hub node connectivity (a higher average node strength and betweenness centrality). These topological alterations were not related to treatment responsiveness. The locations of 'major hub nodes'

and individual nodes exhibiting differences in connectivity between groups was explored, and there were no clear differences found.

In the following sections, a synthesised discussion of the study results including their interpretation and limitations will be presented, followed by a discussion of implications for future work.

6.2 Interpretation

Converging evidence from each study suggests the global network is altered in IGE compared to controls. In particular, the neuronal network in IGE has greater spectral power and a more regular network topology, with altered global nodal connectivity. In addition, there was evidence of a relationship between seizure control and network topology in the graph theoretical EEG analysis. The latter may reflect drug induced changes in people who respond to medication, which renders the network less susceptible to seizures.

Altered neuronal networks in people with IGE compared to controls

Greater spectral power across most of the frequency spectra in widespread scalp regions in the IGE cohorts compared to controls, may reflect a hyperexcitable cortex in the resting state due to greater neuronal synchronisation (Michel et al., 1992, Clemens et al., 2000). This result is consistent with other similar studies (Miyauchi et al., 1991, Clemens et al., 2000, Willoughby et al., 2003, Santiago-Rodríguez et al., 2008, Elshahabi et al., 2015, Niso et al., 2015). The notion that a hyperexcitable cortex increases seizure vulnerability is supported by the finding of elevated spectral power in the immediate pre-ictal period in myoclonic seizures (Sun et al., 2016). Further evidence of a relationship between alterations in spectral power and cortical hyperexcitability is demonstrated by spectral power investigations of AEDs that ostensibly act via reducing glutaminergic excitation (e.g., perampanel, lamotrigine), or by increasing GABAergic inhibition (e.g., valproate) (Routley et al., 2017, Wu and Xiao, 1997, Clemens, 2008, Clemens et al., 2007, Sannita et al., 1989). Such studies all report decreases in spectral power. However, in the study of perampanel (Routley et al., 2017) and one study of valproate (Wu and Xiao, 1997), increased spectral power in some frequency bands was also reported. Despite there being an overall increase in spectral power in IGE in our study, peak alpha frequency was lower. Interpreted in the context of findings from other studies, our results suggest a complex relationship between neuronal oscillations, cortical excitability, and AED effects, with an implication that factors beyond an alteration in cortical hyperexcitability are involved in

seizure control. The latter is supported by our finding of increased spectral power irrespective of seizure control, which is further discussed in the section below.

Differences between IGE and controls were also found in both the EEG and fMRI-based graph theoretical studies of network topology, where a significantly greater characteristic path length in IGE was detected in the fMRI study and nodal metrics were altered in both instances.

A greater characteristic path length reflects a less integrated network and is seen in networks tending toward a regular topology. Since hypersynchrony of the network occurs during a seizure (Li et al., 2007, Wu et al., 2015), and network topology during a seizure becomes more regular in configuration (Ponten et al., 2007, Ponten et al., 2009, Kramer et al., 2010), a resting state network with a regular structure is postulated to make the network more liable to synchronise (van Diessen et al., 2014c). Other IGE network studies have also demonstrated a more regular network in IGE compared to controls, where a higher average clustering coefficient has been found (Chowdhury et al., 2014, Chavez et al., 2010). However, it should be noted that when the characteristic path length metric is considered in isolation, three previous EEG studies (Chowdhury et al., 2014, Lee and Park, 2019, Lee et al., 2020), in addition to our own, and two fMRI studies (Zhang et al., 2011, Liao et al., 2013) have not reported a difference between groups, and one MEG study reported a decreased characteristic path length in the 21–29 Hz frequency band (Elshahabi et al., 2015). Direct comparability with these studies is limited by the use of different modalities, a smaller network in previous EEG studies (up to 23 nodes), and a larger network in the MEG study (275 nodes), which may alter sensitivity to outcomes (van Wijk et al., 2010). Furthermore, the frequency bands in the MEG/EEG studies were defined differently. Our finding of a higher characteristic path length in the group with epilepsy in the fMRI study is similar to a meta-analysis of focal epilepsy studies where functional networks derived from fMRI and EEG/MEG were evaluated in the theta frequency band (van Diessen et al., 2014b). The authors did not detail the boundaries of this frequency band, but conventionally this would be regarded as 4-7 Hz and this, therefore, overlaps with our result. A higher characteristic path length in IGE is also consistent with the significant results for this metric in the structural connectivity studies in our review paper (Xue et al., 2014a, Qiu et al., 2017, Lee and Park, 2019, Pegg et al., 2020a), in addition to a more recently published paper (Lee et al., 2020). This is further consistent with a systematic review where a positively correlated relationship between structural and functional connectivity was described (Straathof et al., 2019).

Differences between IGE and controls in nodal metrics averaged across the network (average node strength/mean degree, or average betweenness centrality) were found in both the fMRI and EEG graph theoretic studies. Interpreted together, these results suggest that there is altered connectivity of network nodes in IGE compared to controls. However, there are differences in whether the average node strength/mean degree was higher or lower in IGE between the fMRI and EEG studies, which makes further interpretation at a physiological level challenging. The picture does not become clearer when considering similar studies; contrary to our own EEG results, a greater mean degree in the 6-9 Hz frequency band has been previously reported (Chowdhury et al., 2014). To my knowledge, nodal measures averaged across the network have not been previously described in fMRI studies of IGE. It is important to note that outcomes between fMRI and EEG/MEG studies may not be directly comparable. This is owing to factors including differences in network density, extent of brain coverage and importantly, dissimilar sensitivities to temporal scale, which may mean that dynamical alterations are captured differently by each modality. It is possible that characteristic path length alterations are temporally stable, whereas nodal metrics may be more influenced by dynamical factors. Similarly, nodal connectivity may vary between or within individuals. This is consistent with the finding of a lack of specific individual nodal regions of altered resting state connectivity in IGE identified in our fMRI study and similar studies (Zhang et al., 2011, Laiou et al., 2019). Notably, each of our graph theoretic studies had different participants, with different proportions of those with WC-IGE (the study population with WC-IGE in the fMRI study comprised a lower proportion). It is clear that the network alterations in the IGE cohort in our EEG analysis were driven by the group with WC-IGE. Thus, results derived from cohorts with differing proportions of patients with WC-IGE may not be directly comparable.

An alternative explanation for the difference in network features in people with IGE compared to controls, is that it represents direct drug effects regardless of epilepsy. However, evidence from other studies in both the spectral power and graph theoretic literature contradicts this. As outlined in the preceding section, overall evidence pertaining to drug effects on spectral power suggests that it is reduced by commonly used AEDs. Where spectral power in medicated and unmedicated individuals with IGE has been compared, one study reported no differences (Miyauchi et al., 1991) and another reported increased spectral power in medicated patients at 2-4 Hz and 7-8 Hz only (Willoughby et al., 2003). Possible effects of specific AEDs were not addressed in these studies. There are limited studies in the literature that have assessed drug effects on network topology. An fMRI connectivity study reported alterations in global efficiency (the inverse of path length), but not clustering coefficient, with topiramate

but not lamotrigine, levetiracetam or valproate (van Veenendaal et al., 2017). Another fMRI study found an alteration in average betweenness centrality, but not small-world index, with carbamazepine but not with other AEDs (Haneef et al., 2015b). Thus, existing studies do not provide evidence that medication commonly taken by participants in our studies (levetiracetam, valproate, lamotrigine) directly explains the result. It was not possible to perform sub-group analyses of individual AEDs in our study as the number of participants taking only one AED was low. The inclusion of a cohort with IGE who are not taking an AED would clarify the possibility of some results being a drug effect but would be practically challenging because typically AED treatment is advised at the point of diagnosis.

The relationship between seizure control and network features in IGE

The main aim of this thesis was to explore a potential relationship between seizure control and global network features. It was postulated that alterations in neuronal networks that underlie epilepsy may also be implicated in AED response. Consistent with the intrinsic severity hypothesis of DRE, which posits that disease severity determines response to treatment (Rogawski and Johnson, 2008), such alterations may be present from the outset. Alternatively, seizure-induced brain plasticity could result in the development of abnormal networks, which inhibit the effect of AEDs and lead to DRE (Fang et al., 2011). Both hypotheses suggest that network abnormalities are on a spectrum, with WC-IGE network anomalies lying between those of DR-IGE and controls.

Evidence that seizure control has an influence on network topology was found in the EEG graph theoretic study only, where a difference in network topology between WC-IGE and controls in the 10-12 Hz frequency band was demonstrated, without significant differences in other group comparisons in the same frequency band. Rather than revealing a spectrum of network abnormalities sensitive to seizure control, this raises the possibility that differences observed between WC-IGE and controls in this frequency band reflect specific drug induced topological changes occurring in the WC-IGE group. These alterations comprise a shift away from a regular topology to a network with stronger small-world network features, and an alteration in network hubs. This perhaps renders the network less vulnerable to seizures than a network that has not undergone drug induced modifications to its structure. Similar findings have been recently reported in a study which assessed the effects of cannabidiol on network topology in patients with Dravet's syndrome who were refractory to AEDs (Anderson et al., 2020). Patients who responded to cannabidiol (defined as those who had a 70% or more

reduction in seizure frequency), exhibited a lower mean degree compared to non-responders in the beta frequency band (in addition to a higher global efficiency and higher modularity).

Potential explanations for a lack of corresponding effect on topology according to seizure control in the fMRI study include that there were proportionally fewer patients with WC-IGE in the fMRI participant cohort, and that each modality potentially has a different sensitivity to capture any differences, as outlined in the preceding section.

In our EEG spectral power study, no relationship with seizure control was identified. This suggests that the cortex remains hyperexcitable in well-controlled epilepsy but that this has less influence on seizure likelihood than the overall network topology. Another possibility is that the difference in AED burden between the two groups affected the results of this comparison.

It would be simplistic to conclude that the identified network topological alterations in the WC-IGE group in our EEG study are alone responsible for reduced vulnerability to seizures. To illustrate this, in a study of network features in people with IGE and healthy first-degree relatives compared to controls (Chowdhury et al., 2014), the same network aberrations that were found in the group with IGE were also present in the first-degree relative group, thus demonstrating that factors beyond these network alterations are necessary for seizures to ensue. Similarly, it is known that any brain, under certain conditions, can transition to a seizure state and therefore how the 'non-epileptic' network becomes vulnerable in such settings is an important consideration. It is possible that the lack of significant difference in network topology in people with DR-IGE compared to controls may be explained by factors that are not considered in static connectivity measures.

Unaccounted for connectivity measures are likely to include dynamic factors which are involved in determining transition to the seizure state (Woldman et al., 2019, Schmidt et al., 2016). In the hypothesis of epilepsy arising from a bi-stable state, it is proposed that the brain can exist in two network states (attractors) and can converge to and transition between the two states via a dynamical bifurcation (Lopes da Silva et al., 2003) (*figure 28*). One state is the interictal resting state, and the other is the seizure state. In a computer model of CAE, state-plane representations of the two stable states using a stimulation of the thalamocortical network were created (Suffczynski et al., 2004); In the normal brain, it was demonstrated that the resting state was distinct from the seizure state, which meant that transition to the seizure state did not occur. In the 'epileptic brain', there was a smaller distance between the two attractors which meant that any fluctuation could readily cause transition to the seizure state.

More recent modelling studies support the notion that the likelihood of transition to the seizure state depends on an interplay between network structure and the excitability of network nodes (Petkov et al., 2014, Lopes et al., 2020). Incorporating our results into this framework, it is possible that in the epileptic brain which responds to medication, the resting state network topology becomes more stable which means that bifurcation to the seizure state is less likely to occur.

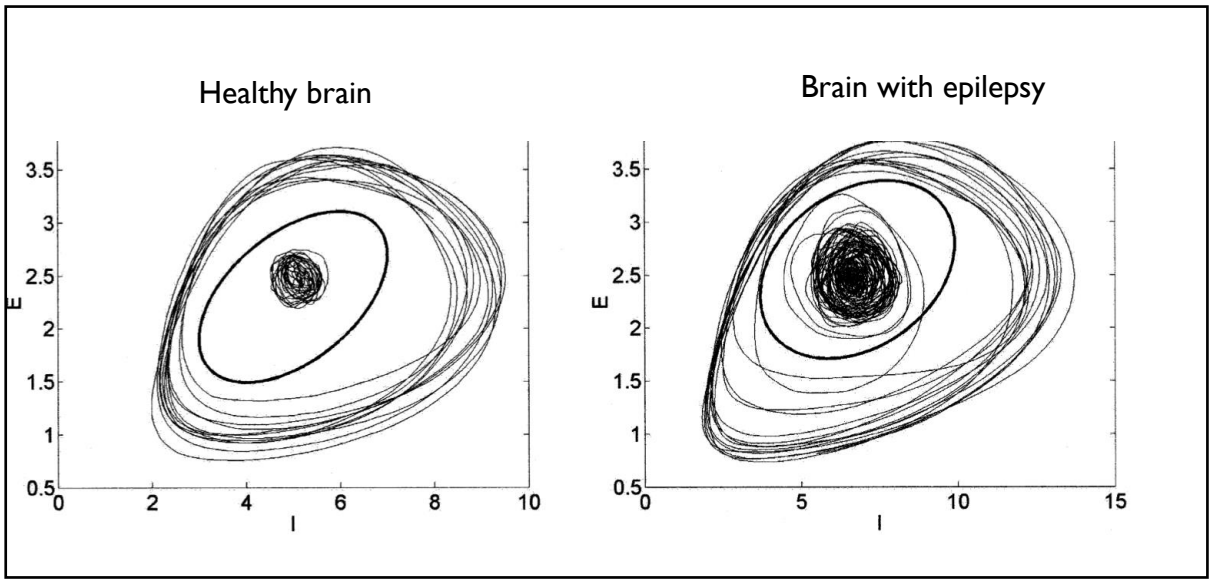

Figure 28. 2D state-plane representations of oscillations in a normal brain and a brain with epilepsy. These were obtained via computer stimulations of the thalamocortical network. The normal resting state is the central cluster of oscillations and the seizure state is represented by the peripheral oscillations. The single thick elliptical shape represents the transition point, where dynamic bifurcation to the seizure state occurs. In someone without epilepsy these two zones are separate from each other and therefore a transition to the seizure state will practically never occur (unless there are extreme alterations to the neuronal environment). In a brain with epilepsy, the distance between the two attractors is much smaller, such that any fluctuation in the critical parameters, or the initial conditions, can give rise to a transition to the seizure state. Figure from F. H. L. da Silva, W. Blanes, S. N. Kalitzin, J. Parra, P. Suffczynski and D. N. Velis, "Dynamical diseases of brain systems: different routes to epileptic seizures," in *IEEE Transactions on Biomedical Engineering*, vol. 50, no. 5, pp. 540-548, May 2003. Copyright 2003 IEEE.

The proposition that the network in people with DR-IGE does not gain adequate drug-induced topological stabilisation provides a different perspective on the network hypothesis of drug resistance. It may also be consistent with a framework that incorporates the inherent severity hypothesis of drug resistant epilepsy. Within this, people with severe epilepsy do not gain seizure control because the network abnormality is more pronounced and, therefore, the amount of medication required to effectively alter the network to a less vulnerable state may

be too great without causing toxicity. As with the original intrinsic severity hypothesis of epilepsy, this alone does not account for people who shift in and out of seizure control, or for people who have a high pre-treatment seizure burden (consistent with severe epilepsy) but who subsequently become seizure free with AEDs. However, these scenarios could be accounted for in a broader network model of drug resistance that incorporates multiple, interactive, pharmacological and neurobiological dynamical factors that together influence the likelihood of the complex resting state network system transitioning to the seizure state *(figure 29)*. For example, a person with epilepsy may not have intrinsically severe network abnormalities but may have frequent seizures due to being sleep deprived and depressed, both of which are known to lower the seizure threshold. However, when an AED is initiated, because that person does not have intrinsically severe epilepsy, the network alters enough to become less vulnerable to seizures and therefore that person become seizure free.

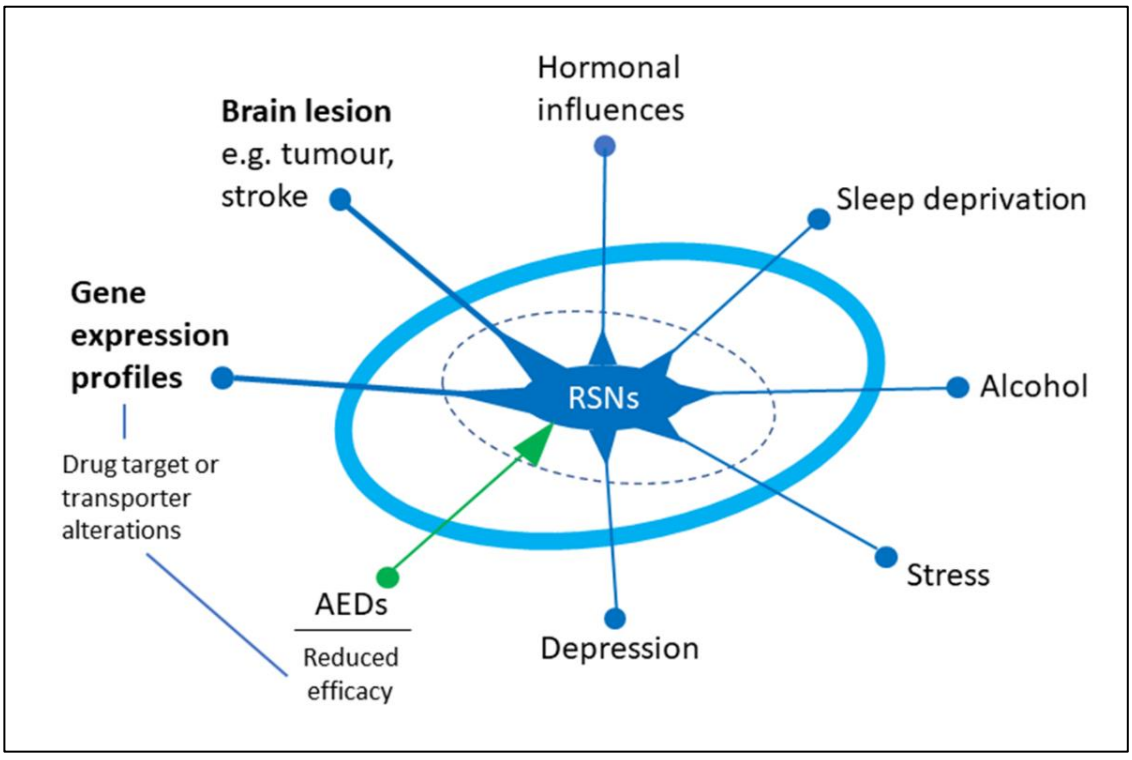

Figure 29. A multifactorial network system model of antiepileptic drug resistance. This is a schematic representation of how multiple neurobiological networks may interact as part of the resting state system in epilepsy. It is hypothesised that intrinsic resting state network topology (RSN) is largely determined by genetic factors and brain structure. Pharmaco-biologically influenced networks may modify the global resting state network and transition (represented by the dashed line) to the seizure state (represented by the light blue ovoid) may occur. The likelihood of transition is dependent upon the extent of intrinsic network abnormality.

Direct AED effects may also be considered to explain the finding of a difference in WC-IGE in the EEG graph theoretic study. However, in view of the lack of alteration in topology in DR-IGE topology, this would imply that people with DR-IGE are less likely to take their prescribed AED. Whilst medication concordance can be an issue in chronic illness, to my knowledge this is not any more likely to occur in those with DR-IGE than those with WC-IGE.

In our patient sample, the question as to whether network alterations have evolved over time, or whether they were present from the outset, remains open. In a recently published similar study, which included an EEG at the time of diagnosis and one year later, network alterations at onset were described (Kim et al., 2020). In this study, graph theoretic metrics in people with controlled JME were compared with those in people with drug resistant JME and controls. Differences in global efficiency and local efficiency between drug resistant participants and controls were reported, with no differences in other group comparisons, and no differences in the other metrics used (mean node strength, characteristic path length, clustering coefficient, small-world index). There was no significant change in metrics between the first and second EEG. Of further consideration is that these results are not consistent with our own. However, the interpretation of this study is likely to be significantly limited by the fact that only four patients with drug resistant epilepsy were included, and outcomes were classified after only one year. This represents a relatively short time period in which to assess the response to two tolerated AEDs and therefore raises concerns about the accuracy of classification of treatment response. To further limit comparability with our own study, only 16 EEG channels were used, data were not filtered into frequency bands, high frequency data was used (which is likely to contain myogenic artefact), some participants were children, and a comparison of graph theoretic metrics between groups for the second EEG was not presented.

6.3 General Limitations

A potential limitation of the analyses relates to the challenges of classifying a patient's drug responsiveness. This may occur due to the natural history of epilepsy whereby a proportion of patients follow a fluctuating course, shifting in and out of seizure control (Brodie et al., 2012). A larger study may allow for the inclusion of this subgroup as a third category. A second potential issue in classifying drug responsiveness is that patients may not be concordant with their prescribed AED, thus they may be inaccurately categorised as drug resistant, when in fact they may have better control of seizures if they were to take an adequate dose of AED. This could potentially dilute potential differences between WC-IGE and DR-IGE and does not

have a clear solution. Thirdly, it is possible that some participants have unrecognised co-existent NEAD or have NEAD alone, without epilepsy. NEAD is characterised by paroxysmal episodes that superficially resemble seizures but are not associated with electrophysiological abnormalities. It is currently understood as a psychological disorder that may be explained by an 'Integrative Cognitive Model' (Reuber and Brown, 2017). NEAD is estimated to be a co-existent diagnosis in 10-50% of people with epilepsy (Benbadis et al., 2001) and misdiagnosis is reported to occur in up to 1 in 5 people diagnosed with epilepsy, some of whom have NEAD (Smith et al., 1999, Benbadis and Allen Hauser, 2000). However, as NEAD typically has a poorer prognosis than epilepsy (Reuber and Elger, 2003), it could be reasoned that people with NEAD misdiagnosed as epilepsy may be more likely to be classified as having DR-IGE than WC-IGE. Therefore, the significant results in the WC-IGE group in are less likely to be affected by this theoretical potential issue. Furthermore, each participant's diagnosis was reviewed independently by two epilepsy specialists, which is expected to mitigate the risk of misdiagnosis.

The cerebral effects of epilepsy may arise through a complex interplay of seizures, cognitive issues, pharmacological side effects and depression. In comparing brain network features in people with WCE to those with DRE, it is recognised that the aforementioned factors are more prominent in DRE and therefore potentially may confound results. However, if these factors had affected our results, it seems likely that greater network alterations would have been identified in the DR-IGE group. Collecting information on depression and cognitive ability in future studies could be considered. However, disentangling these complex effects on brain networks is likely to require prospective longitudinal studies.

Although there is convincing evidence to support the notion of shared pathophysiological and genetic relationships of the various IGE syndromes (Helbig, 2015), it is possible that connectivity features vary between subtypes and as such, our results may be affected by considering them a homogenous group of disorders. However, the number of participants with certain subtypes in our study were too low to perform a meaningful comparison. In a recent study comparing graph theoretic measures in IGE subtypes using EEG, some differences in graph theoretic metrics between absence epilepsy (JAE and CAE combined) and JME were reported, but not between JME and EGTCSA or between absence epilepsy and JME (Lee et al., 2020). This study was potentially limited by only having 16 electrodes and not filtering data into frequency bands. Nevertheless, it suggests that further studies with larger sample numbers are indicated to clarify if IGE subtypes have differing network features.

Another limitation relates to the relatively small sample sizes in the studies. As such, it is possible that the studies were underpowered to detect differences between WC-IGE and DR-IGE. Small sample sizes also increase the probability of type 1 errors (Button et al., 2013). Normal values of network metrics in healthy controls have not been established thus performing a power calculation is limited by the lack of a meaningful parameter to include in such a calculation (Pegg et al., 2020a). The reliability of our findings would be strengthened by reproducing the results in an independent dataset.

The comparison of results between our two graph theoretic studies was limited by the fact that the participant cohorts were different. Therefore, it is not possible to determine if the differences relating to the relative increase or decrease in mean degree/average node strength are due to interindividual differences between participants, or a reflection of differing properties captured by each imaging modality.

A limitation specific to the fMRI analysis is that IEDs may have occurred during data collection. In a study evaluating the effects of IEDs captured on intracranial electrodes on BOLD activation, IEDs have been described to alter both co-localised and distant BOLD signal (Aghakhani et al., 2015). It is therefore possible that the presence of IEDs may confound connectivity measures. A combined EEG-fMRI study may overcome this limitation.

6.4 Future directions

A network analysis of EEGs across time points in the natural history of epilepsy in a prospective study is a clear direction for future work. This would clarify if network differences are present from the outset, or whether they subsequently develop, either as a result of medication or disease progression. Incorporating information relating to cognitive and mood issues would enhance insight into the complex relationship between these factors and cerebral function in epilepsy.

Differences between network topology in the WC-IGE group demonstrate the importance of considering seizure control in the design of future studies that aim to evaluate network connectivity in people with epilepsy compared with controls. This would reduce the possibility of a null effect resulting from counteracting network differences between well-controlled epilepsy and drug resistant epilepsy.

The suggestion of differences in the interictal EEG in people with IGE and WC-IGE compared with controls may be of potential clinical value as a basis to improve the diagnostic capability

of EEG. Current use of routine EEG in the diagnosis of IGE is largely limited to syndromic classification and detection of photosensitivity. It relies upon visual detection of interictal spike-wave discharges. Routine EEG is not used as a diagnostic test because initially, up to around 50% of patients with epilepsy do not have any IEDs (van Donselaar et al., 1992), while false positives occur in around 2% of people without epilepsy (Zivin and Marsan, 1968). Furthermore, 'overinterpretation' of EEGs is not uncommon (Benbadis and Tatum, 2003). In two UK based studies, prevalence rates of epilepsy misdiagnosis have been demonstrated to be around 20% (Scheepers et al., 1998, Leach et al., 2005). A further benefit of the availability of an objectively defined biomarker of epilepsy would be in reducing misdiagnosis and in particular, distinguishing NEAD from epilepsy. The current gold standard for the diagnosis of NEAD is inpatient video telemetry, the purpose of which is to evaluate for the presence of epileptiform discharges during a clinical episode. This is costly, inconvenient to patients, and may be inconclusive (Lawley et al., 2015). Thus, the availability of an interictal EEG biomarker of epilepsy would potentially also improve the care of patients with NEAD. Whilst there are some studies to suggest a difference in network topology between people with NEAD and controls (van der Kruijs et al., 2014, Li et al., 2015b, Ding et al., 2013, Barzegaran et al., 2012), further work to explore network features in people with NEAD compared to those with epilepsy is required. If EEG could also identify people with drug resistant epilepsy at an early stage, it would facilitate a more tailored management approach for this patient group. In addition, it would provide a means to better characterise drug resistant cohorts for pharmacological and epidemiological studies.

Though the results of the fMRI study also suggest potential promise to be developed as a biomarker of IGE, fMRI is perhaps less suitable than EEG at a practical level as it is not readily available and would place an extra, costly, demand on resources (an fMRI scan would be an additional investigation, whereas EEG is typically performed to support a diagnosis of IGE). A further avenue for future consideration is a similar study using MEG. Whilst more expensive and not as widely available as EEG, MEG has the advantage of being less influenced by volume conduction and is more suitable for source reconstruction, thus enabling superior spatial localisation (Brookes et al., 2011). Evidence to support that differing connectivity features according to seizure control may be detected by MEG can be found in two studies which examined the ictal MEG in CAE. Both reported spatial differences in connectivity strengths in those responding to AEDs compared with those who had no response to AEDs (Tenney et al., 2018, Miao et al., 2019).

After potential biomarkers have been identified, an assessment of their ability to infer outcomes at an individual level is paramount. In this regard, the search for clinically useful, interictal EEG features very much remains an area for development. In a study comparing candidate biomarkers for the diagnosis of IGE (Schmidt et al., 2016), the sensitivity for peak occipital alpha power (8-13 Hz) and the mean degree in the 6-9 Hz frequency band was very low (0% and 15.8% respectively, with 100% specificity). The low sensitivity is perhaps unsurprising given that these measures were selected based upon the outcome of just one previous study for each measure (Larsson and Kostov, 2005, Chowdhury et al., 2014). A fundamental requirement in the search for a biomarker is that it must be reproducible in different patient cohorts. As outlined in our review paper (Pegg et al., 2020a), the outcome of graph theoretic alterations demonstrated in the IGE literature is inconsistent, particularly for fMRI studies, which suggests low reproducibility. However, at the current time, it is not known whether such inconsistencies reflect the limitations of using these methods to capture connectivity, or whether it is due to extensive variations in study methodology. Such variations are discussed in our review and particularly relate to network size, data collection modality and the method of determining synchronisation between network areas. Our own experimental results demonstrate that even subtle changes to the methodology (such as the inclusion of negatively correlated connections), may alter the results. Not only does variation in methodology limit study comparability, but it also makes inferring results at a physiological level more challenging. Our review paper concludes with a suggested methodological framework for future graph theoretical analyses, with the aim of improving standardisation. However, to optimally improve study comparability and reproducibility, methodological studies are required to systematically assess how the various choices affect outcome metrics, in addition to a consensus on the preferred methods.

Relatively small sample sizes are likely to be contributing to inconsistent outcomes in the field, due to both an increased risk of type one error (Button et al., 2013) and potential underpowering (as discussed in the section above). Multi-centre collaborations for epilepsy studies would help overcome the issue of small sample sizes. At a larger scale, the Human Connectome Project (Van Essen et al., 2012) and the ENIGMA project (Whelan et al., 2018, Hatton et al., 2020, Sisodiya et al., 2020) provide examples of studies that will improve statistical power in neuroscience studies.

A further implication of this work is the novel insight that it provides into potential mechanisms of AEDs. Our results suggest that examining individual drug effects at the network level (rather than at a cellular level), in relation to seizure control, merits further

consideration. Whilst there is some existing evidence of altered connectivity with certain AEDs (Haneef et al., 2015b, van Veenendaal et al., 2017, Routley et al., 2017), the relationship between network effects and seizure control has only been explored for ethosuximide and cannabidiol, to my knowledge (Anderson et al., 2020, Tenney et al., 2018, Miao et al., 2019). As previously discussed, the number of participants taking monotherapy in our studies was low, which meant this could not be explored.

Although there is converging evidence that phase synchronisation and correlation between signals reflects communication between regions (Canolty and Knight, 2010, Palva et al., 2005, Lachaux et al., 1999), it should be noted that diverse methods to measure coupling exist and the optimal method to capture this complex phenomenon has not been ascertained. Furthermore, assuming stationarity in connectivity analyses is likely to be an oversimplification (Manuca et al., 1998, Jones et al., 2012, Allen et al., 2014). Crucially, how static network representations of resting state networks relate to the emergent dynamics of the complex system they are a part of is a fundamental consideration for further work. It seems likely that the optimal way of capturing brain connectivity is through methods that incorporate the dynamical, multivariate interactions of the network. This notion is supported by the biomarker study referred to above (Schmidt et al., 2016), where a third candidate biomarker derived from the coupling value of individual nodes in a dynamic network model had better sensitivity for IGE than the mean degree metric (57.6% with 100% specificity). Extending beyond the relationship between static measures and dynamic systems, how the multifarious brain networks interact across a range of spatial and temporal scales and influence seizure vulnerability is a compelling question for future research. Relevant temporal scales may include those spanning circadian and multi-day periods, combined phase information from which has shown promise as a biomarker for seizure prediction (Baud et al., 2018). This suggests that abnormalities in these temporally diverse networks are also implicated in seizure susceptibility and warrant further attention in the context of epilepsy drug resistance.

6.5 Conclusions

This thesis explored interictal functional networks in IGE, and the relationship between AED responsiveness and network features. Converging evidence from experimental data derived from fMRI and EEG, demonstrated large-scale network alterations in IGE compared to controls. These alterations included a suggestion of greater cortical hyperexcitability, a more

regular network topology and an alteration in the connectivity of network hubs. The relationship between global network features and seizure control in IGE using spectral power analysis and graph theoretical analysis is a relatively unexplored area that we hypothesised may provide further insight into network alterations. Indeed, our results demonstrate that people with well-controlled IGE have networks that differ from controls. We propose that this reflects AED induced network alterations in people who respond to medication, which renders the network less vulnerable to transitioning to the seizure state. The reason as to why some individuals do not respond to AEDs remains unanswered but may involve complex dynamical interactions between numerous brain networks, influenced by inherent disease severity.

These results are of potential importance in advancing the understanding of mechanisms of epilepsy drug resistance and as a possible basis for further investigation of a biomarker of IGE and DR-IGE. The finding of altered network features according to drug responsiveness demonstrates the importance of considering the degree of seizure control in future studies. The literature as a whole suggests the interpretation of study outcomes in network analysis can be greatly influenced by methodological variations. This highlights the need for consensus on optimal methodological strategies in order to develop this promising area of research into drug resistant epilepsy.

References

R2019a. MATLAB. Natick, Massachusetts: The MathWorks Inc.

ABE, T., SEO, T., ISHITSU, T., NAKAGAWA, T., HORI, M. & NAKAGAWA, K. 2008. Association between SCN1A polymorphism and carbamazepine-resistant epilepsy. *Br J Clin Pharmacol,* 66**,** 304-7.

ABELA, E., PAWLEY, A. D., TANGWIRIYASAKUL, C., YAAKUB, S. N., CHOWDHURY, F. A., ELWES, R. D. C., BRUNNHUBER, F. & RICHARDSON, M. P. 2019. Slower alpha rhythm associates with poorer seizure control in epilepsy. *Annals of Clinical and Translational Neurology,* 6**,** 333-343.

ABELES, M. 1982. Information Codes for Higher Brain Function. *In:* ABELES, M. (ed.) *Local Cortical Circuits: An Electrophysiological Study.* Berlin, Heidelberg: Springer Berlin Heidelberg.

ABREU, R., LEAL, A. & FIGUEIREDO, P. 2018. EEG-Informed fMRI: A Review of Data Analysis Methods. *Frontiers in Human Neuroscience,* 12**,** 29.

ACHARD, S., SALVADOR, R., WHITCHER, B., SUCKLING, J. & BULLMORE, E. 2006. A resilient, low-frequency, small-world human brain functional network with highly connected association cortical hubs. *J Neurosci,* 26**,** 63-72.

ADEBIMPE, A., AARABI, A., BOUREL-PONCHEL, E., MAHMOUDZADEH, M. & WALLOIS, F. 2016. EEG Resting State Functional Connectivity Analysis in Children with Benign Epilepsy with Centrotemporal Spikes. *Front Neurosci,* 10.

ADEY, W. R., ELUL, R., WALTER, R. D. & CRANDALL, P. H. 1967. The cooperative behavior of neuronal populations during sleep and mental tasks. *Electroencephalogr Clin Neurophysiol,* 23**,** 88.

AERTSEN, A. M., GERSTEIN, G. L., HABIB, M. K. & PALM, G. 1989. Dynamics of neuronal firing correlation: modulation of "effective connectivity". *J Neurophysiol,* 61**,** 900-17.

AGCAOGLU, O., WILSON, T. W., WANG, Y.-P., STEPHEN, J. & CALHOUN, V. D. 2019. Resting state connectivity differences in eyes open versus eyes closed conditions. *Human brain mapping,* 40**,** 2488-2498.

AGHAKHANI, Y., BAGSHAW, A. P., BÉNAR, C. G., HAWCO, C., ANDERMANN, F., DUBEAU, F. & GOTMAN, J. 2004. fMRI activation during spike and wave discharges in idiopathic generalized epilepsy. *Brain : a journal of neurology,* 127**,** 1127-1144.

AGHAKHANI, Y., BEERS, C. A., PITTMAN, D. J., GAXIOLA-VALDEZ, I., GOODYEAR, B. G. & FEDERICO, P. 2015. Co-localization between the BOLD response and epileptiform discharges recorded by simultaneous intracranial EEG-fMRI at 3 T. *NeuroImage: Clinical,* 7**,** 755-763.

AICH, T. K. 2014. Absent posterior alpha rhythm: An indirect indicator of seizure disorder? *Indian J Psychiatry,* 56**,** 61-6.

ALLEN, E. A., DAMARAJU, E., PLIS, S. M., ERHARDT, E. B., EICHELE, T. & CALHOUN, V. D. 2014. Tracking Whole-Brain Connectivity Dynamics in the Resting State. *Cerebral Cortex,* 24**,** 663-676.

ALTHOUSE, A. D. 2016. Adjust for Multiple Comparisons? It's Not That Simple. *Ann Thorac Surg,* 101**,** 1644-5.

ANDERMANN, F. & BERKOVIC, S. F. 2001. Idiopathic Generalized Epilepsy with Generalized and Other Seizures in Adolescence. *Epilepsia,* 42**,** 317-320.

ANDERSON, D. E., MADHAVAN, D. & SWAMINATHAN, A. 2020. Global brain network dynamics predict therapeutic responsiveness to cannabidiol treatment for refractory epilepsy. *Brain Communications,* 2.

ANDERSON, J. & HAMANDI, K. 2011. Understanding juvenile myoclonic epilepsy: Contributions from neuroimaging. *Epilepsy Research,* 94**,** 127-137.

ANDRESEN, B. 1993. Multivariate statistical methods and their capability to demarcate psycholophysiologically and neurophysiologically sound frequency components of human scalp EEG. *In:* ZSCHOCKE, S. & SPECKMANNN, E.-J. (eds.) *Basic mechanisms of the EEG.* Boston: Birkhauser.

ANNEGERS, J. F., COAN, S. P., HAUSER, W. A. & LEESTMA, J. 2000. Epilepsy, Vagal Nerve Stimulation by the NCP System, All-Cause Mortality, and Sudden, Unexpected, Unexplained Death. *Epilepsia,* 41**,** 549-553.

ARSLAN, S., KTENA, S. I., MAKROPOULOS, A., ROBINSON, E. C., RUECKERT, D. & PARISOT, S. 2018. Human brain mapping: A systematic comparison of parcellation methods for the human cerebral cortex. *Neuroimage,* 170**,** 5-30.

AURICH, N. K., ALVES FILHO, J. O., MARQUES DA SILVA, A. M. & FRANCO, A. R. 2015. Evaluating the reliability of different preprocessing steps to estimate graph theoretical measures in resting state fMRI data. *Frontiers in neuroscience,* 9**,** 48-48.

BANCAUD, J. 1969. Physiopathogenesis of generalized epilepsies of organic nature (stereo-electroencephalographic study). *The physiopathogenesis of the epilepsies***,** 158-185.

BARABÁSI, A.-L. & ALBERT, R. 1999. Emergence of Scaling in Random Networks. *Science,* 286**,** 509.

BARZEGARAN, E., JOUDAKI, A., JALILI, M., ROSSETTI, A. O., FRACKOWIAK, R. S. & KNYAZEVA, M. G. 2012. Properties of functional brain networks correlate with frequency of psychogenic non-epileptic seizures. *Front Hum Neurosci,* 6**,** 335.

BASSETT, D. S. & BULLMORE, E. 2006. Small-world brain networks. *Neuroscientist,* 12**,** 512-23.

BASTOS, A. M. & SCHOFFELEN, J.-M. 2016. A Tutorial Review of Functional Connectivity Analysis Methods and Their Interpretational Pitfalls. *Frontiers in Systems Neuroscience,* 9**,** 175.

BAUD, M. O., KLEEN, J. K., MIRRO, E. A., ANDRECHAK, J. C., KING-STEPHENS, D., CHANG, E. F. & RAO, V. R. 2018. Multi-day rhythms modulate seizure risk in epilepsy. *Nature Communications,* 9**,** 88.

BAŞAR, E., BAŞAR-EROĞLU, C., KARAKAŞ, S. & SCHÜRMANN, M. 2000. Brain oscillations in perception and memory. *Int J Psychophysiol,* 35**,** 95-124.

BECKMANN, C. F., DELUCA, M., DEVLIN, J. T. & SMITH, S. M. 2005. Investigations into resting-state connectivity using independent component analysis. *Philosophical Transactions of the Royal Society B: Biological Sciences,* 360**,** 1001-1013.

BEGHI, E., CORNAGGIA, C. & THE, R.-G. 2002. Morbidity and Accidents in Patients with Epilepsy: Results of a European Cohort Study. *Epilepsia,* 43**,** 1076-1083.

BEGHI, E., GARATTINI, L., RICCI, E., CORNAGO, D. & PARAZZINI, F. 2004. Direct cost of medical management of epilepsy among adults in Italy: a prospective cost-of-illness study (EPICOS). *Epilepsia,* 45**,** 171-8.

BEHRENS, T. E., BERG, H. J., JBABDI, S., RUSHWORTH, M. F. & WOOLRICH, M. W. 2007. Probabilistic diffusion tractography with multiple fibre orientations: What can we gain? *Neuroimage,* 34**,** 144-55.

BEHRENS, T. E., WOOLRICH, M. W., JENKINSON, M., JOHANSEN-BERG, H., NUNES, R. G., CLARE, S., MATTHEWS, P. M., BRADY, J. M. & SMITH, S. M. 2003. Characterization and propagation of uncertainty in diffusion-weighted MR imaging. *Magn Reson Med,* 50**,** 1077-88.

BEHZADI, Y., RESTOM, K., LIAU, J. & LIU, T. T. 2007. A component based noise correction method (CompCor) for BOLD and perfusion based fMRI. *Neuroimage,* 37**,** 90-101.

BELL, G. S., NELIGAN, A., GIAVASI, C., KEEZER, M. R., NOVY, J., PEACOCK, J. L., JOHNSON, A. L., GOODRIDGE, D. M., SHORVON, S. D. & SANDER, J. W. 2016. Outcome of seizures in the general population after 25 years: a prospective follow-up, observational cohort study. *J Neurol Neurosurg Psychiatry,* 87**,** 843-50.

BELLEC, P., ROSA-NETO, P., LYTTELTON, O. C., BENALI, H. & EVANS, A. C. 2010. Multi-level bootstrap analysis of stable clusters in resting-state fMRI. *Neuroimage,* 51**,** 1126-39.

BENBADIS, S. R., AGRAWAL, V. & TATUM, W. O. T. 2001. How many patients with psychogenic nonepileptic seizures also have epilepsy? *Neurology,* 57**,** 915-7.

BENBADIS, S. R. & ALLEN HAUSER, W. 2000. An estimate of the prevalence of psychogenic non-epileptic seizures. *Seizure,* 9**,** 280-1.

BENBADIS, S. R. & TATUM, W. O. 2003. Overintepretation of EEGs and Misdiagnosis of Epilepsy. *Journal of Clinical Neurophysiology,* 20.

BENJAMINI, Y. & HOCHBERG, Y. 1995. Controlling the False Discovery Rate: A Practical and Powerful Approach to Multiple Testing. *Journal of the Royal Statistical Society: Series B (Methodological),* 57**,** 289-300.

BENTES, C., MARTINS, H., PERALTA, A. R., CASIMIRO, C., MORGADO, C., FRANCO, A. C., FONSECA, A. C., GERALDES, R., CANHÃO, P., PINHO, E. M. T., PAIVA, T. & FERRO, J. M. 2017. Post-stroke seizures are clinically underestimated. *J Neurol,* 264**,** 1978-1985.

BERG, A. T., BERKOVIC, S. F., BRODIE, M. J., BUCHHALTER, J., CROSS, J. H., VAN EMDE BOAS, W., ENGEL, J., FRENCH, J., GLAUSER, T. A., MATHERN, G. W., MOSHE, S. L., NORDLI, D., PLOUIN, P. & SCHEFFER, I. E. 2010. Revised terminology and concepts for organization of seizures and epilepsies: report of the ILAE Commission on Classification and Terminology, 2005-2009. *Epilepsia,* 51**,** 676-85.

BERG, A. T. & SHINNAR, S. 1997. Do seizures beget seizures? An assessment of the clinical evidence in humans. *J Clin Neurophysiol,* 14**,** 102-10.

BERG, A. T., SHINNAR, S., LEVY, S. R., TESTA, F. M., SMITH-RAPAPORT, S., BECKERMAN, B. & EBRAHIMI, N. 2001. Two-year remission and subsequent relapse in children with newly diagnosed epilepsy. *Epilepsia,* 42**,** 1553-62.

BERGER, H. 1929. Über das Elektrenkephalogramm des Menschen. *Archiv für Psychiatrie und Nervenkrankheiten,* 87**,** 527-570.

BERNHARDT, B. C., CHEN, Z., HE, Y., EVANS, A. C. & BERNASCONI, N. 2011. Graph-theoretical analysis reveals disrupted small-world organization of cortical thickness correlation networks in temporal lobe epilepsy. *Cereb Cortex,* 21**,** 2147-57.

BERNHARDT, B. C., HONG, S., BERNASCONI, A. & BERNASCONI, N. 2013. Imaging structural and functional brain networks in temporal lobe epilepsy. *Front Hum Neurosci,* 7**,** 624.

BERNHARDT, B. C., ROZEN, D. A., WORSLEY, K. J., EVANS, A. C., BERNASCONI, N. & BERNASCONI, A. 2009. Thalamo-cortical network pathology in idiopathic generalized epilepsy: insights from MRI-based morphometric correlation analysis. *Neuroimage,* 46**,** 373-81.

BETTUS, G., WENDLING, F., GUYE, M., VALTON, L., RÉGIS, J., CHAUVEL, P. & BARTOLOMEI, F. 2008. Enhanced EEG functional connectivity in mesial temporal lobe epilepsy. *Epilepsy Research,* 81**,** 58-68.

BETZEL, R. F. & BASSETT, D. S. 2017. Multi-scale brain networks. *NeuroImage,* 160**,** 73-83.

BIRN, R. M., MOLLOY, E. K., PATRIAT, R., PARKER, T., MEIER, T. B., KIRK, G. R., NAIR, V. A., MEYERAND, M. E. & PRABHAKARAN, V. 2013. The effect of scan length on the reliability of resting-state fMRI connectivity estimates. *Neuroimage,* 83**,** 550-8.

BISWAL, B., YETKIN, F. Z., HAUGHTON, V. M. & HYDE, J. S. 1995. Functional connectivity in the motor cortex of resting human brain using echo-planar MRI. *Magn Reson Med,* 34**,** 537-41.

BLADIN, C. F., ALEXANDROV, A. V., BELLAVANCE, A., BORNSTEIN, N., CHAMBERS, B., COTÉ, R., LEBRUN, L., PIRISI, A. & NORRIS, J. W. 2000. Seizures after stroke: a prospective multicenter study. *Arch Neurol,* 57**,** 1617-22.

BOHLAND, J. W., WU, C., BARBAS, H., BOKIL, H., BOTA, M., BREITER, H. C., CLINE, H. T., DOYLE, J. C., FREED, P. J., GREENSPAN, R. J., HABER, S. N., HAWRYLYCZ, M., HERRERA, D. G., HILGETAG, C. C., HUANG, Z. J., JONES, A., JONES, E. G., KARTEN, H. J., KLEINFELD, D., KÖTTER, R., LESTER, H. A., LIN, J. M., MENSH, B. D., MIKULA, S., PANKSEPP, J., PRICE, J. L., SAFDIEH, J., SAPER, C. B., SCHIFF, N. D., SCHMAHMANN, J. D., STILLMAN, B. W., SVOBODA, K., SWANSON, L. W., TOGA, A. W., VAN ESSEN, D. C., WATSON, J. D. & MITRA, P. P. 2009. A Proposal for a Coordinated Effort for the Determination of Brainwide Neuroanatomical Connectivity in Model Organisms at a Mesoscopic Scale. *PLOS Computational Biology,* 5**,** e1000334.

BONILHA, L., TABESH, A., DABBS, K., HSU, D. A., STAFSTROM, C. E., HERMANN, B. P. & LIN, J. J. 2014. Neurodevelopmental alterations of large-scale structural networks in children with new-onset epilepsy. *Hum Brain Mapp,* 35**,** 3661-72.

BRANDT, C., BETHMANN, K., GASTENS, A. M. & LÖSCHER, W. 2006. The multidrug transporter hypothesis of drug resistance in epilepsy: Proof-of-principle in a rat model of temporal lobe epilepsy. *Neurobiology of Disease,* 24**,** 202-211.

BRAZIER, M. A. B. & BARLOW, J. S. 1956. Some applications of correlation analysis to clinical problems in electroencephalography. *Electroencephalography and Clinical Neurophysiology,* 8**,** 325-331.

BRODIE, M., BARRY, S., BAMAGOUS, G., NORRIE, J. & KWAN, P. 2012. Patterns of treatment response in newly diagnosed epilepsy. *Neurology.* Hagerstown, MD.

BROIDO, A. D. & CLAUSET, A. 2019. Scale-free networks are rare. *Nature Communications,* 10**,** 1017.

BROOKES, M. J., HALE, J. R., ZUMER, J. M., STEVENSON, C. M., FRANCIS, S. T., BARNES, G. R., OWEN, J. P., MORRIS, P. G. & NAGARAJAN, S. S. 2011. Measuring functional connectivity using MEG: methodology and comparison with fcMRI. *NeuroImage,* 56**,** 1082-1104.

BUCKNER, R. L., ANDREWS-HANNA, J. R. & SCHACTER, D. L. 2008. The brain's default network: anatomy, function, and relevance to disease. *Ann N Y Acad Sci,* 1124**,** 1-38.

BUCKNER, R. L. & VINCENT, J. L. 2007. Unrest at rest: Default activity and spontaneous network correlations. *NeuroImage,* 37**,** 1091-1096.

BULLMORE, E. & SPORNS, O. 2009. Complex brain networks: graph theoretical analysis of structural and functional systems. *Nature Reviews Neuroscience,* 10**,** 186-198.

BUTTON, K. S., IOANNIDIS, J. P. A., MOKRYSZ, C., NOSEK, B. A., FLINT, J., ROBINSON, E. S. J. & MUNAFÒ, M. R. 2013. Power failure: why small sample size undermines the reliability of neuroscience. *Nature Reviews Neuroscience,* 14**,** 365-376.

BUTTS, C. T. 2009. Revisiting the foundations of network analysis. *Science,* 325**,** 414-6.

BUZSAKI, G. 1991. The thalamic clock: emergent network properties. *Neuroscience,* 41**,** 351-64.

BÉNAR, C. G., GROSS, D. W., WANG, Y., PETRE, V., PIKE, B., DUBEAU, F. & GOTMAN, J. 2002. The BOLD response to interictal epileptiform discharges. *Neuroimage,* 17**,** 1182-92.

CADOTTE, A. J., MARECI, T. H., DEMARSE, T. B., PAREKH, M. B., RAJAGOVINDAN, R., DITTO, W. L., TALATHI, S. S., HWANG, D. U. & CARNEY, P. R. 2009. Temporal lobe epilepsy: anatomical and effective connectivity. *IEEE Trans Neural Syst Rehabil Eng,* 17**,** 214-23.

CAEYENBERGHS, K., POWELL, H. W., THOMAS, R. H., BRINDLEY, L., CHURCH, C., EVANS, J., MUTHUKUMARASWAMY, S. D., JONES, D. K. & HAMANDI, K. 2015. Hyperconnectivity in juvenile myoclonic epilepsy: a network analysis. *Neuroimage Clin,* 7**,** 98-104.

CALLENBACH, P. M. C., BOUMA, P. A. D., GEERTS, A. T., ARTS, W. F. M., STROINK, H., PEETERS, E. A. J., VAN DONSELAAR, C. A., PETERS, A. C. B. & BROUWER, O. F. 2009. Long-term outcome of childhood absence epilepsy: Dutch Study of Epilepsy in Childhood. *Epilepsy Research,* 83**,** 249-256.

CAMPBELL, A. E., SUMNER, P., SINGH, K. D. & MUTHUKUMARASWAMY, S. D. 2014. Acute effects of alcohol on stimulus-induced gamma oscillations in human primary visual and motor cortices. *Neuropsychopharmacology,* 39**,** 2104-13.

CANOLTY, R. T. & KNIGHT, R. T. 2010. The functional role of cross-frequency coupling. *Trends Cogn Sci,* 14**,** 506-15.

CASPERS, S., GEYER, S., SCHLEICHER, A., MOHLBERG, H., AMUNTS, K. & ZILLES, K. 2006. The human inferior parietal cortex: Cytoarchitectonic parcellation and interindividual variability. *NeuroImage,* 33**,** 430-448.

CAVAZOS, J. E. & SUTULA, T. P. 1990. Progressive neuronal loss induced by kindling: a possible mechanism for mossy fiber synaptic reorganization and hippocampal sclerosis. *Brain Research,* 527**,** 1-6.

CHAUMON, M., BISHOP, D. V. & BUSCH, N. A. 2015. A practical guide to the selection of independent components of the electroencephalogram for artifact correction. *J Neurosci Methods,* 250**,** 47-63.

CHAVEZ, M., VALENCIA, M., NAVARRO, V., LATORA, V. & MARTINERIE, J. 2010. Functional Modularity of Background Activities in Normal and Epileptic Brain Networks. *Physical Review Letters,* 104**,** 118701.

CHELLA, F., PIZZELLA, V., ZAPPASODI, F. & MARZETTI, L. 2016. Impact of the reference choice on scalp EEG connectivity estimation. *J Neural Eng,* 13**,** 036016.

CHEN, Z., BRODIE, M. J., LIEW, D. & KWAN, P. 2018. Treatment Outcomes in Patients With Newly Diagnosed Epilepsy Treated With Established and New Antiepileptic Drugs: A 30-Year Longitudinal Cohort Study. *JAMA Neurol,* 75**,** 279-286.

CHIANG, S., STERN, J. M., ENGEL, J., LEVIN, H. S. & HANEEF, Z. 2014. Differences in graph theory functional connectivity in left and right temporal lobe epilepsy. *Epilepsy Res,* 108**,** 1770-81.

CHO, J. R., KOO, D. L., JOO, E. Y., YOON, S. M., JU, E., LEE, J., KIM, D. Y. & HONG, S. B. 2012. Effect of levetiracetam monotherapy on background EEG activity and cognition in drug-naive epilepsy patients. *Clin Neurophysiol,* 123**,** 883-91.

CHOUCHI, M., KAABACHI, W., KLAA, H., TIZAOUI, K., TURKI, I. B. & HILA, L. 2017. Relationship between ABCB1 3435TT genotype and antiepileptic drugs resistance in Epilepsy: updated systematic review and meta-analysis. *BMC Neurol,* 17**,** 32.

CHOWDHURY, F. A., WOLDMAN, W., FITZGERALD, T. H., ELWES, R. D., NASHEF, L., TERRY, J. R. & RICHARDSON, M. P. 2014. Revealing a brain network endophenotype in families with idiopathic generalised epilepsy. *PLoS One,* 9**,** e110136.

CHU, C. J., KRAMER, M. A., PATHMANATHAN, J., BIANCHI, M. T., WESTOVER, M. B., WIZON, L. & CASH, S. S. 2012. Emergence of stable functional networks in long-term human electroencephalography. *J Neurosci,* 32**,** 2703-13.

CLAYDEN, J. D. 2013. Imaging connectivity: MRI and the structural networks of the brain. *Funct Neurol,* 28**,** 197-203.

CLEMENS, B. 2008. Valproate decreases EEG synchronization in a use-dependent manner in idiopathic generalized epilepsy. *Seizure,* 17**,** 224-33.

CLEMENS, B., PIROS, P., BESSENYEI, M. & HOLLODY, K. 2007. Lamotrigine decreases EEG synchronization in a use-dependent manner in patients with idiopathic generalized epilepsy. *Clin Neurophysiol,* 118**,** 910-7.

CLEMENS, B., PUSKAS, S., BESENYEI, M., SPISAK, T., OPPOSITS, G., HOLLODY, K., FOGARASI, A., FEKETE, I. & EMRI, M. 2013. Neurophysiology of juvenile myoclonic epilepsy: EEG-based network and graph analysis of the interictal and immediate preictal states. *Epilepsy Res,* 106**,** 357-69.

CLEMENS, B., SZIGETI, G. & BARTA, Z. 2000. EEG frequency profiles of idiopathic generalised epilepsy syndromes. *Epilepsy Res,* 42**,** 105-15.

COHEN, M. X. 2014. *Analyzing Neural Time Series Data : Theory and Practice,* , MIT Press, 2014. ProQuest Ebook Central,, MIT Press.

COHEN, M. X. & GRAFMAN, J. 2014. *Analyzing Neural Time Series Data : Theory and Practice,* Cambridge, UNITED STATES, MIT Press.

COLCLOUGH, G. L., WOOLRICH, M. W., TEWARIE, P. K., BROOKES, M. J., QUINN, A. J. & SMITH, S. M. 2016. How reliable are MEG resting-state connectivity metrics? *Neuroimage,* 138**,** 284-293.

CONTURO, T. E., LORI, N. F., CULL, T. S., AKBUDAK, E., SNYDER, A. Z., SHIMONY, J. S., MCKINSTRY, R. C., BURTON, H. & RAICHLE, M. E. 1999. Tracking neuronal fiber pathways in the living human brain. *Proc Natl Acad Sci U S A,* 96**,** 10422-7.

CRADDOCK, R. C., JAMES, G. A., HOLTZHEIMER III, P. E., HU, X. P. & MAYBERG, H. S. 2012. A whole brain fMRI atlas generated via spatially constrained spectral clustering. *Human Brain Mapping,* 33**,** 1914-1928.

CUI, L. B., WEI, Y., XI, Y. B., GRIFFA, A., DE LANGE, S. C., KAHN, R. S., YIN, H. & VAN DEN HEUVEL, M. P. 2019. Connectome-Based Patterns of First-Episode Medication-Naïve Patients With Schizophrenia. *Schizophr Bull,* 45**,** 1291-1299.

CUTTING, S., LAUCHHEIMER, A., BARR, W. & DEVINSKY, O. 2001. Adult-onset idiopathic generalized epilepsy: Clinical and behavioral features. *Epilepsia,* 42**,** 1395-1398.

DAI, Z., LIN, Q., LI, T., WANG, X., YUAN, H., YU, X., HE, Y. & WANG, H. 2019. Disrupted structural and functional brain networks in Alzheimer's disease. *Neurobiol Aging,* 75**,** 71-82.

DALIC, L. & COOK, M. J. 2016. Managing drug-resistant epilepsy: challenges and solutions. *Neuropsychiatr Dis Treat,* 12**,** 2605-2616.

DAMOISEAUX, J. S., ROMBOUTS, S. A. R. B., BARKHOF, F., SCHELTENS, P., STAM, C. J., SMITH, S. M. & BECKMANN, C. F. 2006. Consistent resting-state networks across healthy subjects. *Proceedings of the National Academy of Sciences,* 103**,** 13848.

DARVAS, F., PANTAZIS, D., KUCUKALTUN-YILDIRIM, E. & LEAHY, R. M. 2004. Mapping human brain function with MEG and EEG: methods and validation. *NeuroImage,* 23**,** S289-S299.

DAVID, O., COSMELLI, D. & FRISTON, K. J. 2004. Evaluation of different measures of functional connectivity using a neural mass model. *NeuroImage,* 21**,** 659-673.

DE BOER, H. M., MULA, M. & SANDER, J. W. 2008. The global burden and stigma of epilepsy. *Epilepsy & Behavior,* 12**,** 540-546.

DE MARTINO, F., ESPOSITO, F., VAN DE MOORTELE, P. F., HAREL, N., FORMISANO, E., GOEBEL, R., UGURBIL, K. & YACOUB, E. 2011. Whole brain high-resolution functional imaging at ultra high magnetic fields: an application to the analysis of resting state networks. *Neuroimage,* 57**,** 1031-44.

DE PISAPIA, N., TURATTO, M., LIN, P., JOVICICH, J. & CARAMAZZA, A. 2012. Unconscious Priming Instructions Modulate Activity in Default and Executive Networks of the Human Brain. *Cerebral Cortex,* 22**,** 639-649.

DELORME, A. & MAKEIG, S. 2004. EEGLAB: an open source toolbox for analysis of single-trial EEG dynamics including independent component analysis. *J Neurosci Methods,* 134**,** 9-21.

DESIKAN, R. S., SÉGONNE, F., FISCHL, B., QUINN, B. T., DICKERSON, B. C., BLACKER, D., BUCKNER, R. L., DALE, A. M., MAGUIRE, R. P., HYMAN, B. T., ALBERT, M. S. & KILLIANY, R. J. 2006. An automated labeling system for subdividing the human cerebral cortex on MRI scans into gyral based regions of interest. *NeuroImage,* 31**,** 968-980.

DESTRIEUX, C., FISCHL, B., DALE, A. & HALGREN, E. 2010. Automatic parcellation of human cortical gyri and sulci using standard anatomical nomenclature. *Neuroimage,* 53**,** 1-15.

DIAZ, B. A., VAN DER SLUIS, S., MOENS, S., BENJAMINS, J. S., MIGLIORATI, F., STOFFERS, D., DEN BRABER, A., POIL, S. S., HARDSTONE, R., VAN'T ENT, D., BOOMSMA, D. I., DE GEUS, E., MANSVELDER, H. D., VAN SOMEREN, E. J. & LINKENKAER-HANSEN, K. 2013. The Amsterdam Resting-State Questionnaire reveals multiple phenotypes of resting-state cognition. *Front Hum Neurosci,* 7**,** 446.

DICKIE, D. A., SHENKIN, S. D., ANBLAGAN, D., LEE, J., BLESA CABEZ, M., RODRIGUEZ, D., BOARDMAN, J. P., WALDMAN, A., JOB, D. E. & WARDLAW, J. M. 2017. Whole Brain Magnetic Resonance Image Atlases: A Systematic Review of Existing Atlases and Caveats for Use in Population Imaging. *Front Neuroinform,* 11**,** 1.

DING, J. R., AN, D., LIAO, W., LI, J., WU, G. R., XU, Q., LONG, Z., GONG, Q., ZHOU, D., SPORNS, O. & CHEN, H. 2013. Altered functional and structural connectivity networks in psychogenic non-epileptic seizures. *PLoS One,* 8**,** e63850.

DONISHI, T., TERADA, M. & KANEOKE, Y. 2018. Effects of gender, digit ratio, and menstrual cycle on intrinsic brain functional connectivity: A whole-brain, voxel-wise exploratory study using simultaneous local and global functional connectivity mapping. *Brain Behav,* 8**,** e00890.

DONNER, T. H. & SIEGEL, M. 2011. A framework for local cortical oscillation patterns. *Trends in Cognitive Sciences,* 15**,** 191-199.

DOUW, L., VAN DELLEN, E., DE GROOT, M., HEIMANS, J. J., KLEIN, M., STAM, C. J. & REIJNEVELD, J. C. 2010. Epilepsy is related to theta band brain connectivity and network topology in brain tumor patients. *BMC Neurosci,* 11**,** 103.

DYHRFJELD-JOHNSEN, J., SANTHAKUMAR, V., MORGAN, R. J., HUERTA, R., TSIMRING, L. & SOLTESZ, I. 2007. Topological determinants of epileptogenesis in large-scale structural and functional models of the dentate gyrus derived from experimental data. *J Neurophysiol,* 97**,** 1566-87.

DÍAZ, G. F., VIRUÉS, T., SAN MARTÍN, M., RUIZ, M., GALÁN, L., PAZ, L. & VALDÉS, P. 1998. Generalized background qEEG abnormalities in localized symptomatic epilepsy. *Electroencephalogr Clin Neurophysiol,* 106**,** 501-7.

DÜZEL, E., PENNY, W. D. & BURGESS, N. 2010. Brain oscillations and memory. *Current Opinion in Neurobiology,* 20**,** 143-149.

EGUÍLUZ, V. M., CHIALVO, D. R., CECCHI, G. A., BALIKI, M. & APKARIAN, A. V. 2005. Scale-free brain functional networks. *Phys Rev Lett,* 94**,** 018102.

EICKHOFF, S. B., THIRION, B., VAROQUAUX, G. & BZDOK, D. 2015. Connectivity-based parcellation: Critique and implications. *Hum Brain Mapp,* 36**,** 4771-92.

EICKHOFF, S. B., YEO, B. T. T. & GENON, S. 2018. Imaging-based parcellations of the human brain. *Nature Reviews Neuroscience,* 19**,** 672-686.

ELSHAHABI, A., KLAMER, S., SAHIB, A. K., LERCHE, H., BRAUN, C. & FOCKE, N. K. 2015. Magnetoencephalography Reveals a Widespread Increase in Network Connectivity in Idiopathic/Genetic Generalized Epilepsy. *PLoS One,* 10**,** e0138119.

ENGEL, A. K., GERLOFF, C., HILGETAG, C. C. & NOLTE, G. 2013a. Intrinsic coupling modes: multiscale interactions in ongoing brain activity. *Neuron,* 80**,** 867-86.

ENGEL, J., JR., THOMPSON, P. M., STERN, J. M., STABA, R. J., BRAGIN, A. & MODY, I. 2013b. Connectomics and epilepsy. *Curr Opin Neurol,* 26**,** 186-94.

ENGLOT, D. J., CHANG, E. F. & AUGUSTE, K. I. 2011. Vagus nerve stimulation for epilepsy: a meta-analysis of efficacy and predictors of response. *J Neurosurg,* 115**,** 1248-55.

FALLON, N., CHIU, Y., NURMIKKO, T. & STANCAK, A. 2016. Functional Connectivity with the Default Mode Network Is Altered in Fibromyalgia Patients. *PLoS One,* 11**,** e0159198.

FANG, M., XI, Z. Q., WU, Y. & WANG, X. F. 2011. A new hypothesis of drug refractory epilepsy: neural network hypothesis. *Med Hypotheses,* 76**,** 871-6.

FELDMANN, M., ASSELIN, M. C., LIU, J., WANG, S., MCMAHON, A., ANTON-RODRIGUEZ, J., WALKER, M., SYMMS, M., BROWN, G., HINZ, R., MATTHEWS, J., BAUER, M., LANGER, O., THOM, M., JONES, T., VOLLMAR, C., DUNCAN, J. S., SISODIYA, S. M. & KOEPP, M. J. 2013. P-glycoprotein expression and function in patients with temporal lobe epilepsy: a case-control study. *Lancet Neurol,* 12**,** 777-85.

FERRO, J. M., CORREIA, M., ROSAS, M. J., PINTO, A. N. & NEVES, G. 2003. Seizures in cerebral vein and dural sinus thrombosis. *Cerebrovasc Dis,* 15**,** 78-83.

FICKER, D. M., SO, E. L., SHEN, W. K., ANNEGERS, J. F., BRIEN, P. C., CASCINO, G. D. & BELAU, P. G. 1998. Population-based study of the incidence of sudden unexplained death in epilepsy. *Neurology,* 51**,** 1270.

FINN, E. S., SCHEINOST, D., SHEN, X., PAPADEMETRIS, X. & CONSTABLE, R. T. 2015. Methodological Issues in fMRI Functional Connectivity and Network Analysis. *In:* TOGA, A. W. (ed.) *Brain Mapping.* Waltham: Academic Press.

FISCHL, B. 2012. FreeSurfer. *Neuroimage,* 62**,** 774-81.

FISHER, R. S., BOAS, W. V. E., BLUME, W., ELGER, C., GENTON, P., LEE, P. & ENGEL JR, J. 2005. Epileptic Seizures and Epilepsy: Definitions Proposed by the International League Against Epilepsy (ILAE) and the International Bureau for Epilepsy (IBE). *Epilepsia,* 46**,** 470-472.

FORNITO, A. & BULLMORE, E. T. 2010. What can spontaneous fluctuations of the blood oxygenation-level-dependent signal tell us about psychiatric disorders? *Curr Opin Psychiatry,* 23**,** 239-49.

FORNITO, A., ZALESKY, A. & BREAKSPEAR, M. 2013. Graph analysis of the human connectome: promise, progress, and pitfalls. *Neuroimage,* 80**,** 426-44.

FORNITO, A., ZALESKY, A. & BULLMORE, E. T. 2010. Network scaling effects in graph analytic studies of human resting-state FMRI data. *Frontiers in systems neuroscience,* 4**,** 22-22.

FORNITO, A., ZALESKY, A. & BULLMORE, E. T. 2016. *Fundamentals of brain network analysis,* Amsterdam, Elsevier.

FOX, M. D. & RAICHLE, M. E. 2007. Spontaneous fluctuations in brain activity observed with functional magnetic resonance imaging. *Nat Rev Neurosci,* 8**,** 700-11.

FOX, M. D., SNYDER, A. Z., VINCENT, J. L., CORBETTA, M., VAN ESSEN, D. C. & RAICHLE, M. E. 2005. The human brain is intrinsically organized into dynamic, anticorrelated functional networks. *Proceedings of the National Academy of Sciences of the United States of America,* 102**,** 9673-9678.

FOX, M. D., ZHANG, D., SNYDER, A. Z. & RAICHLE, M. E. 2009. The global signal and observed anticorrelated resting state brain networks. *Journal of neurophysiology,* 101**,** 3270-3283.

FRASCHINI, M., DEMURU, M., CROBE, A., MARROSU, F., STAM, C. J. & HILLEBRAND, A. 2016. The effect of epoch length on estimated EEG functional connectivity and brain network organisation. *J Neural Eng,* 13**,** 036015.

FRASER, A. M. & SWINNEY, H. L. 1986. Independent coordinates for strange attractors from mutual information. *Physical Review A,* 33**,** 1134-1140.

FREEMAN, L. C. 1978. Centrality in social networks conceptual clarification. *Social Networks,* 1**,** 215-239.

FREI, M. G., ZAVERI, H. P., ARTHURS, S., BERGEY, G. K., JOUNY, C. C., LEHNERTZ, K., GOTMAN, J., OSORIO, I., NETOFF, T. I., FREEMAN, W. J., JEFFERYS, J., WORRELL, G., VAN QUYEN, M. L., SCHIFF, S. J. & MORMANN, F. 2010. Controversies in epilepsy: Debates held during the Fourth International Workshop on Seizure Prediction. *Epilepsy & Behavior,* 19**,** 4-16.

FRIES, P., NEUENSCHWANDER, S., ENGEL, A. K., GOEBEL, R. & SINGER, W. 2001. Rapid feature selective neuronal synchronization through correlated latency shifting. *Nat Neurosci,* 4**,** 194-200.

FRISTON, K. J. 2011. Functional and effective connectivity: a review. *Brain Connect,* 1**,** 13-36.

FUSTER, J. M. 1998. Linkage at the top. *Neuron,* 21**,** 1223-4.

GARCIA-RAMOS, C., BOBHOLZ, S., DABBS, K., HERMANN, B., JOUTSA, J., RINNE, J. O., KARRASCH, M., PRABHAKARAN, V., SHINNAR, S. & SILLANPAA, M. 2017. Brain structure and organization five decades after childhood onset epilepsy. *Hum Brain Mapp,* 38**,** 3289-3299.

GARGOURI, F., KALLEL, F., DELPHINE, S., BEN HAMIDA, A., LEHÉRICY, S. & VALABREGUE, R. 2018. The Influence of Preprocessing Steps on Graph Theory Measures Derived from Resting State fMRI. *Frontiers in computational neuroscience,* 12**,** 8-8.

GARRISON, K. A., SCHEINOST, D., FINN, E. S., SHEN, X. & CONSTABLE, R. T. 2015. The (in)stability of functional brain network measures across thresholds. *Neuroimage,* 118**,** 651-61.

GELISSE, P., GENTON, P., THOMAS, P., REY, M., SAMUELIAN, J. & DRAVET, C. 2001. Clinical factors of drug resistance in juvenile myoclonic. *J Neurol Neurosurg Psychiatry,* 70**,** 240-3.

GHOUGASSIAN, D. F., D'SOUZA, W., COOK, M. J. & O'BRIEN, T. J. 2004. Evaluating the utility of inpatient video-EEG monitoring. *Epilepsia,* 45**,** 928-32.

GIBBS, F. A., GIBBS, E. L. & LENNOX, W. G. 1943. Electroencephalographic classification of epileptic patients and control subjects. *Archives of Neurology & Psychiatry,* 50**,** 111-128.

GLASSER, M. F., COALSON, T. S., ROBINSON, E. C., HACKER, C. D., HARWELL, J., YACOUB, E., UGURBIL, K., ANDERSSON, J., BECKMANN, C. F., JENKINSON, M., SMITH, S. M. & VAN ESSEN, D. C. 2016. A multi-modal parcellation of human cerebral cortex. *Nature,* 536**,** 171-178.

GLOOR, P. 1968. Generalized Cortico-Reticular Epilepsies Some Considerations on the Pathophysiology of Generalized Bilaterally Synchronous Spike and Wave Discharge. *Epilepsia,* 9**,** 249-263.

GLOVER, G. H. 2011. Overview of Functional Magnetic Resonance Imaging. *Neurosurg Clin N Am,* 22**,** 133-9.

GORDON, E. M., LAUMANN, T. O., ADEYEMO, B., HUCKINS, J. F., KELLEY, W. M. & PETERSEN, S. E. 2016. Generation and Evaluation of a Cortical Area Parcellation from Resting-State Correlations. *Cerebral cortex (New York, N.Y. : 1991),* 26**,** 288-303.

GOTMAN, J., GROVA, C., BAGSHAW, A., KOBAYASHI, E., AGHAKHANI, Y. & DUBEAU, F. 2005. Generalized epileptic discharges show thalamocortical activation and suspension of the default state of the brain. *Proceedings of the National Academy of Sciences of the United States of America,* 102**,** 15236-15240.

GOWERS, W. 1881. Epilepsy and other chronic convulsive disorders:

their causes, symptoms and treatment. London: J&A Churchill.

GRANGER, C. W. J. 1969. Investigating Causal Relations by Econometric Models and Cross-spectral Methods. *Econometrica,* 37**,** 424-438.

GRAY, C. M. & SINGER, W. 1989. Stimulus-specific neuronal oscillations in orientation columns of cat visual cortex. *Proceedings of the National Academy of Sciences,* 86**,** 1698.

GREGORY, R. P., OATES, T. & MERRY, R. T. 1993. Electroencephalogram epileptiform abnormalities in candidates for aircrew training. *Electroencephalogr Clin Neurophysiol,* 86**,** 75-7.

GREICIUS, M. D., KRASNOW, B., REISS, A. L. & MENON, V. 2003. Functional connectivity in the resting brain: A network analysis of the default mode hypothesis. *Proceedings of the National Academy of Sciences,* 100**,** 253.

GROBELNY, B. T., LONDON, D., HILL, T. C., NORTH, E., DUGAN, P. & DOYLE, W. K. 2018. Betweenness centrality of intracranial electroencephalography networks and surgical epilepsy outcome. *Clinical Neurophysiology,* 129**,** 1804-1812.

GROSS, J., BAILLET, S., BARNES, G. R., HENSON, R. N., HILLEBRAND, A., JENSEN, O., JERBI, K., LITVAK, V., MAESS, B., OOSTENVELD, R., PARKKONEN, L., TAYLOR, J. R., VAN WASSENHOVE, V., WIBRAL, M. & SCHOFFELEN, J.-M. 2013. Good practice for conducting and reporting MEG research. *NeuroImage,* 65**,** 349-363.

HAGMANN, P., KURANT, M., GIGANDET, X., THIRAN, P., WEDEEN, V. J., MEULI, R. & THIRAN, J. P. 2007. Mapping human whole-brain structural networks with diffusion MRI. *PLoS One,* 2**,** e597.

HALGREN, M., ULBERT, I., BASTUJI, H., FABÓ, D., ERŐSS, L., REY, M., DEVINSKY, O., DOYLE, W. K., MAK-MCCULLY, R., HALGREN, E., WITTNER, L., CHAUVEL, P., HEIT, G., ESKANDAR, E., MANDELL, A. & CASH, S. S. 2019. The generation and propagation of the human alpha rhythm. *Proceedings of the National Academy of Sciences,* 116**,** 23772.

HAMANDI, K., SALEK-HADDADI, A., LAUFS, H., LISTON, A., FRISTON, K., FISH, D. R., DUNCAN, J. S. & LEMIEUX, L. 2006. EEG-fMRI of idiopathic and secondarily generalized epilepsies. *NeuroImage,* 31**,** 1700-1710.

HANEEF, Z., CHIANG, S., YEH, H. J., ENGEL, J., JR. & STERN, J. M. 2015a. Functional connectivity homogeneity correlates with duration of temporal lobe epilepsy. *Epilepsy Behav,* 46**,** 227-33.

HANEEF, Z., LEVIN, H. S. & CHIANG, S. 2015b. Brain Graph Topology Changes Associated with Anti-Epileptic Drug Use. *Brain connectivity,* 5**,** 284-291.

HATTON, S. N., HUYNH, K. H., BONILHA, L., ABELA, E., ALHUSAINI, S., ALTMANN, A., ALVIM, M. K. M., BALACHANDRA, A. R., BARTOLINI, E., BENDER, B., BERNASCONI, N., BERNASCONI, A., BERNHARDT, B., BARGALLO, N., CALDAIROU, B., CALIGIURI, M. E., CARR, S. J. A., CAVALLERI, G. L., CENDES, F., CONCHA, L., DAVOODI-BOJD, E., DESMOND, P. M., DEVINSKY, O., DOHERTY, C. P., DOMIN, M., DUNCAN, J. S., FOCKE, N. K., FOLEY, S. F., GAMBARDELLA, A., GLEICHGERRCHT, E., GUERRINI, R., HAMANDI, K., ISHIKAWA, A., KELLER, S. S., KOCHUNOV, P. V., KOTIKALAPUDI, R., KREILKAMP, B. A. K., KWAN, P., LABATE, A., LANGNER, S., LENGE, M., LIU, M., LUI, E., MARTIN, P., MASCALCHI, M., MOREIRA, J. C. V., MORITA-SHERMAN, M. E., O'BRIEN, T. J., PARDOE, H. R., PARIENTE, J. C., RIBEIRO, L. F., RICHARDSON, M. P., ROCHA, C. S., RODRÍGUEZ-CRUCES, R., ROSENOW, F., SEVERINO, M., SINCLAIR, B., SOLTANIAN-ZADEH, H., STRIANO, P., TAYLOR, P. N., THOMAS, R. H., TORTORA, D., VELAKOULIS, D., VEZZANI, A., VIVASH, L., VON PODEWILS, F., VOS, S. B., WEBER, B., WINSTON, G. P., YASUDA, C. L., ZHU, A. H., THOMPSON, P. M., WHELAN, C. D., JAHANSHAD, N., SISODIYA, S. M. & MCDONALD, C. R. 2020. White matter abnormalities across different epilepsy syndromes in adults: an ENIGMA-Epilepsy study. *Brain,* 143**,** 2454-2473.

HAYASAKA, S. & LAURIENTI, P. J. 2010. Comparison of characteristics between region-and voxel-based network analyses in resting-state fMRI data. *NeuroImage,* 50**,** 499-508.
HE, Y., CHEN, Z. & EVANS, A. 2008. Structural Insights into Aberrant Topological Patterns of Large-Scale Cortical Networks in Alzheimer's Disease. *The Journal of Neuroscience,* 28**,** 4756.
HE, Y., CHEN, Z. J. & EVANS, A. C. 2007. Small-world anatomical networks in the human brain revealed by cortical thickness from MRI. *Cereb Cortex,* 17**,** 2407-19.
HE, Y., WANG, J., WANG, L., CHEN, Z. J., YAN, C., YANG, H., TANG, H., ZHU, C., GONG, Q., ZANG, Y. & EVANS, A. C. 2009. Uncovering intrinsic modular organization of spontaneous brain activity in humans. *PloS one,* 4**,** e5226-e5226.
HELBIG, I. 2015. Genetic Causes of Generalized Epilepsies. *Semin Neurol,* 35**,** 288-92.
HERRMANN, C. S., STRÜBER, D., HELFRICH, R. F. & ENGEL, A. K. 2016. EEG oscillations: From correlation to causality. *Int J Psychophysiol,* 103**,** 12-21.
HESDORFFER, D. C., BENN, E. K. T., CASCINO, G. D. & HAUSER, W. A. 2009. Is a first acute symptomatic seizure epilepsy? Mortality and risk for recurrent seizure. *Epilepsia,* 50**,** 1102-1108.
HESSEN, E., LOSSIUS, M. I., REINVANG, I. & GJERSTAD, L. 2006. Predictors of neuropsychological impairment in seizure-free epilepsy patients. *Epilepsia,* 47**,** 1870-8.
HITIRIS, N., MOHANRAJ, R., NORRIE, J., SILLS, G. J. & BRODIE, M. J. 2007. Predictors of pharmacoresistant epilepsy. *Epilepsy Res,* 75**,** 192-6.
HJORTH, B. 1975. An on-line transformation of EEG scalp potentials into orthogonal source derivations. *Electroencephalogr Clin Neurophysiol,* 39**,** 526-30.
HOLLER, Y., HELMSTAEDTER, C. & LEHNERTZ, K. 2019. Correction to: Quantitative Pharmaco-Electroencephalography in Antiepileptic Drug Research. *CNS Drugs.* New Zealand.
HORSTMANN, M. T., BIALONSKI, S., NOENNIG, N., MAI, H., PRUSSEIT, J., WELLMER, J., HINRICHS, H. & LEHNERTZ, K. 2010. State dependent properties of epileptic brain networks: comparative graph-theoretical analyses of simultaneously recorded EEG and MEG. *Clin Neurophysiol,* 121**,** 172-85.
HUGHES, J. R. 2008. One of the hottest topics in epileptology: ABC proteins. Their inhibition may be the future for patients with intractable seizures. *Neurological Research,* 30**,** 920-925.
HÖLLER, Y., KUTIL, R., KLAFFENBÖCK, L., THOMSCHEWSKI, A., HÖLLER, P. M., BATHKE, A. C., JACOBS, J., TAYLOR, A. C., NARDONE, R. & TRINKA, E. 2015. High-frequency oscillations in epilepsy and surgical outcome. A meta-analysis. *Frontiers in human neuroscience,* 9**,** 574-574.
IBM-CORP 2017. *IBM SPSS Statistics for Windows, version 25.* . Armonk, NY: IBM Corp.
ILAE. 2018. *CAE overview.* https://www.epilepsydiagnosis.org/syndrome/cae-overview.html [Online]. West Harford, USA.: ILAE. [Accessed 09/01/ 2018].
ILAE. 2020a. *Epilepsy with Generalized Tonic-Clonic Seizures Alone.* https://www.epilepsydiagnosis.org/syndrome/egtcsa-overview.html [Online]. [Accessed 16/07/ 2020].
ILAE. 2020b. *JAE overview.* https://epilepsydiagnosis.org/syndrome/jae-overview.html [Online]. West Harford, USA. [Accessed 31/05 2021].
ILAE. 2020c. *JME overview.* https://epilepsydiagnosis.org/syndrome/jme-overview.html [Online]. West Harford, USA. [Accessed 31/05 2021].
IQBAL, N., CASWELL, H. L., HARE, D. J., PILKINGTON, O., MERCER, S. & DUNCAN, S. 2009. Neuropsychological profiles of patients with juvenile myoclonic epilepsy and their siblings: a preliminary controlled experimental video-EEG case series. *Epilepsy Behav,* 14**,** 516-21.
ITURRIA-MEDINA, Y., SOTERO, R. C., CANALES-RODRIGUEZ, E. J., ALEMAN-GOMEZ, Y. & MELIE-GARCIA, L. 2008. Studying the human brain anatomical network via diffusion-weighted MRI and Graph Theory. *Neuroimage,* 40**,** 1064-76.
IWAMOTO, T., KAGAWA, Y., NAITO, Y., KUZUHARA, S. & OKUDA, M. 2006. Clinical evaluation of plasma free phenytoin measurement and factors influencing its protein binding. *Biopharm Drug Dispos,* 27**,** 77-84.

JALLON, P. & LATOUR, P. 2005. Epidemiology of Idiopathic Generalized Epilepsies. *Epilepsia,* 46**,** 10-14.

JAO, T., VÉRTES, P. E., ALEXANDER-BLOCH, A. F., TANG, I. N., YU, Y.-C., CHEN, J.-H. & BULLMORE, E. T. 2013. Volitional eyes opening perturbs brain dynamics and functional connectivity regardless of light input. *NeuroImage,* 69**,** 21-34.

JASPER, H. & KERSHMAN, J. 1941. Electroencephalographic classification of the epilepsies. *Archives of Neurology & Psychiatry,* 45**,** 903-943.

JENSEN, O. & MAZAHERI, A. 2010. Shaping functional architecture by oscillatory alpha activity: gating by inhibition. *Front Hum Neurosci,* 4**,** 186.

JIANG, W., LI, J., CHEN, X., YE, W. & ZHENG, J. 2017. Disrupted Structural and Functional Networks and Their Correlation with Alertness in Right Temporal Lobe Epilepsy: A Graph Theory Study. *Front Neurol,* 8.

JIN, S. H., JEONG, W., SEOL, J., KWON, J. & CHUNG, C. K. 2013. Functional cortical hubs in the eyes-closed resting human brain from an electrophysiological perspective using magnetoencephalography. *PLoS One,* 8**,** e68192.

JO, H. J., SAAD, Z. S., GOTTS, S. J., MARTIN, A. & COX, R. W. 2012. Quantifying Agreement between Anatomical and Functional Interhemispheric Correspondences in the Resting Brain. *PLOS ONE,* 7**,** e48847.

JOHANNESSEN LANDMARK, C., FLØGSTAD, I., SYVERTSEN, M., BAFTIU, A., ENGER, U., KOHT, J. & JOHANNESSEN, S. I. 2019. Treatment and challenges with antiepileptic drugs in patients with juvenile myoclonic epilepsy. *Epilepsy & Behavior,* 98**,** 110-116.

JOLIOT, M., JOBARD, G., NAVEAU, M., DELCROIX, N., PETIT, L., ZAGO, L., CRIVELLO, F., MELLET, E., MAZOYER, B. & TZOURIO-MAZOYER, N. 2015. AICHA: An atlas of intrinsic connectivity of homotopic areas. *Journal of Neuroscience Methods,* 254**,** 46-59.

JONES, D. T., VEMURI, P., MURPHY, M. C., GUNTER, J. L., SENJEM, M. L., MACHULDA, M. M., PRZYBELSKI, S. A., GREGG, B. E., KANTARCI, K., KNOPMAN, D. S., BOEVE, B. F., PETERSEN, R. C. & JACK, C. R., JR. 2012. Non-Stationarity in the "Resting Brain's" Modular Architecture. *PLOS ONE,* 7**,** e39731.

JONES, J. E., HERMANN, B. P., BARRY, J. J., GILLIAM, F. G., KANNER, A. M. & MEADOR, K. J. 2003. Rates and risk factors for suicide, suicidal ideation, and suicide attempts in chronic epilepsy. *Epilepsy & Behavior,* 4**,** 31-38.

JOSEPHS, O. & HENSON, R. N. 1999. Event-related functional magnetic resonance imaging: modelling, inference and optimization. *Philos Trans R Soc Lond B Biol Sci,* 354**,** 1215-28.

KAMINSKI, M. J. & BLINOWSKA, K. J. 1991. A new method of the description of the information flow in the brain structures. *Biological Cybernetics,* 65**,** 203-210.

KAY, B. P., DIFRANCESCO, M. W., PRIVITERA, M. D., GOTMAN, J., HOLLAND, S. K. & SZAFLARSKI, J. P. 2013. Reduced default mode network connectivity in treatment-resistant idiopathic generalized epilepsy. *Epilepsia,* 54**,** 461-470.

KAY, B. P., HOLLAND, S. K., PRIVITERA, M. D. & SZAFLARSKI, J. P. 2014. Differences in paracingulate connectivity associated with epileptiform discharges and uncontrolled seizures in genetic generalized epilepsy. *Epilepsia,* 55**,** 256-263.

KAYSER, J. & TENKE, C. E. 2010. In search of the Rosetta Stone for scalp EEG: converging on reference-free techniques. *Clin Neurophysiol.* Netherlands.

KELLY, A. M. C., UDDIN, L. Q., BISWAL, B. B., CASTELLANOS, F. X. & MILHAM, M. P. 2008. Competition between functional brain networks mediates behavioral variability. *NeuroImage,* 39**,** 527-537.

KHANIN, R. & WIT, E. 2006. How scale-free are biological networks. *J Comput Biol,* 13**,** 810-8.

KHARAZMI, E., PELTOLA, M., FALLAH, M., KERÄNEN, T. & PELTOLA, J. 2010. Idiopathic generalized epilepsies: a follow-up study in a single-center. *Acta Neurologica Scandinavica,* 122**,** 196-201.

KILNER, J. M., KIEBEL, S. J. & FRISTON, K. J. 2005. Applications of random field theory to electrophysiology. *Neurosci Lett,* 374**,** 174-8.

KIM, J., LEE, W. G., PARK, S. & PARK, K. M. 2020. Can we predict drug response by functional connectivity in patients with juvenile myoclonic epilepsy? *Clinical Neurology and Neurosurgery,* 198**,** 106119.

KIM, J. B., SUH, S.-I., SEO, W.-K., OH, K., KOH, S.-B. & KIM, J. H. 2014. Altered thalamocortical functional connectivity in idiopathic generalized epilepsy. *Epilepsia,* 55**,** 592-600.

KIM, J. M., JUNG, K. Y. & CHOI, C. M. 2002. Changes in Brain Complexity during Valproate Treatment in Patients with Partial Epilepsy. *Neuropsychobiology,* 45**,** 106-112.

KLIMESCH, W. 2012. α-band oscillations, attention, and controlled access to stored information. *Trends Cogn Sci,* 16**,** 606-17.

KO, T. S. & HOLMES, G. L. 1999. EEG and clinical predictors of medically intractable childhood epilepsy. *Clin Neurophysiol,* 110**,** 1245-51.

KOPELL, N., ERMENTROUT, G. B., WHITTINGTON, M. A. & TRAUB, R. D. 2000. Gamma rhythms and beta rhythms have different synchronization properties. *Proc Natl Acad Sci U S A,* 97**,** 1867-72.

KRAMER, M. A., EDEN, U. T., KOLACZYK, E. D., ZEPEDA, R., ESKANDAR, E. N. & CASH, S. S. 2010. Coalescence and fragmentation of cortical networks during focal seizures. *J Neurosci,* 30**,** 10076-85.

KRUMHOLZ, A., WIEBE, S., GRONSETH, G., SHINNAR, S., LEVISOHN, P., TING, T., HOPP, J., SHAFER, P., MORRIS, H., SEIDEN, L., BARKLEY, G. & FRENCH, J. 2007. Practice Parameter: evaluating an apparent unprovoked first seizure in adults (an evidence-based review): report of the Quality Standards Subcommittee of the American Academy of Neurology and the American Epilepsy Society. *Neurology,* 69**,** 1996-2007.

KUBICKI, S., HERRMANN, W. M., FICHTE, K. & FREUND, G. 1979. Reflections on the topics: EEG frequency bands and regulation of vigilance. *Pharmakopsychiatr Neuropsychopharmakol,* 12**,** 237-45.

KWAN, P., ARZIMANOGLOU, A., BERG, A. T., BRODIE, M. J., ALLEN HAUSER, W., MATHERN, G., MOSHE, S. L., PERUCCA, E., WIEBE, S. & FRENCH, J. 2010. Definition of drug resistant epilepsy: consensus proposal by the ad hoc Task Force of the ILAE Commission on Therapeutic Strategies. *Epilepsia,* 51**,** 1069-77.

KWAN, P. & BRODIE, M. J. 2000. Early identification of refractory epilepsy. *N Engl J Med,* 342**,** 314-9.

KWAN, P., POON, W. S., NG, H. K., KANG, D. E., WONG, V., NG, P. W., LUI, C. H., SIN, N. C., WONG, K. S. & BAUM, L. 2008. Multidrug resistance in epilepsy and polymorphisms in the voltage-gated sodium channel genes SCN1A, SCN2A, and SCN3A: correlation among phenotype, genotype, and mRNA expression. *Pharmacogenet Genomics,* 18**,** 989-98.

KWAN, P., SCHACHTER, S. C. & BRODIE, M. J. 2011. Drug-resistant epilepsy. *N Engl J Med,* 365**,** 919-26.

LACHAUX, J.-P., RODRIGUEZ, E., MARTINERIE, J. & VARELA, F. J. 1999. Measuring phase synchrony in brain signals. *Human Brain Mapping,* 8**,** 194-208.

LAIOU, P., AVRAMIDIS, E., LOPES, M. A., ABELA, E., MÜLLER, M., AKMAN, O. E., RICHARDSON, M. P., RUMMEL, C., SCHINDLER, K. & GOODFELLOW, M. 2019. Quantification and Selection of Ictogenic Zones in Epilepsy Surgery. *Frontiers in Neurology,* 10**,** 1045.

LAKHAN, R., KUMARI, R., MISRA, U. K., KALITA, J., PRADHAN, S. & MITTAL, B. 2009. Differential role of sodium channels SCN1A and SCN2A gene polymorphisms with epilepsy and multiple drug resistance in the north Indian population. *Br J Clin Pharmacol,* 68**,** 214-20.

LARSSON, P. G. & KOSTOV, H. 2005. Lower frequency variability in the alpha activity in EEG among patients with epilepsy. *Clin Neurophysiol,* 116**,** 2701-6.

LAWLEY, A., EVANS, S., MANFREDONIA, F. & CAVANNA, A. E. 2015. The role of outpatient ambulatory electroencephalography in the diagnosis and management of adults with

epilepsy or nonepileptic attack disorder: A systematic literature review. *Epilepsy & Behavior,* 53**,** 26-30.

LAZAROWSKI, A., SEVLEVER, G., TARATUTO, A., MASSARO, M. & RABINOWICZ, A. 1999. Tuberous sclerosis associated with MDR1 gene expression and drug-resistant epilepsy. *Pediatr Neurol,* 21**,** 731-4.

LEACH, J. P., LAUDER, R., NICOLSON, A. & SMITH, D. F. 2005. Epilepsy in the UK: misdiagnosis, mistreatment, and undertreatment? The Wrexham area epilepsy project. *Seizure,* 14**,** 514-20.

LEE, C., IM, C. H., KOO, Y. S., LIM, J. A., KIM, T. J., BYUN, J. I., SUNWOO, J. S., MOON, J., KIM, D. W., LEE, S. T., JUNG, K. H., CHU, K., LEE, S. K. & JUNG, K. Y. 2017. Altered Network Characteristics of Spike-Wave Discharges in Juvenile Myoclonic Epilepsy. *Clin EEG Neurosci,* 48**,** 111-117.

LEE, D. A., KIM, B. J., LEE, H.-J., KIM, S. E. & PARK, K. M. 2020. Network characteristics of genetic generalized epilepsy: Are the syndromes distinct? *Seizure,* 82**,** 91-98.

LEE, H. J. & PARK, K. M. 2019. Structural and functional connectivity in newly diagnosed juvenile myoclonic epilepsy. *Acta Neurol Scand,* 139**,** 469-475.

LEE, K., KHOO, H. M., LINA, J.-M., DUBEAU, F., GOTMAN, J. & GROVA, C. 2018. Disruption, emergence and lateralization of brain network hubs in mesial temporal lobe epilepsy. *NeuroImage. Clinical,* 20**,** 71-84.

LEUTMEZER, F., LURGER, S. & BAUMGARTNER, C. 2002. Focal features in patients with idiopathic generalized epilepsy. *Epilepsy Res,* 50**,** 293-300.

LI, Q., CAO, W., LIAO, X., CHEN, Z., YANG, T., GONG, Q., ZHOU, D., LUO, C. & YAO, D. 2015a. Altered resting state functional network connectivity in children absence epilepsy. *Journal of the Neurological Sciences,* 354**,** 79-85.

LI, Q., CHEN, Y., WEI, Y., CHEN, S., MA, L., HE, Z. & CHEN, Z. 2017. Functional Network Connectivity Patterns between Idiopathic Generalized Epilepsy with Myoclonic and Absence Seizures. *Frontiers in Computational Neuroscience,* 11**,** 38.

LI, R., LI, Y., AN, D., GONG, Q., ZHOU, D. & CHEN, H. 2015b. Altered regional activity and inter-regional functional connectivity in psychogenic non-epileptic seizures. *Scientific Reports,* 5**,** 11635.

LI, S., LIU, Y. & WANG, Q. 2015c. ABCB1 Gene C3435T Polymorphism and Drug Resistance in Epilepsy: Evidence Based on 8604 Subjects. *Med Sci Monit.*

LI, X., CUI, D., JIRUSKA, P., FOX, J. E., YAO, X. & JEFFERYS, J. G. 2007. Synchronization measurement of multiple neuronal populations. *J Neurophysiol,* 98**,** 3341-8.

LIANG, B., ZHANG, D., WEN, X., XU, P., PENG, X., HUANG, X., LIU, M. & HUANG, R. 2014. Brain spontaneous fluctuations in sensorimotor regions were directly related to eyes open and eyes closed: evidences from a machine learning approach. *Front Hum Neurosci,* 8**,** 645.

LIANG, X., WANG, J., YAN, C., SHU, N., XU, K., GONG, G. & HE, Y. 2012. Effects of different correlation metrics and preprocessing factors on small-world brain functional networks: a resting-state functional MRI study. *PloS one,* 7**,** e32766-e32766.

LIAO, W., ZHANG, Z., MANTINI, D., XU, Q., WANG, Z., CHEN, G., JIAO, Q., ZANG, Y. F. & LU, G. 2013. Relationship between large-scale functional and structural covariance networks in idiopathic generalized epilepsy. *Brain Connect,* 3**,** 240-54.

LIMA-MENDEZ, G. & VAN HELDEN, J. 2009. The powerful law of the power law and other myths in network biology. *Mol Biosyst,* 5**,** 1482-93.

LIN, C. L., DUMONT, A. S., LIEU, A. S., YEN, C. P., HWANG, S. L., KWAN, A. L., KASSELL, N. F. & HOWNG, S. L. 2003. Characterization of perioperative seizures and epilepsy following aneurysmal subarachnoid hemorrhage. *J Neurosurg,* 99**,** 978-85.

LIN, L. C., OUYANG, C. S., CHIANG, C. T., YANG, R. C., WU, R. C. & WU, H. C. 2014. Early prediction of medication refractoriness in children with idiopathic epilepsy based on scalp EEG analysis. *Int J Neural Syst,* 24**,** 1450023.

LIU, J. Y., THOM, M., CATARINO, C. B., MARTINIAN, L., FIGARELLA-BRANGER, D., BARTOLOMEI, F., KOEPP, M. & SISODIYA, S. M. 2012. Neuropathology of the blood-brain barrier and pharmaco-resistance in human epilepsy. *Brain,* 135**,** 3115-33.

LIU, Y., LIANG, M., ZHOU, Y., HE, Y., HAO, Y., SONG, M., YU, C., LIU, H., LIU, Z. & JIANG, T. 2008. Disrupted small-world networks in schizophrenia. *Brain,* 131**,** 945-961.

LOPES DA SILVA, F., BLANES, W., KALITZIN, S. N., PARRA, J., SUFFCZYNSKI, P. & VELIS, D. N. 2003. Epilepsies as dynamical diseases of brain systems: basic models of the transition between normal and epileptic activity. *Epilepsia,* 44 Suppl 12**,** 72-83.

LOPES, M. A., JUNGES, L., WOLDMAN, W., GOODFELLOW, M. & TERRY, J. R. 2020. The Role of Excitability and Network Structure in the Emergence of Focal and Generalized Seizures. *Frontiers in Neurology,* 11**,** 74.

LOPES, M. A., RICHARDSON, M. P., ABELA, E., RUMMEL, C., SCHINDLER, K., GOODFELLOW, M. & TERRY, J. R. 2017. An optimal strategy for epilepsy surgery: Disruption of the rich-club? *PLOS Computational Biology,* 13**,** e1005637.

LOPEZ ZUNINI, R. A., THIVIERGE, J. P., KOUSAIE, S., SHEPPARD, C. & TALER, V. 2013. Alterations in resting-state activity relate to performance in a verbal recognition task. *PLoS One,* 8**,** e65608.

LOPEZ-MUNOZ, F., BOYA, J. & ALAMO, C. 2006. Neuron theory, the cornerstone of neuroscience, on the centenary of the Nobel Prize award to Santiago Ramon y Cajal. *Brain Res Bull,* 70**,** 391-405.

LOSCHER, W., LUNA-TORTOS, C., ROMERMANN, K. & FEDROWITZ, M. 2011. Do ATP-binding cassette transporters cause pharmacoresistance in epilepsy? Problems and approaches in determining which antiepileptic drugs are affected. *Curr Pharm Des,* 17**,** 2808-28.

LOSCHER, W. & POTSCHKA, H. 2002. Role of multidrug transporters in pharmacoresistance to antiepileptic drugs. *J Pharmacol Exp Ther,* 301**,** 7-14.

LOUP, F., WIESER, H. G., YONEKAWA, Y., AGUZZI, A. & FRITSCHY, J. M. 2000. Selective alterations in GABAA receptor subtypes in human temporal lobe epilepsy. *J Neurosci,* 20**,** 5401-19.

LÖSCHER, W. & POTSCHKA, H. 2005. Role of drug efflux transporters in the brain for drug disposition and treatment of brain diseases. *Progress in Neurobiology,* 76**,** 22-76.

MACDONALD, B. K., JOHNSON, A. L., GOODRIDGE, D. M., COCKERELL, O. C., SANDER, J. W. & SHORVON, S. D. 2000. Factors predicting prognosis of epilepsy after presentation with seizures. *Ann Neurol,* 48**,** 833-41.

MAGRI, C., SCHRIDDE, U., MURAYAMA, Y., PANZERI, S. & LOGOTHETIS, N. K. 2012. The amplitude and timing of the BOLD signal reflects the relationship between local field potential power at different frequencies. *J Neurosci,* 32**,** 1395-407.

MALTEZ, J., HYLLIENMARK, L., NIKULIN, V. V. & BRISMAR, T. 2004. Time course and variability of power in different frequency bands of EEG during resting conditions. *Neurophysiol Clin,* 34**,** 195-202.

MANGIN, J. F., JOUVENT, E. & CACHIA, A. 2010. In-vivo measurement of cortical morphology: Means and meanings. *Current Opinion in Neurology,* 23**,** 359-367.

MANUCA, R., CASDAGLI, M. C. & SAVIT, R. S. 1998. Nonstationarity in epileptic EEG and implications for neural dynamics. *Mathematical Biosciences,* 147**,** 1-22.

MARSON, A., BURNSIDE, G., APPLETON, R., SMITH, D., LEACH, J. P., SILLS, G., TUDUR-SMITH, C., PLUMPTON, C., HUGHES, D. A., WILLIAMSON, P., BAKER, G. A., BALABANOVA, S., TAYLOR, C., BROWN, R., HINDLEY, D., HOWELL, S., MAGUIRE, M., MOHANRAJ, R., SMITH, P. E., LANYON, K., MANFORD, M., CHITRE, M., PARKER, A., SWIDERSKA, N., PAULING, J., HUGHES, A., GUPTA, R., HANIF, S., AWADH, M., RAGUNATHAN, S., CABLE, N., COOPER, P., HINDLEY, D., RAKSHI, K., MOLLOY, S., REUBER, M., AYONRINDE, K., WILSON, M., SALADI, S., GIBB, J., FUNSTON, L.-A., CASSIDY, D., BOYD, J., RATNAYAKA, M., FAZA, H., SADLER, M., AL-MOASSEB, H., GALTREY, C., WREN, D., OLABI, A., FULLER, G., KHAN, M., KALLAPPA, C., CHINTHAPALLI, R., AJI, B., DAVIES, R., FOSTER, K., HITIRIS, N., HUSSAIN, N., DOWSON, S., ELLISON, J., SHARRACK, B., GANDHI, V., POWELL, R., TITTENSOR, P., SUMMERS, B., SHASHIKIRAN, S.,

DISON, P. J., SAMARASEKERA, S., MCCORRY, D., WHITE, K., NITHI, K., RICHARDSON, M., PAGE, R., DEEKOLLU, D., SLAGHT, S., WARRINER, S., AHMED, M., CHAUDHURI, A., CHOW, G., ARTAL, J., KUCINSKIENE, D., SREENIVASA, H., VELMURUGAN, SINGARA, ZIPITIS, C. S., MCLEAN, B., LAL, V., GREGORIOU, A., MADDISON, P., PICKERSGILL, T., ANDERSON, J., LAWTHOM, C., WHITLINGUM, G., RAKOWICZ, W., KINTON, L., MCLELLAN, A., ZUBERI, S., KELSO, A., HUGHES, I., et al. 2021. The SANAD II study of the effectiveness and cost-effectiveness of valproate versus levetiracetam for newly diagnosed generalised and unclassifiable epilepsy: an open-label, non-inferiority, multicentre, phase 4, randomised controlled trial. *The Lancet,* 397**,** 1375-1386.

MARSON, A., JACOBY, A., JOHNSON, A., KIM, L., GAMBLE, C. & CHADWICK, D. 2005. Immediate versus deferred antiepileptic drug treatment for early epilepsy and single seizures: a randomised controlled trial. *Lancet,* 365**,** 2007-13.

MARTÍNEZ-JUÁREZ, I. E., ALONSO, M. E., MEDINA, M. T., DURÓN, R. M., BAILEY, J. N., LÓPEZ-RUIZ, M., RAMOS-RAMÍREZ, R., LEÓN, L., PINEDA, G., CASTROVIEJO, I. P., SILVA, R., MIJA, L., PEREZ-GOSIENGFIAO, K., MACHADO-SALAS, J. & DELGADO-ESCUETA, A. V. 2006. Juvenile myoclonic epilepsy subsyndromes: family studies and long-term follow-up. *Brain,* 129**,** 1269-1280.

MARX, E., DEUTSCHLÄNDER, A., STEPHAN, T., DIETERICH, M., WIESMANN, M. & BRANDT, T. 2004. Eyes open and eyes closed as rest conditions: impact on brain activation patterns. *NeuroImage,* 21**,** 1818-1824.

MAZZIOTTA, J., TOGA, A., EVANS, A., FOX, P., LANCASTER, J., ZILLES, K., WOODS, R., PAUS, T., SIMPSON, G., PIKE, B., HOLMES, C., COLLINS, L., THOMPSON, P., MACDONALD, D., IACOBONI, M., SCHORMANN, T., AMUNTS, K., PALOMERO-GALLAGHER, N., GEYER, S., PARSONS, L., NARR, K., KABANI, N., LE GOUALHER, G., BOOMSMA, D., CANNON, T., KAWASHIMA, R. & MAZOYER, B. 2001. A probabilistic atlas and reference system for the human brain: International Consortium for Brain Mapping (ICBM). *Philosophical transactions of the Royal Society of London. Series B, Biological sciences,* 356**,** 1293-1322.

MECHELLI, A., FRISTON, K. J., FRACKOWIAK, R. S. & PRICE, C. J. 2005. Structural covariance in the human cortex. *J Neurosci,* 25**,** 8303-10.

MESULAM, M. M. 1990. Large-scale neurocognitive networks and distributed processing for attention, language, and memory. *Ann Neurol,* 28**,** 597-613.

MESZLÉNYI, R. J., HERMANN, P., BUZA, K., GÁL, V. & VIDNYÁNSZKY, Z. 2017. Resting State fMRI Functional Connectivity Analysis Using Dynamic Time Warping. *Front Neurosci,* 11**,** 75.

MIAO, A., WANG, Y., XIANG, J., LIU, Q., CHEN, Q., QIU, W., LIU, H., TANG, L., GAO, Y., WU, C., YU, Y., SUN, J., JIANG, W., SHI, Q., ZHANG, T., HU, Z. & WANG, X. 2019. Ictal Source Locations and Cortico-Thalamic Connectivity in Childhood Absence Epilepsy: Associations with Treatment Response. *Brain Topogr,* 32**,** 178-191.

MICHEL, C. M., LEHMANN, D., HENGGELER, B. & BRANDEIS, D. 1992. Localization of the sources of EEG delta, theta, alpha and beta frequency bands using the FFT dipole approximation. *Electroencephalography and Clinical Neurophysiology,* 82**,** 38-44.

MICHELOYANNIS, S., PACHOU, E., STAM, C. J., BREAKSPEAR, M., BITSIOS, P., VOURKAS, M., ERIMAKI, S. & ZERVAKIS, M. 2006. Small-world networks and disturbed functional connectivity in schizophrenia. *Schizophrenia Research,* 87**,** 60-66.

MILLER, D. S. 2010. Regulation of P-glycoprotein and other ABC drug transporters at the blood-brain barrier. *Trends Pharmacol Sci,* 31**,** 246-54.

MIRZAEI, A., AYATOLLAHI, A., GIFANI, P. & SALEHI, L. EEG analysis based on wavelet-spectral entropy for epileptic seizures detection. 2010 3rd International Conference on Biomedical Engineering and Informatics, 16-18 Oct. 2010 2010. 878-882.

MIYAUCHI, T., ENDO, K., YAMAGUCHI, T. & HAGIMOTO, H. 1991. Computerized Analysis of EEG Background Activity in Epileptic Patients. *Epilepsia,* 32**,** 870-881.

MOGNON, A., JOVICICH, J., BRUZZONE, L. & BUIATTI, M. 2011. ADJUST: An automatic EEG artifact detector based on the joint use of spatial and temporal features. *Psychophysiology,* 48**,** 229-40.

MOHANRAJ, R. & BRODIE, M. J. 2006. Diagnosing refractory epilepsy: response to sequential treatment schedules. *Eur J Neurol,* 13**,** 277-82.

MOHANRAJ, R. & BRODIE, M. J. 2007. Outcomes of newly diagnosed idiopathic generalized epilepsy syndromes in a non-pediatric setting. *Acta Neurologica Scandinavica,* 115**,** 204-208.

MOHANRAJ, R. & BRODIE, M. J. 2013. Early predictors of outcome in newly diagnosed epilepsy. *Seizure,* 22**,** 333-44.

MOHER, D., LIBERATI, A., TETZLAFF, J. & ALTMAN, D. G. 2009. Preferred reporting items for systematic reviews and meta-analyses: the PRISMA statement. *PLoS Med,* 6**,** e1000097.

MORI, S., CRAIN, B. J., CHACKO, V. P. & VAN ZIJL, P. C. 1999. Three-dimensional tracking of axonal projections in the brain by magnetic resonance imaging. *Ann Neurol,* 45**,** 265-9.

MURPHY, K., BIRN, R. M., HANDWERKER, D. A., JONES, T. B. & BANDETTINI, P. A. 2009. The impact of global signal regression on resting state correlations: Are anti-correlated networks introduced? *NeuroImage,* 44**,** 893-905.

NELIGAN, A., BELL, G. S., JOHNSON, A. L., GOODRIDGE, D. M., SHORVON, S. D. & SANDER, J. W. 2011a. The long-term risk of premature mortality in people with epilepsy. *Brain,* 134**,** 388-395.

NELIGAN, A., BELL, G. S., SANDER, J. W. & SHORVON, S. D. 2011b. How refractory is refractory epilepsy? Patterns of relapse and remission in people with refractory epilepsy. *Epilepsy Res,* 96**,** 225-30.

NEWMAN, M. E. J. 2003. The Structure and Function of Complex Networks. *Computer Physics Communications,* 147**,** 40-45.

NEWMAN, M. E. J. 2008. *Mathematics of Networks. The New Palgrave Encyclopedia of Economics.,* Basingstoke.

NGUGI, A. K., BOTTOMLEY, C., KLEINSCHMIDT, I., SANDER, J. W. & NEWTON, C. R. 2010. Estimation of the burden of active and life-time epilepsy: a meta-analytic approach. *Epilepsia,* 51**,** 883-90.

NICOLETTI, A., SOFIA, V., VITALE, G., BONELLI, S. I., BEJARANO, V., BARTALESI, F., TRAN, D. S., PREUX, P. M., ZAPPIA, M. & BARTOLONI, A. 2009. Natural history and mortality of chronic epilepsy in an untreated population of rural Bolivia: a follow-up after 10 years. *Epilepsia,* 50**,** 2199-206.

NICOLSON, A., APPLETON, R. E., CHADWICK, D. W. & SMITH, D. F. 2004. The relationship between treatment with valproate, lamotrigine, and topiramate and the prognosis of the idiopathic generalised epilepsies. *J Neurol Neurosurg Psychiatry,* 75**,** 75-9.

NISO, G., CARRASCO, S., GUDIN, M., MAESTU, F., DEL-POZO, F. & PEREDA, E. 2015. What graph theory actually tells us about resting state interictal MEG epileptic activity. *Neuroimage Clin,* 8**,** 503-15.

NOLTE, G., BAI, O., WHEATON, L., MARI, Z., VORBACH, S. & HALLETT, M. 2004. Identifying true brain interaction from EEG data using the imaginary part of coherency. *Clinical Neurophysiology,* 115**,** 2292-2307.

PALVA, J. M., PALVA, S. & KAILA, K. 2005. Phase synchrony among neuronal oscillations in the human cortex. *J Neurosci,* 25**,** 3962-72.

PANAYIOTOPOULOS, C. & KOUTROUMANIDI, M. 2017. *Epilepsy 2017. From bench to bedside,* Oxford, ILAE.

PARSONS, N., BOWDEN, S. C., VOGRIN, S. & D'SOUZA, W. J. 2020. Default mode network dysfunction in idiopathic generalised epilepsy. *Epilepsy research,* 159**,** 106254-106254.

PEGG, E. J., TAYLOR, J. R., KELLER, S. S. & MOHANRAJ, R. 2020a. Interictal structural and functional connectivity in idiopathic generalized epilepsy: A systematic review of graph theoretical studies. *Epilepsy Behav,* 106**,** 107013.

PEGG, E. J., TAYLOR, J. R., LAIOU, P., RICHARDSON, M. & MOHANRAJ, R. 2021. Interictal electroencephalographic functional network topology in drug-resistant and well-controlled idiopathic generalized epilepsy. *Epilepsia,* n/a.

PEGG, E. J., TAYLOR, J. R. & MOHANRAJ, R. 2020b. Spectral power of interictal EEG in the diagnosis and prognosis of idiopathic generalized epilepsies. *Epilepsy Behav,* 112**,** 107427.

PENFIELD, W. 1958. Centrencephalic integrating system. *Brain,* 81**,** 231-4.

PENNY, W., FRISTON, K., ASHBURNER, J., KIEBEL, S. & NICHOLS, T. 2006. *Statistical Parametric Mapping: The Analysis of Functional Brain Images.,* London, UK, Academic Press.

PETKOV, G., GOODFELLOW, M., RICHARDSON, M. P. & TERRY, J. R. 2014. A critical role for network structure in seizure onset: a computational modeling approach. *Front Neurol,* 5**,** 261.

PFAFFLIN, M., SCHMITZ, B. & MAY, T. W. 2016. Efficacy of the epilepsy nurse: Results of a randomized controlled study. *Epilepsia,* 57**,** 1190-8.

PIAZZINI, A., CANEVINI, M. P., MAGGIORI, G. & CANGER, R. 2001. Depression and Anxiety in Patients with Epilepsy. *Epilepsy & Behavior,* 2**,** 481-489.

PICTON, T. W., BENTIN, S., BERG, P., DONCHIN, E., HILLYARD, S. A., JOHNSON JR, R., MILLER, G. A., RITTER, W., RUCHKIN, D. S., RUGG, M. D. & TAYLOR, M. J. 2000. Guidelines for using human event-related potentials to study cognition: Recording standards and publication criteria. *Psychophysiology,* 37**,** 127-152.

PITKÄNEN, A., NISSINEN, J., NAIRISMÄGI, J., LUKASIUK, K., GRÖHN, O. H., MIETTINEN, R. & KAUPPINEN, R. 2002. Progression of neuronal damage after status epilepticus and during spontaneous seizures in a rat model of temporal lobe epilepsy. *Prog Brain Res,* 135**,** 67-83.

PITKÄNEN, A. & SUTULA, T. P. 2002. Is epilepsy a progressive disorder? Prospects for new therapeutic approaches in temporal-lobe epilepsy. *The Lancet Neurology,* 1**,** 173-181.

PLACENCIA, M., SANDER, J. W., ROMAN, M., MADERA, A., CRESPO, F., CASCANTE, S. & SHORVON, S. D. 1994. The characteristics of epilepsy in a largely untreated population in rural Ecuador. *J Neurol Neurosurg Psychiatry,* 57**,** 320-5.

PONTEN, S. C., BARTOLOMEI, F. & STAM, C. J. 2007. Small-world networks and epilepsy: graph theoretical analysis of intracerebrally recorded mesial temporal lobe seizures. *Clin Neurophysiol,* 118**,** 918-27.

PONTEN, S. C., DOUW, L., BARTOLOMEI, F., REIJNEVELD, J. C. & STAM, C. J. 2009. Indications for network regularization during absence seizures: weighted and unweighted graph theoretical analyses. *Exp Neurol,* 217**,** 197-204.

POWELL, G. E. & PERCIVAL, I. C. 1979. A spectral entropy method for distinguishing regular and irregular motion of Hamiltonian systems. *Journal of Physics A: Mathematical and General,* 12**,** 2053-2071.

POWER, JONATHAN D., COHEN, ALEXANDER L., NELSON, STEVEN M., WIG, GAGAN S., BARNES, KELLY A., CHURCH, JESSICA A., VOGEL, ALECIA C., LAUMANN, TIMOTHY O., MIEZIN, FRAN M., SCHLAGGAR, BRADLEY L. & PETERSEN, STEVEN E. 2011. Functional Network Organization of the Human Brain. *Neuron,* 72**,** 665-678.

PYRZOWSKI, J., SIEMIŃSKI, M., SARNOWSKA, A., JEDRZEJCZAK, J. & NYKA, W. M. 2015. Interval analysis of interictal EEG: pathology of the alpha rhythm in focal epilepsy. *Scientific Reports,* 5**,** 16230.

QIN, Y., XIN, X., ZHU, H., LI, F., XIONG, H., ZHANG, T. & LAI, Y. 2017. A Comparative Study on the Dynamic EEG Center of Mass with Different References. *Frontiers in Neuroscience,* 11**,** 509.

QIU, W., YU, C., GAO, Y., MIAO, A., TANG, L., HUANG, S., JIANG, W., SUN, J., XIANG, J. & WANG, X. 2017. Disrupted topological organization of structural brain networks in childhood absence epilepsy. *Sci Rep,* 7**,** 11973.

RAJAPAKSE, J. C., GIEDD, J. N. & RAPOPORT, J. L. 1997. Statistical approach to segmentation of single-channel cerebral MR images. *IEEE Transactions on Medical Imaging,* 16**,** 176-186.

RAMON Y CAJAL, S. 1894. The Croonian lecture.—La fine structure des centres nerveux. *Proceedings of the Royal Society of London,* 55.

REMY, S., URBAN, B. W., ELGER, C. E. & BECK, H. 2003. Anticonvulsant pharmacology of voltage-gated Na+ channels in hippocampal neurons of control and chronically epileptic rats. *Eur J Neurosci,* 17**,** 2648-58.

REUBER, M. & BROWN, R. J. 2017. Understanding psychogenic nonepileptic seizures—Phenomenology, semiology and the Integrative Cognitive Model. *Seizure - European Journal of Epilepsy,* 44**,** 199-205.

REUBER, M. & ELGER, C. E. 2003. Psychogenic nonepileptic seizures: review and update. *Epilepsy Behav,* 4**,** 205-16.

RICHARDSON, M. P. 2012a. Large scale brain models of epilepsy: dynamics meets connectomics. *Journal of Neurology, Neurosurgery & Psychiatry,* 83**,** 1238.

RICHARDSON, M. P. 2012b. Large scale brain models of epilepsy: dynamics meets connectomics. *Journal of Neurology, Neurosurgery & Psychiatry,* 83**,** 1238.

RIDSDALE, L., WOJEWODKA, G., ROBINSON, E., LANDAU, S., NOBLE, A., TAYLOR, S., RICHARDSON, M., BAKER, G. & GOLDSTEIN, L. H. 2017. Characteristics associated with quality of life among people with drug-resistant epilepsy. *J Neurol,* 264**,** 1174-1184.

ROGAWSKI, M. A. & JOHNSON, M. R. 2008. Intrinsic severity as a determinant of antiepileptic drug refractoriness. *Epilepsy Curr,* 8**,** 127-30.

ROUTLEY, B., SHAW, A., MUTHUKUMARASWAMY, S. D., SINGH, K. D. & HAMANDI, K. 2020. Juvenile myoclonic epilepsy shows increased posterior theta, and reduced sensorimotor beta resting connectivity. *Epilepsy Research,* 163**,** 106324.

ROUTLEY, B. C., SINGH, K. D., HAMANDI, K. & MUTHUKUMARASWAMY, S. D. 2017. The effects of AMPA receptor blockade on resting magnetoencephalography recordings. *Journal of Psychopharmacology,* 31**,** 1527-1536.

RUBINOV, M. & BULLMORE, E. 2013. Schizophrenia and abnormal brain network hubs. *Dialogues in clinical neuroscience,* 15**,** 339-349.

RUBINOV, M. & SPORNS, O. 2010. Complex network measures of brain connectivity: uses and interpretations. *Neuroimage,* 52**,** 1059-69.

SAAD, Z. S., GOTTS, S. J., MURPHY, K., CHEN, G., JO, H. J., MARTIN, A. & COX, R. W. 2012. Trouble at Rest: How Correlation Patterns and Group Differences Become Distorted After Global Signal Regression. *Brain Connectivity,* 2**,** 25-32.

SALA-LLONCH, R., BARTRÉS-FAZ, D. & JUNQUÉ, C. 2015. Reorganization of brain networks in aging: a review of functional connectivity studies. *Frontiers in Psychology,* 6**,** 663.

SALA-LLONCH, R., SMITH, S. M., WOOLRICH, M. & DUFF, E. P. 2019. Spatial parcellations, spectral filtering, and connectivity measures in fMRI: Optimizing for discrimination. *Human brain mapping,* 40**,** 407-419.

SANDER, J. W. 2003. The epidemiology of epilepsy revisited. *Current Opinion in Neurology,* 16.

SANNITA, W. G., GERVASIO, L. & ZAGNONI, P. 1989. Quantitative EEG effects and plasma concentration of sodium valproate: acute and long-term administration to epileptic patients. *Neuropsychobiology,* 22**,** 231-5.

SANTIAGO-RODRÍGUEZ, E., HARMONY, T., CÁRDENAS-MORALES, L., HERNÁNDEZ, A. & FERNÁNDEZ-BOUZAS, A. 2008. Analysis of background EEG activity in patients with juvenile myoclonic epilepsy. *Seizure - European Journal of Epilepsy,* 17**,** 437-445.

SARVAS, J. 1987. Basic mathematical and electromagnetic concepts of the biomagnetic inverse problem. *Phys Med Biol,* 32**,** 11-22.

SAXENA, N., MUTHUKUMARASWAMY, S. D., DIUKOVA, A., SINGH, K., HALL, J. & WISE, R. 2013. Enhanced Stimulus-Induced Gamma Activity in Humans during Propofol-Induced Sedation. *PLOS ONE,* 8**,** e57685.

SCHAEFER, A., KONG, R., GORDON, E. M., LAUMANN, T. O., ZUO, X. N., HOLMES, A. J., EICKHOFF, S. B. & YEO, B. T. T. 2018. Local-Global Parcellation of the Human Cerebral Cortex from Intrinsic Functional Connectivity MRI. *Cereb Cortex,* 28**,** 3095-3114.

SCHEEPERS, B., CLOUGH, P. & PICKLES, C. 1998. The misdiagnosis of epilepsy: findings of a population study. *Seizure,* 7**,** 403-6.

SCHEFFER, I. E., BERKOVIC, S., CAPOVILLA, G., CONNOLLY, M. B., FRENCH, J., GUILHOTO, L., HIRSCH, E., JAIN, S., MATHERN, G. W., MOSHE, S. L., NORDLI, D. R., PERUCCA, E., TOMSON, T., WIEBE, S., ZHANG, Y. H. & ZUBERI, S. M. 2017. ILAE classification of the epilepsies: Position paper of the ILAE Commission for Classification and Terminology. *Epilepsia,* 58**,** 512-521.

SCHINDLER, K., LEUNG, H., ELGER, C. E. & LEHNERTZ, K. 2007. Assessing seizure dynamics by analysing the correlation structure of multichannel intracranial EEG. *Brain,* 130**,** 65-77.

SCHINKEL, A. H. 1997. The physiological function of drug-transporting P-glycoproteins. *Semin Cancer Biol,* 8**,** 161-70.

SCHMIDT, D. & HAENEL, F. 1984. Therapeutic plasma levels of phenytoin, phenobarbital, and carbamazepine: individual variation in relation to seizure frequency and type. *Neurology,* 34**,** 1252-5.

SCHMIDT, H., PETKOV, G., RICHARDSON, M. P. & TERRY, J. R. 2014. Dynamics on networks: the role of local dynamics and global networks on the emergence of hypersynchronous neural activity. *PLoS Comput Biol,* 10**,** e1003947.

SCHMIDT, H., WOLDMAN, W., GOODFELLOW, M., CHOWDHURY, F. A., KOUTROUMANIDIS, M., JEWELL, S., RICHARDSON, M. P. & TERRY, J. R. 2016. A computational biomarker of idiopathic generalized epilepsy from resting state EEG. *Epilepsia,* 57**,** e200-e204.

SCHNITZLER, A. & GROSS, J. 2005. Normal and pathological oscillatory communication in the brain. *Nature Reviews Neuroscience,* 6**,** 285-296.

SCHOFFELEN, J.-M. & GROSS, J. 2009. Source connectivity analysis with MEG and EEG. *Human Brain Mapping,* 30**,** 1857-1865.

SCHOMER, D. & LOPES DA SILVA, F. 2017. *Niedermeyer's Electroencephalography: Basic Principles, Clinical Applications and Related Fields (7 ed.)*, Oxford University Press.

SCHREIBER, T. & SCHMITZ, A. 1996. Improved Surrogate Data for Nonlinearity Tests. *Physical Review Letters,* 77**,** 635-638.

SCHREIBER, T. & SCHMITZ, A. 2000. Surrogate time series. *Physica D: Nonlinear Phenomena,* 142**,** 346-382.

SCHÖLVINCK, M. L., MAIER, A., YE, F. Q., DUYN, J. H. & LEOPOLD, D. A. 2010. Neural basis of global resting-state fMRI activity. *Proceedings of the National Academy of Sciences,* 107**,** 10238.

SEMAH, F., PICOT, M. C., ADAM, C., BROGLIN, D., ARZIMANOGLOU, A., BAZIN, B., CAVALCANTI, D. & BAULAC, M. 1998. Is the underlying cause of epilepsy a major prognostic factor for recurrence? *Neurology,* 51**,** 1256-62.

SENEVIRATNE, U., BOSTON, R. C., COOK, M. & SOUZA, W. 2017. EEG correlates of seizure freedom in genetic generalized epilepsies. *Neurology: Clinical Practice,* 7**,** 35.

SENEVIRATNE, U., COOK, M. & D'SOUZA, W. 2012. The prognosis of idiopathic generalized epilepsy. *Epilepsia,* 53**,** 2079-2090.

SHACKMAN, A. J., MCMENAMIN, B. W., MAXWELL, J. S., GREISCHAR, L. L. & DAVIDSON, R. J. 2010. Identifying robust and sensitive frequency bands for interrogating neural oscillations. *Neuroimage,* 51**,** 1319-33.

SHAW, A. D., SAXENA, N., E. JACKSON, L., HALL, J. E., SINGH, K. D. & MUTHUKUMARASWAMY, S. D. 2015. Ketamine amplifies induced gamma frequency oscillations in the human cerebral cortex. *European Neuropsychopharmacology,* 25**,** 1136-1146.

SHEFI, O., GOLDING, I., SEGEV, R., BEN-JACOB, E. & AYALI, A. 2002. Morphological characterization of in vitro neuronal networks. *Phys Rev E Stat Nonlin Soft Matter Phys,* 66**,** 021905.

SHEN, X., TOKOGLU, F., PAPADEMETRIS, X. & CONSTABLE, R. T. 2013. Groupwise whole-brain parcellation from resting-state fMRI data for network node identification. *NeuroImage,* 82**,** 403-415.

SHIN, J. W., CHU, K., SHIN, S. A., JUNG, K. H., LEE, S. T., LEE, Y. S., MOON, J., LEE, D. Y., LEE, J. S., LEE, D. S. & LEE, S. K. 2016. Clinical Applications of Simultaneous PET/MR Imaging Using (R)-[11C]-

Verapamil with Cyclosporin A: Preliminary Results on a Surrogate Marker of Drug-Resistant Epilepsy. *AJNR Am J Neuroradiol,* 37**,** 600-6.

SHINNAR, S. & BERG, A. T. 1996. Does antiepileptic drug therapy prevent the development of "chronic" epilepsy? *Epilepsia,* 37**,** 701-8.

SHORVON, S. & LUCIANO, A. L. 2007. Prognosis of chronic and newly diagnosed epilepsy: revisiting temporal aspects. *Curr Opin Neurol,* 20**,** 208-12.

SIEGEL, M., DONNER, T. H. & ENGEL, A. K. 2012. Spectral fingerprints of large-scale neuronal interactions. *Nat Rev Neurosci,* 13**,** 121-34.

SILLANPAA, M. 1993. Remission of seizures and predictors of intractability in long-term follow-up. *Epilepsia,* 34**,** 930-6.

SILLS, G. 2017. Mechanisms of action of antiepileptic drugs. *Epilepsy 2017: From bench to bedside.* Oxford.

SINGH, K. D. 2012. Which "neural activity" do you mean? fMRI, MEG, oscillations and neurotransmitters. *Neuroimage,* 62**,** 1121-30.

SISODIYA, S. M. & MARINI, C. 2009. Genetics of antiepileptic drug resistance. *Curr Opin Neurol,* 22**,** 150-6.

SISODIYA, S. M., WHELAN, C. D., HATTON, S. N., HUYNH, K., ALTMANN, A., RYTEN, M., VEZZANI, A., CALIGIURI, M. E., LABATE, A., GAMBARDELLA, A., IVES-DELIPERI, V., MELETTI, S., MUNSELL, B. C., BONILHA, L., TONDELLI, M., REBSAMEN, M., RUMMEL, C., VAUDANO, A. E., WIEST, R., BALACHANDRA, A. R., BARGALLÓ, N., BARTOLINI, E., BERNASCONI, A., BERNASCONI, N., BERNHARDT, B., CALDAIROU, B., CARR, S. J. A., CAVALLERI, G. L., CENDES, F., CONCHA, L., DESMOND, P. M., DOMIN, M., DUNCAN, J. S., FOCKE, N. K., GUERRINI, R., HAMANDI, K., JACKSON, G. D., JAHANSHAD, N., KÄLVIÄINEN, R., KELLER, S. S., KOCHUNOV, P., KOWALCZYK, M. A., KREILKAMP, B. A. K., KWAN, P., LARIVIERE, S., LENGE, M., LOPEZ, S. M., MARTIN, P., MASCALCHI, M., MOREIRA, J. C. V., MORITA-SHERMAN, M. E., PARDOE, H. R., PARIENTE, J. C., RAVITEJA, K., ROCHA, C. S., RODRÍGUEZ-CRUCES, R., SEECK, M., SEMMELROCH, M. K. H. G., SINCLAIR, B., SOLTANIAN-ZADEH, H., STEIN, D. J., STRIANO, P., TAYLOR, P. N., THOMAS, R. H., THOMOPOULOS, S. I., VELAKOULIS, D., VIVASH, L., WEBER, B., YASUDA, C. L., ZHANG, J., THOMPSON, P. M., MCDONALD, C. R. & GROUP, E. C. E. W. 2020. The ENIGMA-Epilepsy working group: Mapping disease from large data sets. *Human Brain Mapping,* n/a.

SMITH, D., DEFALLA, B. A. & CHADWICK, D. W. 1999. The misdiagnosis of epilepsy and the management of refractory epilepsy in a specialist clinic. *QJM: An International Journal of Medicine,* 92**,** 15-23.

SMITH, S. J. M. 2005. EEG in the diagnosis, classification, and management of patients with epilepsy. *Journal of Neurology, Neurosurgery & Psychiatry,* 76**,** ii2.

SMITH, S. M. 2012. The future of FMRI connectivity. *Neuroimage,* 62**,** 1257-66.

SMITH, S. M., BECKMANN, C. F., ANDERSSON, J., AUERBACH, E. J., BIJSTERBOSCH, J., DOUAUD, G., DUFF, E., FEINBERG, D. A., GRIFFANTI, L., HARMS, M. P., KELLY, M., LAUMANN, T., MILLER, K. L., MOELLER, S., PETERSEN, S., POWER, J., SALIMI-KHORSHIDI, G., SNYDER, A. Z., VU, A. T., WOOLRICH, M. W., XU, J., YACOUB, E., UĞURBIL, K., VAN ESSEN, D. C., GLASSER, M. F. & CONSORTIUM, W. U.-M. H. 2013. Resting-state fMRI in the Human Connectome Project. *NeuroImage,* 80**,** 144-168.

SPENCER, S. S. 2002. Neural networks in human epilepsy: evidence of and implications for treatment. *Epilepsia,* 43**,** 219-27.

SPERK, G., DREXEL, M. & PIRKER, S. 2009. Neuronal plasticity in animal models and the epileptic human hippocampus. *Epilepsia,* 50 Suppl 12**,** 29-31.

SPORNS, O. 2018. Graph theory methods: applications in brain networks. *Dialogues in clinical neuroscience,* 20**,** 111-121.

SPORNS, O., TONONI, G. & KÖTTER, R. 2005. The Human Connectome: A Structural Description of the Human Brain. *PLOS Computational Biology,* 1**,** e42.

SPORNS, O. & ZWI, J. D. 2004. The small world of the cerebral cortex. *Neuroinformatics,* 2**,** 145-62.

STAM, C. J. 2014. Modern network science of neurological disorders. *Nat Rev Neurosci,* 15**,** 683-95.
STAM, C. J., DE HAAN, W., DAFFERTSHOFER, A., JONES, B. F., MANSHANDEN, I., VAN CAPPELLEN VAN WALSUM, A. M., MONTEZ, T., VERBUNT, J. P. A., DE MUNCK, J. C., VAN DIJK, B. W., BERENDSE, H. W. & SCHELTENS, P. 2008. Graph theoretical analysis of magnetoencephalographic functional connectivity in Alzheimer's disease. *Brain,* 132**,** 213-224.
STAM, C. J., JONES, B. F., NOLTE, G., BREAKSPEAR, M. & SCHELTENS, P. 2006. Small-World Networks and Functional Connectivity in Alzheimer's Disease. *Cerebral Cortex,* 17**,** 92-99.
STAM, C. J., JONES, B. F., NOLTE, G., BREAKSPEAR, M. & SCHELTENS, P. 2007a. Small-world networks and functional connectivity in Alzheimer's disease. *Cereb Cortex,* 17**,** 92-9.
STAM, C. J., NOLTE, G. & DAFFERTSHOFER, A. 2007b. Phase lag index: assessment of functional connectivity from multi channel EEG and MEG with diminished bias from common sources. *Hum Brain Mapp,* 28**,** 1178-93.
STAM, C. J. & REIJNEVELD, J. C. 2007. Graph theoretical analysis of complex networks in the brain. *Nonlinear Biomed Phys,* 1**,** 3.
STANLEY, M. L., MOUSSA, M. N., PAOLINI, B. M., LYDAY, R. G., BURDETTE, J. H. & LAURIENTI, P. J. 2013. Defining nodes in complex brain networks. *Front Comput Neurosci,* 7**,** 169.
STARK, D. E., MARGULIES, D. S., SHEHZAD, Z. E., REISS, P., KELLY, A. M. C., UDDIN, L. Q., GEE, D. G., ROY, A. K., BANICH, M. T., CASTELLANOS, F. X. & MILHAM, M. P. 2008. Regional Variation in Interhemispheric Coordination of Intrinsic Hemodynamic Fluctuations. *The Journal of Neuroscience,* 28**,** 13754.
STEPHAN, K. E., HILGETAG, C. C., BURNS, G. A., O'NEILL, M. A., YOUNG, M. P. & KOTTER, R. 2000. Computational analysis of functional connectivity between areas of primate cerebral cortex. *Philos Trans R Soc Lond B Biol Sci,* 355**,** 111-26.
STOLLER, A. 1949. Slowing of the alpha-rhythm of the electroencephalogram and its association with mental deterioration and epilepsy. *J Ment Sci,* 95**,** 972-84.
STRAATHOF, M., SINKE, M. R., DIJKHUIZEN, R. M. & OTTE, W. M. 2019. A systematic review on the quantitative relationship between structural and functional network connectivity strength in mammalian brains. *Journal of cerebral blood flow and metabolism : official journal of the International Society of Cerebral Blood Flow and Metabolism,* 39**,** 189-209.
SUFFCZYNSKI, P., KALITZIN, S. & LOPES DA SILVA, F. H. 2004. Dynamics of non-convulsive epileptic phenomena modeled by a bistable neuronal network. *Neuroscience,* 126**,** 467-84.
SUN, Y., ZHANG, G., ZHANG, X., YAN, X., LI, L., XU, C., YU, T., LIU, C., ZHU, Y., LIN, Y. & WANG, Y. 2016. Time-frequency analysis of intracranial EEG in patients with myoclonic seizures. *Brain Res,* 1652**,** 119-126.
SUPEKAR, K., MENON, V., RUBIN, D., MUSEN, M. & GREICIUS, M. D. 2008. Network analysis of intrinsic functional brain connectivity in Alzheimer's disease. *PLoS computational biology,* 4**,** e1000100-e1000100.
SWARTZ, B. E., HALGREN, E., SIMPKINS, F. & SYNDULKO, K. 1994. Primary memory in patients with frontal and primary generalized epilepsy. *Journal of Epilepsy,* 7**,** 232-241.
SZAFLARSKI, J. P., LINDSELL, C. J., ZAKARIA, T., BANKS, C. & PRIVITERA, M. D. 2010. Seizure control in patients with idiopathic generalized epilepsies: EEG determinants of medication response. *Epilepsy & Behavior,* 17**,** 525-530.
TAN, B., KONG, X., YANG, P., JIN, Z. & LI, L. 2013. The Difference of Brain Functional Connectivity between Eyes-Closed and Eyes-Open Using Graph Theoretical Analysis. *Comput Math Methods Med,* 2013.
TANG, F., HARTZ, A. M. S. & BAUER, B. 2017. Drug-Resistant Epilepsy: Multiple Hypotheses, Few Answers. *Front Neurol,* 8.
TAVAKOL, S., ROYER, J., LOWE, A. J., BONILHA, L., TRACY, J. I., JACKSON, G. D., DUNCAN, J. S., BERNASCONI, A., BERNASCONI, N. & BERNHARDT, B. C. 2019. Neuroimaging and

connectomics of drug-resistant epilepsy at multiple scales: From focal lesions to macroscale networks. *Epilepsia,* 60**,** 593-604.

TENNEY, J. R., KADIS, D. S., AGLER, W., ROZHKOV, L., ALTAYE, M., XIANG, J., VANNEST, J. & GLAUSER, T. A. 2018. Ictal connectivity in childhood absence epilepsy: Associations with outcome. *Epilepsia,* 59**,** 971-981.

THIRION, B., VAROQUAUX, G., DOHMATOB, E. & POLINE, J.-B. 2014. Which fMRI clustering gives good brain parcellations? *Frontiers in Neuroscience,* 8**,** 167.

THOMAS, R. H., STEER, S., GILPIN, T. R., GLASBEY, J. C. D., KING, W. H. & SMITH, P. E. M. 2012. 056 Variability in adult epilepsy prevalence in the UK. *Journal of Neurology, Neurosurgery & Psychiatry,* 83**,** e1-e1.

TIAN, L., WANG, J., YAN, C. & HE, Y. 2011. Hemisphere- and gender-related differences in small-world brain networks: A resting-state functional MRI study. *NeuroImage,* 54**,** 191-202.

TIKKA, S. K., GOYAL, N., UMESH, S. & NIZAMIE, S. H. 2013. Juvenile myoclonic epilepsy: Clinical characteristics, standard and quantitative electroencephalography analyses. *J Pediatr Neurosci.* India.

TISHLER, D. M., WEINBERG, K. I., HINTON, D. R., BARBARO, N., ANNETT, G. M. & RAFFEL, C. 1995. MDR1 gene expression in brain of patients with medically intractable epilepsy. *Epilepsia,* 36**,** 1-6.

TOMSON, T. 2000. Mortality in epilepsy. *J Neurol,* 247**,** 15-21.

TOMSON, T., MARSON, A., BOON, P., CANEVINI, M. P., COVANIS, A., GAILY, E., KÄLVIÄINEN, R. & TRINKA, E. 2015. Valproate in the treatment of epilepsy in girls and women of childbearing potential. *Epilepsia,* 56**,** 1006-19.

TRACY, J. I. 2015. Editorial on "Network Analysis for a Network Disorder: The emerging role of graph theory in the study of epilepsy, by Bernhardt et al. (this issue)". *Epilepsy Behav,* 50**,** 160-1.

TRINKA, E., BAUMGARTNER, S., UNTERBERGER, I., UNTERRAINER, J., LUEF, G., HABERLANDT, E. & BAUER, G. 2004. Long-term prognosis for childhood and juvenile absence epilepsy. *Journal of Neurology,* 251**,** 1235-1241.

TZOURIO-MAZOYER, N., LANDEAU, B., PAPATHANASSIOU, D., CRIVELLO, F., ETARD, O., DELCROIX, N., MAZOYER, B. & JOLIOT, M. 2002. Automated anatomical labeling of activations in SPM using a macroscopic anatomical parcellation of the MNI MRI single-subject brain. *Neuroimage,* 15**,** 273-89.

UHLHAAS, P. J., PIPA, G., LIMA, B., MELLONI, L., NEUENSCHWANDER, S., NIKOLIĆ, D. & SINGER, W. 2009. Neural synchrony in cortical networks: history, concept and current status. *Front Integr Neurosci,* 3**,** 17.

URCHS, S., ARMOZA, J., BENHAJALI, Y., ST-AUBIN, J., ORBAN, P. & BELLEC, P. 2017. MIST: A multi-resolution parcellation of functional brain networks. *MNI Open Research,* 1**,** 3.

URIGÜEN, J. A. 2017. Comparison of background EEG activity of different groups of patients with idiopathic epilepsy using Shannon spectral entropy and cluster-based permutation statistical testing.

VAESSEN, M. J., JANSEN, J. F. A., BRAAKMAN, H. M. H., HOFMAN, P. A. M., DE LOUW, A., ALDENKAMP, A. P. & BACKES, W. H. 2014. Functional and structural network impairment in childhood frontal lobe epilepsy. *PloS one,* 9**,** e90068-e90068.

VAN DELLEN, E., DOUW, L., HILLEBRAND, A., RIS-HILGERSOM, I. H., SCHOONHEIM, M. M., BAAYEN, J. C., DE WITT HAMER, P. C., VELIS, D. N., KLEIN, M., HEIMANS, J. J., STAM, C. J. & REIJNEVELD, J. C. 2012. MEG network differences between low- and high-grade glioma related to epilepsy and cognition. *PLoS One,* 7**,** e50122.

VAN DEN BROEK, S. P., REINDERS, F., DONDERWINKEL, M. & PETERS, M. J. 1998. Volume conduction effects in EEG and MEG. *Electroencephalogr Clin Neurophysiol,* 106**,** 522-34.

VAN DEN HEUVEL, M. P. & POL, H. E. H. 2010. Specific somatotopic organization of functional connections of the primary motor network during resting state. *Human Brain Mapping,* 31**,** 631-644.

VAN DER KRUIJS, S. J., JAGANNATHAN, S. R., BODDE, N. M., BESSELING, R. M., LAZERON, R. H., VONCK, K. E., BOON, P. A., CLUITMANS, P. J., HOFMAN, P. A., BACKES, W. H., ALDENKAMP, A. P. & JANSEN, J. F. 2014. Resting-state networks and dissociation in psychogenic non-epileptic seizures. *J Psychiatr Res,* 54**,** 126-33.

VAN DIESSEN, E., NUMAN, T., VAN DELLEN, E., VAN DER KOOI, A. W., BOERSMA, M., HOFMAN, D., VAN LUTTERVELD, R., VAN DIJK, B. W., VAN STRAATEN, E. C. W., HILLEBRAND, A. & STAM, C. J. 2014a. Opportunities and methodological challenges in EEG and MEG resting state functional brain network research. *Clinical Neurophysiology,* 126**,** 1468-1481.

VAN DIESSEN, E., OTTE, W. M., STAM, C. J., BRAUN, K. P. & JANSEN, F. E. 2016. Electroencephalography based functional networks in newly diagnosed childhood epilepsies. *Clin Neurophysiol,* 127**,** 2325-32.

VAN DIESSEN, E., ZWEIPHENNING, W., JANSEN, F. E., STAM, C. J., BRAUN, K. P. J. & OTTE, W. M. 2014b. Brain Network Organization in Focal Epilepsy: A Systematic Review and Meta-Analysis. *In:* DOESBURG, S. (ed.) *PLoS One.* San Francisco, USA.

VAN DIESSEN, E., ZWEIPHENNING, W. J., JANSEN, F. E., STAM, C. J., BRAUN, K. P. & OTTE, W. M. 2014c. Brain Network Organization in Focal Epilepsy: A Systematic Review and Meta-Analysis. *PLoS One,* 9**,** e114606.

VAN DONSELAAR, C. A., SCHIMSHEIMER, R., GEERTS, A. T. & DECLERCK, A. C. 1992. Value of the electroencephalogram in adult patients with untreated idiopathic first seizures. *Archives of Neurology,* 49**,** 231-237.

VAN ESSEN, D. C., UGURBIL, K., AUERBACH, E., BARCH, D., BEHRENS, T. E., BUCHOLZ, R., CHANG, A., CHEN, L., CORBETTA, M., CURTISS, S. W., DELLA PENNA, S., FEINBERG, D., GLASSER, M. F., HAREL, N., HEATH, A. C., LARSON-PRIOR, L., MARCUS, D., MICHALAREAS, G., MOELLER, S., OOSTENVELD, R., PETERSEN, S. E., PRIOR, F., SCHLAGGAR, B. L., SMITH, S. M., SNYDER, A. Z., XU, J. & YACOUB, E. 2012. The Human Connectome Project: a data acquisition perspective. *Neuroimage,* 62**,** 2222-31.

VAN VEENENDAAL, T. M., DM, I. J., ALDENKAMP, A. P., LAZERON, R. H. C., HOFMAN, P. A. M., DE LOUW, A. J. A., BACKES, W. H. & JANSEN, J. F. A. 2017. Chronic antiepileptic drug use and functional network efficiency: A functional magnetic resonance imaging study. *World J Radiol,* 9**,** 287-294.

VAN WIJK, B. C., STAM, C. J. & DAFFERTSHOFER, A. 2010. Comparing brain networks of different size and connectivity density using graph theory. *PLoS One,* 5**,** e13701.

VARANGIS, E., HABECK, C. G., RAZLIGHI, Q. R. & STERN, Y. 2019. The Effect of Aging on Resting State Connectivity of Predefined Networks in the Brain. *Frontiers in Aging Neuroscience,* 11**,** 234.

VON STEIN, A. & SARNTHEIN, J. 2000. Different frequencies for different scales of cortical integration: from local gamma to long range alpha/theta synchronization. *International Journal of Psychophysiology,* 38**,** 301-313.

VYTVAROVA, E., MARECEK, R., FOUSEK, J., STRYCEK, O. & REKTOR, I. 2017. Large-scale cortico-subcortical functional networks in focal epilepsies: The role of the basal ganglia. *Neuroimage Clin,* 14**,** 28-36.

WANDSCHNEIDER, B., KOPP, U. A., KLIEGEL, M., STEPHANI, U., KURLEMANN, G., JANZ, D. & SCHMITZ, B. 2010. Prospective memory in patients with juvenile myoclonic epilepsy and their healthy siblings. *Neurology,* 75**,** 2161-7.

WANDSCHNEIDER, B., THOMPSON, P. J., VOLLMAR, C. & KOEPP, M. J. 2012. Frontal lobe function and structure in juvenile myoclonic epilepsy: a comprehensive review of neuropsychological and imaging data. *Epilepsia,* 53**,** 2091-8.

WANG, G. & TAKIGAWA, M. 1992. Directed coherence as a measure of interhemispheric correlation of EEG. *International Journal of Psychophysiology,* 13**,** 119-128.

WANG, J., WANG, L., ZANG, Y., YANG, H., TANG, H., GONG, Q., CHEN, Z., ZHU, C. & HE, Y. 2009. Parcellation-dependent small-world brain functional networks: A resting-state fMRI study. *Human Brain Mapping,* 30**,** 1511-1523.

WANG, X., JIAO, D., ZHANG, X. & LIN, X. 2017. Altered degree centrality in childhood absence epilepsy: A resting-state fMRI study. *J Neurol Sci,* 373**,** 274-279.

WANG, Z., ZHANG, Z., JIAO, Q., LIAO, W., CHEN, G., SUN, K., SHEN, L., WANG, M., LI, K., LIU, Y. & LU, G. 2012. Impairments of thalamic nuclei in idiopathic generalized epilepsy revealed by a study combining morphological and functional connectivity MRI. *PLoS One,* 7**,** e39701.

WATTS, D. J. & STROGATZ, S. H. 1998. Collective dynamics of 'small-world' networks. *Nature,* 393**,** 440-2.

WENG, Y., LIU, X., HU, H., HUANG, H., ZHENG, S., CHEN, Q., SONG, J., CAO, B., WANG, J., WANG, S. & HUANG, R. 2020. Open eyes and closed eyes elicit different temporal properties of brain functional networks. *NeuroImage,* 222**,** 117230.

WHELAN, C. D., ALTMANN, A., BOTÍA, J. A., JAHANSHAD, N., HIBAR, D. P., ABSIL, J., ALHUSAINI, S., ALVIM, M. K. M., AUVINEN, P., BARTOLINI, E., BERGO, F. P. G., BERNARDES, T., BLACKMON, K., BRAGA, B., CALIGIURI, M. E., CALVO, A., CARR, S. J., CHEN, J., CHEN, S., CHERUBINI, A., DAVID, P., DOMIN, M., FOLEY, S., FRANÇA, W., HAAKER, G., ISAEV, D., KELLER, S. S., KOTIKALAPUDI, R., KOWALCZYK, M. A., KUZNIECKY, R., LANGNER, S., LENGE, M., LEYDEN, K. M., LIU, M., LOI, R. Q., MARTIN, P., MASCALCHI, M., MORITA, M. E., PARIENTE, J. C., RODRÍGUEZ-CRUCES, R., RUMMEL, C., SAAVALAINEN, T., SEMMELROCH, M. K., SEVERINO, M., THOMAS, R. H., TONDELLI, M., TORTORA, D., VAUDANO, A. E., VIVASH, L., VON PODEWILS, F., WAGNER, J., WEBER, B., YAO, Y., YASUDA, C. L., ZHANG, G., BARGALLÓ, N., BENDER, B., BERNASCONI, N., BERNASCONI, A., BERNHARDT, B. C., BLÜMCKE, I., CARLSON, C., CAVALLERI, G. L., CENDES, F., CONCHA, L., DELANTY, N., DEPONDT, C., DEVINSKY, O., DOHERTY, C. P., FOCKE, N. K., GAMBARDELLA, A., GUERRINI, R., HAMANDI, K., JACKSON, G. D., KÄLVIÄINEN, R., KOCHUNOV, P., KWAN, P., LABATE, A., MCDONALD, C. R., MELETTI, S., O'BRIEN, T. J., OURSELIN, S., RICHARDSON, M. P., STRIANO, P., THESEN, T., WIEST, R., ZHANG, J., VEZZANI, A., RYTEN, M., THOMPSON, P. M. & SISODIYA, S. M. 2018. Structural brain abnormalities in the common epilepsies assessed in a worldwide ENIGMA study. *Brain,* 141**,** 391-408.

WHITFIELD-GABRIELI, S. & NIETO-CASTANON, A. 2012. Conn: a functional connectivity toolbox for correlated and anticorrelated brain networks. *Brain Connect,* 2**,** 125-41.

WILKE, M., LOGOTHETIS, N. K. & LEOPOLD, D. A. 2006. Local field potential reflects perceptual suppression in monkey visual cortex. *Proceedings of the National Academy of Sciences,* 103**,** 17507.

WILLOUGHBY, J. O., FITZGIBBON, S. P., POPE, K. J., MACKENZIE, L., MEDVEDEV, A. V., CLARK, C. R., DAVEY, M. P. & WILCOX, R. A. 2003. Persistent abnormality detected in the non-ictal electroencephalogram in primary generalised epilepsy. *J Neurol Neurosurg Psychiatry,* 74**,** 51-5.

WOLDMAN, W., COOK, M. J. & TERRY, J. R. 2019. Evolving dynamic networks: An underlying mechanism of drug resistance in epilepsy? *Epilepsy Behav,* 94**,** 264-268.

WOLF, P. & BENICZKY, S. 2014. Understanding ictogenesis in generalized epilepsies. *Expert Rev Neurother,* 14**,** 787-98.

WU, X. & XIAO, C. H. 1997. Quantitative pharmaco-EEG of sustained release valproate in epileptics. *Clin Electroencephalogr,* 28**,** 117-20.

WU, Y., LIU, D. & SONG, Z. 2015. Neuronal networks and energy bursts in epilepsy. *Neuroscience,* 287**,** 175-186.

WYART, V. & TALLON-BAUDRY, C. 2008. Neural Dissociation between Visual Awareness and Spatial Attention. *The Journal of Neuroscience,* 28**,** 2667.

XIA, M., WANG, J. & HE, Y. 2013. BrainNet Viewer: A Network Visualization Tool for Human Brain Connectomics. *PLOS ONE,* 8**,** e68910.

XUE, K., LUO, C., ZHANG, D., YANG, T., LI, J., GONG, D., CHEN, L., MEDINA, Y. I., GOTMAN, J., ZHOU, D. & YAO, D. 2014a. Diffusion tensor tractography reveals disrupted structural connectivity in childhood absence epilepsy. *Epilepsy Res,* 108**,** 125-38.

XUE, K., LUO, C., ZHANG, D., YANG, T., LI, J., GONG, D., CHEN, L., MEDINA, Y. I., GOTMAN, J., ZHOU, D. & YAO, D. 2014b. Diffusion tensor tractography reveals disrupted structural connectivity in childhood absence epilepsy. *Epilepsy Research,* 108**,** 125-138.

YAAKUB, S. N., TANGWIRIYASAKUL, C., ABELA, E., KOUTROUMANIDIS, M., ELWES, R. D. C., BARKER, G. J. & RICHARDSON, M. P. 2020. Heritability of alpha and sensorimotor network changes in temporal lobe epilepsy. *Annals of clinical and translational neurology,* 7**,** 667-676.

YANG, H., LONG, X.-Y., YANG, Y., YAN, H., ZHU, C.-Z., ZHOU, X.-P., ZANG, Y.-F. & GONG, Q.-Y. 2007. Amplitude of low frequency fluctuation within visual areas revealed by resting-state functional MRI. *NeuroImage,* 36**,** 144-152.

YAO, D. 2001. A method to standardize a reference of scalp EEG recordings to a point at infinity. *Physiol Meas,* 22**,** 693-711.

YAO, Z., HU, B., XIE, Y., MOORE, P. & ZHENG, J. 2015. A review of structural and functional brain networks: small world and atlas. *Brain Informatics,* 2**,** 45-52.

YEO, B. T. T., KRIENEN, F. M., SEPULCRE, J., SABUNCU, M. R., LASHKARI, D., HOLLINSHEAD, M., ROFFMAN, J. L., SMOLLER, J. W., ZÖLLEI, L., POLIMENI, J. R., FISCHL, B., LIU, H. & BUCKNER, R. L. 2011. The organization of the human cerebral cortex estimated by intrinsic functional connectivity. *Journal of neurophysiology,* 106**,** 1125-1165.

ZALESKY, A., COCCHI, L., FORNITO, A., MURRAY, M. M. & BULLMORE, E. 2012a. Connectivity differences in brain networks. *NeuroImage,* 60**,** 1055-1062.

ZALESKY, A., FORNITO, A. & BULLMORE, E. 2012b. On the use of correlation as a measure of network connectivity. *NeuroImage,* 60**,** 2096-2106.

ZALESKY, A., FORNITO, A., HARDING, I. H., COCCHI, L., YUCEL, M., PANTELIS, C. & BULLMORE, E. T. 2010. Whole-brain anatomical networks: does the choice of nodes matter? *Neuroimage,* 50**,** 970-83.

ZHANG, C., KWAN, P., ZUO, Z. & BAUM, L. 2012. The transport of antiepileptic drugs by P-glycoprotein. *Advanced Drug Delivery Reviews,* 64**,** 930-942.

ZHANG, Z., LIAO, W., CHEN, H., MANTINI, D., DING, J. R., XU, Q., WANG, Z., YUAN, C., CHEN, G., JIAO, Q. & LU, G. 2011. Altered functional-structural coupling of large-scale brain networks in idiopathic generalized epilepsy. *Brain,* 134**,** 2912-28.

ZHENG, G., QI, X., LI, Y., ZHANG, W. & YU, Y. 2018. A Comparative Study of Standardized Infinity Reference and Average Reference for EEG of Three Typical Brain States. *Frontiers in Neuroscience,* 12**,** 158.

ZHONG, C., LIU, R., LUO, C., JIANG, S., DONG, L., PENG, R., GUO, F. & WANG, P. 2018. Altered Structural and Functional Connectivity of Juvenile Myoclonic Epilepsy: An fMRI Study. *Neural Plast,* 2018**,** 7392187.

ZIVIN, L. & MARSAN, C. A. 1968. Incidence and prognostic significance of "epileptiform" activity in the eeg of non-epileptic subjects. *Brain,* 91**,** 751-78.

Blank page